THE MORPHOLOGY AND BIOMECHANICS OF THE MUSCLE ARTICULATION: A
NEW CLASS OF SOFT TISSUE JOINT

Theodore Akira Uyeno

A dissertation submitted to the faculty of the University of North Carolina at Chapel Hill in partial fulfillment of the requirements for the degree of Doctor of Philosophy in the Department of Biology.

Chapel Hill
2007

Approved by:

Dr. W. Kier

Dr. J. Bruno

Dr. J. Carter

Dr. J. Kingsolver

Dr. K. Lohmann

ABSTRACT

THEODORE AKIRA UYENO: The Morphology and Biomechanics of the Muscle
Articulation: A New Class of Soft Tissue Joint
(Under the direction of Dr. William M. Kier)

Joints allow relative motions between the rigid structural elements (termed 'links')

they connect. As joints are crucial for many animal movements used in locomotion, feeding,

and reproduction, an understanding of the biomechanical principles of joint form and

function is essential. There are two categories of animal joints: sliding and flexible. Sliding

joints (e.g. vertebrate and arthropod articulated joints) transmit compressional forces directly

through contact between the links. The shapes of the contact surfaces and their connective

tissue capsules limit their possible motions. Flexible joints include pliable connections which

allow relative motions between the links. They are normally loaded in tension because

compressional forces tend to cause the connection to buckle. As flexible joints are less well-

understood, they are the focus of this dissertation. In particular, I define, describe, and

analyze a new form of flexible joint: the muscle articulation. In muscle articulations, the

pliable connections consist of multiple orientations of muscle fibers or myofibrils arranged as

muscular hydrostats. Arrangements of connective tissue fibers are also important and may

limit shape change and store elastic energy. Together, these soft tissues allow the multi-

functional characteristics of muscle articulations; they connect links, generate motive forces,

create pivot areas, and transmit compressional forces between the links. These arrangements,

with appropriate neural control, may allow muscle articulations to produce a relatively great

diversity and complexity of movements. Three examples of muscle articulations were

examined. First, I described the morphology of the octopus buccal mass in detail. A biomechanical analysis of this morphology generated hypotheses of function that were tested experimentally by correlating muscle activation patterns with beak movement. Second, the morphology and biting movements of the eversible proboscidial jaws of the polychaete *Nereis* were analyzed and found to share key muscle articulation soft tissue characteristics. Third, the morphology of the armed proboscides of the kalyptorhynchs, a group of meiofaunal turbellarian flatworms, was analyzed and identified as a unique muscle articulation of simple and microscopic construction. The comparative analyses of these joints not only identified common muscle articulation characteristics, but demonstrate that this important type of joint has evolved independently in at least three invertebrate phyla.

ACKNOWLEDGEMENTS

This work represents my best effort to become that which my supporters have given a monumental amount of time and energy to develop in me: an integrative organismal biologist. The term "integrative" can mean the use of results of studying one level of organization to help answer questions posed at another: Descriptions of cells and tissues and observations of behavior or patterns of evolution are often mutually informative. For me, the term also describes the use of non-traditional techniques and theory to get things done. Concepts in physiology, engineering, physics, computer science, electronics and other seemingly unrelated disciplines, such as life skills and pedagogy, have all aided the exploration of my ideas. While it is not impressive that I have tried to use these tools to benefit my research, it is impressive that my life and life science educators had the patience to try and teach me. For this I extend my especial thanks to a number of people:

My advisor and trusted mentor Dr. Bill Kier and the members of my doctoral committee, Dr. Ken Lohmann, Dr. Joe Carter, Dr. John Bruno, Dr. Joel Kingsolver, and Dr. Bob Podolsky deserve my thanks for their kind treatment of the many examples of sheer naïveté during the graduate stage of my academic ontogenesis.

My wife Angela and my Mom and Dad (Anna & Thomas) deserve great thanks for their many decades of support. I thank my brother Keith and his family for keeping me company in North Carolina and for letting me hang out with my little nephews.

TABLE OF CONTENTS

LIST OF TABLES

Table

LIST OF FIGURES

Figure

ABBREVIATIONS

º	Degree (s)
µm	Micrometers
3D	Three-dimensional
A	Anterior portion of AMM
AC	Alternating current
AMM	*Octopus* Anterior Mandibular Muscle
AP	Anterior-posterior muscle fibers of the LMM
Bas.mem.	Basement membrane
Bol	Bolster
BP	Buccal palp
Brdg.	Bridge connecting tongues or hook supports
BS	Buccal Sheath
C.I.	Color Index
CD	Central division of the SMM
Circ	Circumferential muscles
cm	Centimeter
CT	Connective Tissue
dB	Decibel
DC	Direct current
DoF	Degree(s) of freedom
DV	Dorsal-ventral muscle fibers of the LMM
E.cone	End cone
EMG	Electromyography
Eso	Esophagus

FFT	Fast Fourier Transform
g	Grams
h	Hours
Hk	Hook
Hk.abd.	Hook abductor muscle
Hk.add.	Hook adductor muscle
Hk.sup.	Hook support
Hz	Hertz, cycles per second
Inf.buc.gang.	Inferior buccal ganglion
Int.buc.conn.	Interbuccal connective
Jun	Junction
kHz	Kilohertz
L	Liters
L.aux.app.	Lateral auxiliary apparatus
Lat	Lateral muscle fibers of the LMM
LB	*Octopus* Lower Beak
LBLW	Lateral wall of Lower Beak
LD	Left division of the SMM
LMM	*Octopus* Lateral Mandibular Muscle
Long	Longitudinal muscle
LW	Lateral Wall
min	minutes
ml	milliliters
mm	millimeters
mmol l^{-1}	millimoles per liter

ms	milliseconds
mV	millivolts
Nod	Nodus
Nod.pore	Nodal pore
P	Posterior portion of AMM
PMM	*Octopus* Posterior Mandibular Muscle
ppt	Parts per thousand
RD	Right division of the SMM
Ret	Retractor muscle
Rost.pore	Rostral pore
s	Seconds
Sept	Septum
Sh.ret.	Sheath retractor muscle
SMM	*Octopus* Superior Mandibular Muscle
Tng	Tongue
Trnk	Trunk muscle
UB	*Octopus* Upper Beak
UBH	Upper Beak Hood
UBLW	Lateral wall of Upper Beak
V	Volts
v/v	by volume
W	Watts

CHAPTER 1
A REVIEW OF JOINTS AND THE MUSCLE ARTICULATION

Introduction

Many movements exhibited during animal behaviors depend on joints. This is

because a joint is the crucial structure that allows a rigid portion of an animal to move

relative to others. Aristotle included this assessment of the importance of joints in the oldest

surviving biomechanical textbook, *De Motu Animalium* (circa 304 BC; Nussbaum, 1985).

Since this time, while many biomechanical studies have advanced our theoretical and

practical understanding of how joint forms relate to their functions, Aristotle's basic

definition and original assessment of the importance of the joint remains unchanged.

Joints are often analyzed in the course of understanding movement and behavior.

However, if the focus is to determine the characteristics of joints themselves, valuable insight

often arises from comparative analyses of joint biomechanics. Therefore, Wainwright et al.

(1982) constructed a general scheme to categorize the wide morphological diversity

exhibited by animal joints. Two general categories were proposed based on range of motion

and how loads are transferred across the joint: *Flexible joints* (Fig. 1A), possess pliable areas

that allow bending, whereas *sliding joints* (Fig. 1B), are formed where the ends of separate

elements contact. As sliding joints include vertebrate and arthropod joints, there are a number

of well-studied examples. However, as flexible joints, and the organisms that seem to make
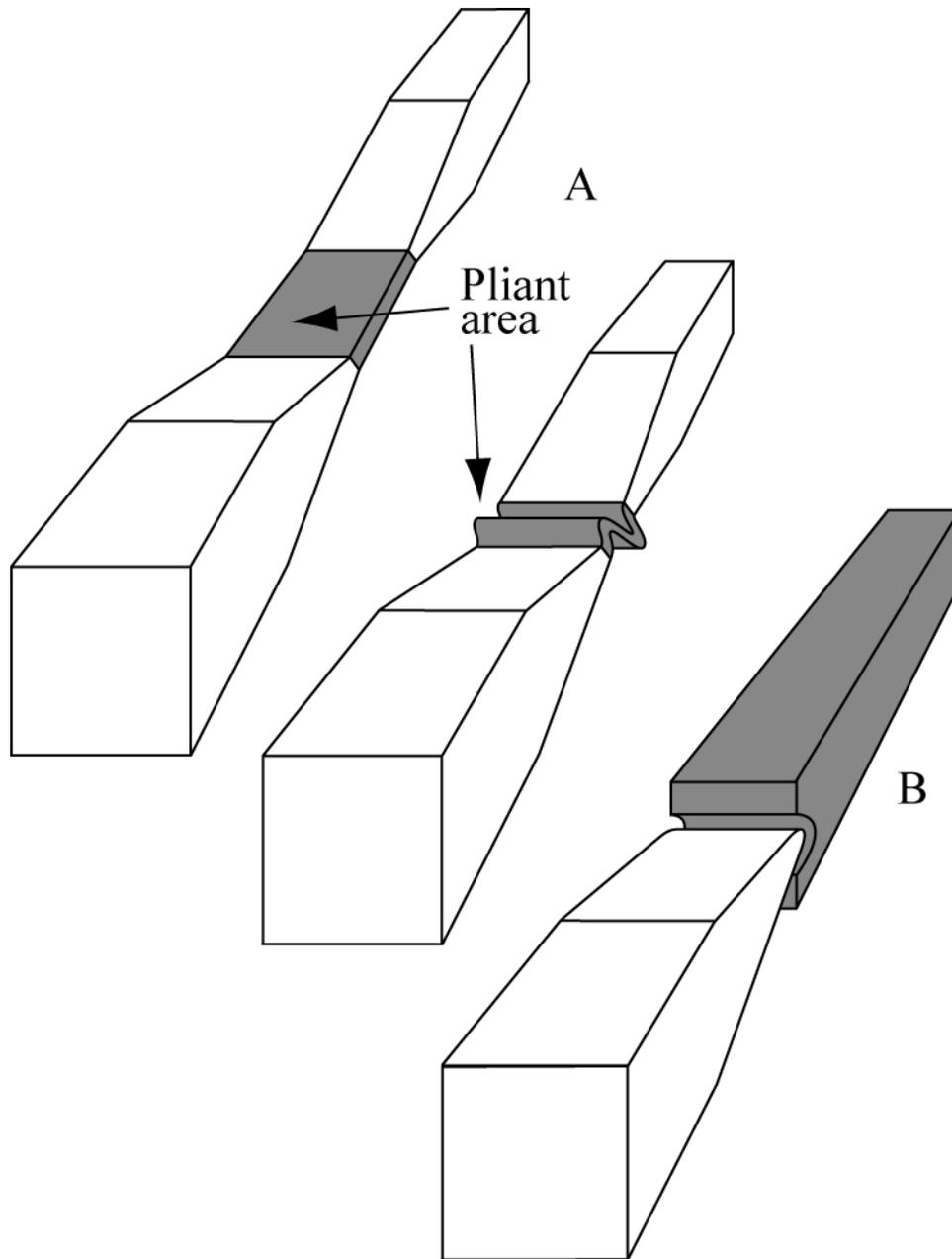
Figure 1. The two broad categories of joints used by animals: A) The strap joint allows bending motions by making use of a thinner, more pliable region. The joint is shown here in tension on the left and buckling under compression on the right. B) The more common sliding joint transmits forces directly from one element to the other through regions that contact one another.

most use of them, have historically received much less attention, they will be the focus of this chapter.

Wainwright et al. (1982) described flexible joints as continuous skeletal elements that possess areas thin enough to allow bending. They noted that these joints are rare and cited the distal leg segments of smaller insects and the joints between valves in polyplacophoran molluscs (chitons) as examples. The limited use of flexible joints was attributed to the tendency of the thin areas to buckle when loaded in compression (Fig. 1A). I have identified a group of flexible joints with a more complex pliable connection that is capable of transmitting and generating a wide range of forces. In this new flexible joint type, which I have termed a "muscle articulation", the rigid elements are connected and separated by muscle and connective tissues. Unlike conventional flexible joints, compressional forces can be transmitted without causing buckling and the joint itself generates force for movement. It is likely that this arrangement allows a greater diversity and complexity of movements.

In this chapter, I describe the characteristics of the muscle articulation and introduce the joints that I have analyzed. I begin by reviewing mechanical concepts and definitions. Then, in order to identify how muscle articulations fit within the joint categorization scheme, I review the structural and mechanical characteristics of previously defined categories. I then review of a number of joints for which complete mechanical analyses exist. While these joints are not muscle articulations, their analyses serve to identify common principles and requirements of joint function and may suggest methods of analysis for muscle articulations. Finally, I summarize the characteristics of muscle articulations and review potential examples of this new category of flexible joint.

The terminology of joint mechanics: What is a joint?

The terminology of joints is derived from engineering and physics. Wainwright et al. (1982) defined the term *joint* from a mechanical point of view: It is the structural area that governs range of motion and allows the transfer of force between two relatively rigid elements. Alexander (1983) noted that these rigid elements are referred to as *links* and formally defined links as the rigid elements that rotate or translate with respect to each other through the relative motions of the joint.

A series of links, connected together by joints, constitutes a *mechanism* (Alexander, 1983), and a *machine* is system of mechanisms that transforms a power source into a desired application of forces and movements (McCarthy & Joskowicz, 2001). Muscle articulations might thus be considered as both a simple mechanism as well as a simple machine.

The term *articulation* is used to describe the physical contact of links within the joint that allows force to be transferred directly from one link to the next. The shapes of the articulating surfaces in sliding joints limit their ranges of motion. Because links do not contact each other in flexible joints, the term articulation is usually only applicable to sliding joints. Thus the use of the term "muscle articulation" deserves explanation: As the links do not touch, the muscle acts as the articulation by limiting the range of motion and transmitting loads between the links.

The motions of any joint can be described by its *degrees of freedom*, of which there are three degrees of rotation and three degrees of translation (Fig. 2). The most flexible joints have all six degrees of freedom, although many, especially articulated sliding joints, have a reduced number for safety and ease of control (Taylor et al., 2000; Wainwright et al., 1982).
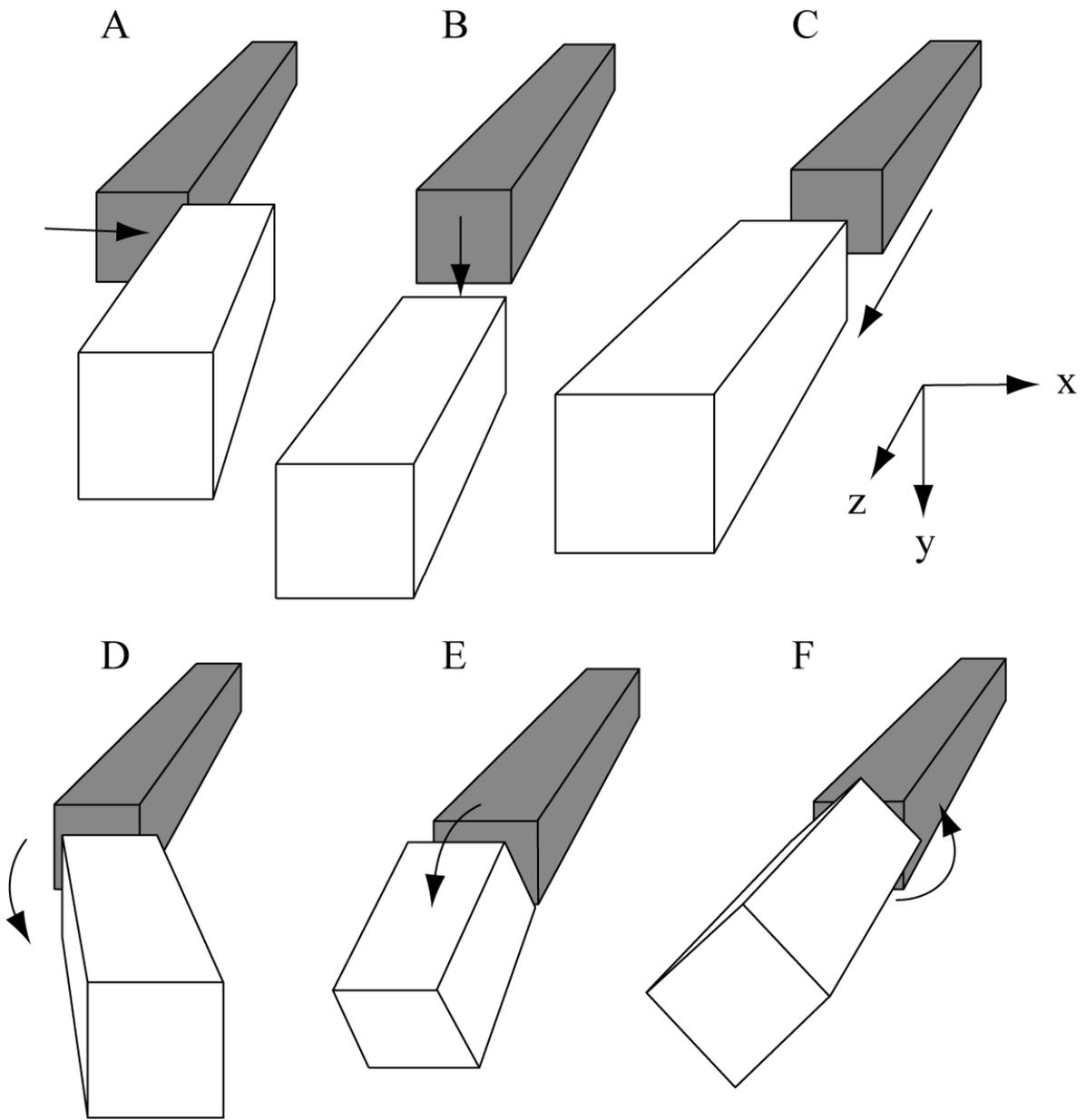
Figure 2. The six degrees of freedom in joint motion: A-C represent the three degrees of translation and D-F represent the three degrees of rotation in all three mutually perpendicular x, y, and z axes. The arrows represent the direction of motion possible by the particular degree of freedom.

Given that machines transform an input force into a desired output, an important characteristic of a machine is its *mechanical advantage*, or the ratio of force output to input (Alexander, 1983). These forces act on the links to move them at certain velocities and thus the ratio of output to input velocity is referred to as the *velocity ratio* (Alexander, 1983). Mechanical advantage and velocity ratio are intimately related. McCarthy and Joskowicz (2001) noted that in machines designed to minimize energy losses due to friction and fatigue, instantaneous input variations in work cancel output variations (engineers refer to this as the principle of virtual work). At a given time (a virtual time increment), because the input and output virtual work cancels, the variation in instantaneous power multiplied by the virtual time increment must equal zero (power input equals power output). Thus, because power is the product of force and velocity, in a system without power dissipation, the mechanical advantage is the inverse of its velocity ratio.

A discussion of joints refers to both rotational and linear forces. Linear forces can be applied in *compression* (a crushing force) or *tension* (a stretching force). *Torque* is a force that causes rotation about an axis. The magnitude of torque is the product of the tangential force and the perpendicular distance from the axis to the line of action of the tangential force. This perpendicular distance is referred to as the *moment arm* (Wainwright et at., 1982, Alexander, 1983).

Surveying joint diversity

Described below are examples of flexible and sliding joints for which detailed analyses exist. They have been selected to illustrate the range of morphological diversity and include exoskeletal and endoskeletal joints, human-engineered mechanical joints, and hydrostatic structures.

Arthropod exoskeletons are a series of hollow cylindrical links. Forces used to bend and straighten arthropod limb joints are created by antagonistic muscle sets that insert on the inner walls of the exoskeleton and on apodemes, or thickened internal attachment surfaces that serve a tendon-like function. Wainwright et al. (1982) noted that there are two types of exoskeletal joints: pliant region joints and condylar joints. Simple pliant region joints are of the flexible joint type; they are hollow cylinders with a thin and resilient section that buckles to allow relative motions of the rigid sections found on either side. Condylar joints are a modification of the pliant region joint in which one (monocondylar) or two (dicondylar) areas of the pliant arthrodial membrane are reinforced to form ball-in-socket or saddle-like joints. Of the two, condylar joints are stronger than pliant region joints because forces transmitted through the joint are directed through the hinge-like reinforced areas.

Hildebrand (1995) noted that vertebrates use endoskeletal joints that are divided into three types: synarthroses, amphiarthroses and diarthroses. Synarthroses, such as cranial sutures, are fibrous joints that allow no movement. Ribs and other amphiarthroses are considered flexible joints because usually the connecting material is composed of cartilage and allows a small range of movement. Diarthroses are capable of the greatest ranges of motion. Here, the articulating surfaces are encased in a bursa sac that contains lubricating synovial fluid. As a sliding joint type, the degrees of freedom and the range of motion of diarthrotic joints are dictated by the morphology of the articular surfaces. (Table 1)

The human engineered joints that serve as components in our machines are well-understood because they are designed to allow a specified range of motion. In building these machines, McCarthy and Joskowicz (2001) note that engineers generally employ a combination of relatively few "primitives" or basic forms of sliding joints (Table 2).

Table 1. A list of types of diarthrotic joints, their degrees of freedom (DoF), a description of their types of movement, and a vertebrate example of the type of joint. Information from Hildebrand, 1995.

Name	Degrees of freedom (DoF)	Description	Example
Hinge	1 rotational DoF	Rotation about an axis in one plane.	The jaw of a cat used to concentrate force
Saddle	2 rotational DoF	Rotation about axes in two planes.	The jaw of a cow use to shear vegetation
Ball-and-socket	3 rotational DoF	Rotation about axes in two directional planes plus twisting in a third.	The human hip joint
Ellipsoid	3 rotational DoF	Rotation about axes in two planes plus twisting in a third. Less movement capable than in the ball-and-socket.	The radio-carpal wrist joint
Pivot	1 rotational DoF	A twisting rotation in one plane.	The occipital bone of the skull
Gliding	1 or 2 translational DoF	Sliding between bones in one or two planes. A third translational DoF would describe a dislocation.	The midcarpal or midtarsal joints

Table 2. Joint primitives commonly used in engineering, the number of associated degrees of

freedom (DoF), a description of the joint motion, and an illustrated example.

Name	Degree of Freedom (DoF)	Description	Example
Rigid	0 DoF	Two links are connected to each other in a rigid fashion	
Revolute	1 rotational DoF	Rotation about only one axis	
Prismatic	1 translational DoF	Sliding along one axis	
Spherical	3 rotational DoF	Rotation about axes in two planes, twisting in the third	
Floating	6 DoF	This is not a primitive joint; it is a composite of several of the above joints. It also describes two disconnected or loosely connected links.	
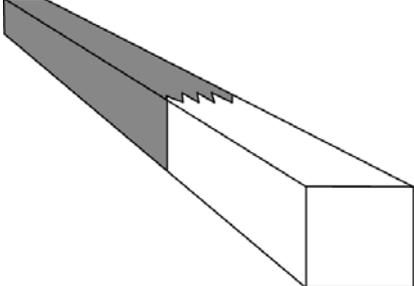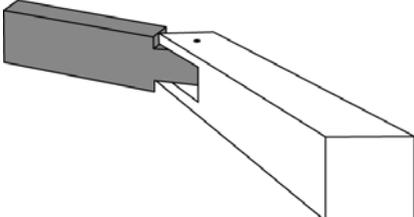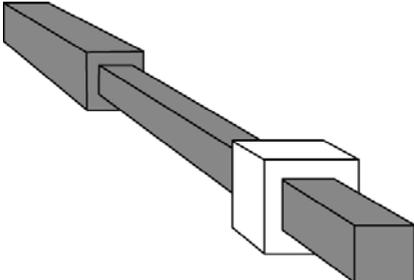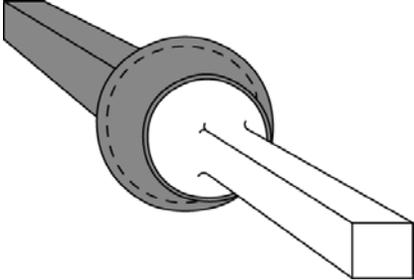
While generally not considered as joints because they do not possess links, classical hydrostatic skeletons, such as the bodies of earthworms and sea anemones, and muscular hydrostats, such as octopus arms and human tongues, may be thought of as a great number of serial joints in between extremely short links. Both classical and muscular hydrostats function by pressurizing internal fluid. The resulting turgidity supports tension and compression created by antagonistic muscles (Wainwright et al., 1982). Classical hydrostats pressurize fluid in a relatively large central cavity. Sea anemones (Fig. 3A) and many vermiform phyla use longitudinal and circumferential muscles within the body wall to pressurize this fluid (Schmidt-Nielsen, 1998). As pressure is omnidirectional, precise direction of force is difficult in organisms reliant on classical hydrostats. Clark (1964) noted that forces were more precisely directed by increasing the number and decreasing the individual volumes of hydrostatic cavities within the body. Kier and Smith coined the term "muscular hydrostat" (Kier & Smith, 1985, Smith & Kier, 1989) to describe the most extreme form. Here, muscle fibers are arranged in multiple orientations to form solid blocks of tissue in which the cavities are maximally reduced to the pressurized fluid within each muscle cell. When muscle fibers contract, their fluid content is pressurized and that region of muscle becomes turgid. Muscle fibers are arranged antagonistically so that the contraction of one orientation will return others to resting length (Figs. 4A-C). As an example, Kier (1982) described the multiple orientations of muscle fibers that form the musculature of cephalopod tentacles (Fig. 3B). Bends are produced by relatively stronger contractions of longitudinal muscles on one side of the body. Overall shortening of the tentacle, or shortening of just one side is resisted by the contraction of appropriate orientations of muscle fibers that keep the diameter constant (Figs. 4C & 4D).

10
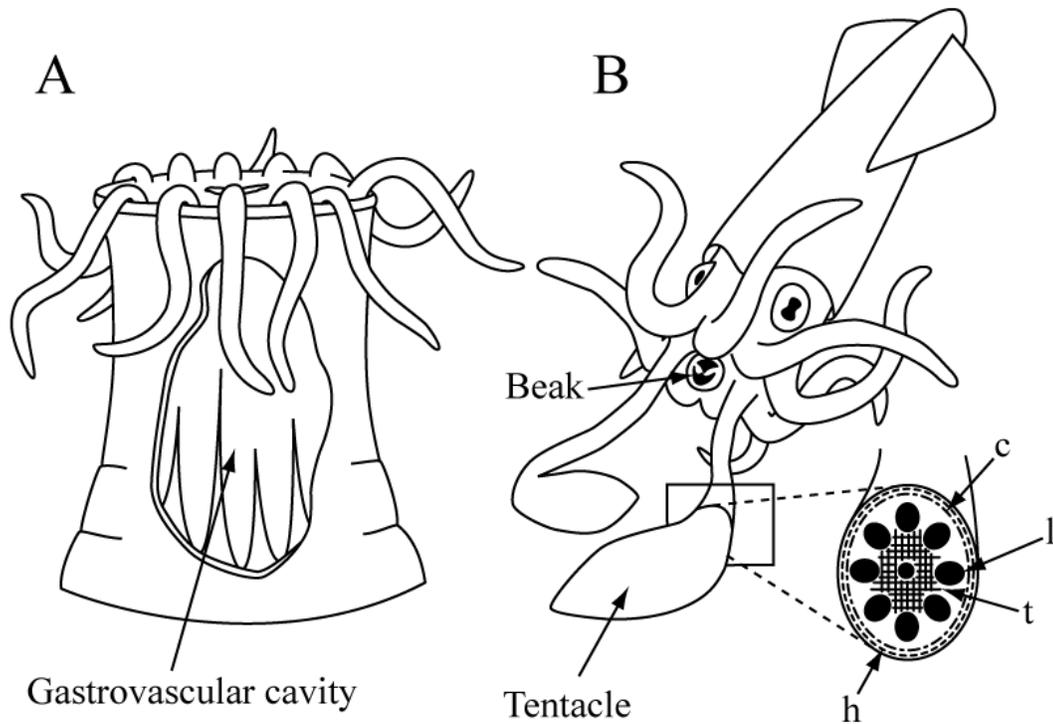
Figure 3. A) A sea anemone's body is supported by a classical hydrostatic skeleton (the body wall is cut away to show the inner space (the gastrovascular cavity) that contains the hydrostatic fluid). B) the arms and tentacles of cephalopods rely on muscular hydrostats. The cross section through one tentacle shows circular (c), longitudinal (l), helical (h), and transverse (t) muscle fiber trajectories that all pack into a solid three-dimensional block of muscle. Here one or more sets of muscle fiber orientations provide antagonistic support for others.
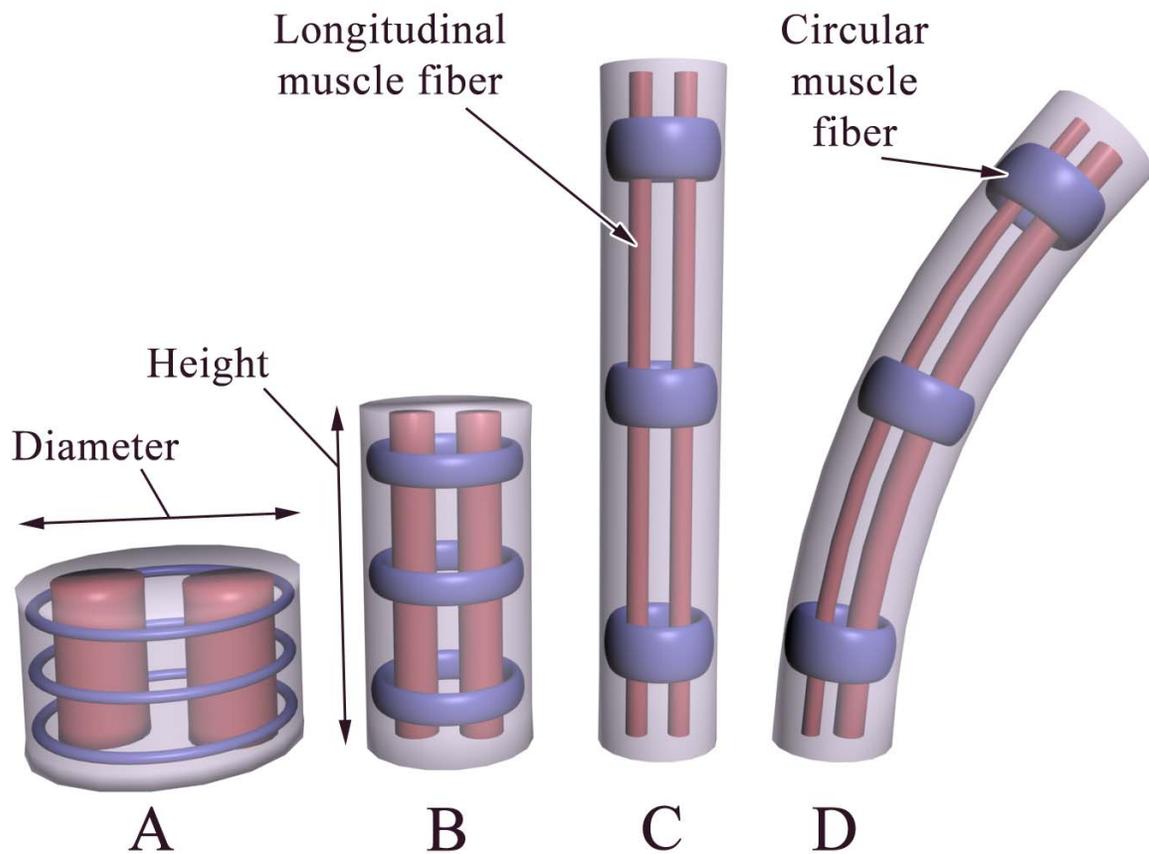
Figure 4. Muscular hydrostats use different orientations of fibers to antagonize each other. Since the volume of a muscular hydrostat cannot change, (A) contraction of longitudinal fibers (two of which are shown here in pink) reduces the height of this cylindrical muscular hydrostat while increasing its diameter relative to that of the resting dimensions (B). (C) Contraction of the circular muscle layer (shown here as three blue bands) increases the height and decreases the diameter of the cylinder. (D) Bending of muscular hydrostats involves asymmetrical muscle contractions: Here the right longitudinal fiber is contracting while the circular muscles are active, resulting in a bending of the muscular hydrostat.

Mechanical analyses of joint examples

Below, I present four well-understood examples: the vertebrate temporomandibular joint, the dicondylar joint of the crab claw, and two human engineered joints for which we have a complete understanding; the lever and the wedge. While none of these joints are considered muscle articulations, their analyses are useful because they identify common and general joint characteristics, as well as useful methods of joint analysis. Additionally, some of the examples show how such analyses might be useful in answering ecological and evolutionary questions.

The temporomandibular joint

The temporomandibular joint is crucial to feeding in mammals and is therefore under strong selective pressure. In the evolution of the mammalian jaw from synapsid reptile ancestors (Fig. 5C & D), Crompton (1963) noted a relative weakening of the joint along with strengthening of its associated muscles. A functional morphological analysis of the links, the joint, and the forces they experience helped explain this evolutionary path.

The increase in the range of functional movements and biting force are strong trends in the evolution of the vertebrate jaw. The diarthrodial craniomandibular joint first appeared in the Silurian ancestors of bony fishes (DuBrul, 1992). This jaw functioned as a simple lever in which closing muscles were positioned between a robust posterior fulcrum, constructed to transmit strong forces, and the biting surface (Fig. 5A). Crompton (1963) noted that biting did not require rotation about the joint that served as a fulcrum, but it did require a large attachment surface for an undivided adductor muscle. This resulted in a limited range of motion as wider gapes required the mandible to rotate. To increase the range of motion and biting force, Noble and Creanor (1992) noted that the evolution of this simple lever into the

13
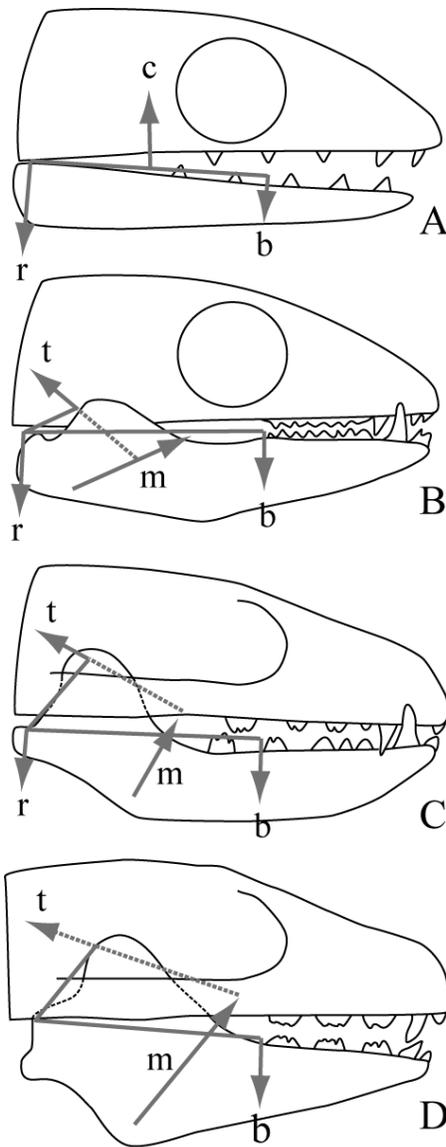
Figure 5. Evolution of the temporomandibular joint. A) An early synapsid reptile. To balance the bite force (b) and the reaction force (r), a single undivided craniomandibular muscle must apply force (c). B-C) Increasingly advanced synapsid reptiles. The divided temporalis and masseter muscles apply forces (t) and (m) respectively, allowing the balancing of bite force (b) with a decreased reaction force (r). D) A mammal or a very advanced synapsid reptile. The bite force (b) is balanced by only force generated by the temporalis (t) and masseter muscles (m). Modified from Alexander, 1983.

14

mammalian temporomandibular joint (Fig. 5D) was accomplished by both a subdivision of the adductor muscle into the masseter, medial pterygoid, and temporalis muscles and by the contact of two formerly unrelated membrane bones (the mandible and temporal bones).

The evolution of the vertebrate jaw has also tended to reduce the reaction forces sustained by the jaw joint during biting. Noble and Creanor (1992) noted that the lower jaws of increasingly advanced synapsids bore large processes to accept divided adductor muscles (the masseter and the temporalis muscles) (Figs. 5B & 5C). This resulted in an increase in mechanical advantage as well as a reduction of the reaction force at the craniomandibular joint. In fact, Crompton (1963) showed that very advanced synapsid reptiles had mammal-like jaws that were capable of balancing the force of a bite on their back teeth using only their temporalis and masseter muscles (Fig. 5D). No contact between the mandible and the cranium was needed and thus no force was transmitted through the craniomandibular joint. While the jaw joint is still required to support opening muscles and to limit the range of possible motions, it is interesting to note that this increase in the complexity of joint functions is a result of a more complex organization of musculature; a characteristic that might be shared by muscle articulations.

The dicondylar crustacean claw

The crustacean claw is an example of an articulated arthropod exoskeletal joint (Wainwright et al., 1982). These claws are the terminal portions of decapod crustacean chelipeds (the 1st pereopod or leg) (Brusca & Brusca, 2003). The bipartite claw is composed of the propodus that bears a fixed finger and the movable dactylus (Fig. 6). The dactylus and the propodus are connected by a dicondylar arthrodial joint that serves as a fixed pivot. This pivot is formed of interlocking condyles (balls) and fossa (sockets) that have evolved to

15
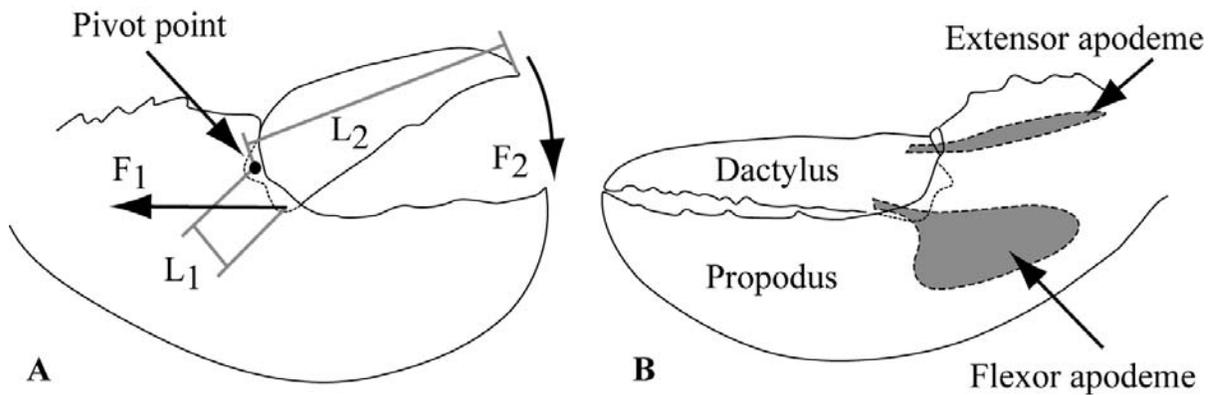
Figure 6. The claws of *Homarus americanus*, the American lobster. A) The crusher claw

showing the length of the input moment arm L_1, the output moment arm L_2, the input force

F_1 and the output force F_2. B) The cutter claw showing the propodus, the dactylus and the

extensor and flexor apodemes. Modified from Elner & Campbell, 1981.

limit range of motion, direct muscular force and transmit loads. The range of motion of the dactylus occurs in one plane in which it rotates about the fixed pivot. The gape of the claw is limited in closing by the occlusion of the cutting surfaces and limited in opening by the abutment of the dorsal surfaces of the dactylus and propodus. Within the hollow dactylus are two ingrowths that serve as tendons (Fig. 6B): the abaxial extensor apodeme and the adaxial flexor apodeme (Alexander, 1983). The apodemes extend from the inner surface of the dactylus into the space inside the propodus where they flare out into a flat sheet. This flaring increases the surface area for pinnate muscle attachment. Taylor (2000) found that crabs of the genus *Cancer* can generate remarkably large claw crushing forces of up to 800 N with corresponding stress in the flexor muscle of up to 2000 kNm^{-2}.

The biomechanical analysis of the dactylus, the propodus, and their dicondylar joint can be used to provide insights into crustacean ecology and evolution. Elner and Campbell (1981) correlated structural characteristics of American lobster (*Homarus americanus*) claws to their ecological function to assess the selective forces acting upon claw morphology. These lobsters have two chelae that differ in shape: The crusher chela (Fig. 6A) has a dactylus and a propodus with flat occluding surfaces, whereas the cutter chela (Fig. 6B) is armed with small sharp teeth. Lobsters use cutter chelae to catch fish and to manipulate and hold objects. The functions of the larger and stronger crusher chelae, despite their name, are not as obvious. As the claw exhibits sexual dimorphism in size and strength, one hypothesis is that it is used in mate selection. Elner and Campbell (1981) measured the mechanical advantage of the chelae and predicted the potential input and output forces (Fig. 6A).

The mechanical advantage of male crusher chelae (0.33) was significantly larger than those of similarly sized females (0.29), while the mechanical advantages of the cutter chelae

were identical (0.16) between sexes. This suggested that the morphology of the cutter chelae is related to prey handling and defense, and that the morphology of the crusher chelae might be related to these same functions, but are also under sexual selection.

The lever and wedge

All variables in the analyses of human engineered joints are known because we can specify them in the design process. The ranges through which the joints permit the links to move can be completely mathematically described. Thus the analyses of two such joints are described here to suggest analytical and modeling methods that may be used to better understand and describe animal joint characteristics.

Typically, artificial mechanisms are analyzed using a process known as kinematic synthesis. Engineers McCarthy and Joskowicz (2001) defined this term as the analysis that determines the configuration and size of the links and the motions required by the joints in order to transform a given input power into a desired output power. The process begins by describing the dimensions and possible positions of each link. Here, the ranges of these positions depend on the magnitude and direction of input and output forces. Next, each joint is described in terms of range of motion and degrees of freedom. With these characteristics defined for each link and joint, the location of any part relative to a predefined base can be described by the kinematic equation (Eq. 1). Here, joints are described as a series of axes (denoted as "S_j") and the links they connect as common normal lines (lines parallel to the long axis of the links, denoted as "A_{ij}").

$$[D]=[Z(\theta_1,\rho_1)][X(\alpha_{12},a_{12})][Z(\theta_2,\rho_2)]\ldots[X(\alpha_{m-1,m},a_{m-1,m})][Z(\theta_m,\rho_m)] \qquad \text{Eq. 1}$$

[D] is the configuration space and represents all the positions obtained as the joint parameters vary over their range of movement. The matrix $[Z(\theta_j,\rho_j)]$ defines screw displacements (a rotation linked to a translation) along the joint axis (S_j) and the matrix $[X(\alpha_{ij},a_{ij})]$ defines screw displacements along the common normal lines (A_{ij}). The paramerters α_{ij},a_{ij} define the dimensions of the links. Parameter θ_j is the angular joint variable for revolute joints and ρ_j is the parameter for prismatic joints.

The lever described here (represented in Fig. 7 as a hand cart) is a bar of rectangular cross section that possesses a bend perpendicular to its long axis. In use, the lever rotates about the bend using a revolute joint that is oriented perpendicular to the plane of the bend. As it has a single link and joint, it is described only by its rotation:

$[D]=[Z(\theta)]$.   Eq. 2

The input velocity of point A (that point at which torque F_{in} is applied) is equal to the product of the moment arm "a" and the angular velocity. As the output velocity of point B is the moment arm "b" times the angular velocity, the velocity ratio is the output moment arm "b" to "a".

The wedge described by McCarthy and Joskowicz (2001), has a right triangular profile and can be considered as two prismatic joints (Fig. 8). The first joint (Eq. 3) is the wedge sliding, in the direction of the applied force, along the ground.

$[D]=[G_1][Z(0,x)][X(\alpha,0)][Z(0,a)][H_1]$,   Eq. 3
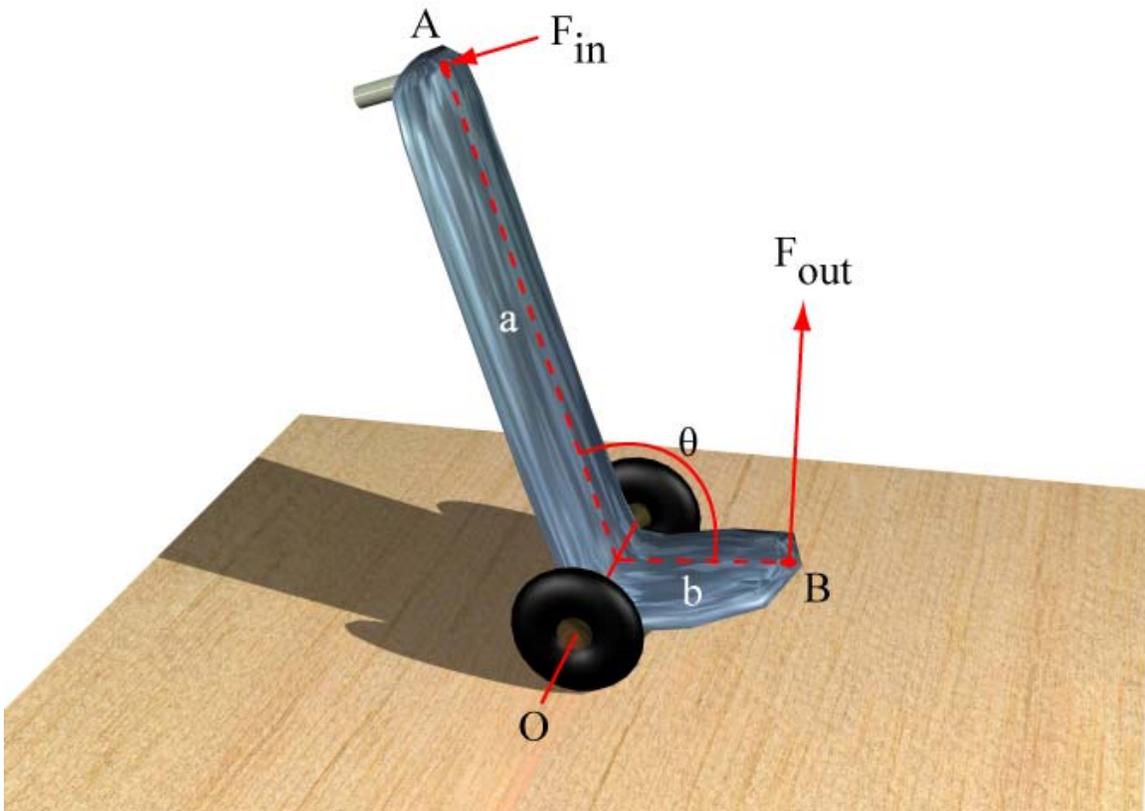
Figure 7. This lever rotates about a revolute joint O. The input force F_{in} applied at point A is the distance **a** away from axis O. The resulting output force F_{out} is generated at point B that is distance **b** from axis O. θ is the angle between segments AO and OB. Modified from McCarthy & Joskowicz, 2001.
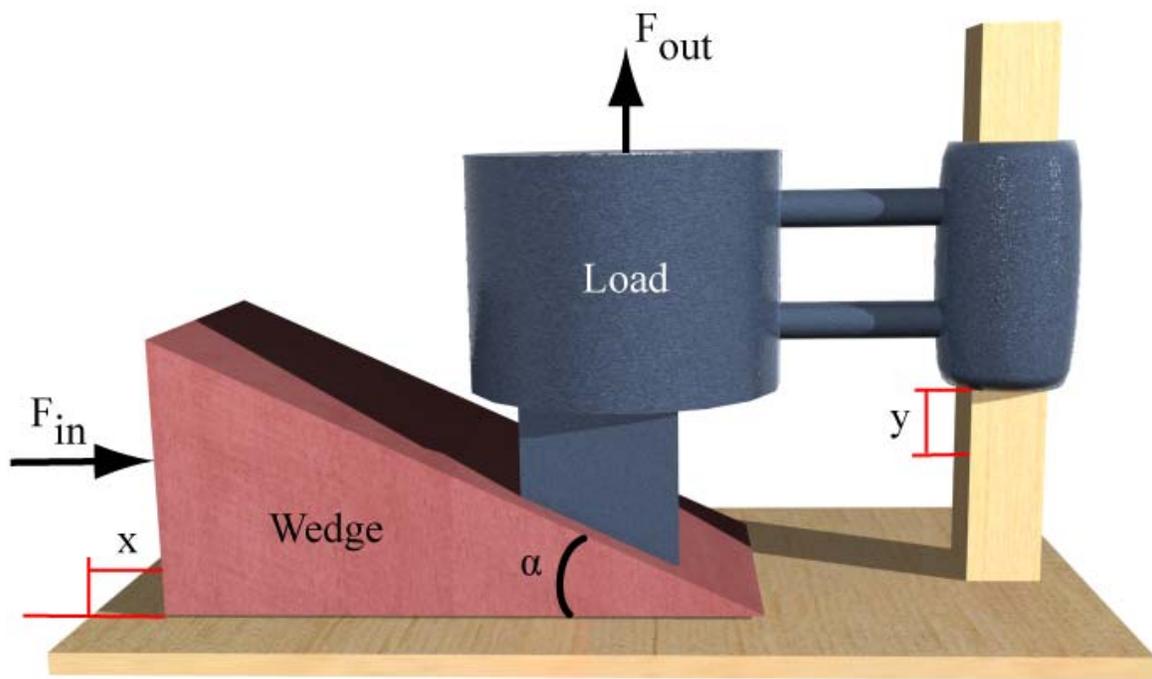
Figure 8. The wedge has a right triangle profile with an angle α. It is moved forward with force F_{in} and a horizontal displacement x. This results in the vertical displacement y of the load with a force F_{out}. Modified from McCarthy & Joskowicz, 2001.

As the triangle has an angle of α at its apex, as it is sliding, it pushes the load up in the direction of the output force. This vertically sliding load represents the second prismatic joint (Eq. 4).

$$[D]=[G_2][Z(0,y)][H_2] \qquad \qquad \text{Eq. 4}$$

$[G_1]$ and $[H_1]$ represent the moving frames for the two joints. McCarthy and Joskowicz (2001) suggested that, in this case, geometry represents a simpler method of analysis. The x and y displacements are related by the changing slope of y and x. The equation of a slope

$$m = (y-b)/x \qquad \qquad \text{Eq.5}$$

where y and x are the vertical and horizontal displacements, m is the slope, calculated by tan α, and b is a constant. The velocity ratio (vertical velocity divided by horizontal velocity) equals the slope in the above equation or tan α. Assuming no power dissipation (zero friction), the mechanical advantage is the inverse of tan α.

The kinematic equations describing the lever and wedge represent complete analyses of these simple devices. Such analyses should be sought by functional biologists; however they can be difficult for complex biological mechanisms with components of unknown material properties or in which *in vivo* length changes are difficult or impossible to measure. As they are typically less interested in the analysis of mechanisms than in their design, engineers use these kinematic equations, but in a process known as inverse kinematics (McCarthy & Joskowicz, 2001). Here, the characteristics of movement are decided upon and

then the possible links positions are expressed in the form of the kinematic equation. Next, joints are selected for their ability to reduce friction, their ease of control, and their ability to safely limit range of motion and fatigue resistant links of correct dimensions are manufactured from materials with appropriate properties.

Common joint characteristics

While the above examples of engineered and animal joints are not muscle articulations, they share some general characteristics. As these features are common to all joints, they may useful in better understanding muscle articulation characteristics.

- As exemplified by derived vertebrate craniomandibular joints, a joint need not bear loads if reaction forces created during biting are balanced by forces generated by the adductor muscles. However, regardless of whether it is provided by a muscle or by the contact of articulating surfaces, there must be a mechanism present to transfer compressive reaction forces between the links.

- While the derived vertebrate craniomandibular joints no longer sustain large bite reaction forces, they are still required to safely limit range of motion. Engineers also consider the safe limitation of undesirable movements when choosing an appropriate joint type to implement and a material from which to build it.

- As muscles, including those that move links, can only actively shorten, they require antagonistic muscles to re-lengthen. Joints provide the structure between two links to support these antagonistic muscle sets.

- The type of joint selected for use in a mechanism is important because it dictates the range of motion and number of degrees of freedom of a link relative to the one to which it is connected.

A missing category of joint: the muscle articulation

The muscle articulation is a previously undescribed animal joint with a number of key characteristics that distinguish them as a unique category within the flexible joints. These traits are summarized below to guide the identification of possible animal examples of the muscle articulation type joint.

- If the soft tissue that connects the rigid links in a muscle articulation is flexible, this flexibility may allow a greater diversity and complexity of motions. The axes of rotation in these joints need not be fixed, or even equal on either side, and thus they relocate to provide the appropriate mechanical advantage to suit the task being performed. Therefore, muscle articulations might take the form of jaws or graspers that may be required to manipulate objects with maneuverability and dexterity.

- While there are limits to the deformations of the soft tissues placed in tension, compression, and torsion, they may not be analogous to the articulation surface features that limit range of motion in many sliding joints. Because these limits might therefore be actively established by muscle articulations, the potential tradeoff for such flexibility could be an increase in the complexity of neuromuscular control.

- The soft muscle and connective tissues that connect the links must serve three distinct roles. First, they must provide function analogous to that of articular surfaces of sliding joints by bearing the forces that are transmitted between the links. Second, they must generate the force that moves the links. Third, the soft tissue must provide skeletal support for antagonistic muscles.

- As the soft tissues between the rigid links of muscle articulations perform the force transmission tasks of an articulation, there may be no contact of the links within the joint.

Examples of potential muscle articulations

With initial descriptions of muscle articulation characteristics resulting from the analyses above, further studies require analyses of actual animal examples. Thus, I describe below the characteristics of four candidate animal joints that suggest they are muscle articulations. As a complete characterization of a muscle articulation includes both a detailed morphological description as well as experimental tests confirming the roles of the soft tissues, only one of these examples, the inarticulate brachiopod, has been fully described. The muscle articulations of the beaks of the octopus, the jaws of errant polychaete annelids, and the eversible hooks of the predatory turbellarian flatworm proboscis have received less attention and are the subjects of my studies described in the following chapters.

Inarticulate brachiopod valves

Superficially resembling molluscan bivalves, inarticulate brachiopods (Fig. 9A) are marine invertebrates that dig burrows using valves that might be connected by a muscle articulation. Since the Ordovician Period, inarticulate brachiopods, such as species of the genera *Lingula* and *Glottidia*, have been ecologically important members of the fauna living in the substrates of shallow seas (Rudwick, 1970). These animals dig U-shaped burrows (Fig. 9B) to orient themselves for the filtration of particulate matter from the surrounding water (Levin, 1999). They dig into the substrate valves first because unlike bivalve molluscs, inarticulate brachiopods do not use a hydraulic foot to pull their valves into the substrate. The fleshy stalk-like pedicle (Fig. 9A) that resembles a bivalve foot is an extension of the

A

Outline of
Valve

Lophophore

1cm

Muscles that
generate valve
movement

Wall of
coelom

Pedicle

Hydrostatic cavity
of pedicle

Burrowing
(Valves moving with
scissor-like motion)

B

1

Feeding Position

2

Valve

Coelom

Pedicle

Sea Floor
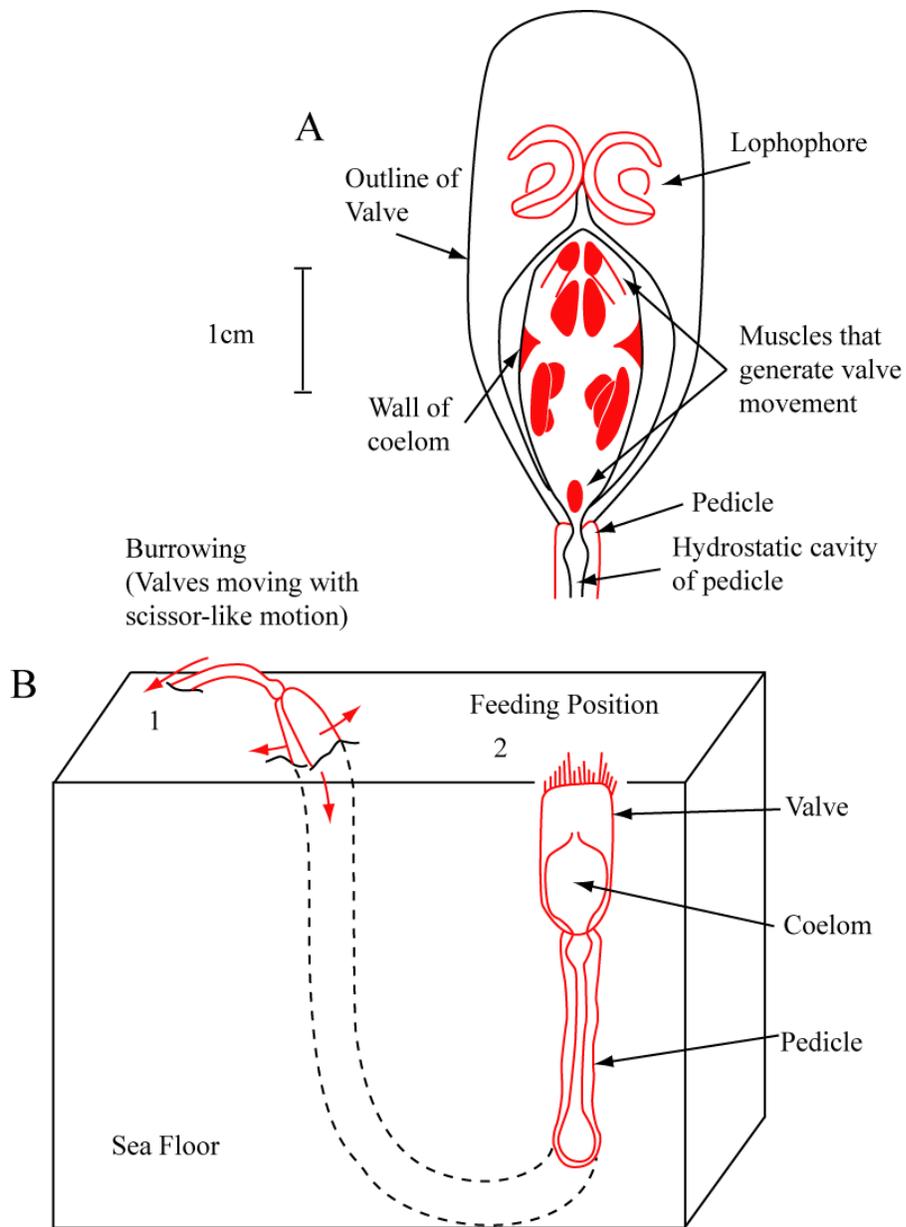
Figure 9. A) a dorsal view of the complex musculature that generates a wide range of complicated valve movements in the brachiopod *Lingula.* B) The burrowing lingulid brachiopod using the pedicle and complex movements of the valves to burrow (1) and attain its feeding position (2). The coelom of the body and pedicle represents a hyrostatically active fluid-filled space. Modified from Trueman and Wong, 1987.

coelomic cavity and is not capable of digging movements. It is instead used to press the valves to the substrate during initial burrowing stages and to hold the animals in its burrow (Fig 9B). Trueman and Wong (1987) described the surprisingly complex digging movements of the valves. Here, inarticulate brachiopods not only have the capacity to open and close the valves in a bivalve-like fashion, but other motions employed, such as side-to-side scissor-like motions and translations of the valves away from each other, represent movements with all six degrees of freedom.

Morphological descriptions (such as Hyman, 1959) show that the valves are connected together by a complex arrangement of muscle and connective tissue (Fig. 9A). The valves are connected, and moved relative to each other, by a complex series of muscle orientations that lie within the coelomic cavity. This cavity that extends into the pedicle, can be pressurized by a second set of muscles that surround the exterior of the coelom wall.

Experimental confirmation of form and function makes the inarticulate brachiopod study unique. Trueman and Wong (1987) hypothesized that since muscles that could pressurize the coelom were present, the cavity might act as a classical hydrostat by becoming turgid and providing compression resistant support for the valves and the muscles that move them. As forces being transferred through the joint were thought to be at their highest when valves were in the adduction phase of their digging movements, the experimental correlation of these adduction movements with increases in coelomic pressure supports this hypothesis.

The joint that allows movement between the valves of inarticulate brachiopods can be considered a muscle articulation. The valves represent rigid links that are connected together and held apart by soft tissue at their posterior ends. These links are capable of a diverse and complex range of digging motions, including movements with all six degrees of freedom.

27

The soft tissue has multiple functions: the complex internal coelomic musculature possess orientations suitable for generating diverse valve movements and the muscle and connective tissues that form the coelom allow pressurization that supports these muscles and bears the compressive reaction forces generated by the digging movements.

While recording electrical activation signals of individual muscles that move the valves during digging would experimentally test their hypothesized functions, our basic understanding of this mechanism as a muscular hydrostat is relatively complete. Other putative muscle articulations are not as well understood as they lack detailed morphological descriptions, testable functional hypotheses, or experiments that explore joint function. Below are introductions to three putative muscle articulations that are not fully characterized. The analyses of the beaks of octopuses, the jaws of nereid polychaetes, and the grasping hooks kalyptorhynch flatworms represent the subject of the remaining chapters.

Cephalopod beaks

The second potential muscle articulation is the joint that connects the two chitinous beaks of extant cephalopod molluscs, such as the nautilus, squid, octopus, and cuttlefish (Nixon and Young, 2003) (Fig. 10). The beaks are capable of complex motions in which the upper beak rotates and translates with six degrees of freedom relative to the lower beak (Boyle et al., 1979a). They are used in crucial cephalopod feeding behaviors that can range from delicate manipulations required to hold food items, to forceful piercing bites that break crustacean armor, and shearing of flesh to sizes appropriate for ingestion (Nigmatullin and Ostapenko, 1976; Nixon, 1987; Kear, 1994). Such diversity of complex motion is possible because the beaks do not directly contact one another within the joint and are instead
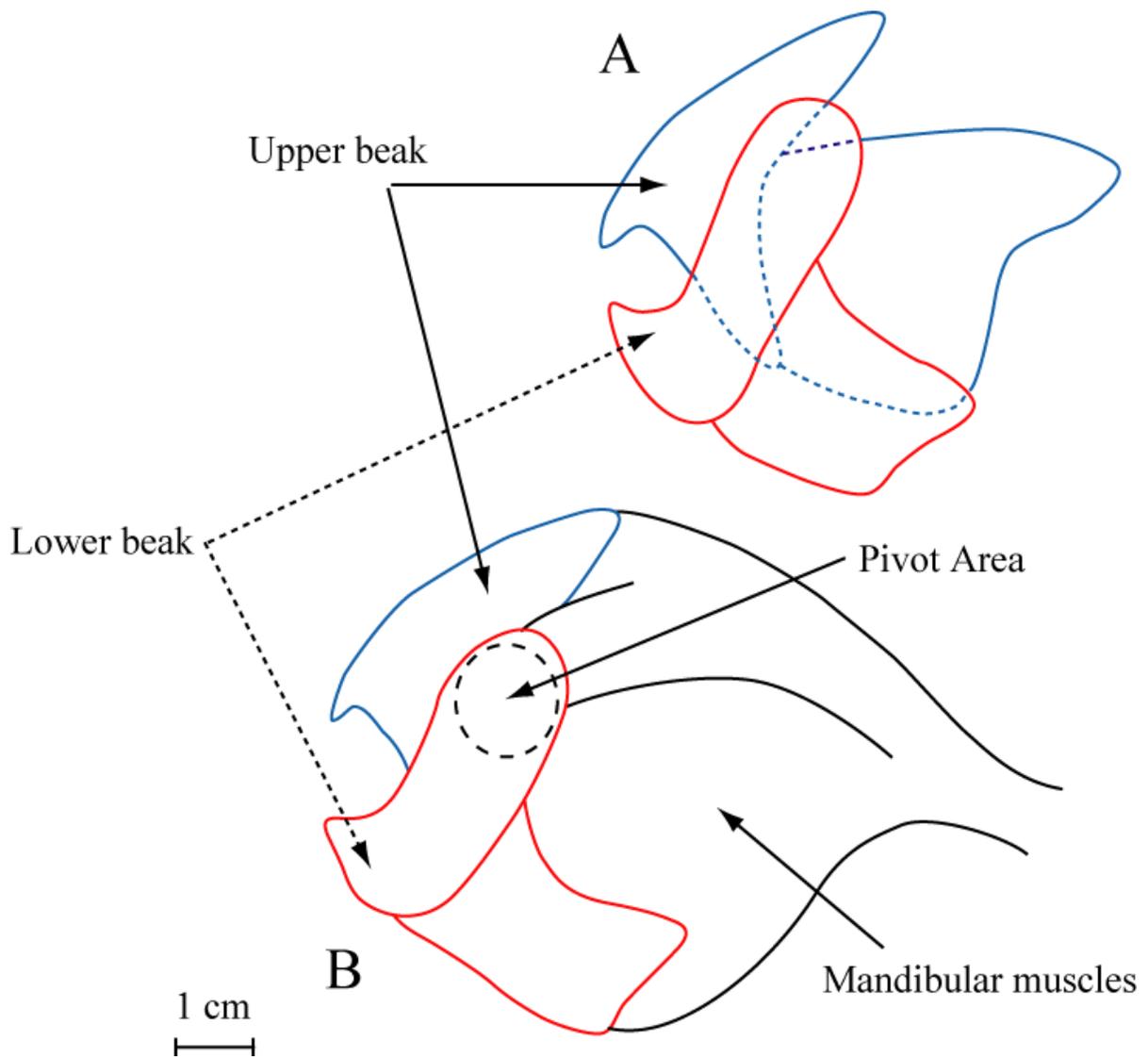
Figure 10. A) The upper and lower beaks of a large octopus. The beaks do not come into contact anywhere other than the biting surfaces. B) The beaks embedded within the mandibular muscles. During biting, the pivot axis of the upper beak relative to the lower one is not fixed and may move within pivot area. Modified from Kear, 1994 and Boyle et al. 1979a.

embedded in a roughly spherical capsule of mandibular muscles known as a buccal mass (Boyle et al., 1979a).

The cephalopod buccal mass (Fig. 10) represents the best opportunity to study muscle articulations in detail; the structure is fairly large and contains a central pattern generator that allows the beak to bite cyclically even when removed from the body (Boyle et al., 1979a, b; Kear, 1994). Previous studies analyzed the morphology and composition of the beaks (Clarke, 1962, 1986; Hunt and Nixon, 1981), the mandibular muscles (Boyle et al, 1979a; Kear, 1994; Tanabe and Fukuda, 1999), the nervous system (Young, 1965, 1971) and experimental tests of muscle function have also been performed (Boyle et al, 1979a,b; Kear, 1994). While the system has received a considerable amount of attention, a number of questions remain. How do the mandibular muscles generate force for opening and closing the beaks, generate skeletal support for muscular antagonism, and transmit forces from one beak to the other? To answer these questions, I first performed a detailed analysis of the morphology of the beaks and soft tissues. This analysis is described in chapter two and includes predictions of muscle function derived from a biomechanical analysis of the structure. I tested these predictions with *in vitro* experiments that are described in the third chapter.

Polychaete jaws

As the functionality of jaw structures benefit significantly from diverse and complex motions, the pharyngeal bulbs of errant polychaetes were considered as possible muscle articulations. Annelids of the class Polychaeta have evolved a wide range of feeding modes; substrate feeders, filterers of particulate matter, parasites, ambush and active predators, and more (Dales, 1962). Of these, errant predators of the sister orders Phyllodocidae and

Nereididae have evolved eversible muscular pharynges (Fig. 10) that are armed with an arrangement of sharp jaws to capture and process prey (Rouse and Pleijel, 2001; Saulnier-Michel, 1992).

While all the armed muscular axial pharynges of both sister orders may be examples of muscle articulations, the common genus *Glycera* (Fig. 11, often sold to ocean pier fishermen as "bloodworms") is described here as an introductory example. These phyllodocid worms possess four stout scleroproteinous jaws that are embedded in the muscle of the pharynx and arranged in a cross pattern. The jaws are hardened by quinine tanning and by the incorporation of iron and copper and are capable of injecting poison produced by an associated gland near the base (Saulnier-Michel, 1992). Observations of the biting behavior of glycerid worms indicate that the jaws are capable of a wide range of motion. Initially, the jaws open as the pharyngeal mass is everted using hydrostatic pressure generated in the body (Saulnier-Michel, 1992). After full eversion, the jaws are then capable of an outward rotation such that the tips of the curved jaws are adducted to a position where they pointing forward or even laterally. Then, upon retraction of the proboscis, the jaws rotate in closing so that the tips touch and even cross in the center.

In chapter four I describe the movements and the morphology of the jaws of the ragworm, *Nereis virens*. This nereidid polychaete offers a number of practical characteristics that lend themselves to a simpler analysis; larger size, commercial availability, a simpler pharyngeal bulb featuring only two jaws, the existence of detailed morphological studies (Pilato, 1968a,b), and a number of descriptions of pharyngeal bulb and jaw function. (Turnbull, 1876; Dorgan et al., 2005).
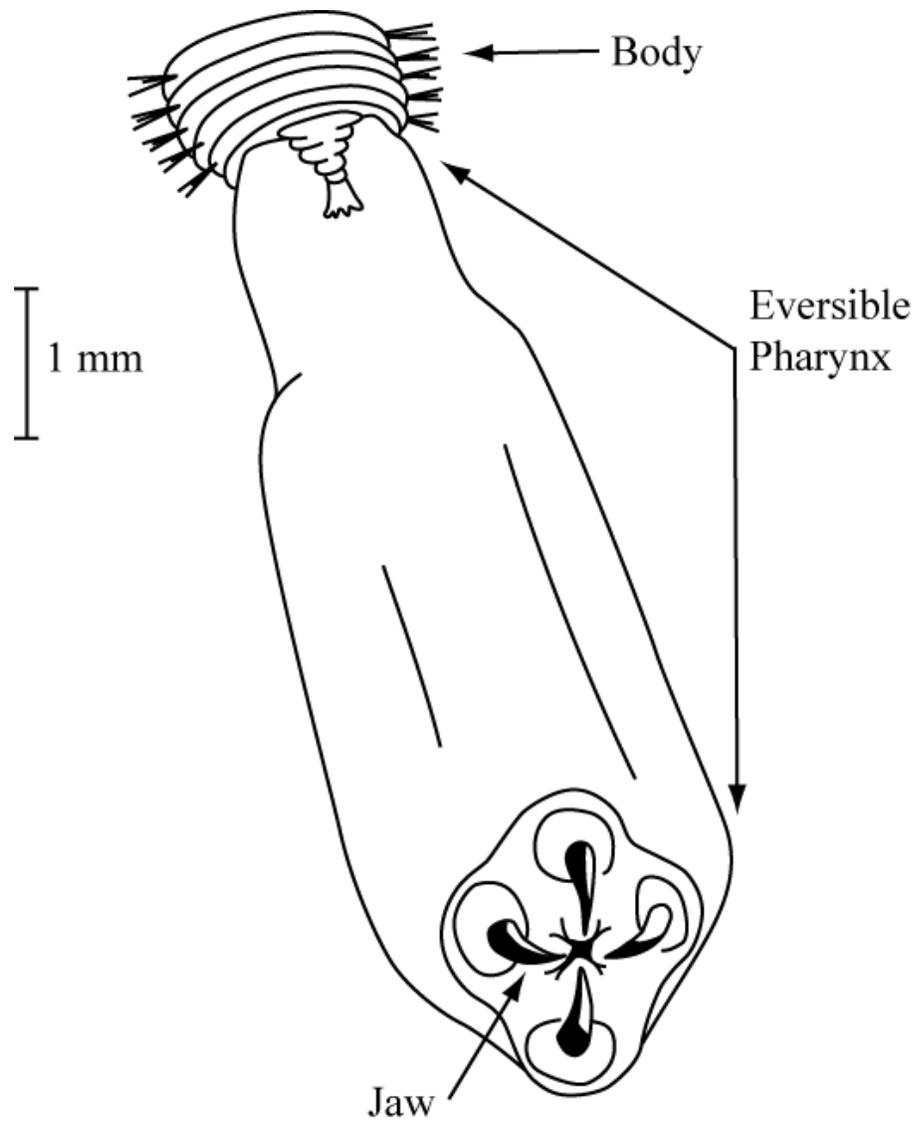
Figure 11. The anterior end of a glycerid polychaete annelid with the large proboscis fully everted and showing the four jaws in a cruciform arrangement.

Kalyptorhynch flatworm hooks

The final potential muscle articulation is the joint that connects the hooks of a prey grasping organ used by turbellarian flatworms (phylum Platyhelminthes) of the order Kalyptorhynchia (Fig. 12). These microscopic organisms are found in the sediment of marine beaches where they live in the aquatic spaces between the grains of sand (Doe, 1976). Kalyptorhynchs are common predators of the meiofauna and catch prey using eversible proboscides that are, in many species, armed with two small hooks to assist in grasping (Karling, 1961). This eversible proboscis is located at the anterior end of the organism and interestingly, is not associated with the ventrally located bulbous stomodeal pharynx (Fig. 11) (Kozloff, 1990).

There are a number of morphological descriptions of the eversible kalyptorhynch proboscides in which the hooks are embedded. At the anterior end are two glandulomuscular hook supports upon each of which are mounted an incurved hook of about 13-16 μm in length (Rieger and Doe, 1975; Doe, 1976). Karling (1961) describes the simple muscular construction of the hook supports as consisting of only two muscle fiber orientations that are thought to be sufficient to open and close the hooks with a wide range of motion after the proboscis is extended from the body.

The proboscis of the kalyptorhynch flatworm represents a unique muscle articulation for analysis because of their microscopic size and apparent simplicity of construction. The details of how the proboscis hooks function are not well understood as the soft tissue components may require a more detailed morphological description. Thus, in chapter five I describe, in detail, the morphology of the glandulomuscular hook supports and propose hypotheses of function of the muscle and connective tissues.
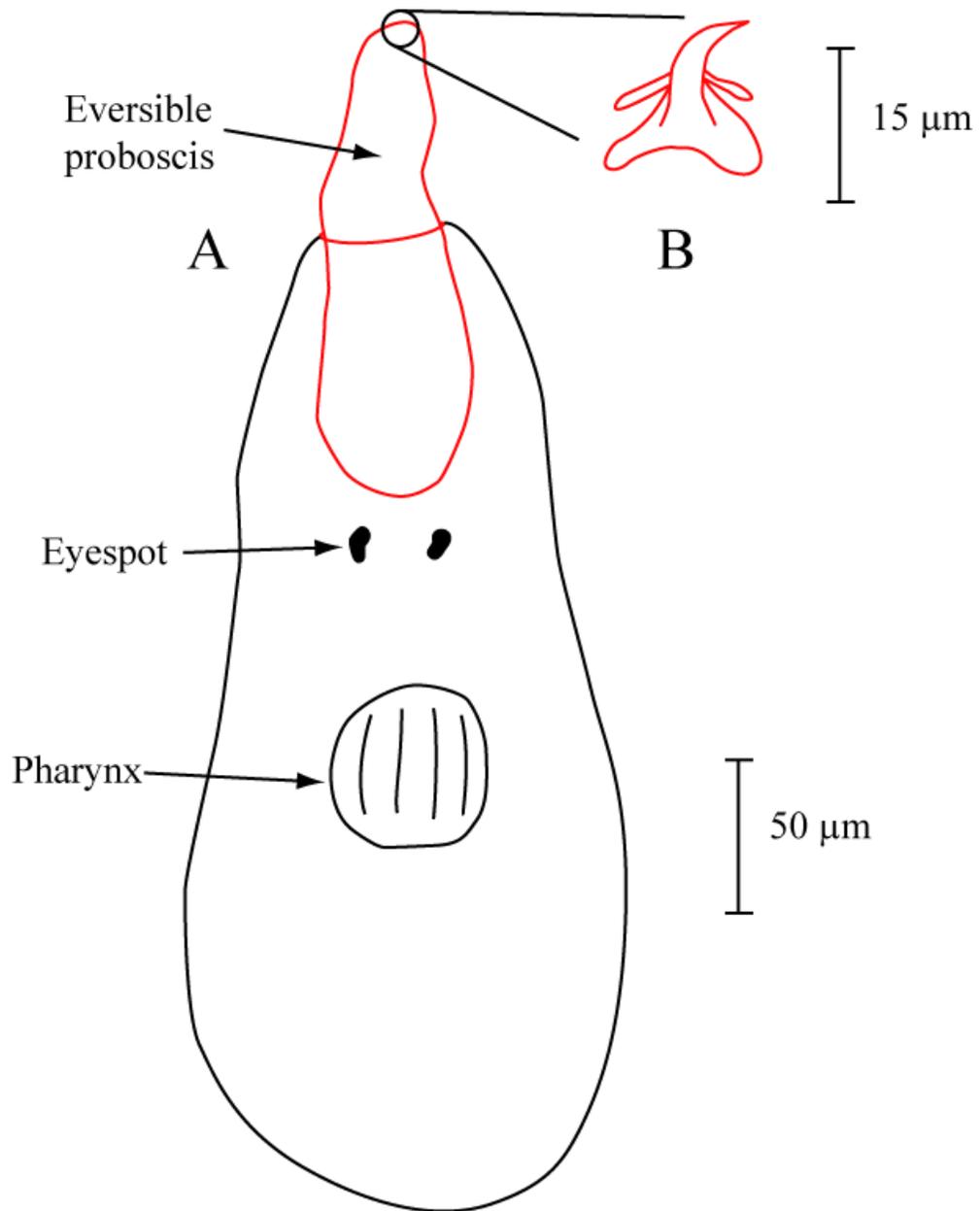
Figure 12. A) Kalyptorhynch (schizorhynch) turbellarian with a partially everted proboscis. Modified from Kozloff, 1990. B) One of two cuticular, inwardly curved hooks located at the tip of the proboscis of a *Gnathorhynchus* kalyptorhynch. Modified from Doe, 1976.

Conclusion

Muscle articulations may be functionally important joints in animals from diverse phyla. This seems especially true in soft-bodied invertebrates that make frequent use of classical or muscular hydrostats, as muscle articulations may often employ these hydrostatic support mechanisms to bear compressive reaction forces. While these hydrostats must be supportive enough to transmit forces from link to link and to support antagonistic muscles that generate motive forces, the flexibility of the muscle and connective tissues may allow both complex and diverse link movements.

The muscle articulation has not been previously recognized as a class of flexible joint, in part because of the difficulty in performing experimental analyses on these structures; long-lived preparations and protocols that allow the recordings of natural movements are rare. In addition, mechanical analyses of hydrostats are difficult. Muscular and classical hydrostats function by changing the relative dimensions, though not volume, of their soft tissue structures. The flexibility of this tissue complicates these analyses because force is generated and transmitted omni-directionally and it is therefore difficult to quantify energy losses and evaluate how friction, fatigue, and viscosity affect function. The predominant use of muscle articulations by soft-bodied invertebrates might have also hindered the detection of the joint. In comparison with vertebrate organisms, only a relatively small subset of charismatic or economically important invertebrates has received much popular attention or academic study.

In the following chapters, I document the diversity of muscle articulation construction and begin to describe common principles of their function. In doing so I hope to establish the basis for a number of future studies: the characterization of the ecological role of muscle

articulations in organismal interactions with the environment; the assessment of the evolution

of muscle articulations in monophyletic groups; the design of potentially practical physical

models to test principles of function; and, as neural input may limit the possible movements

in muscle articulations, the neurobiological characterization of this new type of joint.

CHAPTER 2
THE MORPHOLOGY OF THE CEPHALOPOD BUCCAL MASS

Introduction

In the first chapter, I defined the muscle articulation as a type of flexible joint in

which the rigid links are connected, as well as held apart, by an arrangement of soft muscle

and connective tissue. These tissues may provide hydrostatic support that resist forces that

are transmitted from link to link through the joint, create antagonistic support for muscles

that move the rigid elements relative to each other, and may even form repositionable pivots

and fulcra. The muscle articulation is a type of flexible joint that has not been described

previously. This chapter describes the morphology of one example, the joint between the two

beaks used in feeding by cephalopod molluscs such as the octopus, squid, cuttlefish, and

nautilus.

A detailed description of the form and function of the cephalopod buccal mass is

lacking, in part due to the complex three-dimensional organization of its muscle fibers.

Previous morphological studies (Boyle et al., 1979a, b; Kear, 1994) viewed muscle fiber

bundles individually and thus did not recognize the synergistic role of other muscle fiber

bundles.

An analysis of the cephalopod buccal mass that includes both form and function is

crucial. Not only is a complete biomechanical analysis required to characterize the basic

principles of the muscle articulation joint, but it is of use in understanding cephalopod

biology as well. As a critical feeding structure, buccal mass functional characteristics may be

crucial in understanding cephalopod ecology and evolution. To provide background for this study, I begin by surveying previous studies that describe the anatomy and the ecological function of the buccal mass. As the beaks serve as the links in this putative muscle articulation, I then review their morphology and evolution. This is followed by a review of previous studies that investigate the functional morphology of the mandibular muscles that form the muscle articulation joint. In these reviews, I identify areas where more morphological details are required. I then provide a detailed morphological description of the buccal mass and propose hypotheses of function.

The function of the cephalopod buccal mass

Extant cephalopods include the members of two subclasses: the Nautiloidea (*Nautilus*) and the Coleoidea. Within the coleoids, there are currently six subclasses; the Octopoda (octopuses), Teuthida (squids), Sepiida (cuttlefish), Sepiolida (Bobtail squids), and the rare Spirulida (the Ramshorn squid) and Vampyromorphida (the Vampire squid) (Voss, 1977, Bonnaud et al., 1997; ITIS, 2007). These cephalopods are almost exclusively predators that have adapted to most marine habitats (Nixon & Young, 2003), including deep trenches and seamounts (Nesis, 1993) and even hydrothermal vents (Tunnicliffe et al., 1998). Their success may be due, in part, to their ability to feed on a wide range of prey, including crustaceans, fishes, gastropods, bivalves, cephalopods, polychaetes, ophiuroids, and foraminiferans (Nigmatullin & Ostapenko, 1976; Wells, 1978; Nixon & Budelmann, 1984; Nixon, 1987; Hanlon & Messenger, 1996; Nixon & Young, 2003). Consuming this wide range of prey depends in part on the use of a pair of mobile beaks (or jaws, or mandibles) that are embedded within a muscular buccal mass.

Perhaps the best-studied coleoids belong to the family Octopodidae as a number of extensive behavioral (Hanlon & Messenger, 1996), neuroanatomical (Young, 1971), physiological (Wells, 1978), and life history (Nixon & Mangold, 1996) studies have focused on the ubiquitous and speciose genus *Octopus*. Feeding by octopodids involves manipulation of the food by the suckers and web of the eight arms (Steer & Semmens, 2003) while the various structures that form the buccal mass are used in further processing. The buccal mass is used in boring or crushing of shells (Arnold & Arnold, 1969; Nixon, 1969, 1979a,b, 1980; Nixon et al., 1980; Nixon & Maconnachie, 1988; Cortez et al., 1998; Voight, 2000), the piercing of hard external skeletons, followed by the injection of immobilizing saliva (Ghiretti, 1959, 1960; Cariello & Zanetti, 1977), and the mastication of tissue (Altman & Nixon, 1970; Kear 1994). This reduction of food items is crucial for cephalopods as they maintain the ancestral molluscan characteristic in which the esophagus passes through the brain (Messenger & Young, 1999)

Anatomy of the buccal mass

The buccal mass is a roughly spherical structure that lies in front of the brain, within a sinus formed by the base of the arms. (Boyle et al., 1979a; Kear, 1994; Nixon & Young, 2003) (Fig. 13). It is loosely attached within the sinus by the esophagus and the enclosing buccal membrane, a pigmented web of folded skin that is attached to the arms. The buccal membrane surrounding the beaks is folded into inner and outer lips (Nixon & Young, 2003). The exposed muscles of the buccal mass into which the beaks are embedded are covered by the buccal mass sheath, a thin tough membrane of connective tissue and epithelium (Tanabe & Fukuda, 1999).
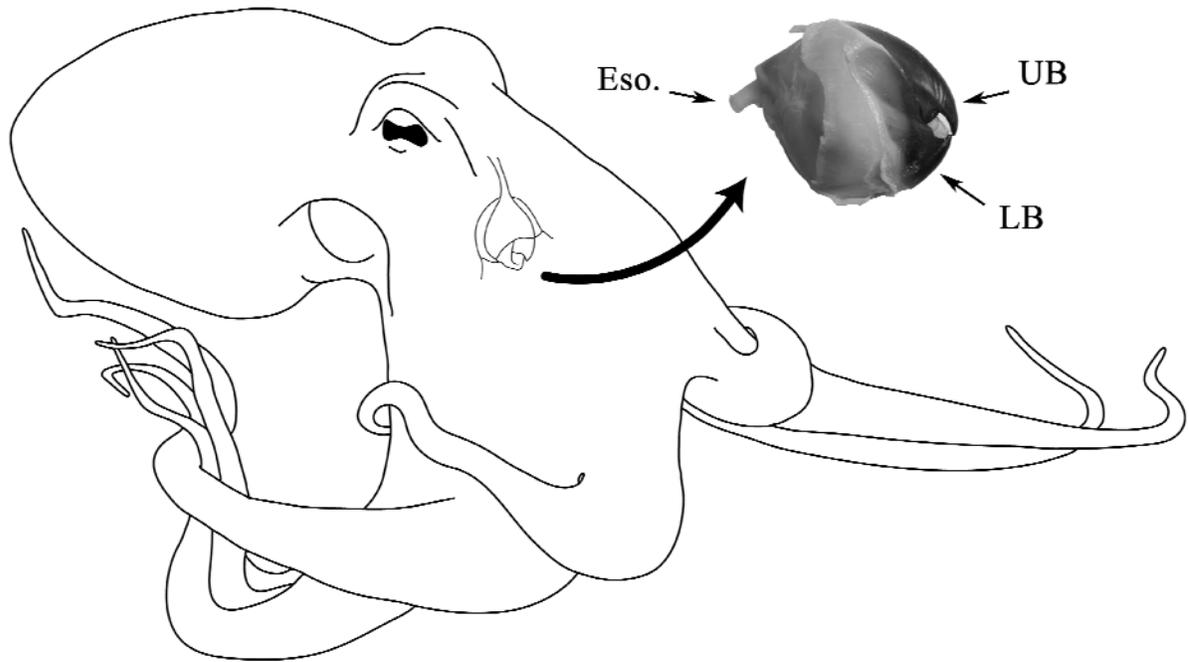
Figure 13. A drawing of the position of the buccal mass within *Octopus bimaculoides*. The inset photo shows the left side of the buccal mass and the orientation of the buccal mass in the descriptions that follow: the dorsal surface is up, the ventral surface is down, the chitinous beaks (UB, upper beak; LB, lower beak) mark the anterior end of the buccal mass and the esophagus (Eso.) is posterior. Note that the beaks are depicted here in an opened position. (Modified from Uyeno & Kier, 2005)

The orientation of the buccal mass varies in cephalopods of different body morphologies (Boyle et al., 1979a, b; Kear, 1994). Although the long axis of the esophagus of benthic octopods is normally vertical, the isolated buccal mass will be described here with the long axis of the esophagus horizontal. This makes the orientation of the buccal mass identical to that of pelagic cephalopods, such as most cuttlefish and squids. The tips of the beaks will be described as anterior, the esophagus as posterior, the upper beak as dorsal, and the lower beak as ventral. The buccal mass is bilaterally symmetrical about the sagittal plane.

The buccal mass is composed of several structures. The chitinous upper and lower beaks are attached to each other by the mandibular muscles (Young, 1965; Boyle et al, 1979a, b; Kear, 1994). These superficial muscles are responsible for generating the force that moves the beaks. The upper beak partially fits within the lower beak, forming an internal buccal cavity. Within this cavity are found a number of other structures associated with feeding: the lateral buccal palps, salivary papilla, salivary glands, radula and radular support apparatus, and the pharyngeal opening to the esophagus (Nixon & Young, 2003). During the biting movement, the more mobile upper beak moves relative to the lower beak. This is because the radular apparatus includes two cylindrical muscular hydrostatic supports (or bolsters) that serve as anchors to which the lower beak is firmly attached (Young, 1991; Messenger & Young, 1999). The radular apparatus itself is a mobile tongue-like structure that bears the radula, a toothed ribbon that used as a rasp to reduce the size of food items (Altman & Nixon, 1970; Messenger & Young, 1999). The palps, papilla, and glands are used to bore through shells (Nixon, 1979a, b, 1980; Nixon et al, 1980; Nixon & Boyle, 1982; Nixon & Maconnachie, 1988), direct food to the pharynx (Guerra et al. 1988), and secrete digestive enzymes (Nixon, 1984) and neurotoxins (Gage et al, 1976; Hwang et al. 1989).

The morphology and evolution of the beaks

Although beak shapes are roughly similar among extant cephalopods (Kear, 1994), there are small differences in beak morphology between cephalopod orders. Clarke (1986) defined the terminology used in identifying and cataloging the beaks, which are found as undigested gut contents in cetaceans (Clarke, 1962), pinnipeds (Mori et al, 2001), fish (Lu & Ickeringill, 2002), and birds (Santos et al., 2001). Both upper and lower beaks resemble U-shaped troughs in which the anterior portions are folded back upon themselves to create a biting surface and a hood (Fig. 14). The upper beak differs from the lower beak in possessing a pronounced hood, a sharp rostrum and lateral walls of large surface area, whereas the lower beak is characterized by exaggerated wings and a round anvil-like rostrum and jaw angle. Although this general form is similar among extant octopods, sepioids, and teuthoids, there are some consistent differences. Decapod (sepioid and teuthoid) upper beaks have relatively longer hoods and a larger space behind the hood but a smaller lateral wall area. Decapod lower beaks have more pointed rostra and shorter (the distance between the jaw angle to the posterior end of the crest) but deeper (the dorsoventral width) lateral walls (Kear, 1994).

Boletzky (2007) reviewed the evolution of the upper and lower beaks. The cephalopod upper beak is thought to be homologous with the jaw of scaphopods (Shimek & Steiner, 1997), and those present in monoplacophorans (Haszprunar & Schaefer, 1997), and gastropods (Luchtel et al. 1997; Voltzow, 1994; Gosliner, 1994). The origin of the lower beak is unclear. Based on histological sections of developing embryos, Boletzky (1999, 2007) suggested that the lower beak might arise from the same anlage that gives rise to the upper. In particular, the derivatives of the lateral parts of the primordium unite ventrally in the sagittal plane of the buccal mass to form the lower beak.

Figure 14. Diagram of the upper (blue) and lower (red) beaks of *O. bimaculoides*. Both beaks are U-shaped in cross section and the anterior end is folded over itself to form the biting surfaces (i.e. the rostrum and the jaw angles). The upper beak has enlarged lateral walls that fit within, but do not contact the lower beak. The lower beak has enlarged wings and a reduced hood relative to the upper beak. (Modified from Uyeno & Kier, 2007.)
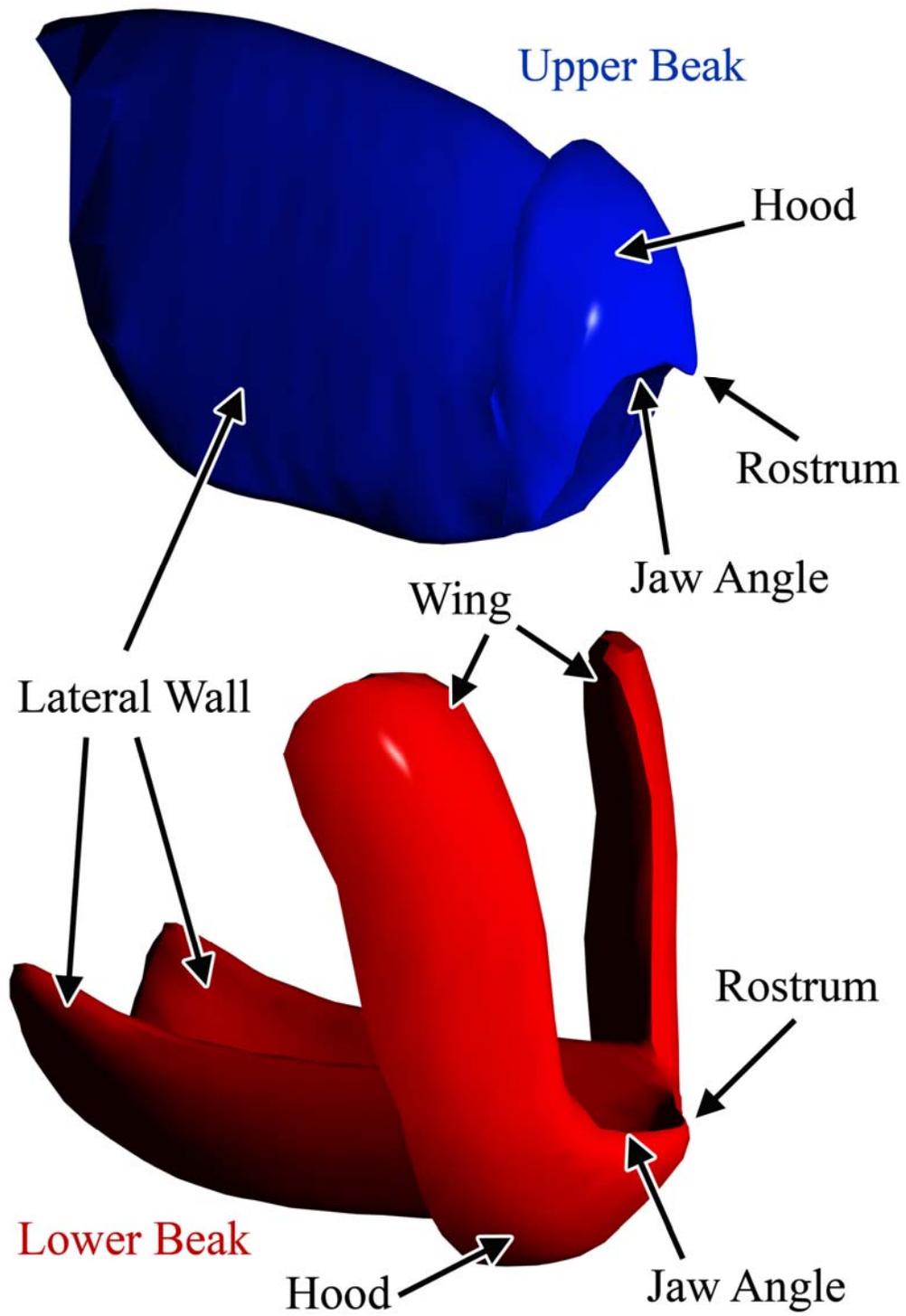
Figure 14

The general trough shape of the upper and lower beaks are seen in fossilized beaks from Carboniferous coleoids (Tanabe & Fukuda, 1999), but a different shape is found in the Ammonoidea (Late Silurian to the end of the Cretaceous), an extinct subclass that evolved from the bactritoid nautiloids (Lehmann, 1981) yet are thought to be more closely allied with coleoids than with modern *Nautilus* (Monks & Palmer, 2002). The upper beaks of ammonoids were similar in shape to those of other cephalopods, but the morphology of the lower beak, called an aptychus, is different. First described by Giebel (1849), aptychi were often misidentified as brachiopods or crustaceans until they were found in association with the upper beaks and shells of ammonoids (Frye & Feldmann, 1991). Complete assemblages are rare, probably because the aptychi often separated from the buoyant shells during decomposition. A further complication is that the term aptychus refers to two different structures. A diaptychus (=aptychus *sensu stricto*) is now thought to be a nautiloid operculum (Fig. 15A) (Holland, et al., 1978, Turek, 1978). The other structure, the anaptychus (Fig. 15B) probably served as an ammonoid lower beak (Moore & Sylvester-Bradley, 1957; Lehmann, 1970).

The anaptychus is large relative to the upper beak and lacks a calcified rostrum. Early speculation was that it functioned by partially occluding the shell aperture. However, most now agree that its main use was probably as a lower jaw; either as a scoop or shovel (Lehmann, 1972) or a true biting jaw (Tanabe et al., 1980). If the anaptychus and the ancestral nautiloid lower jaw are homologous, the biomechanical analysis of this variation in shape might provide novel functional information. Such comparisons, however, might not be feasible as most anaptychi are preserved as flat carbonaceous smears in shale and have lost their three-dimensional and soft tissue characteristics (Frye & Feldmann, 1991).
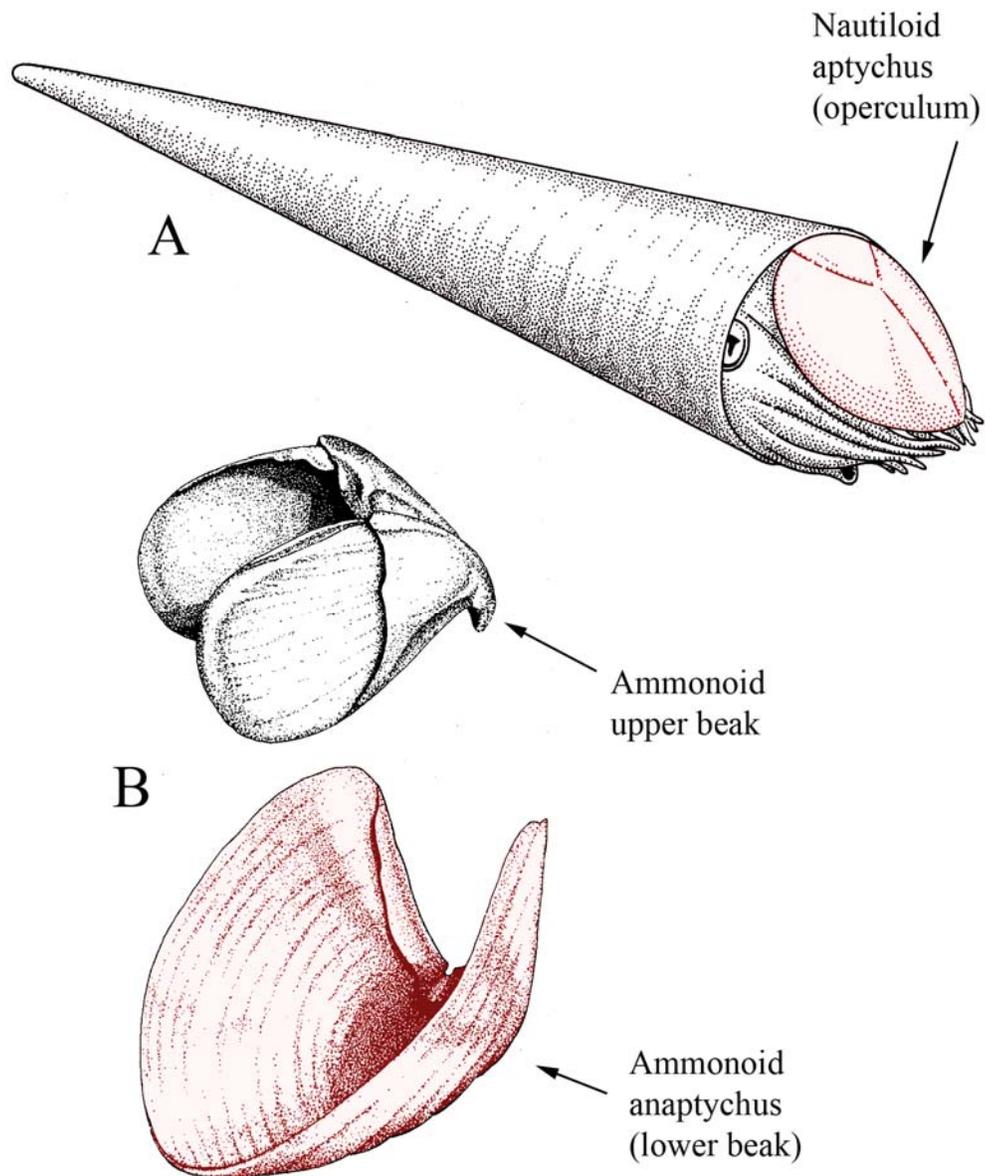
Figure 15. Cephalopod aptychi (structures highlighted in red) A. The nautiloid diaptychus (or aptychus, *sensu stricto*) reconstructed from fossilized orthoconic nautiloids in which the aptychopsid plates were found *in situ* (modified from Turek, 1978); B. The ammonoid anaptychus reconstruction illustrated here showing its *in vivo* relation to the upper beak, suggesting its probable function as a lower beak/operculum (modified from Lehmann, 1971).

The upper and lower beaks of extant coleoids are formed of a chitin-protein complex (Hunt & Nixon, 1981). The percentage of chitin versus protein varies between species and also depends on location in the beak. In *Octopus*, the rigid rostra and crests are 6.0-7.8% chitin and 92.2-94.0% protein while the more flexible lateral walls and wings contain 10.8-12.3% chitin and 87.7-89.2% protein. While modern coleoids do not calcify their surfaces (Tanabe et al, 1980), further analysis by Lowenstam et al. (1984) showed that *Nautilus* harden the chitin-protein complex of their beaks with five different minerals (calcite, aragonite, brushite, phosphatic material, and weddelite) depending on the flexibility or wear resistance characteristics needed. The beak material of all cephalopods is secreted by a single layer of tall columnar cells known as beccublasts, which also serve to attach the mandibular muscles to the beaks (Dilly & Nixon, 1976).

The buccal mass mandibular muscles

Cephalopod beaks are moved by the actions of the mandibular muscles, a term used by Young (1965) in his description of the buccal nervous system in *Octopus*. Since then, there have been two functional morphological descriptions of the buccal mass.

Boyle et al. (1979a) described three mandibular muscles in the buccal mass of *Octopus vulgaris*: the paired lateral mandibular muscles and the superior mandibular muscle. They recorded electromyograms from various locations in the muscles of isolated buccal masses and observed activity during closing, but were unable to find locations of muscle activity during beak opening movements.

In a later study that focused on 23 species of coleoid cephalopods, Kear (1994) described an additional inferior mandibular muscle originally identified by Altman (unpublished notes; see Kear, 1994). Kear (1994) also described the cyclical beak

47

movements of *Eledone cirrhosa, Sepia officinalis, Loligo forbesi,* and *Alloteuthis subulata.* Focusing on isolated buccal mass preparations of *S. officinalis* and *A. subulata* she described five discrete positions during a full bite cycle (Fig 16): 1) resting, 2) opening, 3) fully open, 4) closing, and 5) closed and retracted. During this cycle, she noted that the axis of rotation of the upper beak during biting movements varied and thus was not restricted to a single location. She stimulated various locations of the musculature electrically and observed that closing was elicited at most locations. Stimulation of the area near the inferior buccal ganglion elicited an entire bite cycle. Only simultaneous stimulation near the centers of the paired lateral mandibular muscles resulted in a strong opening movement. It is unclear, however, how these muscles open the beaks.

As details of beak operation are still obscure, the goal of this chapter is to describe the morphology of the muscles and connective tissues of the buccal masses of *Octopus bimaculoides, Sepia officinalis,* and *Lolliguncula brevis* in order to explore the roles of the various mandibular muscles in beak movements and muscle articulation function.

Materials and methods

Four adult specimens of *Octopus bimaculoides* (70–99 g wet weight) were obtained from the National Resource Center for Cephalopods (formerly of Galveston, TX). After a resting period of at least 2h, each octopus was quickly and lightly anaesthetized using 2.5% ethanol in seawater (O'Dor et al., 1990). When the specimens no longer showed ventilation or arm movement, the brains were bisected and the buccal masses were removed and placed in small glass bowls containing aerated seawater chilled to 17°C. Endogenous bite cycles performed by the excised buccal masses were observed prior to their immediate fixation for at least 48 h in buffered formalin in seawater (10% v/v; Kier, 1992). One specimen was

48
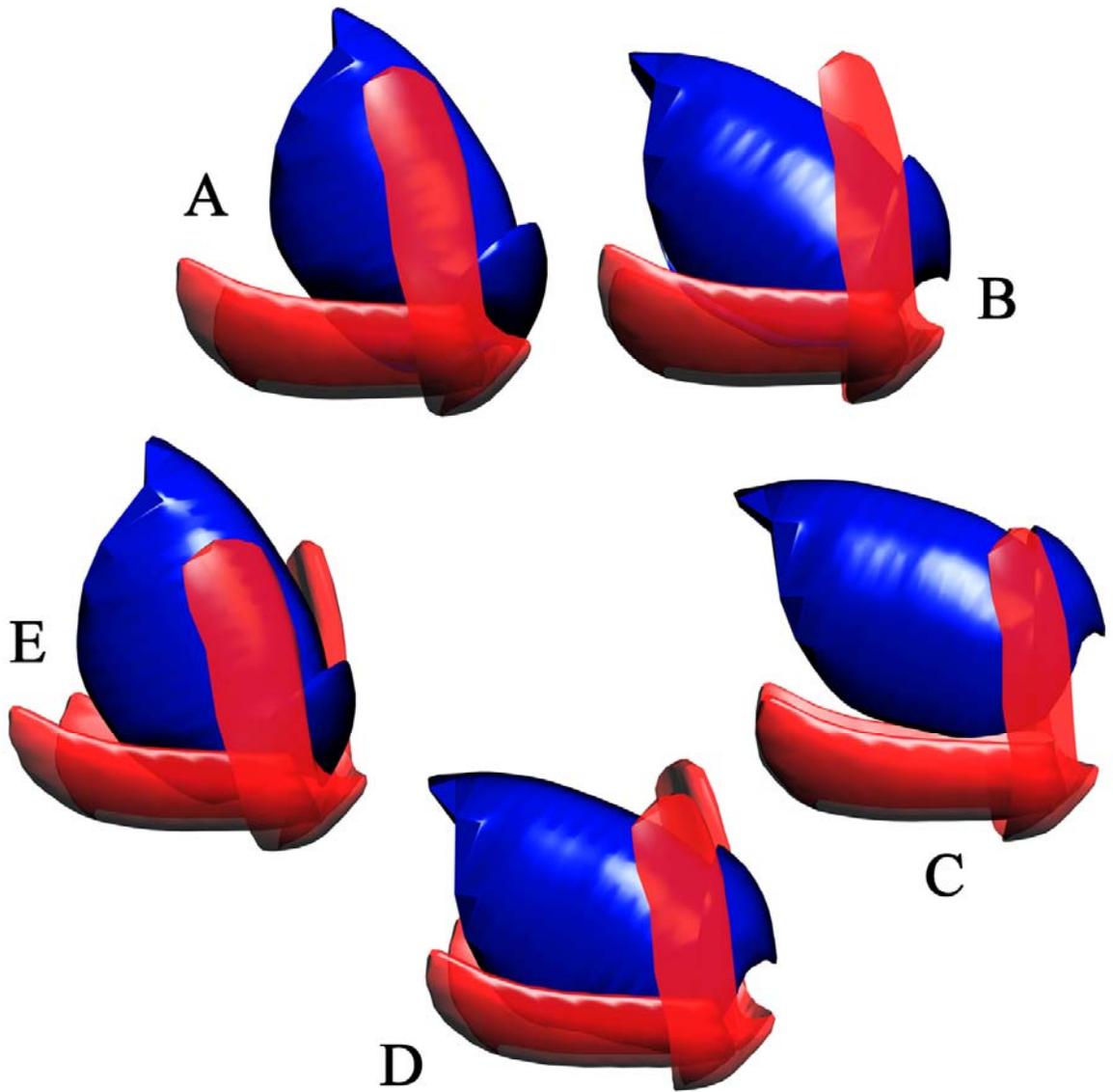
Figure 16. Diagram illustrating movement of the upper beak (blue) with respect to the anchored lower beak (red), of *Octopus bimaculoides*, during a stereotypical bite cycle (description follows Kear, 1994). Position A, resting; B, opening; C, fully open; D, closing; E, closed and retracted.

dissected to identify major features of the buccal mass musculature (such as discernable muscle divisions, overall shape, and origins and insertions). During the dissection, digital photographs and measurements were taken of the beaks and muscles to provide reference data for a three-dimensional model. The remaining buccal masses were reserved for histological processing. Fixation weakens the beccublast connection between the beaks and the musculature and I was able to remove the beaks in two larger specimens prior to embedding, and thus facilitating the microtomy. The larger buccal masses without beaks were dehydrated, embedded in paraffin (Paraplast Plus, Monoject Scientific, St. Louis, MO), and serially sectioned using disposable steel knives at 10 μm, one each in transverse, parasagittal, and frontal planes. The sections were stained using Milligan's Trichrome stain and Picro-Ponceau with Hematoxylin stain on alternate slides (Kier, 1992) and examined by brightfield and polarized light microscopy. The former location of the beaks was apparent in the sections because the beccublasts could be observed lining the space formerly occupied by the beaks. Particular attention was focused on documenting muscle fiber trajectories. Those fibers with trajectories potentially arranged as a muscular hydrostat were defined as a single muscular functional unit.

A three-dimensional model of the muscles and connective tissues was constructed using 3D modeling software (Anim8or, http://www.anim8or.com). The basic shape of the beak and muscles was drawn using digital photographs of the dissection and then outlines were digitized for manipulation by the software. The dimensions of the model were then adjusted by matching approximately 300 points on the model to measurements of corresponding points in the dissected buccal mass.

The buccal masses of the cuttlefish, *Sepia officinalis* (five specimens; 280–440 g wet weight; supplied by the National Resource Center for Cephalopods, Galveston, TX) and of the brief squid, *Lolliguncula brevis* (six specimens; 18–24 g wet weight; collected by short trawl, University of North Carolina Institute of Marine Science, Morehead City, NC) were examined. Serial sections of *S. officinalis* were cut in transverse, frontal, and parasagittal planes using the procedures described above. The beaks of *L. brevis* were small and thin enough to cut with a microtome and tungsten carbide or long edge glass Ralph knives (Bennett et al., 1976) so intact buccal masses were dehydrated, embedded in a cold-polymerizing glycol methacrylate plastic resin (Technovit 7100, Structure Probe, Inc., West Chester, PA), and serially sectioned at a thickness of 3 μm in transverse, parasagittal, and frontal planes. Every tenth section was collected and stained using Toluidine blue stain (2% Toluidine blue O (C.I. 52040) in 2% sodium borate; modified from Burns, 1978).

Results

Morphology of the Beaks and the Mandibular Muscles

The following descriptions and images rendered from the 3D computer model are based on analyses of the buccal mass of *Octopus bimaculoides*. The morphology of the beaks and mandibular muscles of *Sepia officinalis* and *Lolliguncula brevis* were similar and all significant differences are noted below.

Four mandibular muscles are described here: the paired left and right lateral mandibular muscles, the anterior mandibular muscle, the posterior mandibular muscle, and the superior mandibular muscle (Fig. 17).

Figure 17. A series of computer renderings of three sets of beaks of *Octopus bimaculoides* with attached mandibular muscles. The left set, labeled A, shows the muscles attached to the beaks. The center set, labeled B, shows the upper and lower beaks separated with the mandibular muscles originating on the respective beaks. The right set, labeled C, shows the beaks and mandibular muscles separated. The color convention is as follows: the lower beak is red, the upper beak is dark blue, the superior mandibular muscle (SMM) is green, the lateral mandibular muscles (LMM) are purple, the anterior mandibular muscle (AMM) is yellow, and the posterior mandibular muscle (PMM) is light blue. (Modified from Uyeno & Kier, 2007)
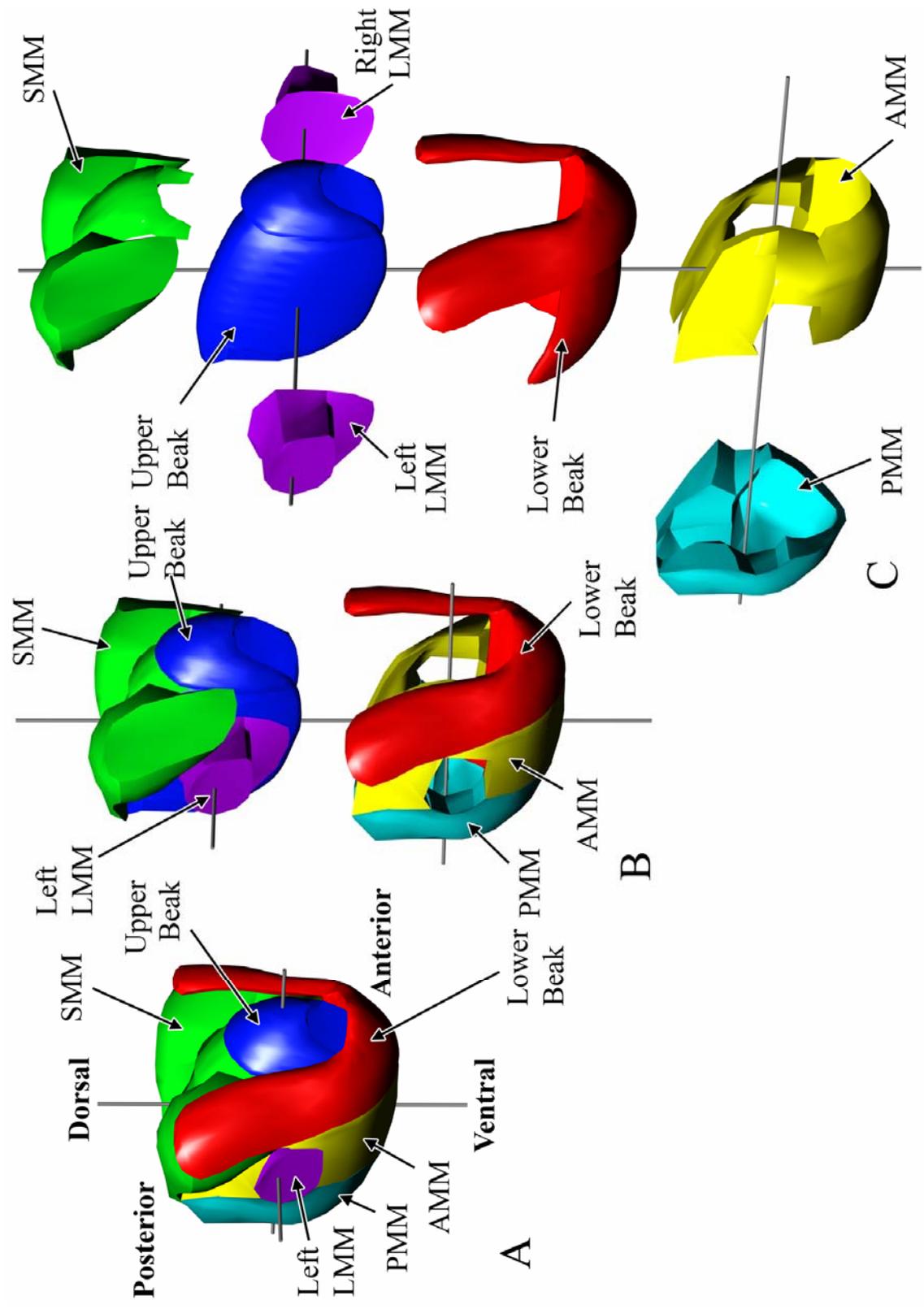
Figure 17

Upper and Lower Beak

The upper and lower beaks of all three species do not contact each other within the buccal mass. Figure 18 is a frontal section from the lower quarter of the buccal mass of *Lolliguncula brevis* in which the lack of contact between the lower and upper beak lateral walls can be seen. Instead, the upper and lower beaks slide by each other. The only points at which the beaks make contact are at the occlusion of the rostra and jaw angles (i.e., those surfaces that are used for shearing food).

The beaks of the three coleoids are similar in overall morphology. The beaks of *Sepia officinalis* (a sepioid) and *Lolliguncula brevis* (a teuthoid) are less robust than those of the octopod *Octopus bimaculoides*. The rostra of *O. bimaculoides* are much less pointed than those of *S. officinalis* and *L. brevis* and the lower beak rostrum of *O. bimaculoides* is especially well-rounded. The lower beak of *O. bimaculoides* has relatively large lateral wings that provide large surfaces for muscle attachment. The hood of the upper beak of *O. bimaculoides* is relatively shorter and broader than that of *S. officinalis* and *L. brevis*.

I identified beak positions within the buccal mass throughout the bite cycle by observing the movements of exposed portions of the beaks and by comparing sections of buccal masses that had been fixed in different positions. The bite cycle of the isolated buccal mass of *Octopus bimaculoides* is very similar to that described by Kear (1994) for *Sepia officinalis* and *Alloteuthis subulata*. I did not observe and could not evoke bite cycles in the freshly dissected buccal masses of *Lolliguncula brevis*. Figure 16 shows a summary of the beak orientations of *Octopus bimaculoides* at each step in the bite cycle.
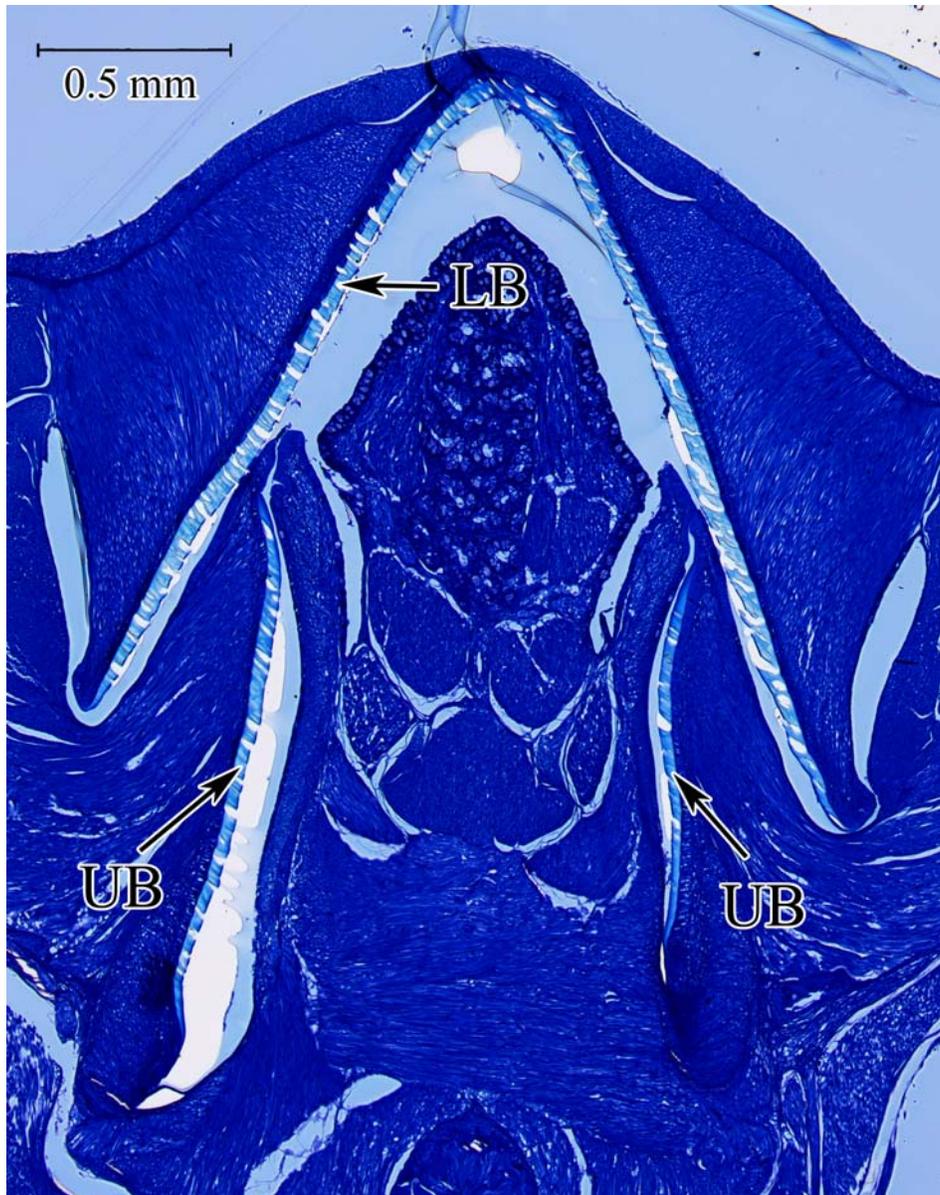
Figure 18. Micrograph of a frontal section of the buccal mass of *Lolliguncula brevis*. The anterior is towards the top of the micrograph. The section is at a level where both the lower beak (LB) and upper beak (UB) are visible in the same plane. The lateral walls and the crest of the lower beak are cut obliquely. The lower edges of the left and right lateral walls of the upper beak are also visible. This is as close together as the upper and lower beaks were observed; they do not contact one another. Brightfield microscopy of 3.0-μm thick glycol methacrylate section.

Lateral Mandibular Muscle

Gross morphology.

The symmetrical left and right lateral mandibular muscles are robust cylinders of muscle tissue that are surrounded by connective tissue. The lateral mandibular muscles have their origin on the lateral walls of the upper beak and a somewhat smaller insertion on the surrounding connective tissue (Fig. 19a). The lateral mandibular muscles of *Lolliguncula brevis* and *Sepia officinalis* are relatively smaller in volume with respect to the size of the beaks than those of *Octopus bimaculoides*.

The 3D reconstruction of the right lateral mandibular muscle shown in Figure 19a illustrates a shape that corresponds to the partially opened position of the beak bite cycle. Comparing similar sections taken from buccal masses of *Lolliguncula brevis* that were fixed in different stages of the bite cycle revealed that the shape of the lateral mandibular muscles changes during movement. From the position illustrated in Figure 19a (which corresponds to the "opening" position in Fig. 16B), the diameter of the lateral mandibular muscles increase and the length of the muscles (measured from the origin to the insertion) decrease as the gape of the beaks widens. As the beaks close, the shape of the cylindrical lateral mandibular muscles become longer and thinner. The lateral mandibular muscles are longest and thinnest when the beaks are in the closed and retracted position and the lateral mandibular muscles are displaced anteriorly by the anterior mandibular muscle and posterior mandibular muscle. Figure 19c is a photomicrograph of a transverse section taken through the middle of the buccal mass. The lateral mandibular muscle in this image appears spherical because all orientations of fibers within the muscle are contracted and the support usually offered by the beaks to hold the shape of the lateral mandibular muscle is not present. Also apparent in this

Figure 19. a: A right rear quarter view of the right lateral mandibular muscle in *Octopus bimaculoides* (the rostra are pointing to the right). The right lateral mandibular muscle, shown in purple, is roughly cylindrical and flared at its base. The transparent plane indicates the section plane of the micrograph shown in c. b: A right rear quarter view of the lateral mandibular muscles without the beaks showing the orientations of muscle fibers of the right lateral mandibular muscle. The red fibers originate on the lateral wall of the upper beak and extend laterally towards their insertion on the buccal sheath. Those fibers at the edges of the lateral mandibular muscle curve because the medial surface is larger than the lateral surface. The blue fibers are oriented dorsoventrally. The green fibers are oriented anteroposteriorly and therefore have an orientation perpendicular to the other two sets of fibers. c: Micrograph showing a transverse section of the left lateral mandibular muscle at its thickest part. The left margin of the lateral mandibular muscle is left in the image. The dorsal surface is towards the top. A portion of the left lateral wall of the upper beak (l. LW) and the buccal sheath (BS) are visible. The lateral mandibular muscle appears round as the beaks were removed and the lateral mandibular muscles are contracted. Note that there are three orientations of muscle fibers. Some fibers (1) are oriented laterally (visible as horizontal fibers in the plane of section) extending from the lateral wall (l. LW) to the buccal sheath (BS). Additional fibers (2) are oriented in the plane of section in a dorsal-ventral orientation. Fibers oriented in an anterior-posterior direction (3) are visible in transverse section. Note that these numbered fiber orientations correspond to the colored fiber orientations in b (1 = red, 2 = blue, 3 = green). Brightfield microscopy of 10-μm paraffin section stained with Milligan's Trichrome.

A

B

0.5 mm

CT

1.LW

2

3

BS

1

C
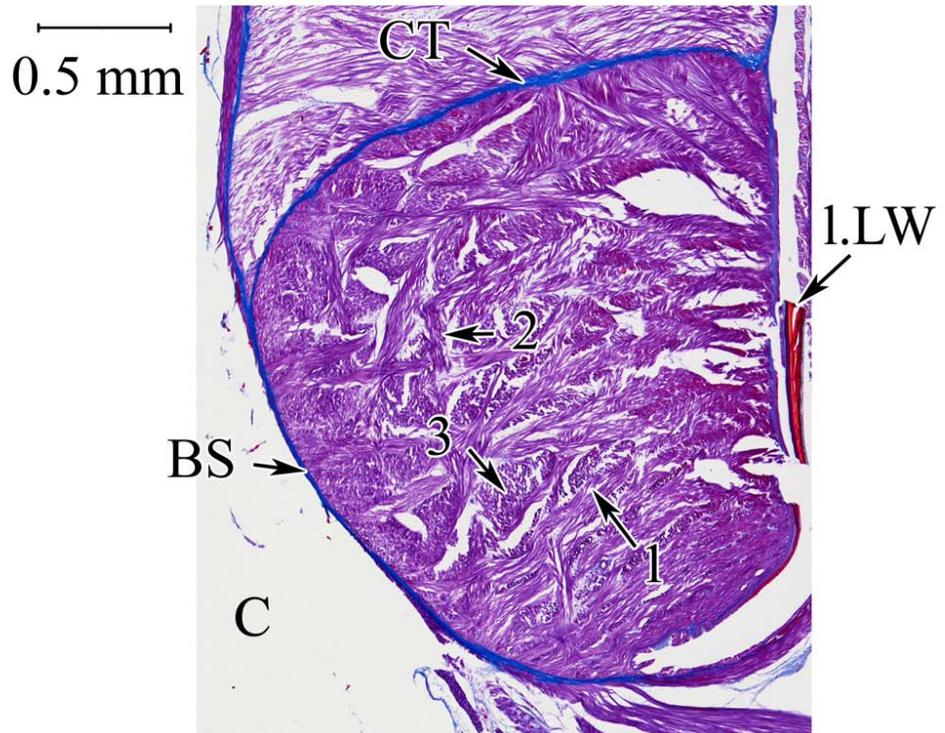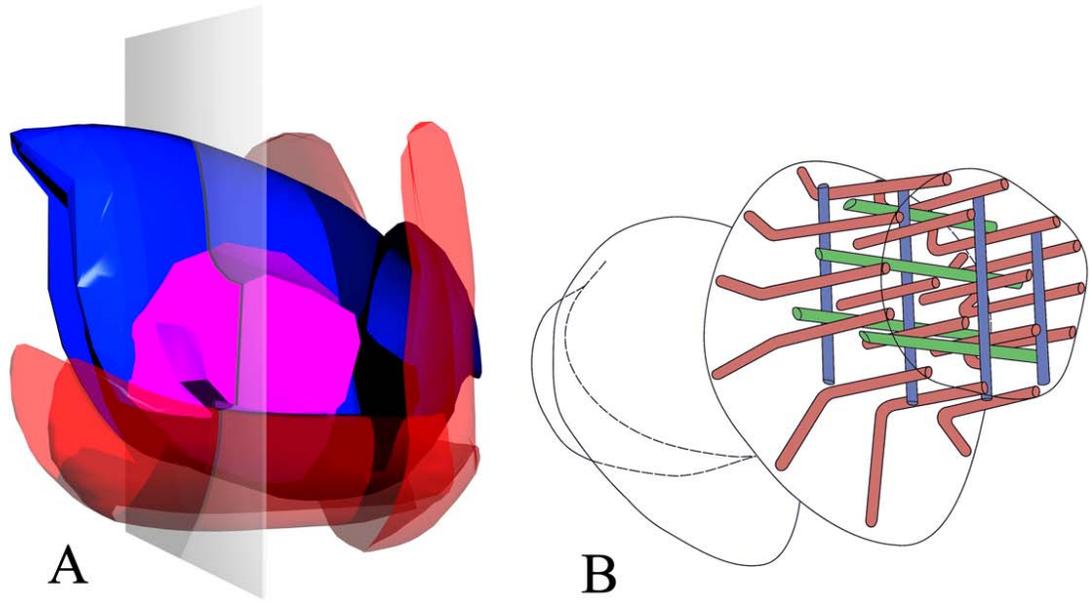
Figure 19

photomicrograph (Fig. 19c) is the separation of the lateral mandibular muscles from surrounding muscles by a sheet of connective tissue.

<u>Fiber orientation.</u>

The orientation of lateral mandibular muscle fibers varies as a function of position. Many fibers run parallel to the long axis of the muscle from their origin to insert on the buccal mass sheath or the connective tissue sheet that surrounds the muscle (the red fibers in Fig. 19b). When these fibers are relaxed and elongated, they follow a curve from their attachment at the origin on the beak so that the lateral mandibular muscles taper from origin to insertion. Contracted fibers of this orientation can be seen in the photomicrograph of Figure 19c as extending from the space formerly occupied by the upper beak lateral wall to the buccal mass sheath. A smaller number of fibers are arranged in planes perpendicular to the long axis of the cylinder. These fibers can be seen in Figure 19c as either transversely sectioned fibers (depicted in Fig. 19b as the green fibers) or as fibers oriented in the plane of the section (depicted in Fig. 19b as the blue fibers) and perpendicular to the more numerous fibers that run parallel to the long axis of the lateral mandibular muscles.

Anterior Mandibular Muscle

<u>Gross morphology.</u>

The anterior mandibular muscle originates on the lateral walls and, as a thin layer, on the crest of the lower beak and follows the curve of the crest dorsally (Fig. 20a). It is also firmly attached to the overlying buccal sheath. The anterior mandibular muscle extends dorsally along the lower beak lateral walls and then across the gap between the upper and lower beaks to its insertion adjacent to the crest on the lateral walls of the upper beak. The left and right dorsal extensions of the anterior mandibular muscle are not oriented in a

Figure 20. a: A right rear quarter view of the anterior mandibular muscle in *Octopus bimaculoides* (the rostra are pointing to the right). The anterior mandibular muscle (yellow) is a broad muscle that partially fills the space within the upper beak hood and completely fills the space within the lower beak hood. The transparent plane identifies the section plane of the micrograph shown in c. b: A right rear quarter view of the anterior mandibular muscle without the beaks. Arrows indicate the trajectory of muscle fibers. The fibers of the anterior mandibular muscle run in a roughly parallel direction from their origin on the lateral walls of the lower beak, around the anterior edge of the lateral mandibular muscles, to the lateral walls of the upper beak. c: Micrograph showing the left half of a frontal section of the middle of the buccal mass of *Octopus bimaculoides*. Anterior is towards the right. The section is at a plane just below the midline of the buccal mass. The left lateral wall of the lower beak (LBLW), the left side of the hood of the upper beak (UBH) and the beccublasts that attach to the left lateral wall of the upper beak (UBLW) are visible. Two portions of the anterior mandibular muscle are visible. The anterior part (A) lies anterior to a crease formed by the proximity of the lateral wall of the lower beak to the hood of the upper beak. The posterior part (P) lies between this crease and the left lateral mandibular muscle (l. LMM). Note that along most of the cross section of the anterior mandibular muscle the fibers are cut in cross section, denoting a dorsoventral orientation. The posteriormost fibers, however, show a more oblique orientation as they are following the anterior edge of the contracted left lateral mandibular muscle (l. LMM). Brightfield microscopy of 10-μm paraffin section stained with Milligan's Trichrome.

60

A

B

1.LMM

P

0.5 mm

A

C   UBLW   UBH   LBLW
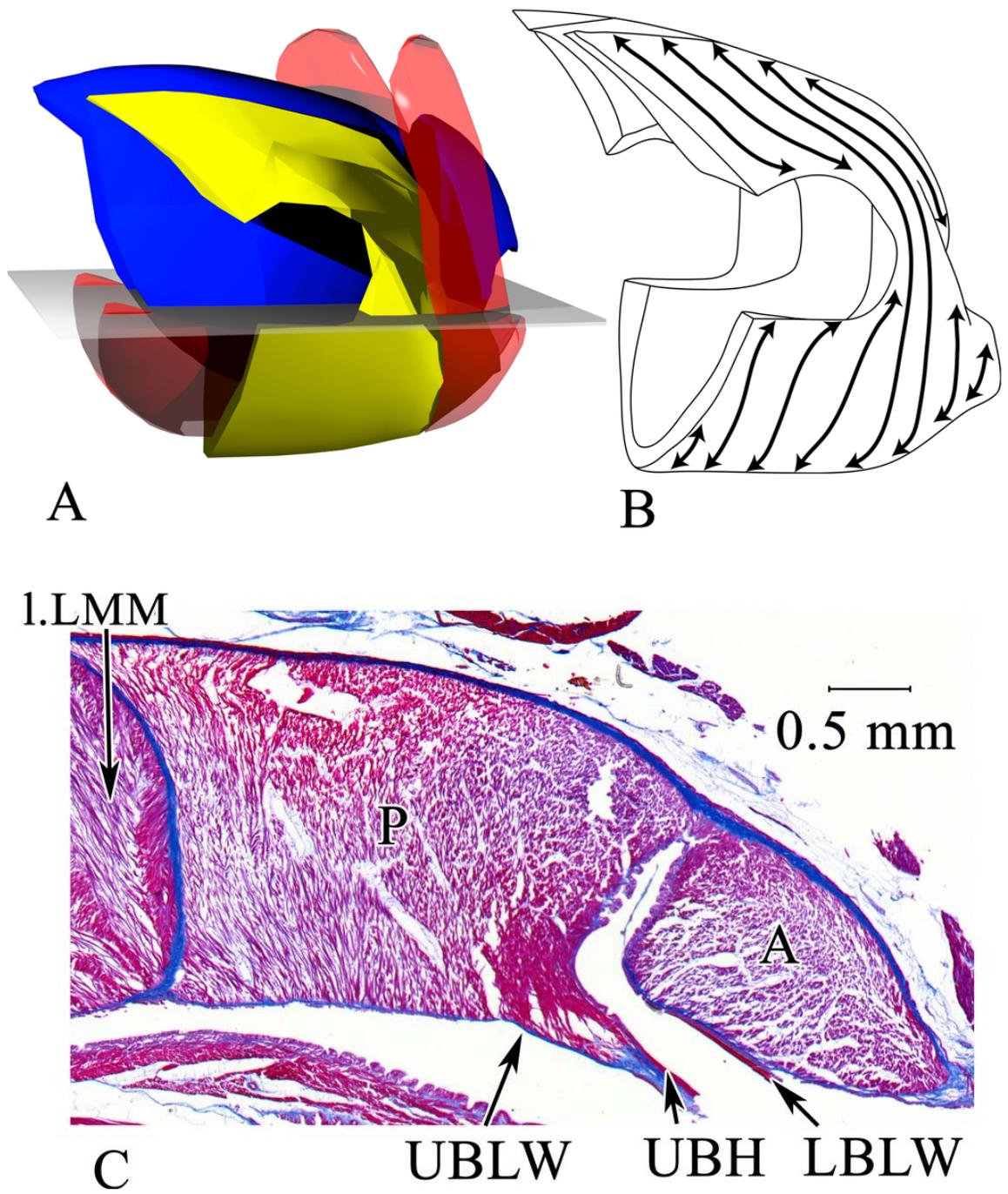
Figure 20

straight trajectory between the origin and insertion points. Instead, as depicted in Figure 20b, they take a curving path around the connective tissue sheet that surrounds the anterior edges of the lateral mandibular muscles. In all the cephalopods observed in this study, the borders between the anterior mandibular muscle and the central division of the superior mandibular muscle are difficult to define within and near the hood of the upper beak, but can be recognized by differences in muscle fiber orientation. The borders between the anterior mandibular muscle and posterior mandibular muscle on the lower beak crest are also defined by differences in muscle fiber orientation as there are no connective tissue divisions at these borders.

Comparisons of sections of buccal masses with the beaks in different positions reveal that the anterior mandibular muscle shortens dorsoventrally with a corresponding increase in thickness during beak closing.

Fiber orientation.

As shown in Figure 20b, the anterior muscle fibers of the anterior mandibular muscle follow a direct course as they extend from their origin along the lateral walls of the lower beak to their insertion on the upper beak or the buccal sheath. The fibers ventral to the lateral mandibular muscles, however, must curve anteriorly and either insert on the sheet of connective tissue that encloses the lateral mandibular muscles or, if their position is sufficiently anterior, continue to curve around the anterior edge of the lateral mandibular muscles and insert high on the lateral walls of the upper beak. The anterior mandibular muscle fibers that lie dorsal and posterior to the lateral mandibular muscles also have a curved trajectory, as they originate on the lateral mandibular muscle connective tissue sheet and then curve posteriorly towards their insertion high on the upper beak lateral wall. The

curvature of the anterior mandibular muscle fibers around the lateral mandibular muscle can be seen in Figure 20c, a photomicrograph of a frontal section through the left half of the anterior mandibular muscle and left lateral mandibular muscle. The dorsoventrally oriented fibers of the anterior mandibular muscle are cut in transverse section along most of the cross-sectional area of the muscle. As the lateral mandibular muscle is contracted, it is displacing the fibers of the anterior mandibular muscle that curve around its anterior out of a dorsoventral orientation and these anterior mandibular muscle fibers are thus obliquely cut. Many of the fibers that originate on the ventral surface of the lower beak lateral walls extend towards, and insert on, the buccal mass sheath and are thus cut in longitudinal section in Figure 20c. In *Octopus bimaculoides* there is a small number of anterior mandibular muscle fibers situated near the lower edge of the lateral mandibular muscles that originate on the lateral mandibular muscle connective tissue sheet and extend into the anterior mandibular muscle along a path that is perpendicular to the majority of the other anterior mandibular muscle fibers.

Posterior Mandibular Muscle

Gross morphology.

The posterior mandibular muscle is the smallest and thinnest of the four mandibular muscles. It is a thin sheet of fibers that originates on the crest of the lower beak and inserts on the upper beak lateral wall inferior to the crest (Fig. 21a). The slightly thicker anterior portion of the posterior mandibular muscle curves around the lateral mandibular muscles. The posterior of this muscle forms the posterior wall of the buccal cavity as the muscle extends from the end of the lateral walls of the lower beak up to a level just below the esophagus. It connects, therefore, to the structures that occupy the cavity within the beaks.

Figure 21. a: A right front quarter view of the posterior mandibular muscle in *Octopus bimaculoides* (the rostra are to the right). The posterior mandibular muscle (light blue) covers the posterior opening of the upper and lower beak and anchors the structures within the buccal cavity. The transparent plane identifies the section plane of the micrograph in c. b: A right front quarter view of the posterior mandibular muscle without the beaks showing the trajectory of muscle fibers. The fibers of the posterior mandibular muscle are similar to those of the anterior mandibular muscle, in that they run in a roughly parallel direction from their origin on the lateral walls of the lower beak to the lateral walls of the upper beak. They differ, however, in curving around the posterior edges of the lateral mandibular muscles. c: Micrograph of the left half of a frontal section from the lower half of the buccal mass of *Octopus bimaculoides*. Posterior is towards the left. The posterior mandibular muscle (PMM) is the thinnest mandibular muscle. The fibers of the posterior mandibular muscle are oriented in the plane of this section. They interdigitate with the muscles of the organs within the buccal cavity and with the mandibular muscles. Note the left bolster (l. Bol) and the muscles of the left buccal palp (l. BP) that fill the buccal cavity. The spaces between the posterior mandibular muscle and the organs of the buccal cavity are artifacts. Brightfield microscopy of 10-μm paraffin section stained with Milligan's Trichrome.

A

B

C

PMM

0.5 mm

l.Bol

l.BP
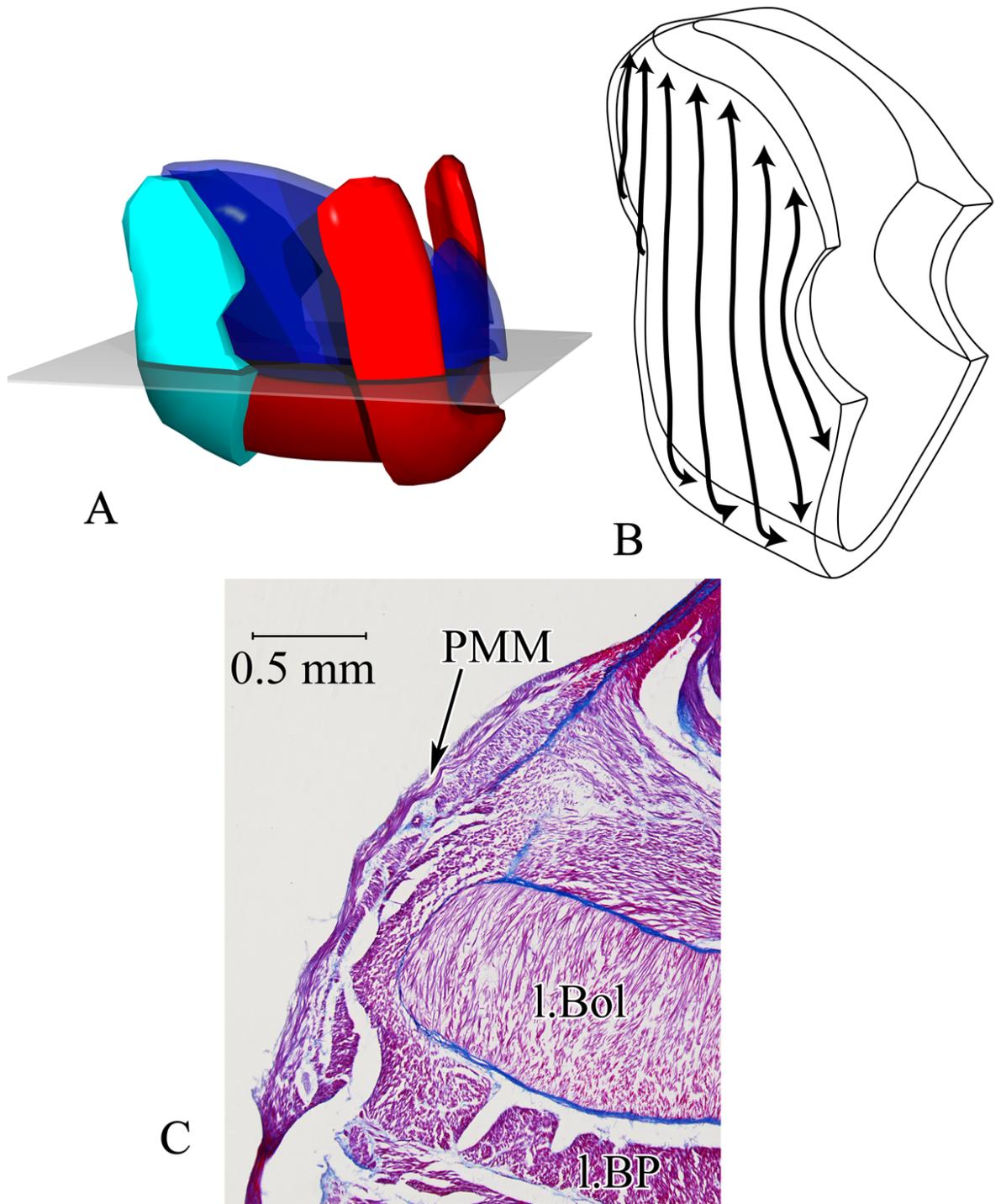
Figure 21

The posterior mandibular muscles in *Sepia officinalis* and *Lolliguncula brevis* appear

relatively thicker than that of *Octopus bimaculoides* with respect to upper beak length.

Fiber orientation.

The fiber orientation of the posterior mandibular muscle is primarily dorsoventral,

except where the anterior portion of the posterior mandibular muscle curves around the

lateral mandibular muscles (Fig. 21b). It is difficult to distinguish the posterior mandibular

muscle from the anterior mandibular muscle where they both originate on the crest of the

lower beak. The border is distinguished by tracing the fibers up to the lateral mandibular

muscles and comparing their trajectories.

The posterior mandibular muscle fibers follow the posterior contours of the lateral

mandibular muscles. Beyond the edge of the upper and lower beak lateral walls, the posterior

mandibular muscle fibers interdigitate with the muscle fibers of the buccal palps, the bolsters,

and the radula retractor muscles to enclose the buccal cavity. The photomicrograph of Figure

21c is a frontal section of the posterior mandibular muscle enclosing the buccal cavity

showing its relative size and connection to the structures of the buccal cavity. The level of

the section is just below the point where the esophagus exits from the buccal mass.

Superior Mandibular Muscle

Gross morphology.

The superior mandibular muscle (Fig. 22a) is a robust dorsal muscle that lies above

the level of the esophagus. It originates primarily as a central division along the crest of the

upper beak. Its origin includes the entire area of the upper beak crest as well as a large area

within the hood. Extending from their origins on the central division and the dorsalmost

portions of the upper beak lateral walls are two robust left and right divisions that extend to

Figure 22. a: A right front quarter view of the superior mandibular muscle in *Octopus bimaculoides* (the rostra are pointing to the right). The superior mandibular muscle (green) is the largest muscle that connects the upper and lower beaks. The transparent plane identifies the section plane of the micrograph in c. b: A right front quarter view of the superior mandibular muscle without the beaks showing the three divisions. The green arrows show the trajectories of the muscle fibers of the right division. These fibers originate within the posterior central division and insert on the right lateral wing of the lower beak. The trajectories of the fibers in the central division are indicated by blue arrows. These fibers originate and insert along the entire crest of the upper beak. The left division is symmetrical with the right division. The red arrows represent muscle fiber directions within the left division. The left division fibers also originate on the posterior central division, but insert on the left lateral wing of the lower beak. c: Micrograph of a frontal section of the dorsal portion of the buccal mass of *Octopus bimaculoides*. The anterior is to the right. The micrograph shows the left (LD) and right (RD) divisions of the superior mandibular muscle extending from the midline out to their insertion points on the left (l. LW) and right (r. LW) lateral wings of the lower beak. The central division (CD) of the superior mandibular muscle that exists between the hood and crest of the upper beak is also shown. The space surrounded by blue connective tissue in the center of the section is the area once occupied by the crest of the lower beak (removed). Brightfield microscopy of 10-μm thick paraffin section stained with Milligan's Trichrome.
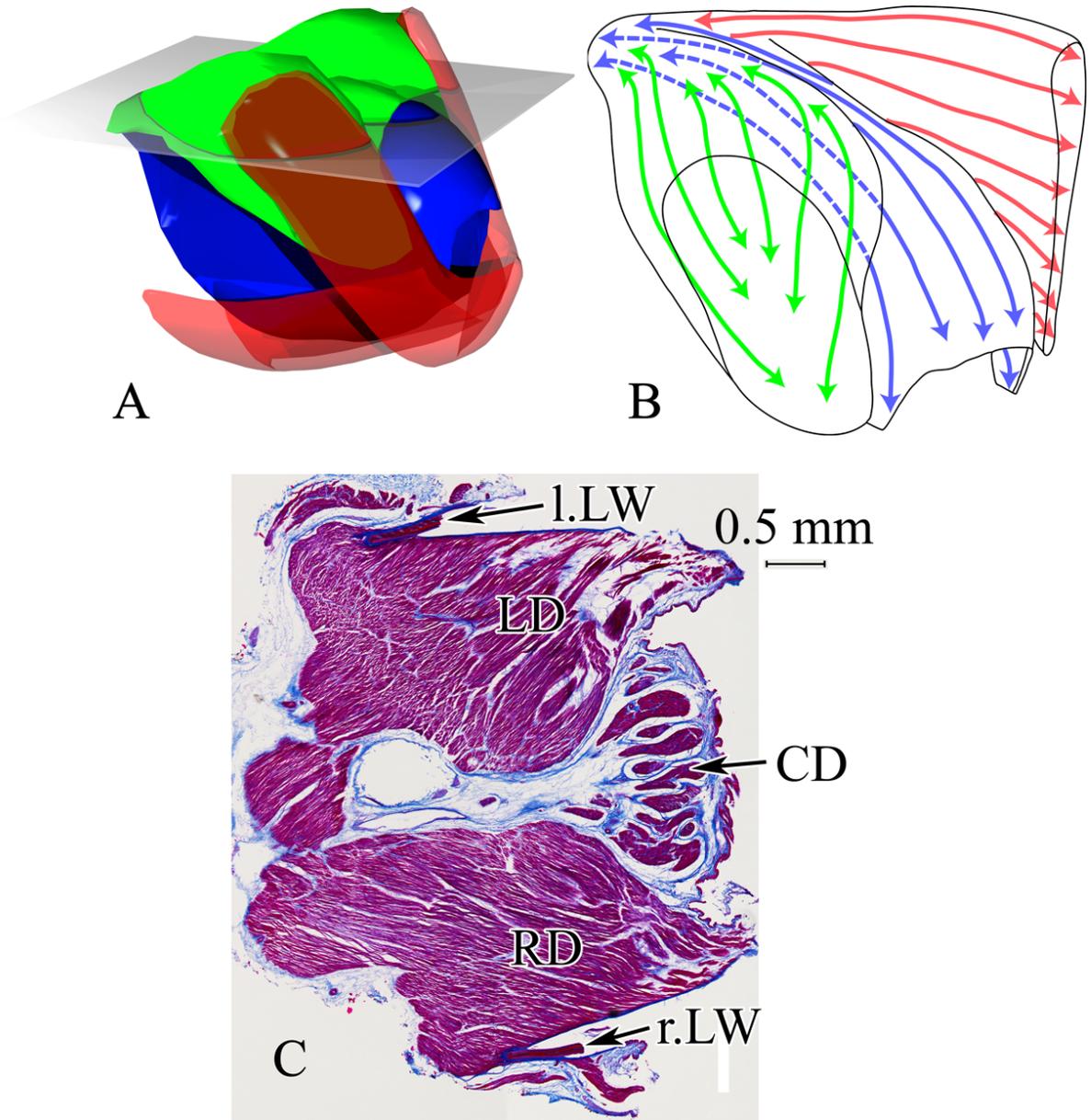
Figure 22

their insertion on the left and right wings of the lower beak. The gross morphology of the superior mandibular muscle is similar in *Octopus bimaculoides*, *Lolliguncula brevis,* and *Sepia officinalis.* The cross-sectional areas of the left and right divisions of the superior mandibular muscle are relatively large compared with the posterior mandibular muscle and anterior mandibular muscle. As the beak closes and retracts, the left (Fig. 22b, shaded red) and right (Fig. 22b, shaded green) divisions of the superior mandibular muscle shorten and increase in cross-sectional area. Observations of isolated *Octopus bimaculoides* buccal masses during beak closure and retraction show the left and right divisions of the superior mandibular muscle becoming so short and thick that they contact each other over the dorsal surface of the central division (Fig. 22b, shaded blue).

Fiber orientation.

Muscle fibers in the right (Fig. 22b, green arrows) and left (Fig. 22b, red arrows) divisions run approximately straight from their origins in the central division and along the dorsal edges of the upper beak lateral wall, to their insertion on the lower beak wings. The muscle fibers within the central division (Fig. 22b, blue arrows) originate along the entire surface of the upper beak crest and follow an anterior-posterior trajectory. Figure 22c is a photomicrograph of a frontal section of the dorsal portion of the buccal mass in which the superior mandibular muscle is somewhat contracted.

The superior mandibular muscle can be seen here extending from the central division below to its insertion points on the left and right lateral wings of the lower beak. The central division can also be seen in this section as fibers, between the two lateral divisions, extending into the region between the hood and crest of the upper beak.

69

Buccal Mass Connective Tissue Sheath

The buccal mass is enclosed by a sheet of connective tissue fibers that are oriented in the plane of the sheath. Fiber orientations in the sheath vary as a function of location. The fibers of the sheath surrounding the lateral mandibular muscles show preferred orientation in the dorsoventral direction. The orientation of the connective tissue fibers overlying the divisions of the superior mandibular muscle varies, but a significant proportion of the fibers are aligned along the long axis of the superior mandibular muscle divisions. The connective tissue associated with the beccublasts within the hoods of the upper and lower beaks show three orientations. Two orientations are mirror images of each other, running from left posterior to right anterior and vice versa. Most of the fibers, however, are arranged perpendicular to the long axis of the beaks, extending from the left side to the right. The fibers are highly birefringent and have the staining properties of collagen. The buccal mass sheath is continuous with the connective tissue sheath surrounding the lateral mandibular muscles as well as with the connective tissue associated with the beccublasts. Frontal or parasagittal sections show that the buccal mass sheath varies in thickness with the thickest portions found in anterior areas of the upper and lower beaks where the buccal mass sheath is continuous with the beccublast connective tissue.

Discussion and Conclusion

The two rigid beaks do not contact one another, but are instead associated with, and embedded in, four muscle groups and the entire structure is enclosed in a connective tissue sheath. How do these muscle and connective tissues generate the complex beak movements during biting and manipulation of food? How is the force required for movement and antagonistic support transmitted if the beaks are not in contact with one another? To begin

70

answering these questions, I will analyze the beak movements during a bite cycle and focus on the origin, insertion, and fiber trajectories of the muscles to predict whether a given muscle is shortened or elongated in a given phase of the bite cycle, and how force is transmitted during movement.

Postulates of mandibular muscle function

The same endogenous motions of the beaks were observed in isolated buccal masses of *Octopus bimaculoides* (Fig. 16) as were observed in the cephalopod species investigated by Boyle et al. (1979 a, b) and Kear (1994). These cyclical beak movements were used to determine the distance between origins and insertions of the four mandibular muscle groups. As contraction of a muscle may result in a decrease in distance between the origin and insertion, a change in these distances suggests muscle activity. The hypothesized muscle activities during a bite cycle based on this analysis are summarized in Table 3.

The lateral mandibular muscles (Fig. 19) are hypothesized here to function in opening movements and in creating a pivot around which the upper beak can rotate relative to the lower beak. In *Octopus bimaculoides*, the lateral mandibular muscles include an extensive network of muscle fibers oriented perpendicular to the fibers extending from origin to insertion, and may thus function as muscular hydrostats (Kier and Smith, 1985). Since the lateral mandibular muscles are constant in volume, contraction of the perpendicular fibers will elongate the other fibers and vice versa, providing a potential mechanism for antagonism of the two fiber orientations and the control of shape change in the lateral mandibular muscle. The contraction of the fibers of the lateral mandibular muscle that extend from origin to insertion will likely cause the buccal mass sheath to move medially towards the lateral wall of the upper beak and, because it is essentially constant in volume, the diameter of the lateral

71

Table 3. Summary of hypothesized muscle activity during the bite cycle of the coleoid buccal mass

	Mandibular Muscles			
	Lateral	Anterior	Posterior	Superior
Closed		✓		✓
Opening	✓		✓	
Opened	✓		✓	
Closing			✓	✓
Retracted		✓		✓

A check mark indicates activity of the muscle during that phase of the cycle. These beak positions correspond to those illustrated in Figure 4. A, Closed; B, Opening; C, Opened; D, Closing; E, Closed.

mandibular muscle will increase and lengthen the fibers of perpendicular orientation. This shape change in the lateral mandibular muscle may displace the anterior mandibular muscle, the posterior mandibular muscle and the lateral divisions of the superior mandibular muscle and move the upper beak away from the lower beak. Thus, the lateral mandibular muscles may be responsible for elongation of the other muscles. This proposed function is consistent with earlier observations by Kear (1994), who elicited opening by stimulation at the location of the lateral mandibular muscle. Contractions of the anterior mandibular muscle and the posterior mandibular muscle around the circumference of the lateral mandibular muscles may re-elongate the lateral mandibular muscles to their resting length. In addition, the extensive network of fibers perpendicular to the long axis in the lateral mandibular muscles of *Octopus bimaculoides* might also play a role in re-elongation of the lateral mandibular muscle. Also, simultaneous contraction of the perpendicular fibers and the parallel fibers of the lateral mandibular muscle may provide a means of increasing the stiffness of the muscle so that it can function as a pivot around which movement can occur.

The muscle fibers of the anterior mandibular muscle (Fig. 20) probably function in closing the upper and lower beak, but two different movements are possible. If no other muscles are active, anterior mandibular muscle contraction probably functions to bring the two beaks together in a shearing motion that moves the upper beak posteriorly with respect to the lower beak. Simultaneous activity of the lateral mandibular muscles may provide a pivot, and since the anterior mandibular muscle fibers are curved around the lateral mandibular muscles, anterior mandibular muscle contraction causes the rotation of the rostrum of the upper beak into the rostrum of the lower beak during closing.

73

The posterior mandibular muscle (Fig. 21) might also function in two ways, depending on the activity of the other muscles. When contracting alone, it probably brings the upper and lower beaks together. When contraction of the posterior mandibular muscle occurs simultaneously with activity of the lateral mandibular muscles, opening of the beak may occur; the fibers of the posterior mandibular muscle connect the two beaks posterior to the lateral mandibular muscles so that if the lateral mandibular muscles serve as a pivot, contraction of the posterior mandibular muscle will bring the posterior portions of the beaks together, thereby causing the rostra to rotate apart. Indeed, in the previous study by Kear (1994), simultaneous electrical stimulation of the musculature defined here as posterior mandibular muscle and lateral mandibular muscle resulted in beak opening. In *Sepia officinalis*, the posterior mandibular muscle is relatively thicker in cross section and therefore may contribute more force to the opening and closing motions than does the posterior mandibular muscle of *Octopus bimaculoides*.

The superior mandibular muscle (Fig. 22) most likely closes the beaks. Contractions of the robust rami move the upper beak in a ventral-anterior direction and bring the biting surfaces of the beaks together. The simultaneous activation of the superior mandibular muscle and the posterior mandibular muscle may be responsible for the closed and retracted position that Kear (1994) described as the resting position (Fig. 16A).

Summary of novel findings

The following is a summary of the differences between morphological description, terminology, and functional roles proposed here and those of Boyle et al. (1979 a, b) and Kear (1994). Boyle et al. (1979a) identified two muscles, the superior mandibular muscle and lateral muscles which incorporated the anterior mandibular muscle, posterior mandibular

74

muscle, and lateral mandibular muscles. They noted that the superior mandibular muscle and several areas of the lateral muscles were active during closing. They suggested that opening was at least partially passive.

Kear (1994) described four muscles, the superior mandibular muscle, the inferior mandibular muscle (which incorporated the anterior mandibular muscle and portions of the posterior mandibular muscle), the thin sheet of longitudinal muscles below the buccal sheath (which incorporated the posteroventral portion of the posterior mandibular muscle), and the lateral mandibular muscles (which incorporated the lateral mandibular muscles and portions of the anterior mandibular muscle and posterior mandibular muscle that spanned the beaks). Kear (1994) identified the lateral mandibular muscles as functioning as a pivot, and the superior mandibular muscle as providing most of the closing force with the inferior mandibular muscle providing for a closing-shearing action. The contraction of the posterior portions of the lateral mandibular muscles was proposed for opening movements.

There are several novel insights in the current study. The lateral mandibular muscles are recognized here as muscular hydrostats and are therefore capable of opening the beaks on their own as well as acting as an antagonist for the other mandibular muscles. The posterior mandibular muscles might also aid in opening the beaks in the manner described by Kear (1994) of her lateral mandibular muscles. The superior mandibular muscle probably closes the beaks by drawing the rostra closer together, while the anterior mandibular muscle probably closes the beaks while retracting the upper beak relative to the lower one. These proposals are consistent with the electromyographical recordings and stimulation experiments of Boyle et al. (1979a) and Kear (1994).

Further investigations

In the following chapter, the proposed functions of the various beak muscles are tested experimentally. Because preparations of isolated beaks spontaneously undergo repetitive cycles of biting that resemble natural movements in intact specimens, electromyograms can be recorded from the mandibular muscles while monitoring movement. This allows a definitive test of the predictions of muscle activity (Table 3) proposed here. This morphological study of the cephalopod buccal mass is the first analysis of an animal joint as a muscle articulation. To further describe the diversity of these joints, I attempt to identify additional muscle articulations by investigating feeding structures used in other invertebrate phyla that rely on hydrostatic mechanisms. Thus, in chapter 2, I examine the hooks of marine interstitial kalyptorhynch turbellarian flatworms (Karling, 1961), and in chapter 3, the jaws of errant nereid polychaetes (Pilato, 1968). These have been analyzed because previous studies have identified characteristics similar to those described in the cephalopod buccal mass, such as a relatively limited number of rigid elements that are embedded in muscle and are not in contact. The major goal of further morphological studies is to explore the possible importance of muscle articulations to invertebrates and to identify general principles of muscle articulation structure and function.

CHAPTER 3

TESTING THE FUNCTIONAL ROLE OF THE MUSCLE OF THE OCTOPUS BUCCAL

MASS IN BEAK MOVEMENTS

Introduction

> *Structure without function is a corpse; function without structure is a ghost.*

> (Vogel & Wainwright, 1969)

No form exists without a function and no function exists without a formal cause and context (Wainwright, 1988). Thus, the goals of biomechanical studies are to complete a full morphological characterization as well as to identify how the mechanism works during natural movements. In this endeavor, however, Gould and Lewontin (1979), by asking if architectural spandrels exist to display iconic mosaics or to simply fill triangular spaces formed by the intersection of arches, challenge us to resist inappropriate associations of structures to their perceived adaptive functions. Thus, the use of strong inference methods (Platt, 1964), resulting in the testing and unambiguous denial of all but one hypothesis of function, are crucial in evaluating the muscle articulation.

While structural details and their functions are inseparable without losing overall perspective, the complexity of biomechanical analysis is reduced by first describing morphology and then addressing the function of the structures. My analysis of the octopus buccal mass follows such a progression: The preceding chapter (Ch. 2) described the detailed three-dimensional morphology of the muscle and connective tissues of the buccal mass. Analysis of this morphology generated hypotheses of the role of these muscles in support and

movement. The octopus buccal mass represents a good model system to test these hypotheses because it can be employed in *in vitro* experiments and previous studies have described aspects of the neuroanatomy and behavior. This chapter describes experiments designed to test the hypotheses of function of the octopus buccal mass musculature.

Aspects of morphology important for beak movement

In Chapter 2 I described five mandibular muscles that are responsible for beak movement: the superior, left and right lateral, anterior, and posterior mandibular muscles. These connect the beaks of *Octopus bimaculoides* to each other and to a connective tissue sheath that encapsulates the buccal mass.

The superior mandibular muscle is a robust dorsal muscle with three divisions. It originates along the crest of the upper beak and includes a central division and left and right divisions that extend anteroventrally to insert on the enlarged wings of the lower beak. These robust left and right divisions constitute the bulk of the superior muscle and include fibers oriented parallel to the line from origin to insertion.

The lateral mandibular muscles are robust, cylindrical, and symmetrically paired muscles originating on a large area of the left and right lateral walls of the upper beak. The muscle extends laterally and has a somewhat smaller insertion on the buccal mass sheath. Three different orientations of muscle fibers are observed. The first group of fibers originates on the lateral walls of the upper beak and extends parallel to the long axis of the muscle to insert on the buccal mass sheath. The other two groups of muscle fibers are perpendicular to the orientation of the first as well as to each other, one group oriented dorsoventrally and the other anteroposteriorly.

The anterior mandibular muscle is relatively thin and originates on the anterior portion of the lower beak crest and overlying buccal mass sheath and follows the curve of the crest dorsally to insert on the lateral walls of the upper beak just below the level of the upper beak crest. Its muscle fibers follow a direct course from origin to insertion.

The posterior mandibular muscle is the smallest and thinnest of the mandibular muscles. It is a thin sheet of muscle that originates on the posterior region of the lower beak crest and extends directly to an insertion on the lateral walls of the upper beak below its crest. As the posterior edges of the trough-like beaks are open, the posterior mandibular muscle, along with the overlying buccal mass sheath, forms the posterior wall of the buccal cavity and serves to contain and secure the buccal complex within the buccal cavity.

The inferior buccal ganglion (Fig.23), which receives input from the superior buccal lobe of the brain through the paired interbuccal connectives, is thought to control the activation sequence of the mandibular muscles (Young, 1965, 1971). Boyle et al. (1979b) noted that the inferior buccal ganglion functions as a central pattern generator that is probably modulated by sensory feedback from the musculature and the brain. After severing the interbuccal connectives and excising the buccal mass, it performs biting movements that are similar to *in vivo* movements with respect to the position of the upper beak relative to the lower one throughout each bite cycle. Boyle et al. (1979b) first described this bite cycle, and Kear (1994) later modified the description (Fig. 24). As my observations agree with those of Kear (1994), I use her terminology here. There are five phases during which the upper beak is: (A) closed in its resting position; (B) opening; (C) fully opened; (D) closing; (E) closed with the upper beak rostrum retracted behind the lower beak rostrum.

Figure 23. Front and rear quarter views of a whole buccal mass of O. bimaculoides and the approximate corresponding computer visualization (Left = rear quarter views; right = front quarter views). Computer visualization model images show dorsovental, anteroposterior, and left-right axes that passes through the center of the buccal mass. (Eso., esophagus; Inf. buc. gang., Inferior buccal ganglion (approximate internal location); Int. buc. conn., Interbuccal connective (severed end); LMM, lateral mandibular muscle; SMM, superior mandibular muscle; AMM, anterior mandibular muscle; PMM, posterior mandibular muscle; LB, Lower beak; UB, Upper beak; Sheath, buccal mass sheath (note cut edge where sheath is attached to the buccal membrane); Radula, radula and odontophore complex).
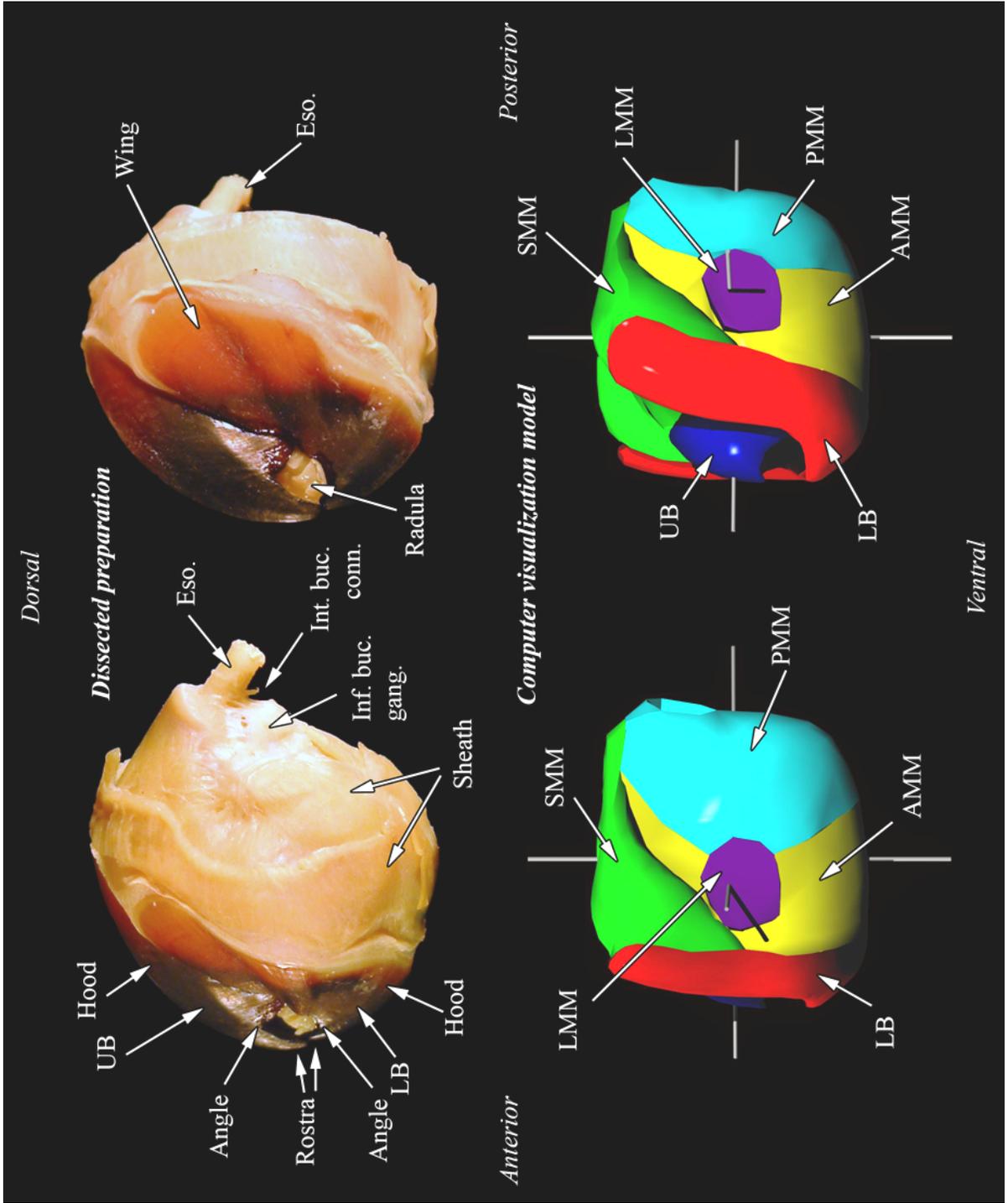
Figure 23
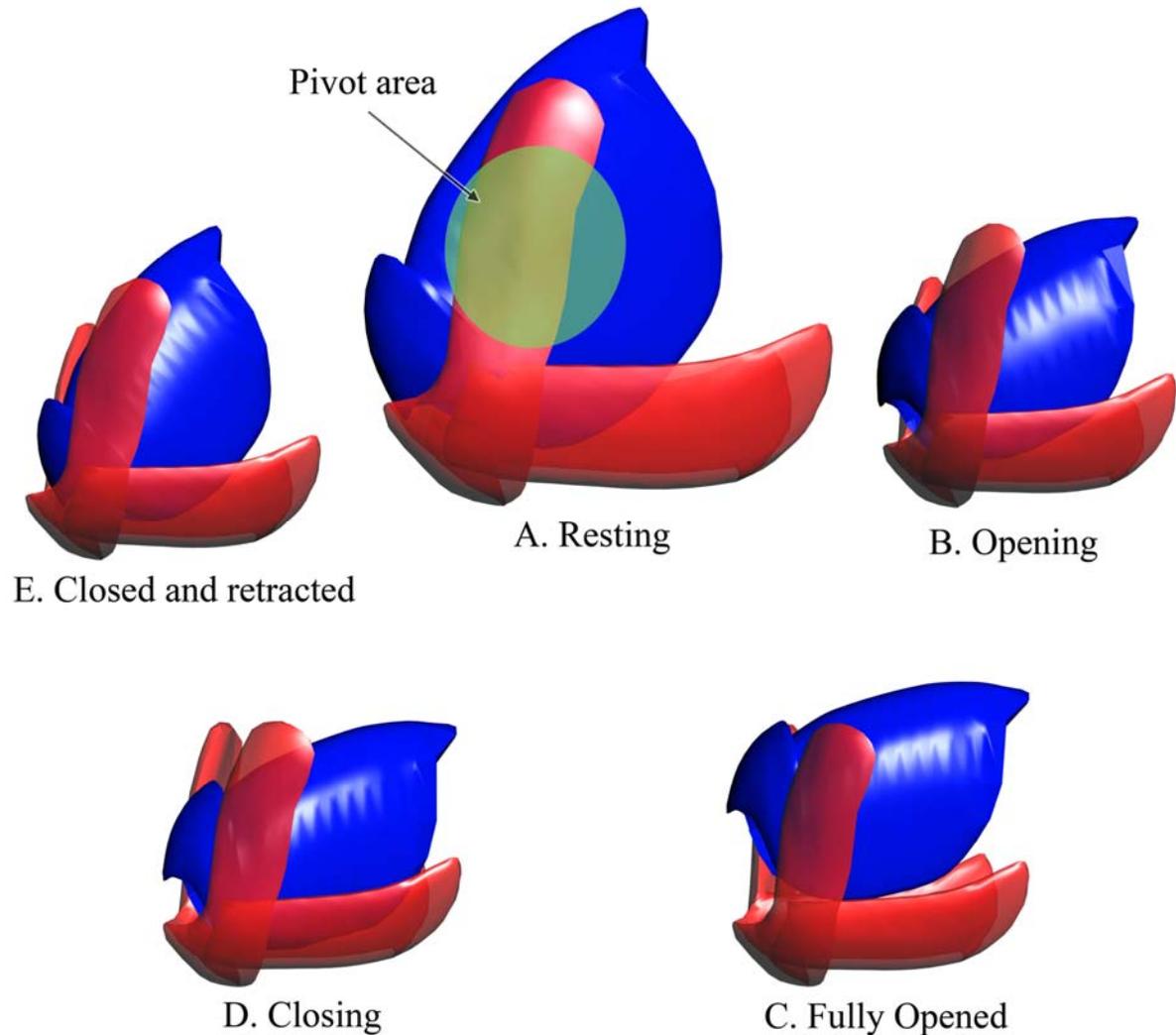
Figure 24. Schematic diagram illustrating the movement of the upper beak (opaque blue) relative to the lower beak (semi-transparent red) during the bite cycle [description follows Kear (1994) and is redrawn from Uyeno and Kier (2005)]. (A) Closed in its resting position (beaks relatively enlarged to illustrate pivot area); (B) opening; (C) fully opened; (D) closing; (E) closed with the upper beak rostrum retracted behind the lower beak rostrum. The axis around which the beaks pivot was observed to be located anywhere in the pivot area indicated in A (resting).

Hypothesized functions of the buccal mass muscles

 My goal is to understand the function of a muscle articulation by examining how the muscles of the octopus buccal mass open, close and otherwise move the beaks. In Chapter 2, I proposed hypotheses of function of the muscle in opening the beaks during the biting cycle. Analysis of this crucial bite cycle phase was therefore a major focus of this study. I summarize below the hypotheses generated from the morphological analysis (Ch. 2) of the role of the various muscles in opening and in other beak movements and describe experimental tests for each.

<u>The superior mandibular muscle</u>

I hypothesize that contraction of the superior mandibular muscle (Fig. 23, SMM, colored green) closes the beaks. Contraction of fibers in the left and right divisions connecting the crest of the upper beak and the wings of the lower beak is predicted to bring the beaks, and especially the rostra, closer together in a closing motion (Fig. 25A). As these lateral divisions of the superior mandibular muscle are robust muscles with a relatively large cross sectional area, I hypothesize that they provide most of the closing force.

Previous studies have provided some evidence that the superior mandibular muscle functions in closing. Boyle et al. (1979a, b) clamped the lower beak of *Octopus vulgaris* and attached a strain gauge to the upper beak with a thread. This approach allowed beak movements to be monitored, although with some mechanical loading from the apparatus. Fine wire electromyography was used to record mandibular muscle electrical activity. Recordings were made during both spontaneous bite cycles as well as evoked bites, in which the ligatured interbuccal connectives were stimulated electrically. Boyle et al. (1979a, b)

concluded that the superior mandibular muscle was active while the beaks were held closed. They also suggested that the superior mandibular muscle was responsible for beak retraction.

In a later study of a variety of coleoid cephalopod buccal masses, Kear (1994) also clamped the lower beak and attached a strain gauge to the upper beak. The superior mandibular muscle was stimulated electrically at five locations along the central division. Stimulation resulted in closing movements at every point tested, but unlike the report of Boyle et al. (1979b), no retraction was observed. In this study, I observed the effect of superior mandibular muscle contraction on upper beak movement without mechanical loading.

The lateral mandibular muscles.

I hypothesize that the paired lateral mandibular muscles (Fig. 23, left and right LMMs colored purple) generate force for opening movements and also help create a dynamic pivot around which beak movements occur. The cylindrical lateral mandibular muscles (Fig. 25) consist of densely packed three-dimensional arrays of muscle. Since they are essentially constant in volume, I hypothesize that contraction of fibers that are parallel to the long axis (Fig. 25, the red lateral fibers of the central diagram) causes the muscle to become shorter and increase in diameter and circumference. This action might push the upper beak away from the lower one because the muscle originates on the lateral wall of the upper beak and passes over the lateral wall edges of the lower beak. The lateral mandibular muscles are the only sizeable muscle groups that include muscle fiber orientations capable of generating the force required to open the beaks. Thus, the definitive test of this hypothesis is whether the beaks can open in the absence of lateral mandibular muscle activity.
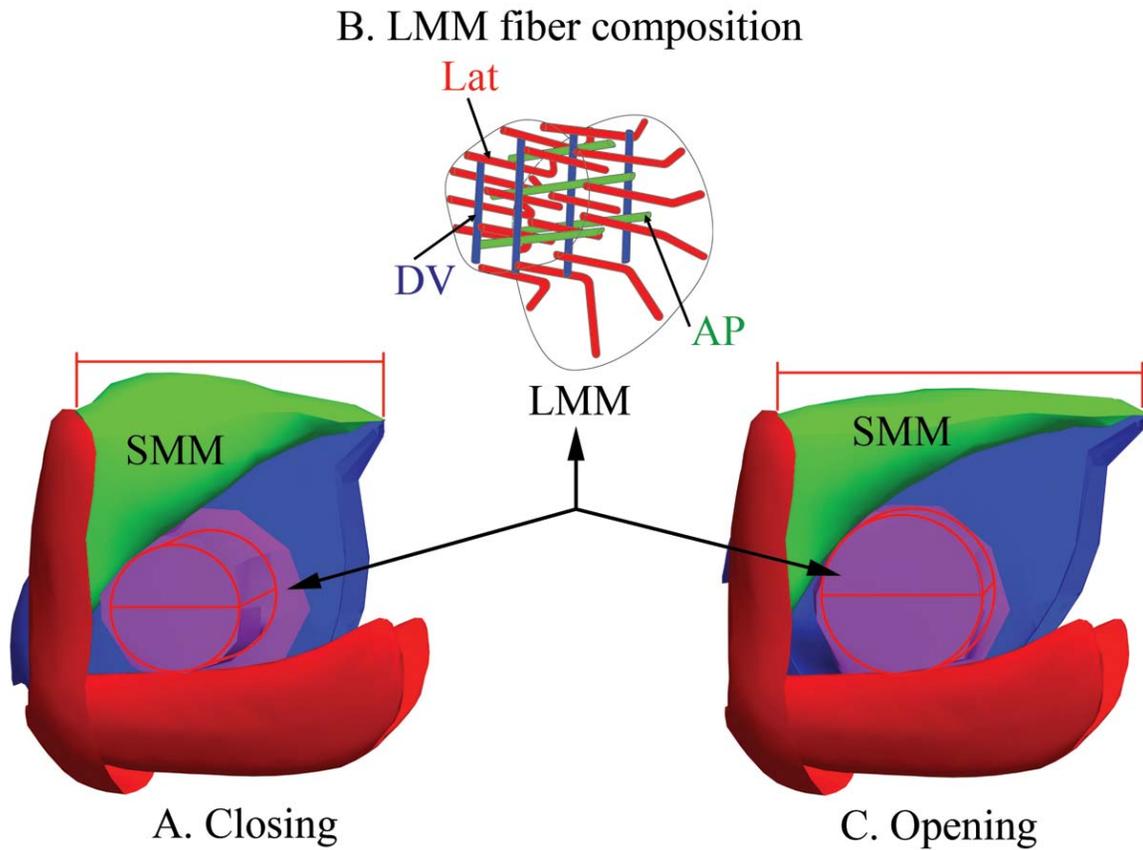
Figure 25. A left side schematic diagram of the hypothesized muscle action during (A) closing and (C) opening states of the superior (SMM, green) and lateral (LMM, purple) mandibular muscles showing dimensional changes seen in the experimental preparation (lower beak, red; upper beak, blue). The central diagram (B) illustrates the cylindrical lateral mandibular muscle with the three fiber orientations: Lat, lateral fibers (red); AP, anterior–posterior fibers (green); DV, dorsal–ventral fibers (blue).

The muscle fiber arrangement within the lateral mandibular muscles suggests that they may also serve as a dynamic pivot for the beaks. The fibers that are parallel to the long axis of the lateral mandibular muscles (Fig. 25, red lateral fibers of the central diagram) may elongate the other fiber orientations [the dorsoventral (Fig. 25, blue fibers in the central diagram) and anteroposterior muscle fibers (Fig. 25, green fibers in the central diagram)] that are arranged perpendicularly to the long axis. As the co-contraction of the perpendicular dorsal–ventral and anterior–posterior fiber orientations will elongate the parallel lateral fibers, the three muscle orientations might serve as antagonists of one another, controlling the shape and stiffness of the lateral mandibular muscle in the manner of many muscular hydrostats. Thus, it is important to note the potential dual function of the lateral mandibular muscles; they might generate force not only for beak opening, but may also be activated with other muscles to stabilize and control the hinge axis or pivot around which the two beaks rotate. This would allow, for instance, the superior mandibular muscle to contract and modulate the angle between the two rostra, instead of simply bringing the two beaks closer together. If the lateral mandibular muscles aid in forming a dynamic pivot for the beaks, they might show activity not only during opening movements but during other beak movements as well.

The hypothesized functions of the lateral mandibular muscle described above differ from previous proposals, in part because they incorporate additional morphological information. Boyle et al. (1979a) observed electrical activity only during closing movements and were unable to record from muscle locations that were active during opening. They therefore considered opening to be a passive movement resulting from the flexion of the lateral walls of the upper beak (Boyle et al., 1979b). Kear (1994) simultaneously stimulated

the buccal mass near the location of the left and right lateral mandibular muscles and found that this opened the beaks. Stimulation of only one side resulted in lateral movement of the upper beak. Interpretation of electrical stimulation experiments is difficult because it is unclear which of the muscles in the lateral portion of the buccal mass were stimulated. Indeed, the inferior mandibular ganglion itself may have been stimulated.

Kear (1994) described the lateral mandibular muscles as originating on the lateral wall of the upper beak and extending both to the ventral side of superior mandibular muscle and to the lateral walls of the lower beak. She suggested that contraction of these fibers pulled the posterior edges of the lateral walls of the upper and lower beaks together. Although Kear (1994) did not identify the pivot mechanism she identified the location of the axis of rotation as being between the lateral mandibular muscles and beak rostra. She concluded that contractions drawing together the posterior portions of the beaks would lever the rostra apart using the pivot area as a fulcrum. The fibers described by Kear (1994) as connecting the upper and lower beak lateral walls were not observed in the lateral mandibular muscles of *Octopus bimaculoides*, or the other species I investigated in the preceding chapter (Ch. 2), so this mechanism cannot function in these species.

Kear (1994) also noted the outward flexion, described by Boyle et al. (1979b), of the upper beak lateral walls. Could this outward flexing cause a shape change in the beaks that would result in opening of the rostra? Presumably this would occur by the flexing of the crest in a way that levers the upper beak rostrum dorsally. This mechanism predicts areas of flexibility of the upper beak itself that can cause shape change. I tested for this possibility as well.

<u>The anterior and posterior mandibular muscles</u>.

Located anterior to both the lateral mandibular muscles (Fig. 23, LMM, colored purple) and the general pivot area around which the beaks rotate (Fig. 24A), the anterior mandibular muscle (Fig. 23, AMM, colored yellow) possesses fibers that connect the upper and lower beaks and is thus hypothesized to function in their closing. The location of the posterior mandibular muscle (Fig. 23, PMM, colored light blue) is opposite to that of the anterior mandibular muscle: it is located posterior to both the lateral mandibular muscles and the beak pivot area. As the posterior mandibular muscle fibers directly connect the two beaks, it is likely that their contraction brings the posterior edges of the beaks together. Because it is positioned posterior to the pivot area, if the pivot area is actively forming a fulcrum, the posterior mandibular muscles may aid beak opening. However, if the pivot area is inactive, then the contraction of the posterior mandibular muscle fibers might simply contribute to the overall closing of the beaks. Given the relatively small cross-sectional areas of these two muscles (see Ch. 2), the forces generated by the anterior and posterior mandibular muscles might be relatively lower than those generated by the superior and lateral mandibular muscles.

Materials and Methods

Fourteen adult *Octopus bimaculoides* (Pickford/ McConnaughey 1949) (91–254 g wet mass), obtained from Aquatic Research Consultants, Inc. (San Pedro, CA, USA) were lightly anaesthetized using 2–3% ethanol in seawater for 2.5–7 min until arm activity ceased (O'Dor et al., 1990). After the specimen was relaxed, the brain was bisected, the interbuccal connectives were severed, and the buccal mass was removed and placed in a glass test chamber containing chilled (17°C) artificial seawater (NaCl, 470 mmol l^{-1}; KCl, 10 mmol l^{-1};

$CaCl_2 \cdot 6H_2O$, 60 mmol l^{-1}; $MgCl_2 \cdot 6H_2O$, 50 mmol l^{-1}; glucose, 20 mmol l^{-1}; Hepes, 10 mmol l^{-1}; adjusted to pH 7.8 with 2.0 mol l^{-1} NaOH) (Milligan et al., 1997). During the experiment, the buccal mass was allowed to rest, unrestricted and ventral surface down, on the bottom to minimize mechanical loading of the joint. Bipolar fine wire electrodes were implanted in the muscles and a pair of silver/silver chloride electrodes was glued to the upper and lower beak rostra and wired to a custom movement monitor circuit (Fig. 26; Appendix I).

The electromyography electrodes were fabricated from Teflon-insulated, half annealed, single stranded stainless steel wire with a bare diameter of 75 µm (A-M Systems, Inc., Carlsborg, WA, USA). Approximately 0.5 mm of insulation was removed from the staggered electrode tips (Basmajian & Stecko, 1962). The inner sharp edge of a hypodermic needle was chamfered (Loeb & Gans, 1986) to prevent damaging the electrode wire. The electrode tips were inserted into the end of the needle and the remaining electrode wire was then folded over the chamfered edge of the needle tip. The needle was then used to insert the electrodes in the muscle of interest and then withdrawn (Parker, 1968), leaving the hooked electrodes embedded in the tissue.

The electrodes were implanted into the left and right divisions of the superior mandibular muscle and the left and right lateral mandibular muscles (Fig. 26). I was unable to reliably implant electrodes into the anterior or posterior mandibular muscles because they were too thin. The signals from four sets of electrodes were fed to a four channel differential AC amplifier (A-M Systems, Inc. Model 1700) and digitized at 5 kHz per channel using a Powerlab 4/20 (AD Instruments, Inc., Colorado Springs, CO, USA) analog to digital conversion unit. The electrodes were dissected out at the end of each experiment to confirm
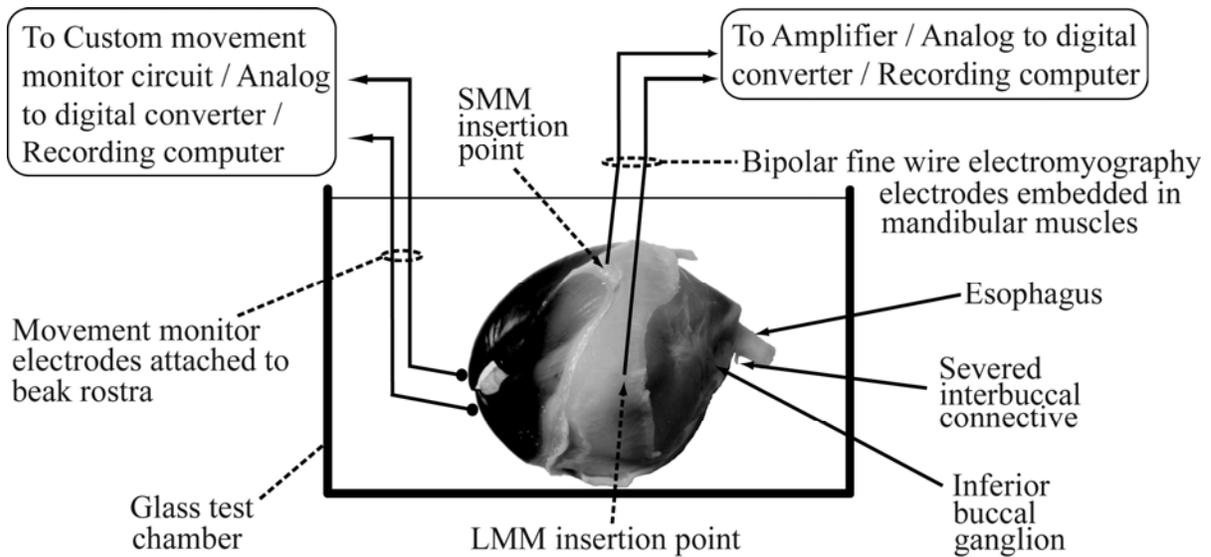
Figure 26. Schematic diagram of the isolated buccal mass preparation showing

electromyography electrode locations in the musculature, and movement monitor electrode

locations on the beak rostra. Also shown are the esophagus, the ligated interbuccal

connectives and the approximate location of the inferior buccal ganglion underneath the

buccal mass sheath.

placement. In two of the preparations, the upper and lower beaks were dissected so as to completely free them from their surrounding mandibular muscles. This was done in order to assess the potential for beak openings based on flexure of the lateral walls. The interbuccal connective and areas adjacent to the electrodes were also electrically stimulated (2.5 v at 60 Hz for 2.5 s) in five of the healthiest preparations (Boyle et al., 1979a).

Beak movements were monitored by a custom movement monitoring circuit (Uyeno & Hsiao, 2007). The details of the construction and use of this device are provided in Appendix I. It measured the resistance between two silver/silver chloride ball electrodes affixed with cyanoacrylate glue to the rostra (Fig. 26). The circuit converted the resistance into an amplified voltage output signal that was fed to a Powerlab 4/25 analog to digital conversion unit. The calibration of the circuit allowed linear distance changes between the electrodes and hence the beaks to be recorded. These data and the electromyographical data were simultaneously recorded to a computer hard drive.

The electromyographical data were analyzed using a routine written for Matlab 7 (MathWorks, Natick, MA, USA) (See Appendix II). The data were DC adjusted to set the mean to zero, rectified (full wave) and then smoothed using a lowpass, second order Butterworth filter with a time constant of 79.5 ms. A Fast Fourier Transform (FFT) frequency domain plot was used to confirm that the cutoff frequency associated with 79.5 ms retained enough resolution to display all pertinent frequencies. Movements were correlated with the electromyographical activity. Onset of activity was calculated using a Matlab 7 routine that automatically determined the standard deviation of the rectified electromyogram signal during a 1 s steady state period prior to muscle activation. Muscle activation onset time was defined as the time at which a threshold of 2.5 standard deviations was reached.

These automatic onset events were visually confirmed and then correlated with movement monitor activity.

Results

Observations of the general bite cycle

The buccal mass preparations of *O. bimaculoides* survived for between 14 and 110 min after being removed. Three phases of beak movement were observed. The first phase, which lasted approximately one quarter of the preparation lifetime, was characterized by strong cycles of biting with a periodicity of 15–20 s (Fig. 27). The typical cycle involved prolonged full opening punctuated by rapid closing and reopening. With age, the time between rapid closings increased and became more variable until it reached 500 s or more, or until no bite cycles occurred. As the bite cycle slowed, the beaks gradually did not open as fully, decreasing to less than half opened. The second phase, which lasted approximately one half of the lifetime of the preparation, was characterized by a simplification of mandibular muscle activation patterns. This resulted in independent activation of the lateral and superior mandibular muscles that could be correlated with beak movements. Only large openings and closings appeared to have continued from the autonomous biting cycle in the first phase, as smaller modulatory and positional movements are not present in the second phase. In this phase, the upper beak translated dorsally in an opening movement (moving from position A to C in Fig. 24) while the closing movement was abbreviated (moving directly from position C to E in Fig. 24): the rotational component of the upper beak closing movement was eliminated, reducing the closure to a combined closing and retraction movement. The third phase of the preparation occurred as the beaks closed and remained in the closed and

92
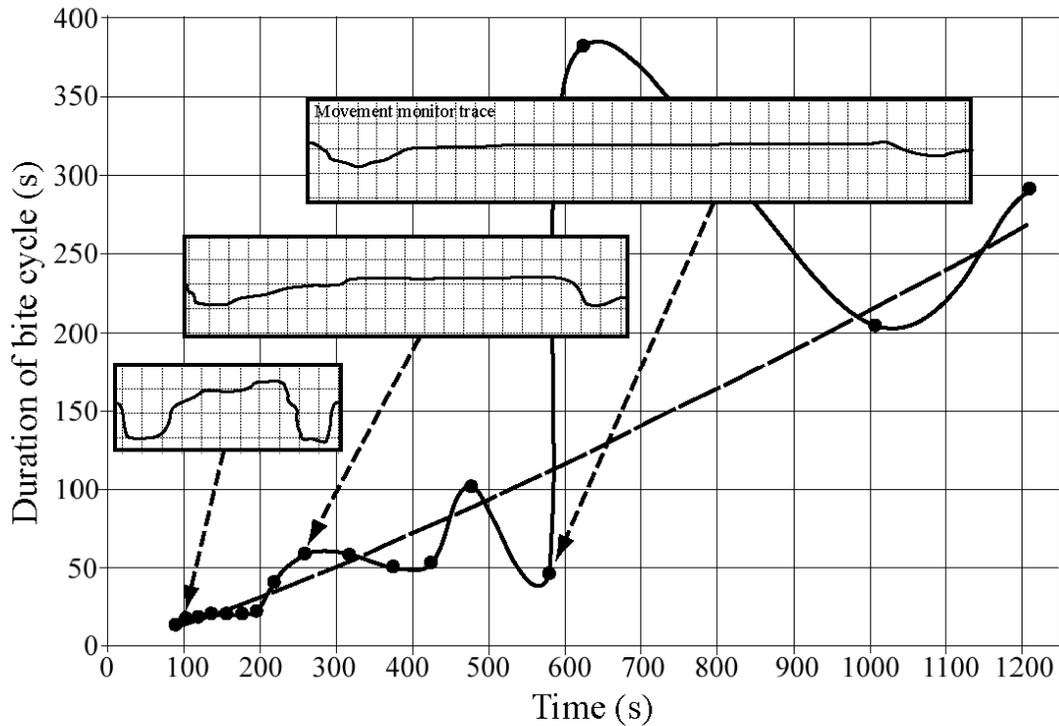
Figure 27. Graph of duration of the bite cycle as a buccal mass preparation ages. The movement monitor traces on the insets represent the relative distance between the upper and lower beaks with respect to time. A rise in the inset traces indicate opening. Although the cyclical beak movements became smaller and the duration became longer as time progressed, the beak was capable of powerful stochastic bites up to the end of the life of the preparation (in this case 2100 s).

retracted position. Although no spontaneous movements were observed, movements could be elicited in this stage by direct electrical stimulation until the preparation died.

Although perhaps more representative of *in vivo* function, analysis of the muscle activation patterns during the first cyclical biting phase (Fig. 28) is difficult because both the superior and lateral mandibular muscles were simultaneously active in almost all phases of the cycle. In the second phase, however, the pattern included only sequential opening, closing, and retraction of the beaks and these frequent movements could be correlated with isolated activity of the left and right lateral mandibular muscles and of the lateral divisions of the superior mandibular muscle. The following is a summary of the muscle activity and correlated beak movements observed in the second stage.

Muscle activity correlated with movements

The electromyographical activities of the lateral and the superior mandibular muscles correlated with beak movements are described below and summarized in Table 4.

Table 4. Mandibular muscle activity correlated with movement of the beaks

	Mandibular muscles				
	Superior (%)	Lateral (%)	Both active (%)	No activity (%)	Total (%)
Openings	51 (27.4)	186 (100)	51 (27.4)	0 (0%)	186 (38.0)
Closings	118 (73.3)	79 (49.1)	50 (31.1)	14 (8.7)	161 (32.9)
No movement	124 (86.7)	107 (74.8)	88 (61.5)		143 (29.1)
				Total	490 (100)
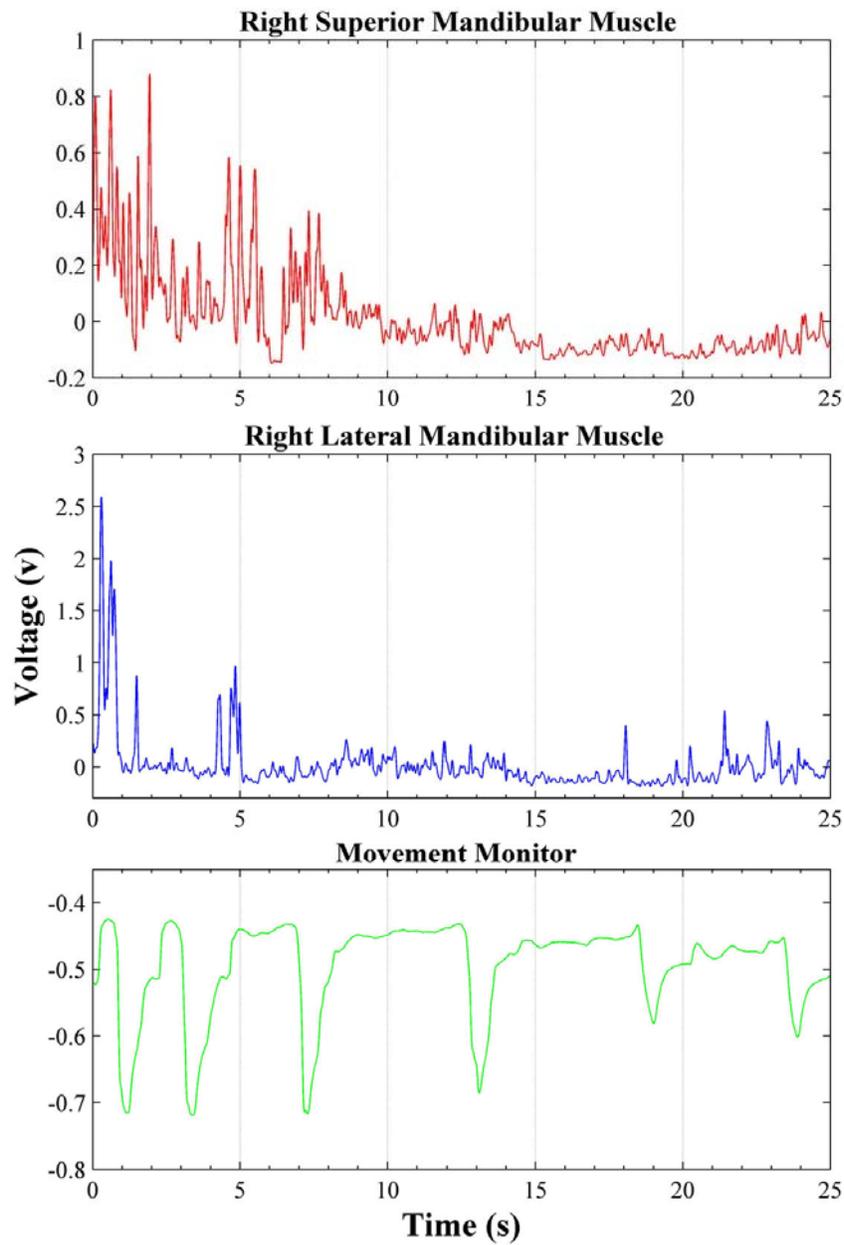
Figure 28. Plots of rectified, averaged electromyograms of the right superior mandibular muscle (A) and the right lateral mandibular muscle (B) correlated with the output of the monitor of beak position (C) during the cyclical biting of a freshly excised beak preparation. The muscle activation patterns are complex and difficult to correlate with beak movements.

Beak opening

The lateral mandibular muscles were active in 100% of all openings. The lateral mandibular muscles were the only muscles active during 72.6% of beak openings and were coactive with the superior mandibular muscle in 27.4% of all openings. Fig. 29 shows an example of three bursts of activity from the left lateral mandibular muscle correlated with three brief beak openings from a half-opened gape. The activity of the left superior mandibular muscle does not show any obvious correlation with beak movements.

Beak closing

The superior mandibular muscle was active either by itself or coactive with the lateral mandibular muscle during 73.3% of all closing motions. The superior mandibular muscle was the only muscle active during 42.2% of all closings and was coactive with the lateral mandibular muscles during 31.1% of all closings. The lateral mandibular muscles were the only muscles active during 18.0% of all closings. In 8.7% of closings neither the superior nor lateral mandibular muscles were recorded as being active. Fig. 30 shows two bursts of superior mandibular muscle activity that correlate with beak closing movements. The largest superior mandibular muscle activity occurs during contact between the upper and lower beaks.

Muscle activity without correlated beak movement

In 29.1% of all muscle activations the superior and lateral mandibular muscles were observed to be active in the absence of beak movement. Both showed activity in the absence of beak movements in 18.0% of all muscle activations. The lateral mandibular muscles were active by themselves in 3.8% of the cases and the superior mandibular muscle was active by itself in 7.3% of cases.

96

Figure 29. Plots of the raw electromyograms (top) with rectified and then averaged signals plotted successively below from the left superior mandibular muscle (A) and left lateral mandibular muscle (B). The bottom traces are the correlated output from the monitor of beak position. Note that beak opening is correlated with activity of the left lateral mandibular muscle.

Figure 29
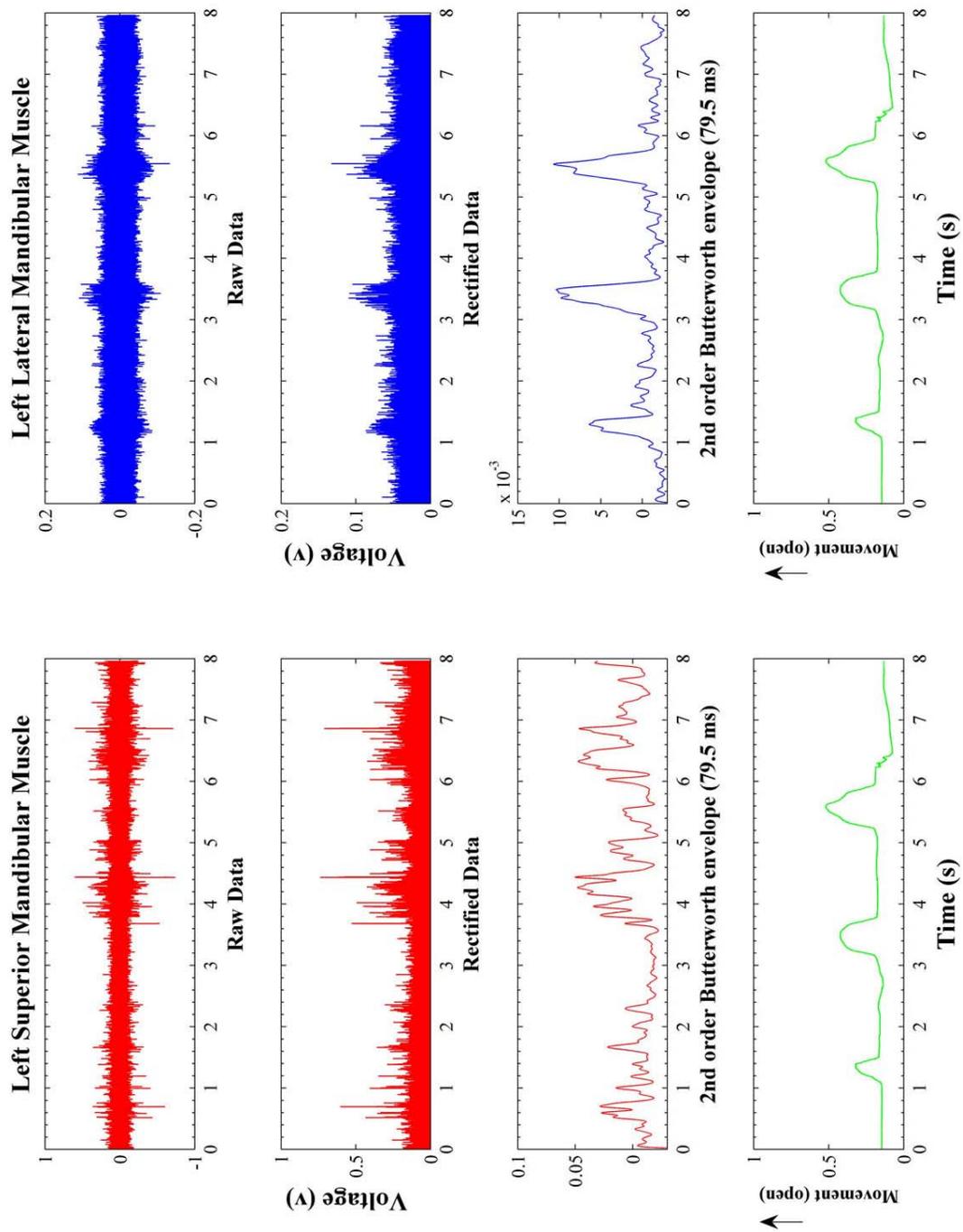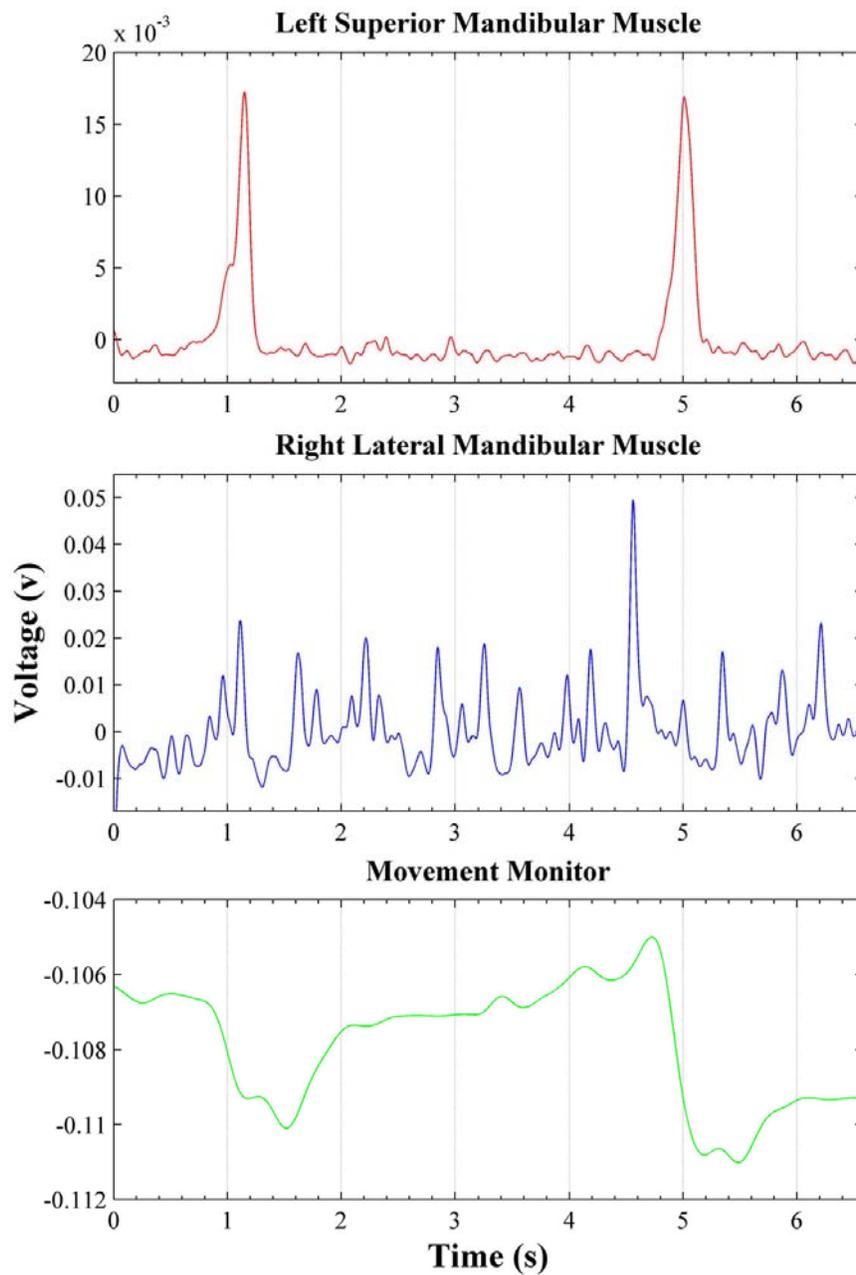
Figure 30. Plots of rectified, averaged electromyograms of the left superior mandibular muscle (upper red trace) and the right lateral mandibular muscle (middle blue trace) correlated with the output of the monitor of beak position (lower green trace). Note that beak closing is correlated with superior mandibular muscle activity.

Observations of beak activity during direct nerve and muscle stimulation.

Electrical stimulation of the beak musculature and nerves was also attempted in order to explore the functional role of the musculature in beak movements. Stimulation of the left or right divisions of the superior mandibular muscle results in asymmetrical beak closing. For example, if the right division is stimulated, the upper beak rostrum closes to the right of the lower beak rostrum. Likewise, stimulation of either the left or right lateral mandibular muscle results in an asymmetrical opening movement. For instance, stimulation of the left lateral mandibular muscle results in opening between the left sides of the upper and lower beaks, but little change on the right. This causes the upper beak to rotate around the anterior–posterior axis, rolling the upper beak by as much as 30° relative to the lower beak. Stimulation of the interbuccal connectives, the neural pathway that connects the brain to the inferior buccal ganglion, elicits a nearly complete bite cycle, in which only the retraction phase seemed to be diminished. The vigor and completeness of the bite cycle decreased as the preparation aged.

Observations of beak movements

It is possible to observe beak movements in an isolated buccal mass of *O. bimaculoides* because portions of both the lower and upper beak are visible. The rostrum, angle and hood of the upper and lower beaks are exposed, and the enlarged lateral wings of the lower beak are also visible (e.g. Fig. 23). During biting movements, the lower beak remains stationary relative to the buccal mass, regardless of the direction of movement of the upper beak or whether the buccal mass is resting on its side, dorsal surface or ventral surface. The upper beak shows five degrees of freedom of movement relative to the lower beak: (1) rotation about the dorsal–ventral axis or yaw; (2) rotation about the anterior–posterior axis, or roll; (3) rotation about the left–right axis, or pitch; (4) translations along the dorsal–ventral

axis; and (5) translations along the anterior–posterior axis. Side to side translations were not observed, but were approximated by a combination of yaw and roll movements. This diverse array of beak movements would be impossible with a simple hinge joint between the two beaks. The musculature that serves as the joint thus allows shearing between the beaks along multiple axes. In addition, it provides for an axis of rotation that can be repositioned within the pivot area, a zone that includes most of the lateral mandibular muscles and an area dorsal and anterior to them.

Flexibility of the freshly dissected beak

The stiffest areas of *O. bimaculoides* beaks are a dark, opaque brown/black color. Less stiff areas are a lighter shade of brown and the most flexible and thinnest areas are tan-colored or transparent. The only flexible areas of the freshly dissected upper beak are the lateral walls, which are capable of flexing outward. Maximal outward flexing results in a 30–40% increase in distance between the lower edges of the upper beak lateral walls. The flexible areas of the lower beaks include the tips of the lateral wings and the posterior edges of the lateral wall. There is a sharp demarcation approximately half way between the jaw angle and the tip of the lateral wing where the wing becomes lighter in color, more flexible and thinner. A more graded demarcation exists near the posterior tips of the lateral walls of the lower beak. Neither the upper nor the lower beaks are capable of significant longitudinal bending, perhaps due in part to their U-shaped cross-section and consequent large second moment of area. Thus, the rostra and crests do not move relative to each other.

Discussion

Kear (1994) noted that the most conclusive evidence for the role of the various muscles in beak movements requires *in vivo* intramuscular electromyography records during

feeding. Although *in vivo* experiments are indeed preferable, they present substantial experimental difficulties because implanting electrodes requires invasive surgery close to the brain, electrode placement cannot be assured because the buccal mass is encapsulated within the base of the arm musculature, and post-operative movements of the octopus often dislodge embedded electrodes (Kear, 1994).

The excised buccal mass preparation is a useful alternative approach. Boyle et al. (1979a) found the autonomous biting movements of the excised beak to be similar to normal beak movements. They suggest that the bite cycle is under the control of a central pattern generator in the inferior mandibular ganglion, which is part of the excised preparation, and thus the similarity to *in vivo* movements is less surprising (Boyle et al., 1979a). The biting cycles of the initial phase of the preparation are similar to those observed *in vivo*, but they are difficult to analyze because of the complexity of movement. Although this complexity is probably more representative of the full range of muscle function in the intact animal, analysis of the less complex, discrete movements found in the second phase is more instructive because the opening, closing, and retracting movements are similar to those of the normal bite cycle and isolated muscle activity can be correlated with specific beak motions. I did not observe this second phase of activity in preparations of the other coleoids studied [the Atlantic brief squid *Lolliguncula brevis* (Blainville 1823) or the cuttlefish *Sepia officinalis* Linnaeus 1758] perhaps because these movements are more apparent in species (such as *Octopus bimaculoides*) in which excised buccal mass preparations have a longer life span.

Assessment of functional hypotheses for the mandibular muscles

The superior mandibular muscle

The superior mandibular muscle is active during the majority of the beak closings and during all of the rapid closings in which the beaks clamp together quickly. This, together with the morphological analysis (Ch. 2) that showed that this muscle contains the largest number of muscle fibers in an orientation that could effect this motion, suggest that the superior mandibular muscle is the prime force generator in beak closure. This muscle is also co-active with the lateral mandibular muscle in 27% of openings, suggesting also that it may either stabilize the beaks or modulate the movements produced by other beak muscles.

The lateral mandibular muscles

No beak openings occurred in the absence of lateral mandibular muscle activity. The lateral mandibular muscles were identified previously as the only muscles that have a fiber arrangement that could produce opening force and they are likely to be the major beak opening muscles postulated in Chapter 2. The competing hypothesis does not seem to be valid: Contraction of the lateral mandibular muscles probably does not elevate the upper beak by flexing the lateral walls. No shape change that results in the movement of the upper beak was observed in the freshly dissected beak. I did observe flexing of the lateral walls in the buccal mass preparation, but agree with Kear's (1994) assessment that this flexion probably accommodates the movement of the palps and radula/ odontophore complex.

Mandibular muscles as a dynamic hinge

In addition to producing the force required to open the beaks, I hypothesized in Chapter 2 that the lateral mandibular muscles may also form a pivot for other beak motions. My experimental results are consistent with this hypothesis, but do not provide a definitive test. If the lateral mandibular muscles are only involved in opening the beaks, activity would be observed only during these motions. I also observed them to be active, often in concert

with the superior mandibular muscle, during closing and during phases without motion. These data suggest that the lateral mandibular muscles may modulate the effects of superior mandibular muscle contraction during the production of complex beak movements, but I cannot determine from my data whether they are simply stabilizing beak movements or if they are serving a more dynamic role in altering the location of the pivot between the two beaks. A definitive test of this hypothesis will require more precise three-dimensional kinematics in conjunction with finer scale sampling of electrical activity from the musculature.

<u>The anterior and posterior mandibular muscles</u>

I was unable to record from either the anterior or the posterior mandibular muscles because the muscle layers were too thin to implant electrodes and the connective tissue sheath surrounding the buccal mass complicated their placement. Although I was unable to test the functional predictions for these muscles it is likely that they produce less force than the superior and lateral mandibular muscles because of their small cross-sectional areas (see Ch. 2). Based on the fiber arrangement, the anterior mandibular muscle may retract the upper beak. The posterior mandibular muscle may maintain tonus of the posterior buccal wall and perhaps, in conjunction with the lateral mandibular muscles, open the beak (Kear, 1994). Tests of these predictions will require a novel experimental approach.

Summary of the opening and closing movement

<u>Closing</u>

The superior mandibular muscles were active during the majority of beak closures, especially the rapid ones of large amplitude. In approximately one quarter of the cases, in which closing was slower and of smaller amplitude, activity was observed only in the lateral

mandibular muscle or no activity was seen in either the lateral or superior mandibular muscles. This suggests three possibilities: the anterior or posterior mandibular muscles may be able to close the beak; elasticity of the buccal sheath may close the beaks; or movement of structures within the buccal cavity, such as the bolsters or the radula/odontophore complex may close the beak.

These conclusions are in general agreement with the data provided by previous studies. Boyle et al. (1979a) correlated the activity of the superior mandibular muscle with both closing and retraction movements. Kear (1994) observed closing movements without retraction in response to stimulation of the superior mandibular muscle. She attributed the retraction to either an artifact of the experimental setup used by Boyle et al. or the activity of the inferior mandibular muscle. In Chapter 2, I re-described anterior portions of the inferior mandibular muscle as the anterior mandibular muscle. The anterior mandibular muscle may indeed be active in retraction, but as described above, I was unable to implant electrodes in this muscle to explore its function.

Opening

I observed the lateral mandibular muscles to be active during every beak opening and thus conclude that their activity is required for this movement. In addition, during opening movements, I observed the axis of rotation of the upper beak relative to the lower beak varied and could be located over a rather large area that includes the lateral mandibular muscles (Fig. 24A). These results differ in some respects from those of previous studies. Boyle et al. (1979a) were unable to correlate any muscular activity to beak opening movements and proposed a passive mechanism. I am uncertain why Boyle et al. (1979a) did not observe muscle activity during opening, but Kear (1994) suggested that the buccal mass sheath may

have insulating properties that hampered recordings. Kear (1994) stimulated the center of the lateral mandibular muscles and found this produced the strongest opening movements. Her results are thus in general agreement with my observations, although she suggested a different opening mechanism (see above).

Conclusions and future directions

The cephalopod buccal mass is a flexible joint in which the lateral mandibular muscle functions as a muscular hydrostat, providing force for opening of the beaks. The superior mandibular muscle probably produces the majority of the closing force. Co-contraction of the superior mandibular muscle and lateral mandibular muscles may stabilize beak movements and might also provide a means of actively controlling the position of the hinge between the beaks. The upper and lower beaks are connected by the lateral mandibular muscles so that they bear any reactive forces generated by the bite and thus they replace the function of the contacting surfaces of articulating skeletal elements. These three functions, a pivot, an antagonistic muscle, and the element that bears compressive and shear forces, are all provided by soft tissue and represent the key functional characteristic of the muscle articulation. Such an arrangement may allow a larger range of motion and greater number of degrees of freedom than a more conventional articulated joint. In the case of the buccal mass, five degrees of freedom were identified (anterior–posterior and dorsal–ventral translations as well as rotations in all three orthogonal planes). A potential trade-off for the gain of this flexibility may be the increased complexity of neuromuscular control that is required to produce this diversity of movement. In cephalopods, an inferior buccal ganglion pattern generator is thought to organize cyclical biting movements that are modulated by input from the brain. This may represent an attempt to reduce the complexity of central nervous control.

There are a number of areas in which further studies should occur. First, as muscle articulation joints might be a more common biomechanical feature than previously recognized, other examples should be investigated in order to identify general functional principles. In documenting this diversity, the feeding and manipulation structures of soft-bodied invertebrates deserve close scrutiny as the morphology, function, and neurobiological control of these joints may provide the diverse and complex motions required of these multifunctional structures. To begin this process, the eversible jaws of marine polychaetes (Ch. 4) and the hooks of interstitial turbellarians (Ch. 5) will be studied as they appear to share many characteristics with the buccal mass of cephalopods. Second, novel use of relatively new technology may allow *in vivo*, three-dimensional recordings that could result in a more complete assessment of muscle function: Magnetic resonance imaging techniques (e.g. Neustadter et al., 2002) that use short durations in order to generate a series of records through time would be useful in better assessing functions associated with complex shape changes in the muscles and buccal mass sheath with respect to the beaks. Third, as neurological input, and not morphology, of the cephalopod buccal mass, may control the range of beak motion, a neurobiological analysis of this joint should be particularly instructive in the basic characterization of muscle articulation function and control. Finally, the diversity and complexity that characterize the motions of animal muscle articulations might be of practical use; perhaps natural examples can inspire aspects of function and design in artificial muscle articulation joint mechanisms.

CHAPTER 4

THE FUNCTIONAL MECHANICS OF RAGWORM JAWS AS A MUSCLE

ARTICULATION

Introduction

In previous chapters, I analyzed animal joint categories (Ch.1) and suggested that flexible joints are under-studied. In particular, I have identified an undescribed type of flexible joint termed a muscle articulation. I reviewed the joint of inarticulate brachiopod valves (Ch. 1), described the morphology (Ch. 2) and function (Ch. 3) of the octopus buccal mass, and suggested that these joints share principles of structure and function. A flexible joint that incorporates a muscular hydrostatic mechanism may allow great diversity and complexity of movement by providing support, generating movement, and bearing joint compression.

This chapter investigates a putative muscle articulation used by a successful group of animals unrelated to those previously studied: the raptorial polychaete annelids. The muscular pharyngeal bulb of the ragworm (or clamworm), *Nereis virens* Sars, 1860, (Fig. 31) supports the motions of two stout jaws used in feeding, defense, and burrowing behaviors. During these activities, this joint accommodates a jaw gape that exceeds that of other muscle articulations.

Annelids are the most complex of all vermiform phyla; they possess a distinct head region, a complete gut, and a coelom that is segmented into metameres by septa (Kozloff,
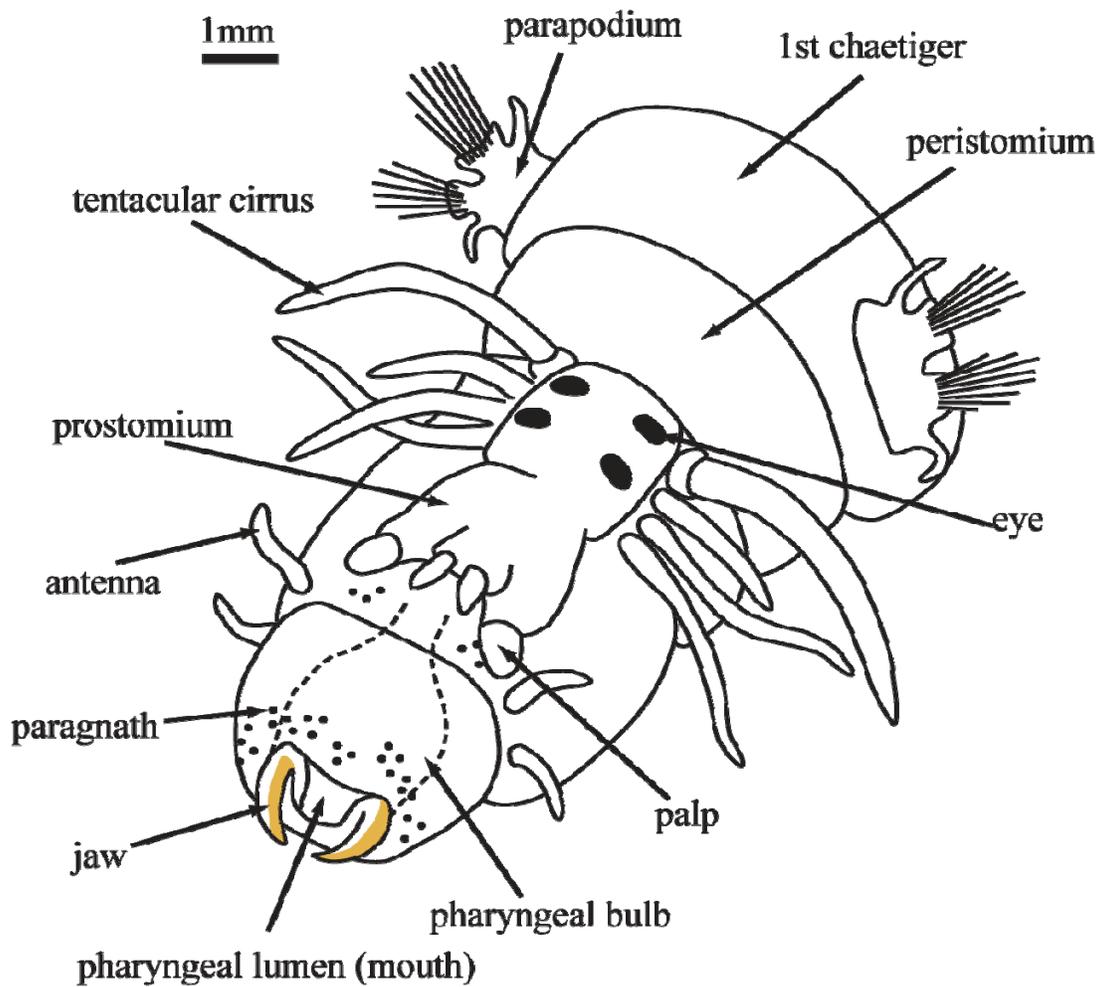
Figure 31. A three-quarter, dorso-frontal view of *Nereis virens*, Sars, 1860. Depicted here is the first body segment (chaetiger) and the head (peristomium and prostomium) with the pharyngeal bulb everted. See text for details.

1990). The segmented coelom allows annelids to locomote with more effective movements than non-segmented worms because the pressure in each section acts as an isolated classical hydrostatic skeleton (Clark, 1964). The body segments (chaetigers) are located posterior to a distinct head region (Fig. 31) formed of two specialized segments; a peristomium that often bears tentacular cirri and the pharynx (Kozloff, 1990), and a prostomium that typically bears the eyes, antennae and sensory palps (Fauchald & Rouse, 1997). Annelids live anywhere that sufficient water is available and owe their success to body plan versatility and the adaptability of the foregut to a diversity of ecological niches (Brusca & Brusca, 2003).

The largest, most diverse, and oldest class of annelids, the Polychaeta, has foreguts that are often modified as armed and eversible stomodeal pharynges that might include a muscle articulation. I begin my assessment of these structures with a brief description of the diversity of polychaete pharynges and feeding modes.

Comprising approximately 63% of all described annelid species (Pechenik, 2000), polychaetes typically live in marine habitats ranging from the intertidal zone to extreme depths. There are, however, a few brackish and freshwater species and at least two terrestrial forms (Brusca & Brusca, 2003). Polychaetes have traditionally been divided into two general groups: the errant, mobile species that live on or in the substratum and the sedentary species that live in simple burrows or protective tubes (Pechenik, 2000). A more ecologically and biomechanically significant categorization of polychaetes that is based on feeding modes was described by Fauchald and Jumars (1979). Here polychaetes can be selective or non-selective deposit feeders, raptorial predators, filter feeders, or even, as in the case of the hydrothermal vent species *Riftia pachyptila*, form autotrophic relationships with symbiotic bacteria (Markert et al., 2007). The comparative analysis of pharynx morphology and ecological

function has been particularly useful in the development of modern theories of polychaete evolution (e.g. Rouse & Fauchald, 1997).

Evolution of the polychaete pharyngeal bulb

Dales (1962) identified a major trend in polychaete evolution that included pharynx position and construction. The plesiomorphic condition is represented by a simple ventral pharynx used by deposit and filter feeders. Subsequently, major evolutionary changes involved either or both the relocation of the pharynx to an axial position and the muscularization of the simple pharyngeal wall to become a fortified pharyngeal bulb. A simple pharynx of axial position evolved independently in the scolecids (non-selective deposit feeders) and the spionids (selective feeders which use grooved feeding palps). The family Eunicidae evolved a ventral muscular bulb which supports complex jaw plates used by both sedentary tube dwellers as well as errant predators (Brusca & Brusca, 2003). Of interest to this study is the axial muscular bulb because it might represent a muscle articulation. Axial muscular bulbs are thought to have evolved a number of times; however, they are most prominently found in the order Phyllodocida (Rouse & Fauchald, 1997) in which they support two large embedded jaw elements.

I studied a phyllodocid from the family Nereidae, because they are large, common, and economically important. Below I review studies of the ecology, natural history, and morphology that consider the form and function of the jaws and bulb.

Natural history and ecology of nereid worms

Nereids comprise a monophyletic and speciose family (Fauchald, 1977; Bakken & Wilson, 2005) which is common in shallow marine habitats but which also occurs in the deep sea, estuaries, freshwater streams, and even temporary rainwater puddles in moist terrestrial

111

environments (Wilson, 2000). It is perhaps their adaptable feeding habits that allow nereids to assume the diverse ecological roles required to exist in these varied environments. Indeed, Goerke (1971) and Fauchald and Jumars (1979) found a variety of feeding habits even within the single genus *Nereis* (N.B. generic synonyms include *Alitta, Hediste,*and *Neanthes*). *Nereis pelagica*, *Nereis virens* and *Nereis diversicolor* are omnivorous, feeding on algae (see also Copeland & Wieman, 1924), detritus, and invertebrates such as small crustaceans, other polychaetes, and even small bivalves (Lewis & Whitney, 1968; Commito, 1982; Ambrose 1984a, b; Commito & Shrader, 1985). Specialists include the carnivorous *Nereis fucata*, a species commensal with crabs, and the herbivore *Nereis brandti*, which feeds primarily on green algae. Additionally, a number of omnivorous species are also known to supplement feeding by directly absorbing dissolved organic matter (Stephens, 1968).

The species investigated in this study, *Nereis virens*, is widely distributed. It is found on both sides of the North Atlantic and northern Pacific oceans (Wilson & Ruff, 1988) living in high densities near the low water mark of sandy and muddy shores, under cobbles and boulders of rocky shores and under attached algae (Pettibone, 1963). Its range extends as far south as France in Europe and to Virginia off the east coast of the United States. In the north of the Pacific Ocean, it has been recorded from Alaska to central California, in the Bearing Sea, and off the coasts of Japan (Wilson & Ruff, 1988). Because of its ecological importance to local trophic structure (Commito, 1982), commercial importance as fish bait [and the resulting threat of over harvesting, see Brown (1993)], use as a model organism in physiology (Bryan & Gibbs, 1979) and endocrinology research (Hofmann & Schiedges, 1984) and as an indicator organism in environmental research (Goerke, 1979), periodic

assessments focus on both the European (e.g. the United Kingdom; Olive, 1993) and North American (e.g. the United States, Wilson & Ruff, 1988) populations of *Nereis virens*.

Use of the pharyngeal bulb

Nereis virens uses pharyngeal bulb eversions and quick and forceful jaw movements in feeding, defense, and burrowing.

The feeding modes and diets of *Nereis* species vary greatly (Goerke, 1971) even though morphological variation of the jaws and pharyngeal bulb may be small (Pilato, 1968a) and the jaw movements (Turnbull, 1876; Gross 1921; Copeland & Wieman, 1924) are similar. A generalized biting movement has been observed: the proboscis is rapidly turned inside out so that the pharyngeal bulb is placed in the anteromost position (Fig. 31) with the jaws positioned in a half-opened gape. The jaws are opened and closed to cut algal blades or large prey. Smaller pieces of food are then grasped with the jaws and the bulb is retracted.

Nereis virens also uses armed pharyngeal bulbs in defense behaviors. As the preferred prey of many fishes, *Nereis virens* is especially vulnerable when swimming in the open water column. Thus, they are extremely thigmotactic (Copeland & Wieman, 1924) and spend most of their time in loose flexible tubular burrows within mud or under stones (Turnbull, 1876). *Nereis virens* preferentially feeds from the mouth of these mucous-lined burrows (Fauchald & Jumars, 1979; Wilson & Ruff, 1988) and will vigorously defend them against predators and conspecific competitors (Turnbull, 1876; Gross, 1928; Evans, 1973; Miron et al., 1992a, b; Lewis et al, 2003). These defensive behaviors use pharyngeal bulb movements that are roughly similar to prey capture and food item manipulation: quick extensions of the pharyngeal bulb followed by a forceful closing of the jaws as the proboscis retracts. A single bite is capable of cutting the body of an adult conspecific competitor in half (Turnbull, 1876).

The bulb of *Nereis virens* is also used in burrowing though muddy or fine sandy substrates (Pettibone, 1963; Reise, 1981). Studies by Dorgan et al. (2005, 2006) have shown that cohesive muddy and sandy sediments behave like elastic solids, and the pharyngeal bulb is used in burrowing by causing cracks to propagate through the substrate. Instead of digging or pushing its way through the substrate, the worm extends its pharyngeal bulb and uses it as a wedge to propagate a discoidal crack in the direction of travel. The function of the jaws in crack propagation burrowing has not yet been considered.

Jaw morphology and paleontology

Preserved polychaete jaws, or "scolecodonts" (Croneis & Scott, 1933), are well represented in the fossil record. Since their earliest descriptions, such as those by Eichwald (1854), these microfossils have become important in biostratigraphy and polychaete phylogeny (Toomey et al. 1974). By analyzing descriptions of complete jaw apparatuses, Jansonius and Craig (1971) found evolutionary changes to be relatively apparent and identified twenty Paleozoic polychaete genera. Of these, however, they were only able to identify four genera that might represent ancestors of modern families. Nonetheless, phyllodocid scolecodonts are well-represented throughout much of the Paleozoic, being most diverse in the Upper Ordovician, Silurian, and Devonian. The oldest known specimens occur in Lower Ordovician rocks (Szaniawski, 1996).

Jansonius and Craig (1971) established the terminology used to describe scolecodonts and to some extent, jaws of extant polychaetes. A large number of these terms describe the multi-element articulating jaw assemblages of the ventral muscular pharynges of eunicid polychaetes. The terminology associated with the non-articulated jaws of nereid polychaetes (Fig. 32) is simpler, as they comprise fewer elements: two sharp, hook-shaped jaws and an

array of smaller inclusions known as paragnaths (Fig. 31). *Paragnaths* are small, button-shaped teeth found in various places on the pharynx in highly variable numbers which may vary with age, size, feeding regime, salinity, and nature of the sediment (Zghal & Amor, 1986). The left and right *jaws* resemble open-ended cones with curved anterior tips. These sickle-shaped extended tips are known as *falx* when very strongly curved (Fig. 32A). In nereid jaws (Fig. 32D-E), because the tips are somewhat less pronounced, they are referred to as *fangs*. A series of teeth, or *denticles*, are found along the hardened *inner margin* formed at the sharp edge of the *inner face* (Birkedal et al., 2005). The opening at the base of the cone is referred to as the *myocoele opening* and leads to an inner space known as an *antrum* or *myocoele*. The myocoele opening creates the inner and outer surface area to which the pharyngeal bulb musculature attaches.

Polychaete jaws are formed by hardening of specific areas of the pharyngeal epithelium (Paxton, 2004). Whereas some eunicid polychaetes periodically shed jaw elements and replace them with larger ones, others have elements which grow throughout the lifetime of the animal (Paxton, 1980). The presence of small channels extending throughout the jaws of *Nereis* species suggest that they are remodeled throughout life (Birkedal et al., 2005). Lichtenegger et al. (2003) demonstrated that the jaws are composed of glycine- and histidine-rich protein fibers and that the areas requiring wear resistance or stiffening are biomineralized by an inorganic zinc-chloride compound.
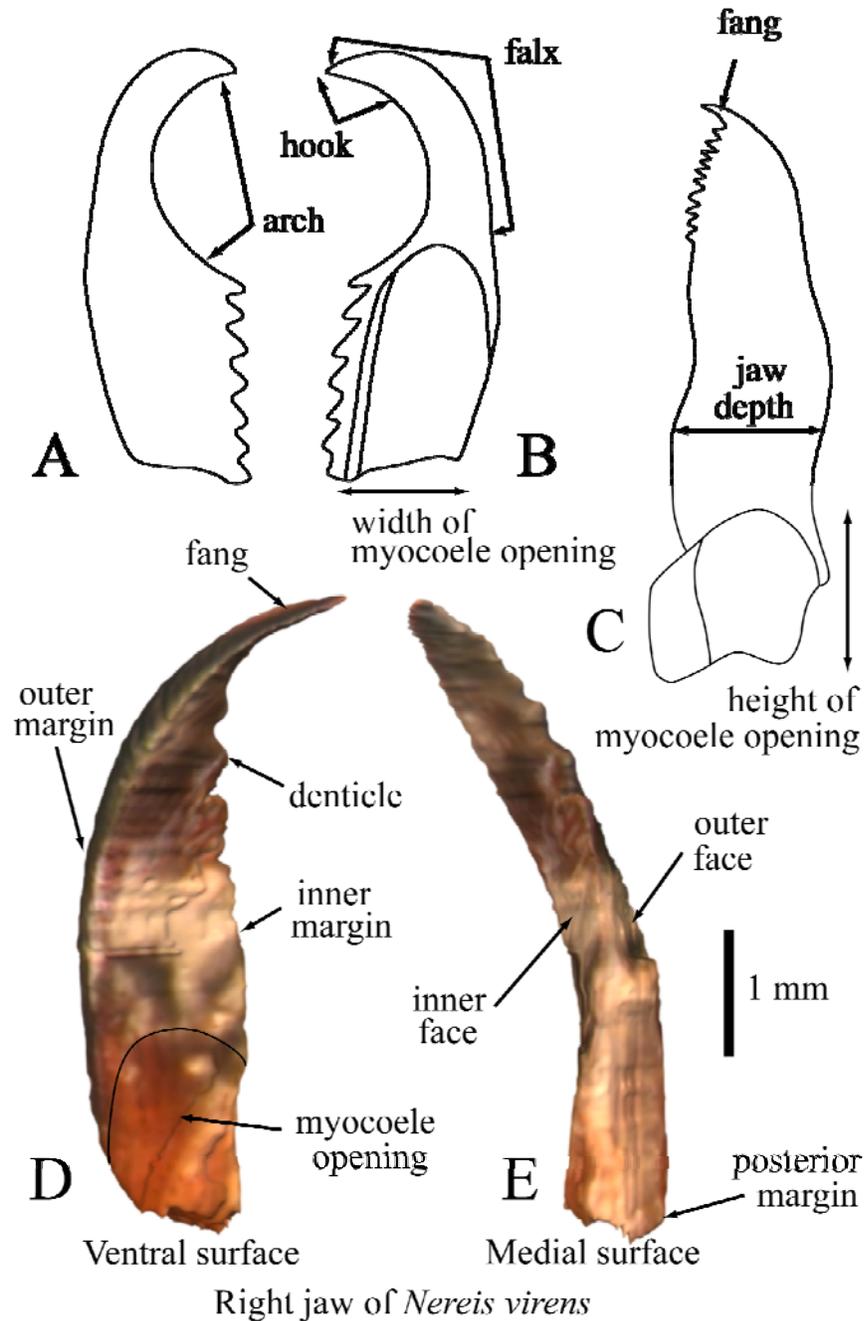
Figure 32. Illustrations of various jaw elements. A-C, Eunicid jaws (from Jansonius & Clark, 1971); A and B show a jaw element with a robust falx and flaired myocoele opening; C shows a deep jaw element with a small fang. D-E show a ventral and medial view of a three-dimensional digitized model of the right jaw of *Nereis virens*. See text for explanation of terms.

Pharyngeal bulb morphology and functional hypotheses

Pilato (1968a, b) described the morphology of the pharyngeal bulb and proboscidial eversion and retraction musculature in *Perinereis cultrifera* (Grube, 1840). The descriptions are useful here because the structures are similar in *Perinereis* and *Nereis* (Pilato, 1968a). Additionally, these studies attempted to describe the morphology from a functional perspective, whereas many previous descriptions emphasized systematics and taxonomy (eg. Ehlers, 1864; Regnard 1913).

Pilato's separate treatments of the proboscis (1968b) and the pharyngeal bulb (1968a) mechanisms reflect their independent functions. The proboscis includes structures external to the pharyngeal bulb that are responsible for eversions and retractions. Eversions are thought to be hydraulic, using coelomic fluid pressure generated by the body wall musculature. Pilato (1968b) noted that antagonistic adductor muscles may help orient the proboscis as it is being everted and retract it. The pharyngeal bulb is described by Pilato (1968a) as the terminal anterior portion of the foregut that has evolved thick muscular walls. Superficially, the morphology of the bulb seems simple; it resembles a dorsoventrally flattened prolate eliptoid in which the left and right jaws are embedded on either side of an anterior pharyngeal opening (mouth) that extends through the center of the bulb to exit posteriorly as the esophagus. The musculature that forms the bulb, however, is complex; it contains many muscle fiber groups that vary in orientation relative to each other.

To facilitate the description of this complex intrinsic bulb musculature, Pilato (1968a) categorized the muscle groups into those that originate on the jaws and those that do not. The muscles that originate on the jaws include thirteen pairs of jaw protractors and retractors, jaw base adductors and abductors, jaw fang adductors, and jaw elevator and depressor muscles.

He named them according to their hypothesized roles in jaw movement, but these actions have not been confirmed experimentally. Muscles not directly attached to the jaws include eight orientations of muscle fibers that tend to be dispersed throughout the three-dimensional bulb structure, and are named for their orientations rather than their actions: the superficial circular, transverse and longitudinal fibers, radial fibers, dorsoventral transverse fibers and posterolateral fibers.

Pilato (1968a) intended his analysis purely as a morphological description to be used as a basis for future functional studies. Thus he does not advance functional hypotheses further than the muscle group names indicate. One difficulty in assessing the function of muscle groups with varying orientations is in understanding how the contraction of one orientation affects others. This is because the muscle fibers might not be organized as discrete bundles and might instead be dispersed in an interdigitating pattern to form a three-dimensional block of solid muscle. Further, the function of fibers that originate on the jaws and insert of the flexible surface of the bulb might be difficult to interpret; would their contractions reposition the jaws or simply deform the bulb surface? Given these outstanding issues, I identify areas in which additional morphological detail may help in generating hypotheses of jaw function. As the solid block of muscle contains varying fiber orientations, it may constitute a muscular hydrostat capable of providing the functions of a muscle articulation. Thus, the first goal is to describe the pharyngeal bulb of *Nereis virens* and to compare its muscle morphology to that of *Perinereis cultrifera* in order to assess whether this structure is a muscle articulation with muscle fibers organized as one or more multifunctional muscular hydrostats. Second, only the muscle fibers have been described in detail. As the presence of non-muscular components may be functionally significant, the connective tissue

of the pharyngeal bulb is also described. Finally, as direct *in vitro* and *in vivo* techniques are not currently possible with *Nereis virens*, I conducted a video analysis of aggressive biting behavior associated with burrow defense in order to estimate contraction and elongation distances of various muscle fiber orientations during biting. These measurements provide a preliminary test of the hypotheses of muscle function.

Materials and methods

Twelve adult (~200 mm length) *Nereis virens* specimens were donated by Peter Cowin of Seabait (Maine) L.L.C. (Franklin, ME), a commercial polychaete aquaculture company. The specimens were maintained in two 19 L glass aquaria fed by a continuous flow of aerated artificial seawater (21°C, 35-38 ppt salinity) filtered by a larger aquarium system with an 1890 L sump. Twelve glass tubes of 10 mm inner diameter were cut to 200mm lengths and fire-polished to smooth the openings. These served well as artificial burrows when placed on the bottom of each tank. Specimens were put on a 10h light: 14h dark cycle and were fed every other evening with small single pieces of either shrimp or squid.

Eight specimens were processed for histology. They were quickly anaesthetized using 1.5% ethanol in seawater (adapted from O'Dor et al., 1990) until they did not respond to touch. Then the pharyngeal bulb was exposed by a ventral incision made from the 6th body segment to the tip of the peristomium. In two specimens, the anterior ends were then cut off at the 6th body segment and fixed whole. These were used in gross anatomical dissections to identify and photograph major pharyngeal bulb features (such as overall shape, position of the jaws, and visible muscle groups). In six specimens, the pharyngeal bulbs were dissected free from the proboscis walls and the protractor and retractor muscles and then immediately

119

fixed for at least 48 h in buffered formalin in seawater (10% v/v, Kier, 1992) and prepared

for serial sectioning. The jaws of one bulb were dissected out in order to avoid the

complications of microtome sectioning through hard materials. The bulb was dehydrated,

embedded in paraffin (Paraplast Plus, Monoject Scientific, St. Louis, MO), and serially

sectioned in the transverse plane using disposable steel knives at 10-12μm. These sections

were stained using Milligan's Trichrome stain and Picro-Ponceau with Hematoxylin stain on

alternate slides (Kier, 1992) and examined by brightfield microscopy. I found that removal of

the jaws caused excessive damage to the surrounding tissue and therefore the remaining

bulbs were embedded in glycol methacrylate plastic (JB-4, Structure Probe, Inc. West

Chester, PA) and serially sectioned in transverse, parasagittal, and frontal planes using either

tungsten carbide or long edge glass Ralph knives (Bennett et al., 1976) at a thickness of 2.5

μm. Every fifth section was collected and stained using either a Toluidine blue stain (2%

Toluidine blue O (C.I. 52040) in 2% sodium borate; modified from Burns, 1978) or a

Toluidine blue/Basic fuchsin stain [1% Toluidine blue O (C.I. 52040) in 1% sodium borate

and 0.1% Basic fuchsin (C.I. 42510); modified from Blaauw et al., 1987] in order to

differentiate muscle and connective tissue. Sections were examined by brightfield and

polarized light microscopy.

A three-dimensional model of the muscles and connective tissues was constructed

using 3D modeling software (Anim8or, http://www.anim8or.com). The basic outline of the

pharyngeal bulb was drawn using digital photographs of the dissection and then section

outlines were digitized for incorporation into the model. The dimensions of the model were

then adjusted by matching approximately 150 points on the model to measurements of

corresponding points in the pharyngeal bulb. The jaws that were removed from the paraffin

embedded bulb were optically digitized using a custom made microscope stage that precisely rotated the jaw through 360° in 22.5° increments. In consultation with Dr. Pollefeys and Dr. Vicci (UNC-CH Computer Science Department), computer generated contours of the jaws from the resulting photomicrographs were then recombined to form a high resolution three-dimensional reconstruction of the jaws.

The last four specimens were observed to record behaviors involving pharyngeal bulb movements. A custom glass aquarium was built (150mm height x 150mm width x 600mm length) with a frame that held a mirror below it angled at 45°. This allowed simultaneous digital video recording of both a side and bottom view of specimens either guarding their glass tube burrows or burrowing through a single layer of 15 mm clear glass balls. Digital video recordings (30 frames per second; 530 lines of horizontal resolution) of bites performed as part of burrow guarding behaviors were analyzed frame by frame using Adobe Photoshop CS2 (Adobe systems Inc., San Jose, CA) and Image J (a public domain Java version of the image processing and analysis program NIH Image; http://rsb.info.nih.gov/) to identify changes in jaw positions when they were exposed during pharyngeal eversions.

Results

Jaw morphology

The terminology describing the jaws of *Nereis virens* follows Jansonius and Craig (1971). As the jaw description is based on only two adult, farm raised specimens, the variation within natural populations has not been assessed. The conic jaws (Fig. 32 D-E) have a left and right chiral symmetry, are relatively shallow in their lateral thickness (termed "jaw depth"; Fig. 32C), and bear a twisting curve along their lengths that result in an inward and slightly ventrally pointing fang. The jaws are dorsoventrally compressed to form a

ventral and a dorsal face (usually referred to as an "inner" and "outer" face because of the length-wise twisting curve of the jaws) and thus a sharp inner (or medial) and a broader outer (or lateral) margin. The myocoele opening at the base is slightly flaired, allowing for greater muscle attachment surface area, and leads to a large myocoele that extends somewhat into the denticles. There are approximately six free denticles that are separated by narrow spaces along the inner margin. The free denticles have a strong anterior inclination towards the fang. The posterior end of each jaw, approximately half of its length, is embedded within the tissue of the pharyngeal bulb.

Pharyngeal bulb musculature

The pharyngeal bulb of *Nereis virens* resembles a bilaterally symmetrical, dorsoventrally flattened prolate elliptoid with the foregut lumen extending through the center along the long axis (Fig. 33A). The esophagus extends from the posterior end of the pharyngeal bulb and the jaw tips protrude from the anterior end on either side of the mouth or pharyngeal opening. The muscular proboscis wall is attached to the pharyngeal bulb at a location lateral to where the jaws protrude. As many of the muscle fiber orientations of this bilaterally symmetrical muscle mass (Fig. 33B) resemble those of *Perinereis cultrifera* (Pilato, 1968a), I use consistent terminology in the description of *Nereis virens*. I use images of three-dimensional computer models to describe the complex orientations of muscle fibers. The fibers in the illustrations are fewer in number and larger in size than in life.

<u>Jaw elevators and depressors</u>

Rather than being organized into two discrete muscle groups, the jaw elevator and depressor muscle fibers (Fig. 34) are interspersed in between other muscle fiber orientations.
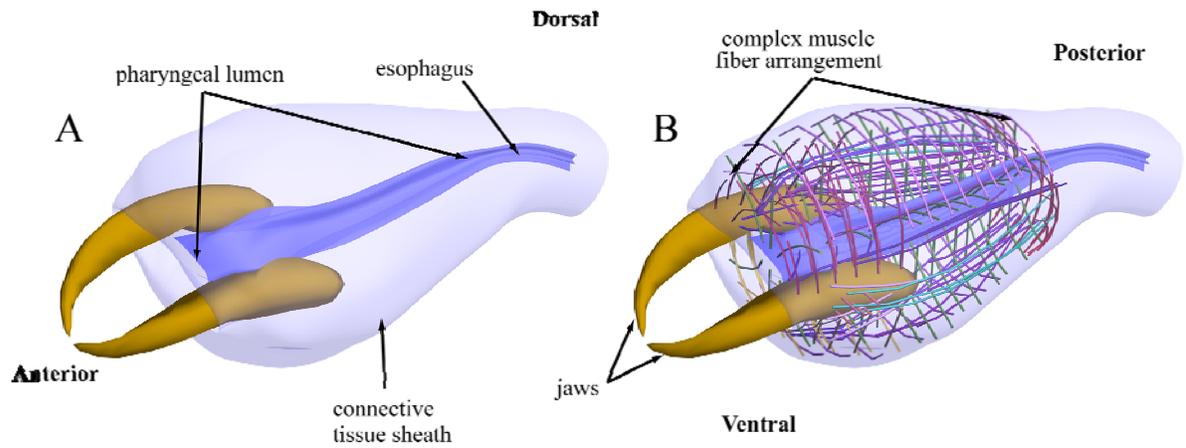
Figure 33. An antero-dorsal three-quarter left side view of the three-dimensional reconstruction of the pharyngeal bulb. A) The bulb without muscle fibers. B) The bulb showing all fiber orientations. Note the orientation of this view as it is used as an inset to aid understanding of orientations of other structures in subsequent images.
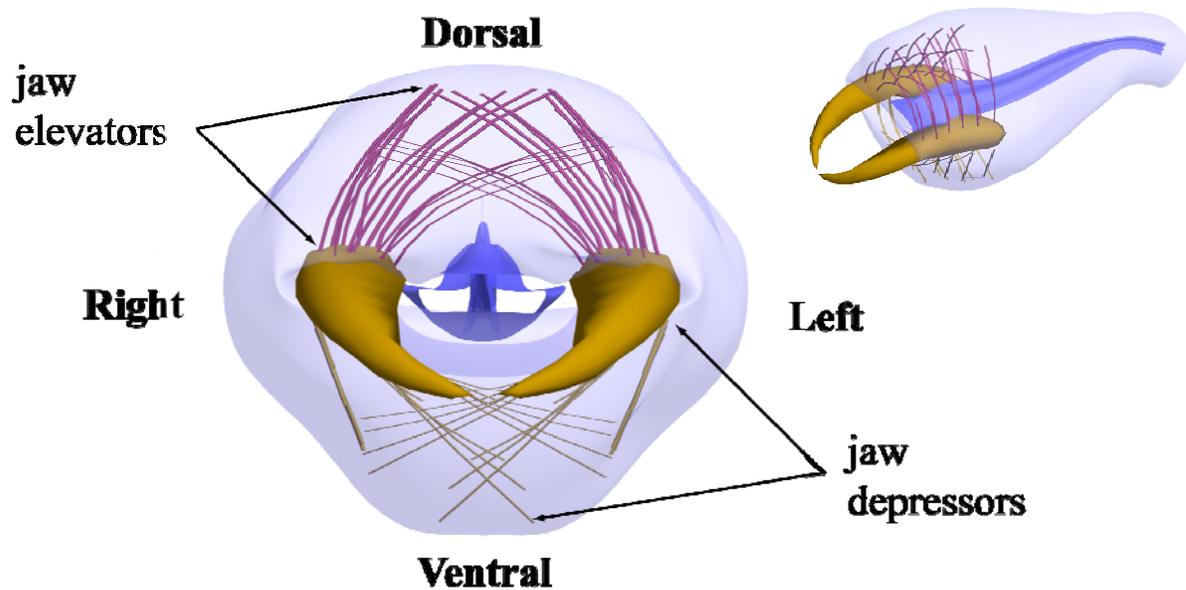
Figure 34. An anterior view of the dorsal jaw elevator (mauve) and ventral jaw depressor (gold) muscle fibers. Note that these fibers cross over each other above and below the foregut lumen.

The left fibers extend over the midline to cross the right fibers. Also, other muscle fiber orientations, such as the superficial longitudinal and transverse fibers and the lumen dilators, regularly pass in between the elevator and depressor muscle fibers. The jaw elevators (also appearing in figs. 36 & 40) originate on the outer (dorsal) face of the left and right jaws and extend medio-dorsally in a curved radiating pattern towards the dorsal surface of the bulb where they insert on the pharyngeal bulb connective tissue sheath. The jaw depressors originate on the inner (ventral) face of the left and right jaws and extend in a similar radiating pattern to insert on the connective tissue sheath of the bulb's ventral surface.

Lumen dilators

The lumen dilators (Figs. 35 & 36) are radial muscle fibers that are dispersed along the longitudinal axis of the pharyngeal bulb. The fibers originate on the lumen walls of the foregut and extend radially in all directions to the outer surface of the bulb and insert on the surrounding connective tissue sheath.

Jaw adductors

The jaw adductors are muscle fibers that originate along the medial posterior surfaces of the jaws (Fig. 37). These points of origin include both external jaw surfaces as well as the surface within the myocoele opening. These fibers are divided into anterior and longitudinal adductors depending on their insertion points. The anterior adductor fibers insert along the lateral surfaces of the anterior portion of the foregut within the pharyngeal bulb. The fibers of the longitudinal adductors extend toward the posterior of the pharyngeal bulb where they insert on the basal bulb muscle fibers at the posterior end of the bulb and the beginning of the esophagus.
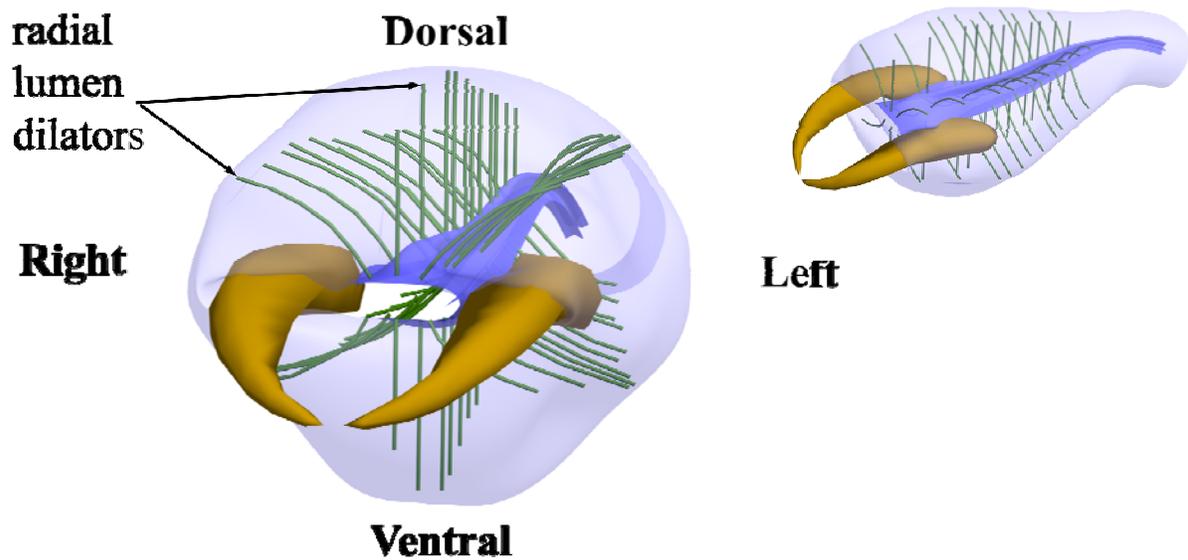
Figure 35. Anterior view of the pharyngeal bulb (rotated slightly to the right) showing the lumen dilator muscle fibers (green) extending radially from the foregut lumen wall to the outer surface of the bulb.
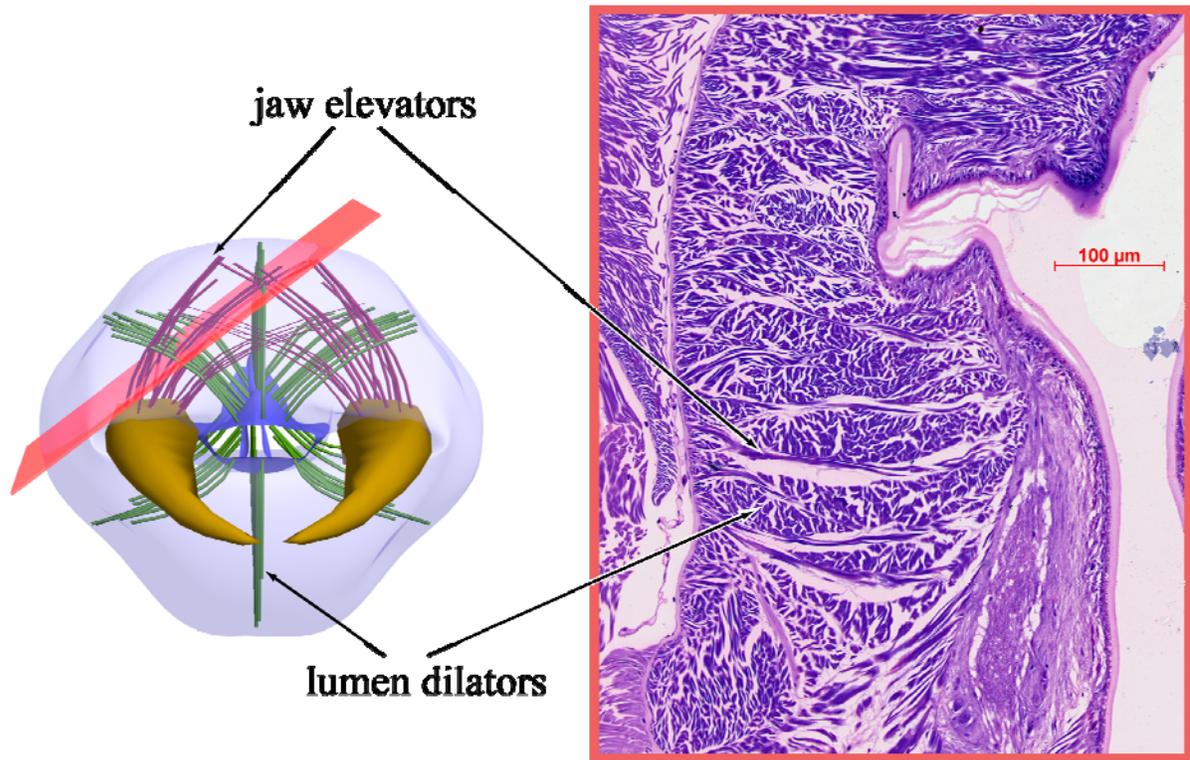
Figure 36. Left: anterior view of the pharyngeal bulb showing the elevator muscle fibers (mauve), the lumen dilator muscle fibers (green) and a red oblique frontal section plane indicating the approximate section corresponding to the histological micrograph on the right. The micrograph shows the interdigitation of the jaw elevator and the radial lumen dilator muscle fibers. Brightfield micrography of section stained with Toluidine blue/Basic fuchsin.
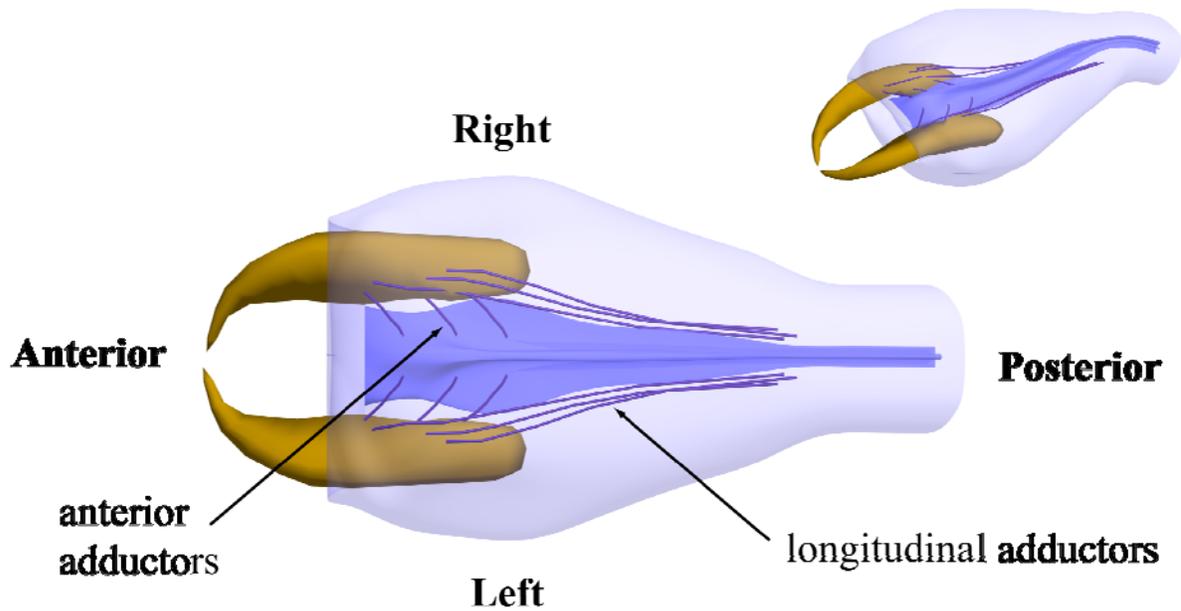
Figure 37. A dorsal view of the pharyngeal bulb showing the adductor muscle fibers (dark blue). These fibers separate into the anterior and the longitudinal fiber orientations. They insert on the medial jaw surface as well as within the myocoele.

<u>Jaw abductors, protractors, and retractors</u>

The jaw abductor, protractor, and retractor muscle fibers (Fig. 38) cross and interdigitate with one another. They originate on the lateral most posterior surfaces of the jaws. The abductors are short fibers that extend radially from their origin to insert on the connective tissue sheath surrounding the lateral edges of the pharyngeal bulb. The protractors originate on the extreme postero-lateral edges of the jaws and extend anteriorly to insert on the connective tissue sheath in the area lateral to where the jaws emerge from the bulb musculature. The retractors are longitudinal fibers that extend from their origin to insert on the basal bulb muscle fibers at the posterior end of the pharyngeal bulb.

<u>Deep longitudinal muscle fibers</u>

The deep longitudinal muscle fibers are found between the posterior margin of the jaws and the posterior end of the bulb. They might represent retractor and longitudinal adductor muscle fibers that have subdivided in this area as they are longitudinally oriented and insert on the posterior end of the bulb. However, tracing these fibers back to their origin on the jaws is difficult since groups of these fibers seem to end near the posterior edge of the jaws, and thus might originate within the muscle itself. I describe the deep longitudinal muscle fibers (Fig. 39) as a unique group.

<u>Superficial longitudinal and transverse muscles</u>

The superficial longitudinal and transverse muscle fibers (Figs. 40 & 41) lie just inside the connective tissue sheath at the surface of the bulb. The superficial transverse muscle fibers are separated into dorsal and ventral halves such that their origins and insertions are located along the lateral surfaces of the bulb (Fig. 40). The superficial longitudinal fibers have an anterior origin on the connective tissue sheath at the opening of
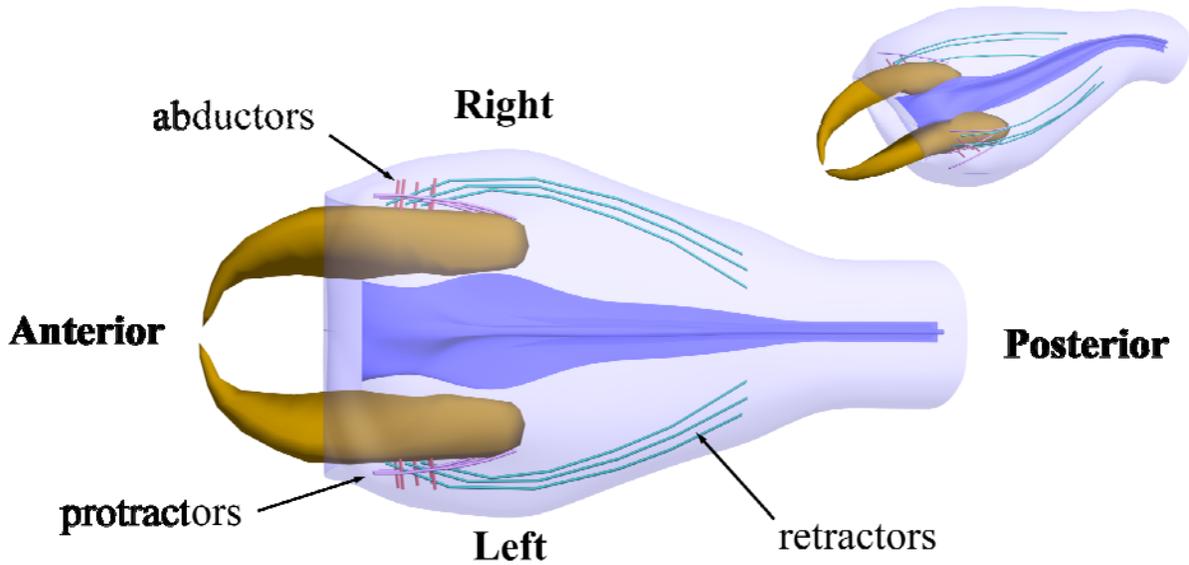
Figure 38. A dorsal view of the pharyngeal bulb showing the abductor (pink), the protractor (light purple), and the retractor (teal) muscle fibers of the lateral jaw surface. The abductors and protractors insert on the connective tissue sheath and the retractors insert in the area of the basal bulb musculature.
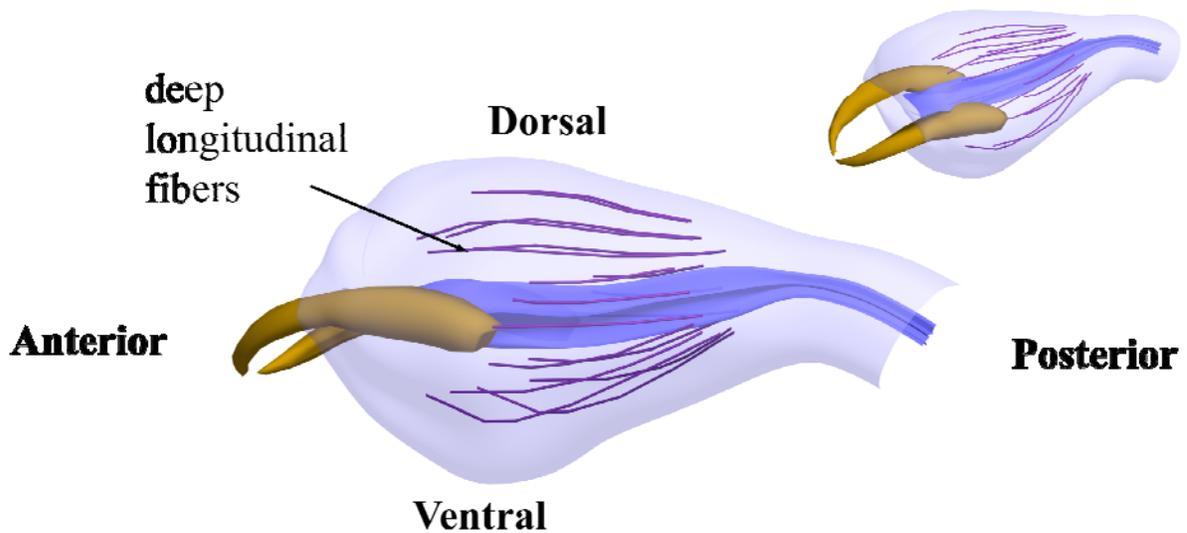
Figure 39. A postero-lateral view of the pharyngeal bulb showing the deep longitudinal muscle fibers (dark purple). There may be a number of origins (see text) but the insertion is in the area of the basal bulb musculature.
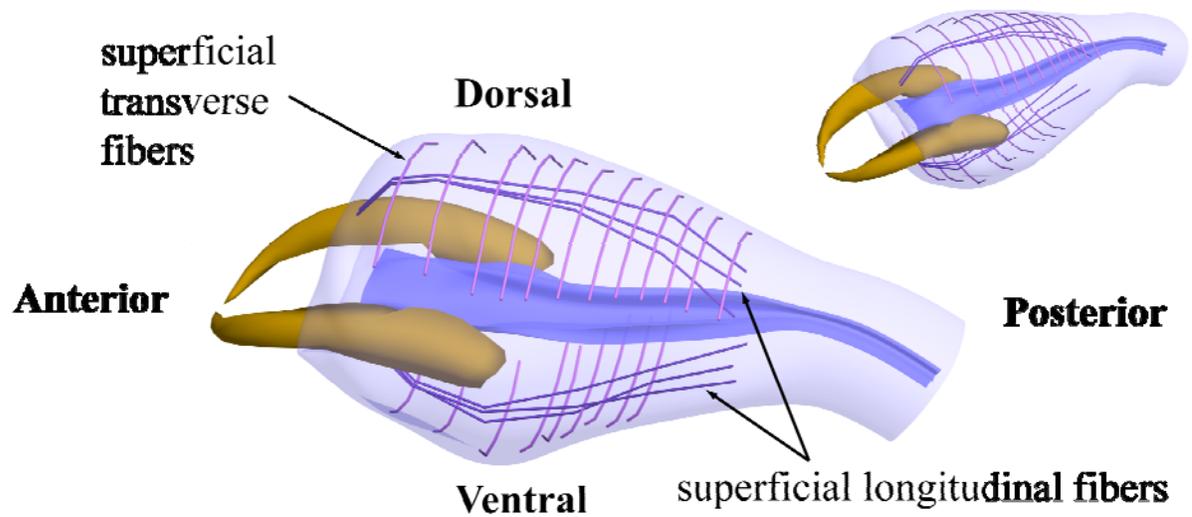
Figure 40. A slightly posterior, dorso-lateral view of the superficial longitudinal muscle fibers (light mauve) and the superficial transverse fibers (light purple). These muscle fiber layers are closely associated with the connective tissue sheath. The transverse fibers are superficial to the longitudinal fibers.
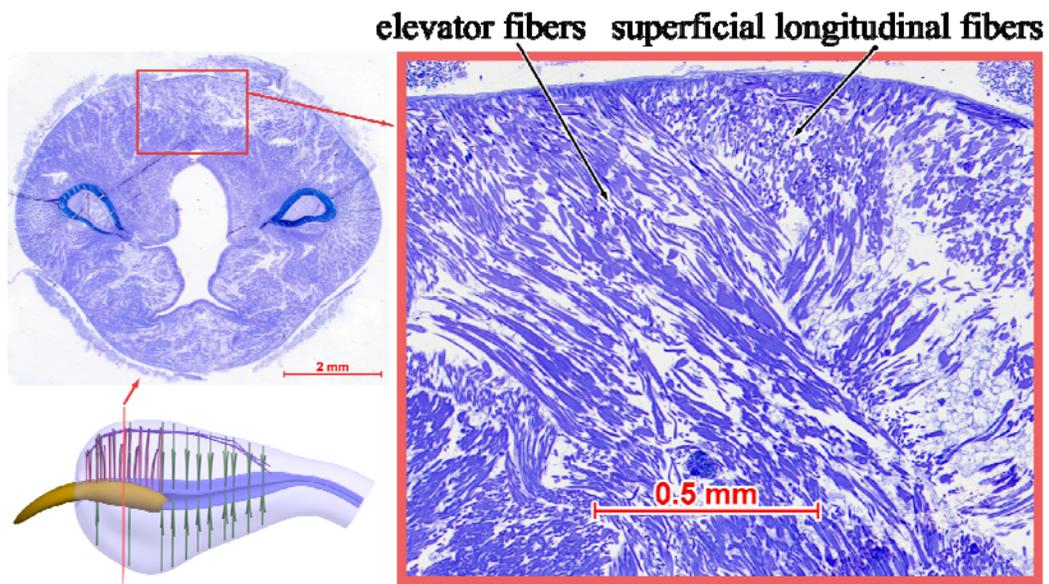
Figure 41. The inset on the lower left shows the pharyngeal bulb with the jaw elevator fibers (pink), the radial lumen dilator fibers (green) and the superficial longitudinal fibers (light mauve). The red plane indicated on the bulb shows the approximate location of the transverse histological section above. The red box shows the location of the magnified area shown to the right. The magnified area shows the crossing left and right elevator fibers and the superficial longitudinal fibers. Brightfield micrography of section stained with Toluidine blue.

the pharynx and extend to insert on the posterior end of the pharyngeal bulb and its basal

bulb muscle fibers (Fig. 42). As these fiber orientations are closely associated with the

surface of the bulb, they interdigitate with the perpendicular fibers (most notably the lumen

dilators) that insert on the connective tissue sheath.

Basal bulb musculature

The basal bulb musculature marks the posterior end of the pharyngeal bulb and is

represented by an array of fibers that originate and insert on the dorsal and ventral portions of

the connective tissue sheath (Figs. 42 & 43). These fibers curve toward the anterior as they

approach the surface of the bulb such that the overall array resembles a cup with the opening

pointed towards the jaws (Fig. 43). There is an interruption at the center of the medial fibers

(the center of the cup's base) through which the esophagus leaves the pharyngeal bulb. This

dorsoventral orientation of basal bulb fibers interdigitate with many fibers of other

orientations; lateral (the posterior-most superficial transverse fibers), radial (lumen dilator

fibers), and longitudinal fiber orientations (superficial longitudinal fibers, jaw retractor

fibers, and jaw adductor fibers).

Pharyngeal mass connective tissue sheath

A thin sheath of connective tissue fibers surrounds the pharyngeal bulb (Fig. 44). This

thin layer is closely apposed to underlying superficial muscle fibers and contains connective

tissue fibers that are highly birefringent and show staining characteristics typical of collagen.

The fibers show a crossed-fiber arrangement with an angle of 22° relative to the long axis of

the pharyngeal bulb. No analogous connective tissue sheath was observed in the foregut

lumen wall.
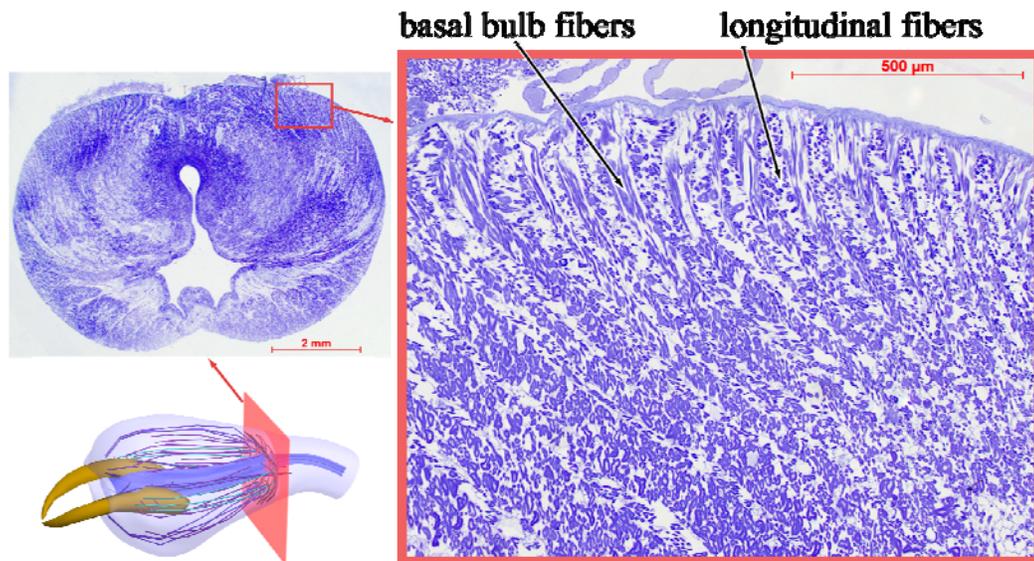
Figure 42. The inset on the lower left shows the pharyngeal bulb with the longitudinally arranged fibers (the dorsal and ventral superficial longitudinal fibers (light mauve), the jaw retractors (teal), the jaw abductors (dark blue), and the deep longitudinal fibers (dark purple)) and the basal bulb muscle fibers (dark red). The red plane indicated on the bulb shows the approximate location of the transverse histological section shown above. The red box shows the location of the magnified area shown to the right. The magnified area shows the highly interspersed basal bulb (obliquely cut) and longitudinal fibers (transversely cut). Brightfield micrography of section stained with Toluidine blue.
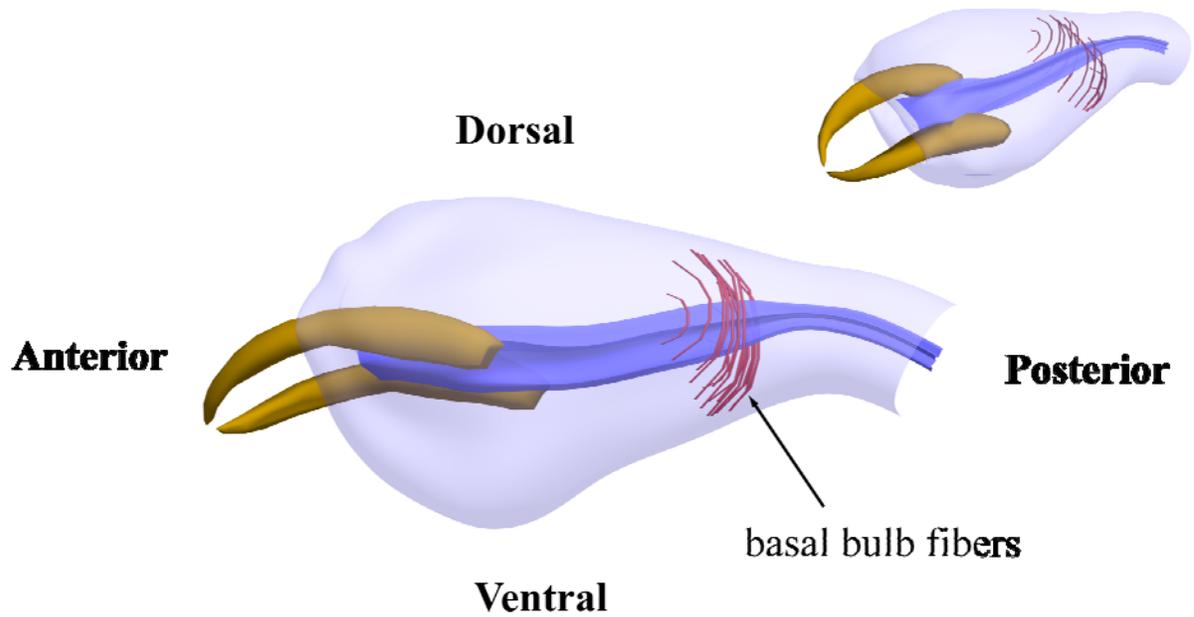
Figure 43. A slightly ventral postero-lateral view of the pharyngeal bulb showing the basal bulb fibers (dark red). These fibers are oriented dorsoventrally and mark the end of the pharyngeal bulb.
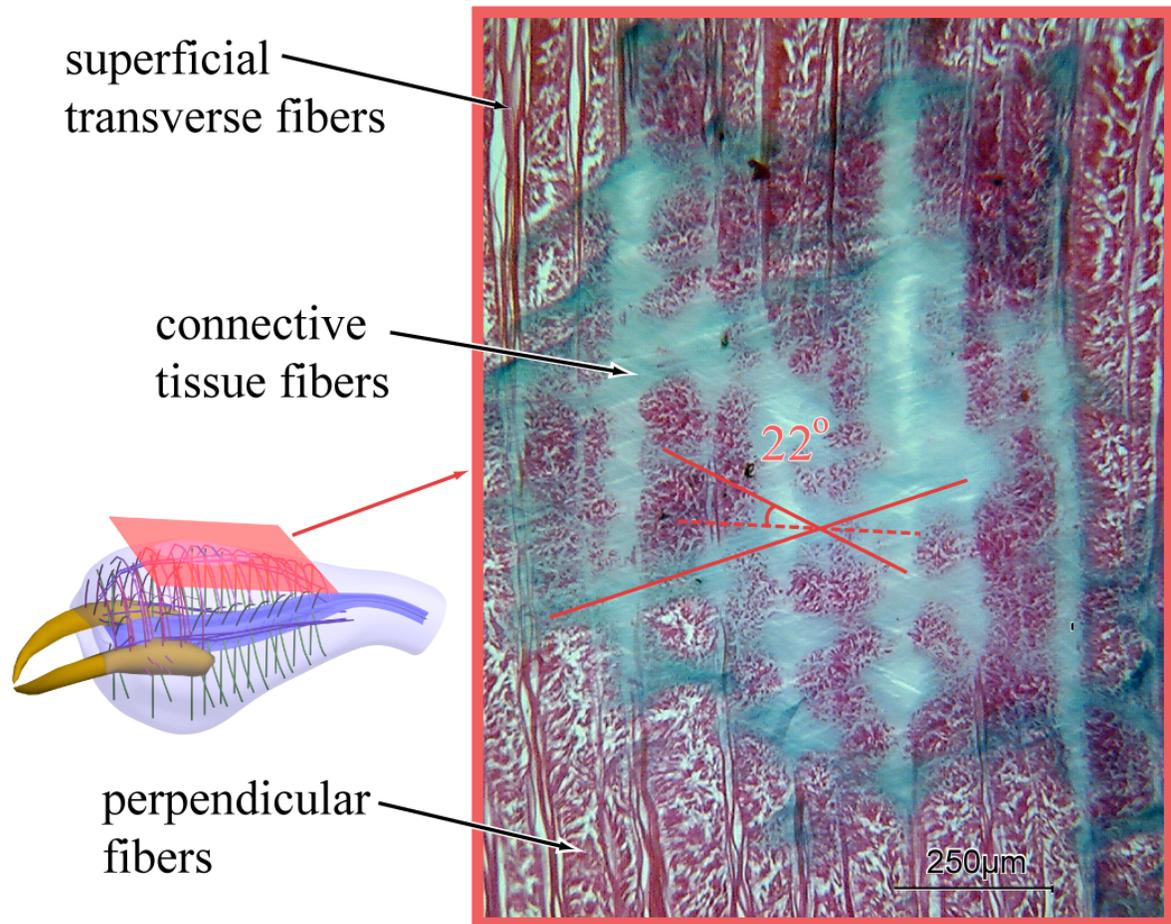
Figure 44. The inset on the left shows a slightly antero-dorsal left lateral view of the pharyngeal bulb with radial lumen dilator fibers (green), superficial longitudinal fibers (light mauve), and superficial transverse fibers (light purple). The obliquely frontal red plane indicates the approximate level of the section appearing to the right. The histological micrograph shows the superficial transverse fibers, the perpendicular fibers that insert on the connective tissue sheath and the connective tissue fibers that are arranged in a crossed fiber array. The anterior of the histological micrograph is oriented towards the left of the page. Thus, the helical connective tissue fibers form an angle of 44° relative to each other and 22° relative to the longitudinal axis of the bulb. Polarized light micrography of paraffin section stained with Milligan's Trichrome stain.

Jaw movements during defense of burrows

When perturbed, *Nereis virens* usually back into and wedges its body deep within the burrow. If an individual has occupied a particular tube for several hours, it will perform bites that are thought to function in defending the opening of the burrow (Turnbull, 1876). Quickly advancing a short distance out of the burrow, the pharyngeal bulb is everted, often with a lateral sweep of the head, and a quick biting movement is made. Usually a retraction into the burrow follows, but occasionally additional bites occur in which retraction ceases and the worm advances and bites again. The typical bites, consisting of nearly symmetrical left and right jaw rotations and translations, can be tracked by observing the exposed fang position and orientation in a series of video fields (Fig. 45). Motion analysis of the ventral view represents an appropriate initial investigation of pharyngeal bulb function because it avoids complications associated with the jaws being obscured as they bite into items. Four animals and 15 bites of this type were videotaped. Of these, the sequence shown in Figure 45 represents the bite with the widest range of gapes that was clearly recorded, although common phases of movement could be distinguished in all bites recorded.

Below I describe a generalized defensive biting motion. Relative phases of movements, rather than specific durations and displacements are reported because these phases can be performed with considerable variation in the speed, timing, and linear and angular displacements of the jaws. All jaw movement seems to occur within a single, approximately mid-frontal plane. Because the timing of the bites is difficult to predict well enough to video record from an appropriate side view, I was not able to determine the angle of this plane relative to the longitudinal axis. I estimate, however, that this plane could be pitched ventrally up to approximately 10° relative to the horizontal.

Figure 45. Video frames of jaw movements during a portion of a typical burrow defense bite. Shown on the abscissa are the jaw positions measured as gape angle formed between the jaws during sequential video frames indicated by time on the ordinate. The upper inset shows how the angle was measured between the jaws and lower inset shows the pivot area on the jaw. This biting sequence represents the widest gape recorded.

Gape angle

Time (seconds)

Gape angle formed by jaws

Pivot area

138
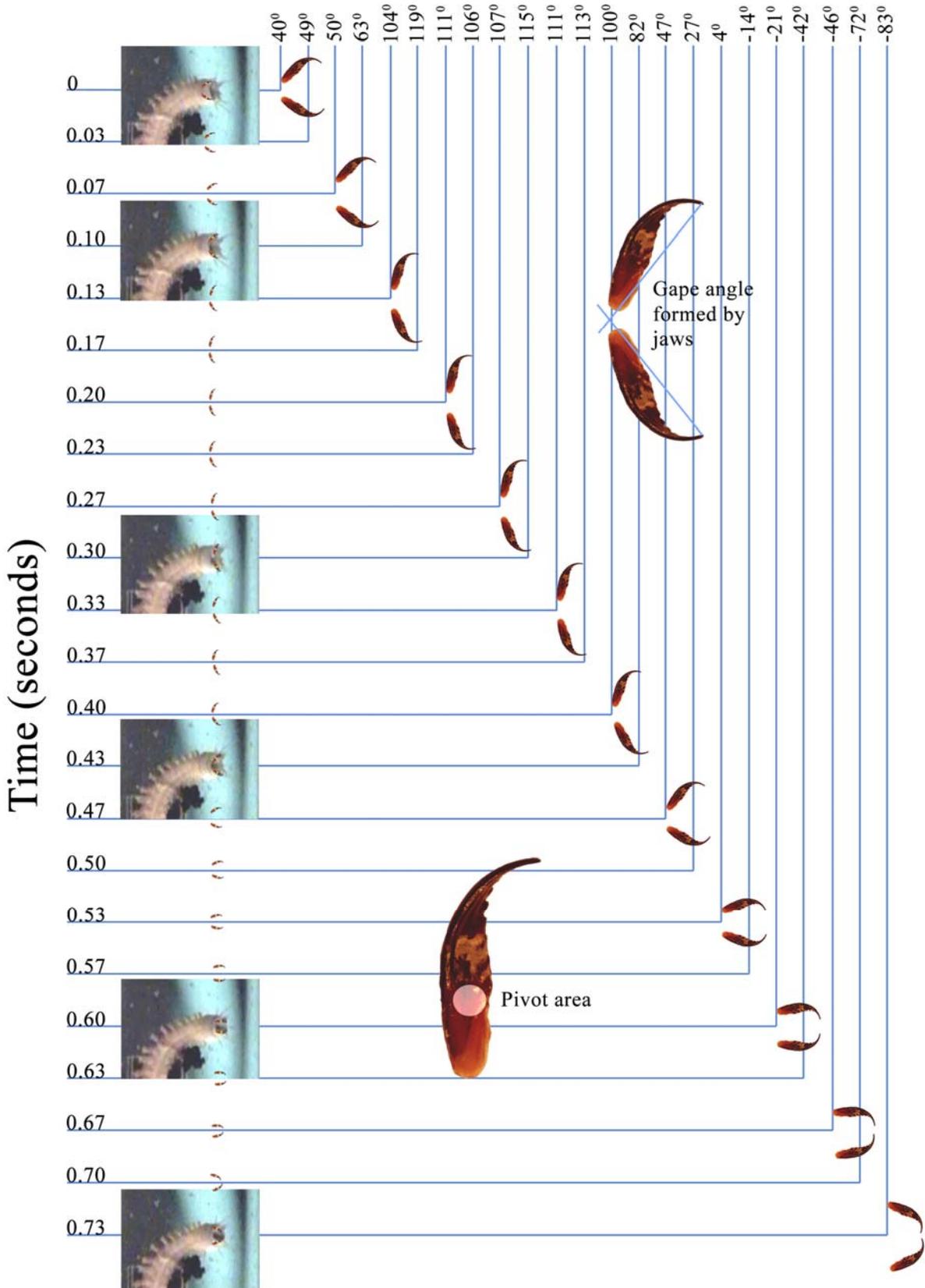
The initial stage of the bite begins with eversion of the proboscis. There is slight jaw rotation as the posterior end of the bulb is everted past the prostomial opening. As a result, when the anterior halves of the jaws become exposed they are already opened with a gape of approximately 40° (e.g. Fig. 45, 0 sec.). Finally, as the bulb is fully everted, the jaws begin a lateral translation that correlates with an increase in the diameter of the pharyngeal opening (Fig. 45, 0.03-0.1 sec). After this translation separates the jaws, the gape between the fangs is further widened by jaw rotation up an angle of 115° (That angle formed between the tips and the center of the bases of the jaws; Fig. 45, upper inset, 0.3 sec). During this movement, the center of rotation is not fixed but may occur anywhere within an area just posterior of the longitudinal center of each jaw (Fig 45, lower inset).

Subsequent movements involve jaw closure (Fig. 45, 0.4-0.73 sec). The jaws were found to rotate past the point where they are parallel (Fig.45, 0.73 sec, -83^{0}). In bites associated with burrow defense, jaw closing usually occurs simultaneous with retraction of the proboscis: In bites associated with feeding, repeated rotations and translations open and close the jaws to grasp and manipulate the food. Simultaneous closure of the jaws and retraction of the pharyngeal bulb requires that the jaws rotate toward the medial axis so that their fangs touch or even cross over each other as they enter the peristomium.

I recorded a second pharyngeal bulb behavior during burrowing through a field of loosely packed glass balls that were roughly double the diameter of the thickest body segment (Fig. 46). The worms used bulb eversions to move the balls out of their path. I observed that the fangs are often pointed forward and slightly exposed when the pharyngeal bulb is maximally everted (Fig. 46, frame 7).
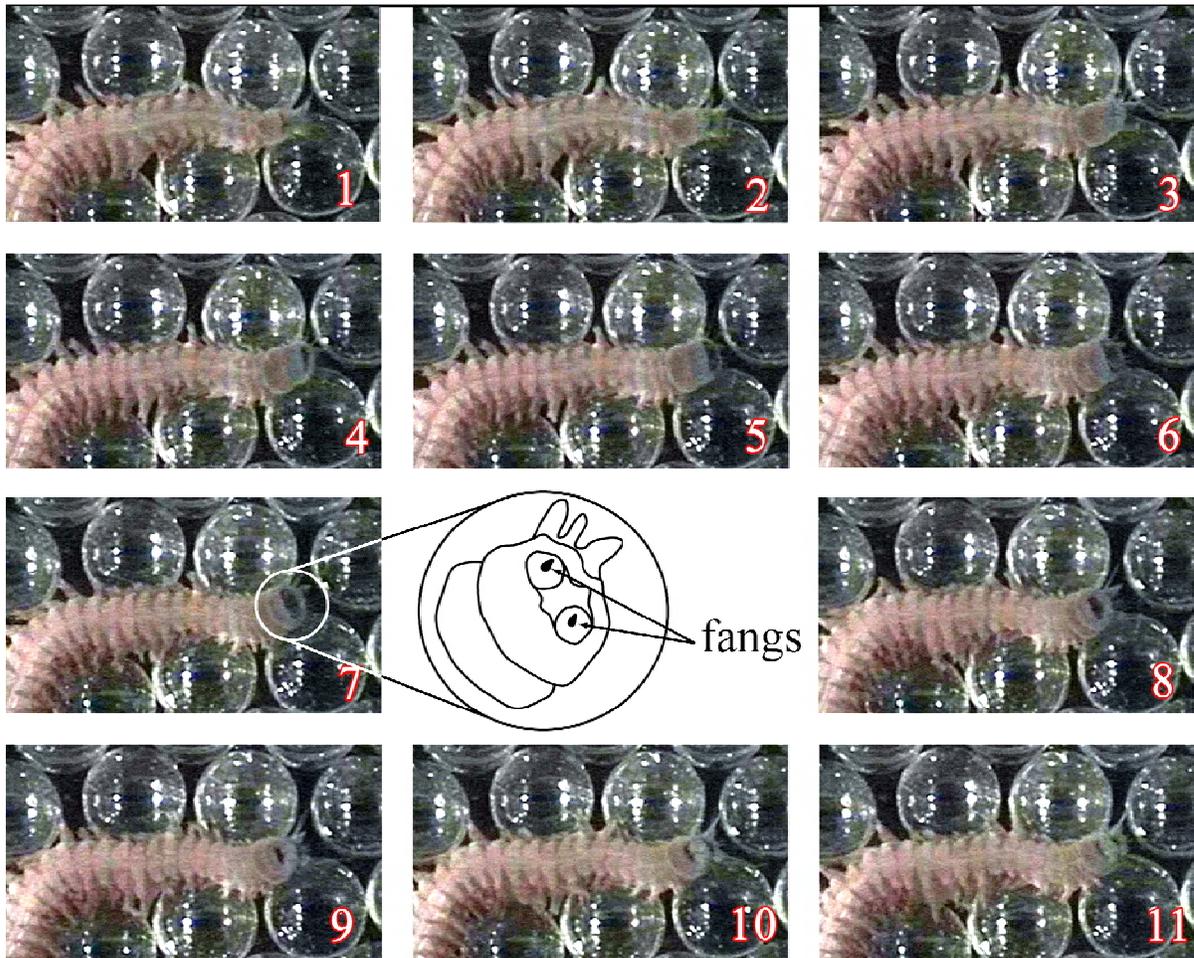
Figure 46. A sequence of eleven frames of video taken of the ventral surface of *Nereis virens*.

Here the worm is everting its proboscis to use its pharyngeal bulb as a wedge to move

between clear glass 1cm balls. The fangs (tips of the jaws) are exposed during this movement

(see frame 7 and accompanying illustration).

Discussion

Summary and analysis of novel morphological findings

I have observed two important aspects of nereid pharyngeal bulb morphology that have not been reported previously.

First, I have described a connective tissue sheath with staining properties of collagen surrounding the pharyngeal bulb. It has a crossed fiber arrangement with an angle of 22° relative to the long axis of the bulb. It may not have previously been detected because it is a thin layer that is closely apposed to the underlying transverse and longitudinal muscles, and previous studies did not employ histological stains that differentiate between muscle and connective tissues.

Second, the muscle fibers are described here, not as discrete muscles or large bundles, but instead as small bundles of fibers with similar orientations that interdigitate with fibers of other orientations dispersed throughout the solid muscular pharyngeal bulb wall. To generate hypotheses of function, I consider the possibility that this three-dimensional arrangement of muscle fibers could be a muscular hydrostat that serves the multiple functional roles required of a muscle articulation.

The connective tissue sheath

The connective tissue sheath surrounding the pharyngeal bulb may be crucial to the function of this putative muscle articulation because it may constrain shape changes and store elastic energy. Similar connective tissue fiber arrays provide structural reinforcement, control shape, transmit stresses, and store elastic energy in many soft-bodied invertebrates (Thompson & Kier, 2001).

Clark and Cowey (1958) noted that shape change in cylindrical worms can be limited by tension bearing connective tissue fibers arranged as left- and right-handed helices that wrap the bodies of these worms. The length of the fibers and body volume are considered to be essentially constant and there is thus a characteristic fiber angle relative to the long axis for any given body length. As the body shortens, the fiber angle increases. As the body extends the fiber angle decreases, becoming nearly longitudinal. When the body is circular in cross-section, the fibers are placed in tension and limit further elongation or shortening. When the volume of a cylinder with a crossed fiber connective tissue sheath is maximized, the connective tissue fibers assume a geometrically unique angle of 54.5° relative to the longitudinal axis. Because the volume is maximal, the fibers are in constant tension, and thus no elongations or contractions are possible. As this does not allow any length change, animal volumes rarely approach this limit (Clark, 1964). I hypothesize that the function of the pharyngeal bulb sheath may, in part, be to limit the length and diameter changes of the bulb. Since the measured connective tissue fiber angle of 22° is lower than 54.5°, this might suggest that the bulb was fixed for histology while elongated and might be capable of becoming shorter and wider before again being mechanically limited by the sheath.

Collagen is a fibrous protein found in the connective tissues of almost every animal phylum. It is a tough biomaterial (high work of fracture) that is well-suited to applications that place it in tension (Vogel, 2003). Thus, one function may be to resist changes in length: Ward and Wainwright (1972) found that fibers organized as right and left helices of low angle relative to the long axis of squid mantle tunics might serve to resist length changes while permitting changes in diameter required for the jetting power stroke. Because collagen fibers can stretch about ten percent beyond their resting lengths (Vogel, 2003) they may

function in another capacity; biomechanical studies of cephalopod mantles (Gosline &

Shadwick, 1983a, b, Thompson & Kier, 2001), suckers (Kier & Smith, 1990, 2002), and fins

(Kier, 1989; Kier et al., 1989; Johnsen & Kier, 1993) suggest that an array of collagen fibers

may serve as an elastic energy storage mechanism in soft bodied invertebrates. Thus, an

additional hypothesis for the functional significance of the polychaete bulb sheath is that it

may be a non-muscular method of antagonizing and returning stored energy provided by

muscular contraction. The sheath might aid re-elongation of the fibers that decrease the bulb

length, such as the deep and superficial longitudinal fibers, or increase the bulb diameter,

such as the radial lumen dilator fibers or jaw adductor muscle fibers. Re-elongation of jaw

adductor muscles by the sheath during closing movements may represent the return of elastic

energy stored during jaw abduction. Future studies that measure changes in muscle fiber

length and consider the roles of the pharyngeal bulb sheath as both a mechanical limit to

shape change and an elastic component capable of storing and returning energy are required

to clarify the function of this array of crossed connective tissue fibers.

Muscular hydrostats of the pharyngeal bulb

The pharyngeal bulb musculature most likely performs the multiple functions

required of a muscle articulation: it opens and closes the jaws by rotating them and by

translating them during changes in the diameter of the foregut lumen; it provides antagonistic

support to the muscles that generate these motive forces; it may bear the compression that is

transferred between the jaws; and it can form a pivot for each jaw. These functions may be

supported by a three-dimensional array of muscle with highly interdigitated orientations

functioning as a muscular hydrostat. This hypothesis requires that, in addition to considering

the function of individual fiber trajectories, the simultaneous actions of multiple fiber

143

orientations must also be considered. Co-activation of multiple orientations likely results in a function different from what might occur during single or sequential activations. I describe below a novel functional interpretation of the pharyngeal bulb morphology as a muscular hydrostat with specialized, but interconnected, anterior and posterior halves.

The posterior half of the pharyngeal bulb may resist longitudinal compression and act as a bolster or support for the muscles that move the jaws. The dorsoventrally oriented basal bulb muscle fibers are perpendicular to a group of longitudinal fibers (Fig. 42; the deep and superficial longitudinal fibers and the posterior ends of the jaw elevator and depressor fibers). Additionally, most of the basal bulb fibers are arranged obliquely relative to the lumen dilator muscle fibers in this area and the basal bulb and longitudinal fibers are perpendicular to the superficial transverse fibers. This complex organization of muscle fibers may function as a muscular hydrostat. The orientation of the basal bulb muscle fibers suggests that their isolated contraction would dorsoventrally flatten the posterior end of the bulb. The co-contraction of other muscle fiber orientations, however, in addition to shape limitations imposed by the connective tissue sheath, might result, not in movement, but in increase in the stiffness of this zone. This stiffening of the posterior half of the bulb might provide support for anterior muscle fibers that support and move the jaws.

As the jaws are embedded in the anterior half, the muscle fibers responsible for moving the jaws, creating pivots, and resisting compression are located here. While there is no obvious border between the anterior and posterior portions of the musculature of the pharyngeal bulb, the differences in fiber orientations may reflect a difference in function. I hypothesize that lateral translation of the jaws, the support for pivoting of the jaws (Fig. 45, lower insert), and the support that allows longitudinal adductor and abductor muscle fibers to

rotate the jaws open and closed are generated by a mechanism that includes the lumen dilator muscle fibers, the superficial transverse muscle fibers, and the surrounding connective tissue sheath. The jaws are embedded within the bulb wall and interrupt the course of the radial lumen dilator fibers. The radial muscles on either side of the jaws are represented by the anterior adductor (Fig. 37) and abductor (Fig. 38) muscle fibers. Thus, there is a full compliment of radial fibers that surround the jaws and that might function to thin the pharyngeal walls by bringing the inner foregut and outer bulb surfaces closer together. When this occurs, both the inner and outer circumferences increase because the bulb musculature volume is essentially constant. This circumferential increase may be controlled by the superficial transverse fibers or limited by the connective tissue sheath. Thus, the lateral translation of the jaws and the widening of the mouth during the initial stages of a bite may be explained by this increase in circumference of the lumen and exterior.

The jaws were observed to rotate laterally to widen the gape in the second stage of the bite. I hypothesize that the tissue of the anterior bulb wall becomes stiff because the radially arranged fibers are either limited by the connective tissue sheath or antagonized by simultaneously active superficial transverse fibers. This stiffening of the tissue may support the position of the jaws and provide a pivot against which the longitudinal adductors may act in closing and the abductors in opening. Contraction of these longitudinal fibers may not compress the length of the bulb because of the stiffening of the posterior half.

Observations of pharyngeal bulb function

The hypotheses of muscle activity during support and movement have not been tested experimentally. I attempted to develop an isolated pharyngeal bulb preparation analogous to that of the isolated octopus buccal mass preparations (Ch. 3), but the pharyngeal bulb ceased

functioning and did not exhibit biting behavior when removed. Future, experimental studies involving improvements in these preparations or novel *in vivo* measurements are needed to test the hypotheses proposed here.

During burrow defense bites (Fig 45), the jaws are rotated and translated in a roughly mid-frontal plane. This suggested that the jaw elevator and depressor muscle fibers may stabilize dorso-ventral jaw movements. As the bite begins, translation of the jaws away from the bulb midline opened the gape between the fangs. This occurred simultaneously with the dilation of the pharyngeal opening, suggesting that the translation was caused by radial muscle fibers. The width of the gape was then increased by jaw rotation in which the symmetrical left and right pivots were located in an area posterior to the center of each jaw's long axis (Fig. 45, lower inset). The longitudinal abductor muscle fibers originate immediately anterior to this location. This suggests that the posterior half of the jaw is supported while the anterior portion is adducted or abducted by the longitudinally arranged muscle fibers. Because these jaw movements are not used to bite, it is likely that little reaction force is transmitted through the pharyngeal wall. Jaw opening concurrent with an increase in the diameter of the pharynx suggest that the radial muscle fibers of the anterior bulb may stiffen, providing the compression resisting element required to support these movements.

Video observations of *Nereis virens* burrowing through a field of glass balls suggest a locomotory function for the jaws. The jaw fangs are exposed briefly as the bulb is used as a wedge to propagate cracks (Fig. 46, frame 7). The jaw tips seem to be held fixed with the fangs pointed forwards. The force of the forward proboscidial thrust may thus be focused at

146

the tips of the jaws and could be useful in exerting point loads to develop cracks in the elastic medium.

Summary and future directions

The novel findings summarized below include morphological details and functional interpretations. Although my behavioral observations are consistent with these hypotheses, further experimental studies based on novel experimental techniques are required for definitive tests.

The first important novel morphological detail provided here is the description of the connective tissue sheath that has staining characteristics of collagen. The sheath is formed of crossed fibers oriented at 30° to the longitudinal axis. Both the composition and the orientation of the fibers are important to the hypothesized function of the sheath. The sheath may constrain shape changes, store elastic energy that may be returned during jaw closures, and, with contraction of radial muscle fibers, provide antagonistic support for the jaw pivots.

The second novel morphological detail is the identification of two independent pharyngeal bulb portions with interdigitating muscle fiber orientations that might function as a muscular hydrostat. The posterior portion may stiffen (by co-contraction of the longitudinal, superficial transverse, basal bulb, and radial fibers) and provide support for muscle fibers originating on the jaw. The anterior portion has muscle fiber orientations that might support the jaws (radially arranged fibers and superficial transverse fibers), opening (abductors) and closing (adductors) the jaws, and stabilizing dorsoventral jaw movements (elevators and depressors). I hypothesize that radial muscle fibers (i.e. lumen dilators) in this area, along with the connective tissue sheath and superficial transverse muscle fibers, create a

compression-resisting element that allows the foregut lumen to remain open during jaw motions.

The joint between the left and right jaws of the eversible axial muscular pharyngeal bulb of *Nereis virens* is likely to be a muscle articulation. The joint is formed of muscle and connective tissues arranged as a muscular hydrostat that serves the multiple roles required of previously described muscle articulations: the soft tissues separate and connect the jaws; they bear compression transferred across the joint; and they generate the force that moves the jaws. While the nereid bulb possesses characteristics common with the previously described muscle articulations, it also exhibits several novel characteristics. The range of motion of the jaws may be limited by the crossed fiber connective tissue sheath because it might constrain the maximum diameter of the pharyngeal mass. Thus, analogous to sliding joints, muscle articulation joints may also have mechanical limits to their range of motion and degrees of freedom. Although mechanical limits may be imposed, there is also evidence that range of motion may be limited by neural input. As an example, neural input might control the jaw elevator and depressor muscle fibers to limit the lateral sweep of the opening and closing jaws to approximately a mid-frontal plane. Finally, the description of the nereid pharyngeal bulb has increased our understanding of the morphological diversity of muscle articulation joints. These joints may have evolved independently in at least three unrelated phyla (inarticulate brachiopods, cephalopods, and jawed polychaetes) to serve critical functions typically related to feeding and defense. The independent evolution of the muscle articulation emphasizes the potential importance of this joint type to many soft-bodied invertebrates.

Additional research is required to characterize further the nereid pharyngeal bulb muscle articulation. While this study has clarified details of the muscle and connective tissue

fiber arrays and made a preliminary investigation of function, little is known about how the musculature is controlled in order to generate the complex and diverse movements required by the many nereid feeding and defense behaviors. Further studies involving *in situ* recording of muscle activation while simultaneously recording the natural biting motions of the jaws are needed. These studies will be challenging, however, because the wide range of jaw motions and the small size of the bulb and its fiber bundles may impede accurate and stable placement of electromyography electrodes. Magnetic resonance imaging techniques may be useful to record changes in bulb dimensions and thereby suggest which muscle fiber orientation is active. Additionally, if appropriate physical models of the pharyngeal bulb can be engineered, they may be useful in testing aspects of joint function. Finally, further efforts to describe novel muscle articulations are important as they allow exploration of the diversity of structure and function of these joints. Thus, in the next and final chapter I analyze the grasping organ of a kalyptorhynch turbellarian flatworm as a muscle articulation of unique construction and microscopic size.

CHAPTER 5

THE MORPHOLOGY OF THE PROBOSCIS OF THE KALYPTORHYNCH

FLATWORM (*CHELIPLANA* SP.)

Introduction

The muscle articulation joints of cephalopod beaks (Ch. 2 & 3) and polychaete worm jaws (Ch. 4) include complex, three-dimensional arrangements of muscle fibers that function as muscular hydrostats. These structures bear compressional forces transmitted through the joint, move the links or jaw elements, and generate support for muscular antagonism and pivot formation. Connective tissues might limit shape changes and antagonize muscular contractions. In this chapter, I analyze the morphology of the proboscis that bears two grasping hooks in a sand-dwelling turbellarian flatworm of the sub-order Kalyptorhynchia (Fig. 47) (Brusca & Brusca, 2003). The kalyptorhynch joint is unique among those I describe here because it is microscopic and of relatively simple construction.

I begin the morphological analysis by describing the environment in which the kalyptorhynch proboscis is used. I then briefly review kalyptorhynch phylogeny and evolution, as this proboscis is armed with two hooks and is thought to have evolved from unarmed precursors. Finally, I review what is known of kalyptorhynch feeding behavior and previous morphological studies of the hooks and proboscis musculature. I describe and analyze muscle and connective tissue fiber organizations in order to generate hypotheses of function, but experimental tests are not possible at this time. In the conclusion, I summarize
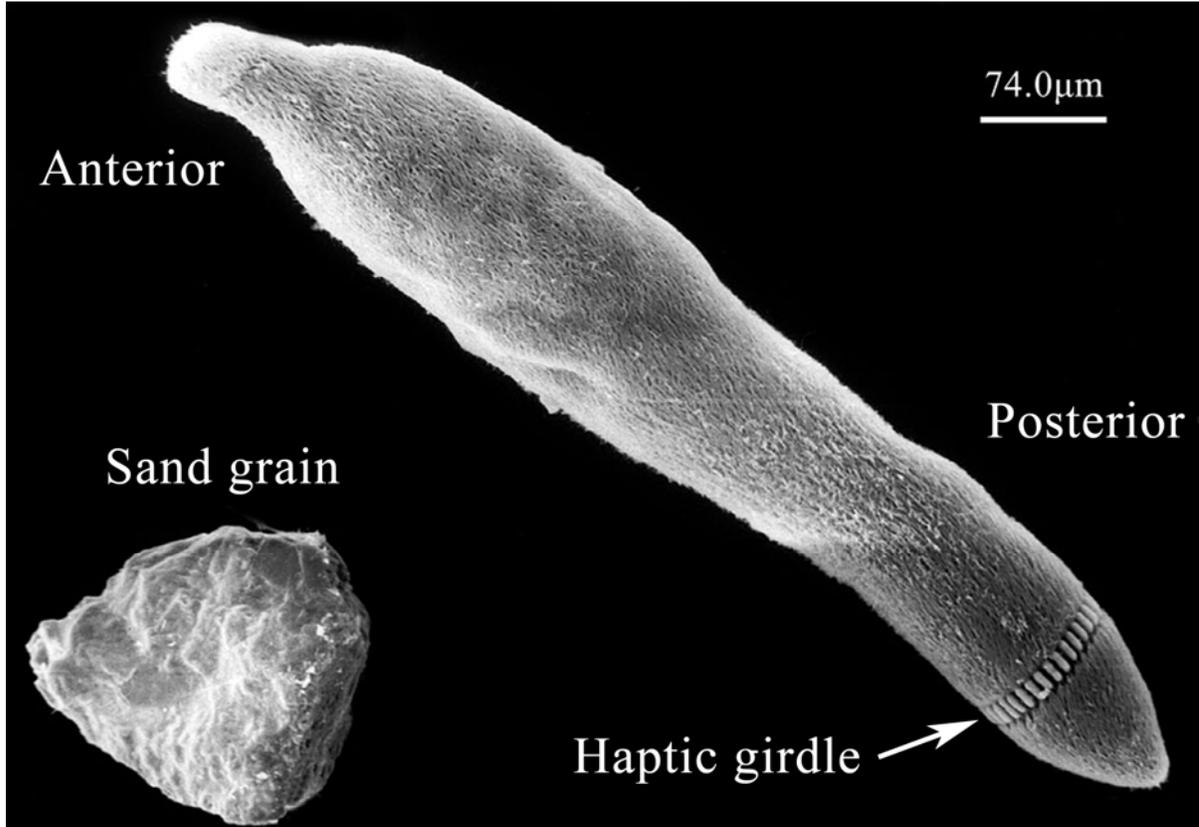
Figure 47. Scanning electron microscope image of *Cheliplana* sp. beside a grain of sand. The

proboscis is located within the proboscidial sheath that is partially projecting from the

anterior end of this specimen. The haptic girdle is a collection of glandular papilla (Karling,

1989) (Photo provided by and used with permission of Dr. Matthew Hooge, University of

Maine)

common muscle articulation characteristics, assess the importance of these joints, and identify general areas that require further study.

Kalyptorhynch flatworms as meiofauna

Kalyptorhynch flatworms belong to the meiofauna, a taxonomically diverse group of infaunal organisms exhibiting numerous morphological adaptations to a unique aquatic environment. Remane (1933) first recognized that the smallest infaunal metazoans formed a unique community [termed "meio-" fauna by Mare (1942)]. With body lengths that range from 100 to 1000μm, they are small enough to live in the water-filled interstices between grains of marine sediments (Brusca & Brusca, 2003). Most extant phyla (24 of the approximately 34 recognized) include members that are specialized for interstitial life (Giere, 1993). A common specialization is a highly miniaturized, soft, and elongate body that facilitates movement through small interstices (Ricci & Balsamo, 2000). Major phyla present in the meiofauna include cnidarians, gnathostomulids, nemerteans, nematodes, gastrotrichs, kinorhynchs, rotifers, sipunculids, molluscs, annelids, tardigrades, arthropods, and echinoderms (Robertson et al., 2000).

Free-living turbellarian flatworms are common predators among the meiofauna of sandy, and to a lesser extent, muddy marine substrates (Martens & Schockaert, 1986). The predatory turbellarian studied here belongs to the suborder Kalyptorhynchia (Fig. 48). In addition to the small, soft, and cylindrical body, kalyptorhynchs possess an anterior eversible proboscis that is separate from the posteroventral pharynx (Pechenik, 2004; Brusca & Brusca, 2003). Some kalyptorhynch proboscides are armed with stout hooks that facilitate

Figure 48. Micrograph of unidentified *Cheliplana* species from Northern California.

Structural terminology used is from Karling (1989). (Photo provided by and used with

permission of Dr. Matthew Hooge, University of Maine)
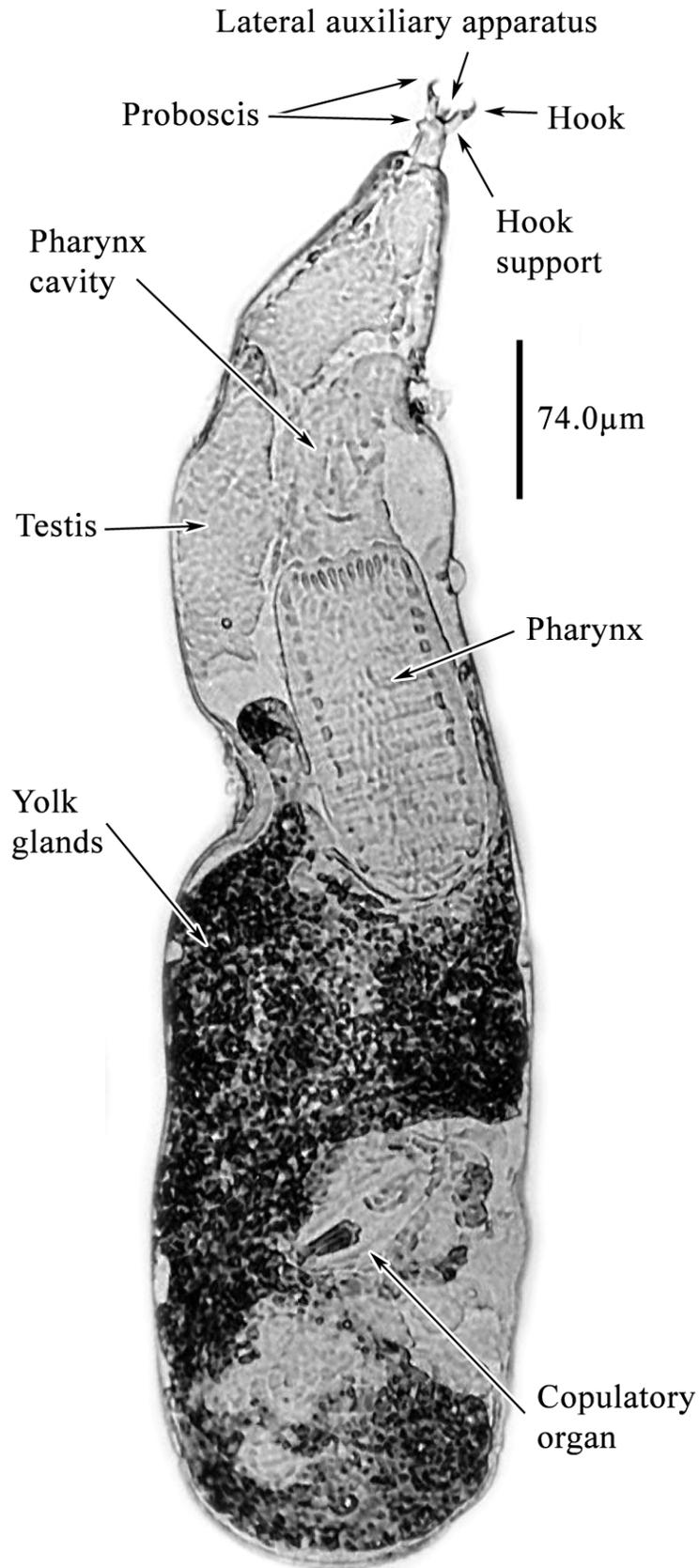
Figure 48.

capturing prey (Rieger et al., 1991; Karling, 1961). As the hooks do not contact each other in the joint, these proboscides might include a muscle articulation.

Kalyptorhynch taxonomy and systematic relationships

Kalyptorhynchs are common meiofaunal predators belonging to the phylum Platyhelminthes and class Turbellaria (Karling, 1961; Beauchamp, 1961; Maly et al. 1980; Brusca & Brusca, 2003). The undescribed species of kalyptorhynch studied here was identified as belonging to the genus *Cheliplana* Beauchamp, 1927 (syn. *Rhinepera*; Meixner, 1928; see Karling, 1983) based on body morphology, reproductive morphology (Hooge, pers. comm.), and proboscidial features (Karling, 1983). The relatively speciose genus *Cheliplana* [with approximately two dozen described species (Karling, 1983)] is most often associated with the orders Rhabdocoela (Littlewood et al., 1999; Brusca & Brusca, 2003) or Neorhabdocoela (Beauchamp, 1961). This discrepancy occurs because of taxonomic uncertainties associated with the possible polyphyletic nature of turbellarian flatworms (Smith et al., 1986; Ehlers, 1986). *Cheliplana* is classified within both these orders because it possesses both a bulbous pharynx and a simple, saclike gut without diverticula (Greek: *rhabd-*, rod; *coel-*, hollow).

The genus *Cheliplana* belongs to the suborder Kalyptorhynchia (Graff, 1905) (Greek: *calypt-*, hidden; *rhynch-*, snout) because it possesses a well-developed, fully-sheathed, and retractable proboscis (Karling, 1947, 1949, 1950; Beauchamp, 1961; Schilke, 1970). Kalyptorhynchs are monophyletic (Littlewood, 1999) and are subdivided into two natural groups, the eukalyptorhynchs and the schizorhynchs, based on proboscidial morphology (Karling, 1961; Doe, 1976). Eukalyptorhynch proboscides are referred to as the conorhynch type because the eversible, distal end is more or less cone-shaped (Fig. 49AB). The anterior

Figure 49. The diversity of kalyptorhynch proboscides. A. The unarmed eukalyptorhynch conorhynch proboscis features an endcone formed of longitudinal muscles (A1, extended; A2, contracted to forming a cup); B. The armed conorhynch proboscis (B1, hooks open; B2, hooks closing); C. Movement in the unarmed schizorhynch proboscis (Longitudinal view of tongues opening as hook abductors contract (C1) and closing as trunk muscles contract (C2); Transverse view of tongues opened (C3) and curled (C4)); D. A 3-D visualization of a schizorhynch proboscis with a widely connected bridge (D1). Note the nodal pore at the base; Anterior (D2) and posterior (D3) sections through the proboscis at levels indicated. E. Karling's (1961) karkinorhynch proboscis opening sequence, E1 illustrates the retracted proboscis resting position with hooks closed, E2 shows the sheath being retracted the hooks opening, E3 shows the hooks opened and the proboscis fully extended; F. A diascorhynch proboscis opening (F1) and closing (F2). Note the presence of the hook adductors. Drawn from illustrations and text descriptions of Karling (1961).

Bas. mem.	Basement membrane
Brdg.	Bridge connecting tongues or hook supports
Circ.	Circumferential muscles
E. cone.	End cone
Hk.	Hook
Hk. abd.	Hook abductor muscle
Hk. add.	Hook adductor muscle
Hk. sup.	Hook support
Jun.	Junction
L. aux.app.	Lateral auxiliary apparatus
Long.	Longitudinal muscle
Nod.	Nodus
Nod. pore	Nodal pore
Ret.	Retractor muscle
Rost. pore	Rostral pore
Sept.	Septum
Sh. ret.	Sheath retractor muscle
Tng.	Tongue
Trnk.	Trunk muscle

Figure 49

157
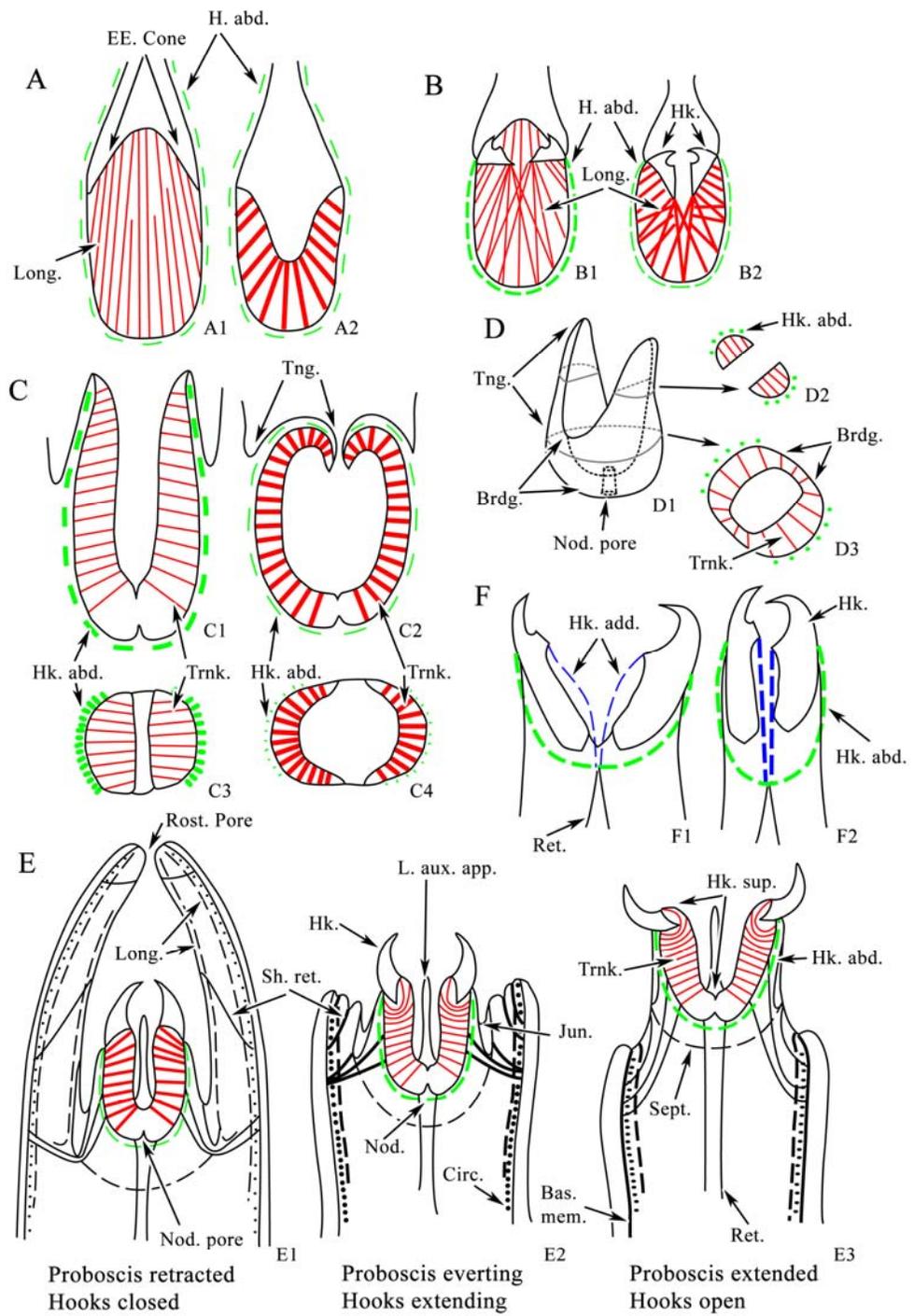
end of schizorhynch (Greek: *schiz-*, cleft) proboscides (Fig. 49CD) is split into two halves or

tongues (Rieger et al., 1991). In the families Karkinorhynchidae (e.g. *Cheliplana*) (Fig. 49E)

and Diascorhynchidae (Fig. 49F) (Meixner, 1928), these tongues are reduced in length and

bear a pair of stout hooks used as pincers to grab prey.

Evolution of armed and unarmed kalyptorhynch proboscides

Opposable hooks have evolved independently in both conorhynch (Fig. 49B) and

schizorhynch (Fig. 49EF) proboscides (Rieger et al., 1991). The more plesiomorphic

conorhynch condition is an unarmed cone-shaped end cap (Rieger et al., 1991) composed

mainly of inner longitudinal muscle strands (De Vocht, 1991). De Vocht (1991) found no

nuclei within the conorhynch, and thus these longitudinal strands could represent bundles of

myofibrils (Fig. 49A). These longitudinal bundles of myofibrils extend from the basement

membrane of the anterior epithelial covering of the cone and the fibrous septum between the

body wall and the posterior margin of the proboscis (De Vocht, 1989). Their contraction is

thought to pull the tip of the cone posteriorly until it is inverted into a cup shape (Fig.49A2),

and a thin layer of superficial circular muscles may re-extend them. Suction generated by

inverting the conorhynch might aid glands that produce sticky secretions to capture prey

(Rieger et al., 1991). The two hooks of armed conorhynchs (Fig. 49B) are described by Doe

(1976) as resembling jaws embedded at the point where the sheath connects to the proboscis.

These opposable hooks close and open by contraction of specialized muscles derived from

the longitudinal myofibril bundles of the unarmed conorhynch (Rieger et al., 1991).

Thought to have evolved from the unarmed conorhynch proboscis (based on

morphological parsimony), the unarmed schizorhynch proboscis consists of two

dorsoventrally opposed halves connected to a variable degree at the base (Beauchamp, 1961;

158

Karling, 1961). The halves may be nearly independent and connected only by a small strip or bridge (Fig. 49C; e.g. *Clyporhynchus*; Karling, 1947) or may be broadly connected such that they appear fused (Fig. 49D; e.g. *Placorhynchus*; Meixner 1938). Each half is referred to as a lip or *tongue* in unarmed proboscides and as a base unit, muscle bulb, hook carrier or *hook support* if the structure carries a hook. Tongues, such as those found in the family Schizorhynchidae (Schilke, 1970), resemble tapering tentacles composed of myofibril bundles that are oriented transversely to the long axis of the proboscis (Fig. 49C). Contraction of these myofibril bundles is thought to flatten the tongues, curl them medially, and wrap around the prey (Fig. 49C 2, 4). Antagonistic lateral longitudinal muscle fibers are thought to straighten or shorten the tongues (Karling, 1961; Rieger et al., 1991). Armed hook supports most likely evolved from unarmed tongues (Beauchamp, 1961) and are found in three schizorhynch families. Schilke (1969) described small, straight, needle-like teeth carried on the distal end of the tongues in the family Nematorhynchidae. Members of the family Karkinorhynchidae (Fig. 49E) have more substantial incurved hooks at the tips of relatively short hook supports (Karling, 1961; Rieger et al., 1991). In *Cheliplana*, the hooks may or may not bear a single tooth-shaped process along their inside or medial edges (Karling, 1961). The largest and most developed hooks are found in the family Diascorhynchidae (Fig. 49F) (Beauchamp, 1961; Karling, 1961). Here, complex hooks resemble jaws, sometimes with several interlocking medial processes (Rieger et al., 1991).

Proboscidial hooks may have evolved as an adaptation to the meiofaunal lifestyle. Because kalyptorhynchs are relatively large meiofaunal predators, their soft, cylindrical bodies may navigate larger spaces between sand grains while the armed proboscis may be particularly suitable for removing prey from smaller gaps (Meixner, 1938). Using the hooks

159

to hold the prey, the flatworm then feeds by moving to larger spaces and folding in half in order to transfer the food to their posteroventral pharynx (Karling, 1961). Meixner (1925) described eukalyptorhynch body musculature as particularly suited to the task of bending the anterior body and proboscis towards the pharynx. The requirement for large feeding spaces may explain why kalyptorhynchs are present in greater densities in sandy substrates with larger and more variable interstitial spaces than in fine particulate mud (Karling, 1961; Martens & Schockaert, 1986).

The development and functional morphology of the armed schizorhynch proboscis

The development of rigid schizorhynch hooks has been studied (Rieger & Doe, 1975, Doe, 1976). The common reference to these hooks as "cuticular" (e.g., Karling, 1961) suggests that they are formed as an extracellular material secreted by the epidermis. Instead, Rieger and Doe (1975) noted that they are closely associated with, and may be derivatives of, the basement lamina of the proboscis and sheath epithelium. Doe (1976) noted that a number of gland cells underlie the hollow hooks of *Cheliplana*. During ontogeny these gland cells secrete hook material into the basement lamina. In some schizorhynchs, these gland cells may later be used to produce narcotizing or poisonous secretions; although Karling (1961) notes that most karkinorhynch hooks are closed at the anterior tips.

Additional structures, termed *lateral auxiliary apparati* (Fig. 49E), are present on the right and left sides of the hook supports in most karkinorhynchs (Karling, 1961; Shilke 1970). These semi-rigid, papilliform extensions are present either singly or in pairs on either side. Karling (1961) noted that *Cheliplana* has two weakly cuticularized lateral auxiliary apparati that are often difficult to observe. In the closely related genera *Cheliplanilla* and *Rhinepera*, these semi-rigid, rod-shaped structures are 24-29µm long, tapered, and curve

160

inwards at their distal points. The function of these structures is uncertain; they may be feelers, or guide the expansion and retraction of the proboscidial pore and sheath, or, as found in *Baltoplana magna* (Karling, 1950), they may serve as excretory tubes for glands.

Karling (1961) noted that Graff first described the kalyptorhynch proboscis in 1882 as a probing sensory organ and later (1913) documented its grasping function. Since then, the proboscidial morphology of a number of kalyptorhynch families, and a number of *Cheliplana* species (e.g. Brunet, 1968; Schilke, 1970) have been described. Most of these descriptions, however, have a taxonomic focus and do not consider function. One study (Karling, 1961) considered a number of schizorhynch proboscides from a functional point of view, and thus provides a solid foundation for this study.

The general structure and movement of the proboscis in *Cheliplana* is summarized below (Fig. 49E). When inverted, karkinorhynch proboscides are held within a sheath in the anterior portion of the body. The sheath is essentially a canal formed by the infolding of the body wall (Rieger et al., 1991). Ultrastructural details available for eukalyptorhynch sheaths (De Vocht, 1989, 1991) show that they are formed of a cellular and several syncytial belts through which a number of glands extend. A rostral pore (Fig. 49E1) through which the proboscis emerges is formed at the point where the body wall folds in. Thus, the sheath extends from the pore to where it joins the base of the proboscis hook supports. The glandulomuscular hook supports themselves are sheathed in a 1-2 μm thick syncytial epidermis (Doe, 1976) that is connected to the epidermis of the body at a point termed the *junction*. In schizorhynchs, a post-rostral muscle-free reticulum that contains a connective tissue framework, termed a *nodus*, is present at the posterior end of the proboscis (Karling, 1961; De Vocht & Schockaert, 1999). At the center of the nodus is a small *nodal pore* (Fig.

161

49D1), through which pass ducts of glands that lie within the body (Karling, 1961). The posterior end of the proboscis in most schizorhynchs (the differentiation is less obvious in karkinorhynchs) is divided from the surrounding parenchyma of the body by a *septum* (Fig. 49E3) of extracellular matrix and muscles that demarcate a *post-rostral bulb* region (Karling, 1961).

The proboscis emerges through the anterior rostral pore during eversion. Because there are no proboscis protractor muscles, the proboscis is exposed by the combined dilation of the rostral pore and retraction of the rostral wall (Fig. 49E). Some proboscis extension does occur and is caused by pressure generated by superficial circumferential body muscle contraction (Karling, 1961; Rieger et al., 1991). While everted, the two opposable hooks may open and close (Beauchamp, 1961) with independent, asymmetric motions (Karling, 1961) and with a wide range of motion along the dorsoventral axis (Hooge, pers. comm.). The proboscis is withdrawn into its sheath using proboscis retractor muscles that insert on the nodus and originate within the body beyond the post-rostral bulb septum (Karling, 1961).

Opening and closing hook movements are generated by the dorsal and ventral hook supports. These movements are reported to occur in the mid-sagittal plane (Karling, 1961), although this may be an artifact of *in vivo* microscope observations that use squash preparations to lightly restrain the animal. The symmetrical dorsal and ventral *trunk muscles* (or longitudinal muscle rows, or inner longitudinal muscles, or confusingly, radial muscles; see below) and *hook abductor muscles* (or external longitudinal muscles, or divaricator muscles) of the hook supports generate karkinorhynch hook movement (Karling 1961).

Karkinorhynch trunk muscles probably evolved from the longitudinal myofibril bundles of the eukalyptorhynch conorhynch proboscis end cone (Fig. 49A) (Beauchamp,

1961; Karling, 1961). When inverted, the end cone becomes cup-shaped, and this mechanical reconfiguration reorients the longitudinal myofibrils such that those located at the edges of the cone appear as radially oriented myofibrils in longitudinal sections (Fig. 49A1-2). The schizorhynch proboscis (Fig. 49CD) resembles a mid-sagittal portion of this cup and thus the two hook supports of *Cheliplana* (Fig. 49E) possess short radial or transverse myofibrils that originate on the medial edge of the hook supports and insert on the lateral edge. Within each trunk muscle, the transverse myofibril bundles are arranged in two longitudinal stacks that extend from the base of the hook support to its anterior end within the hook (Karling, 1961). The bases of the hook supports in *Cheliplana*, *Cheliplanilla*, *Rhinepera*, and probably other species, are firmly attached to the proboscidial bulb septum by the nodus (Karling, 1961).

Karling (1961) noted that all karkinorhynch hook supports have hook abductor muscles formed of longitudinally arranged muscle fibers that are located lateral to the trunk muscles (Fig. 49E). They originate on the nodus and extend along the lateral surfaces of the hook supports to insert on the outer or lateral hook margins. In diascorhynch hook supports (Fig. 49F), there are also adductor (occlusor) muscle fibers that originate on the nodus and extend to the inner or medial margins of their complex, jaw-like hooks (Karling, 1961). Note that adductor muscles are not present in karkinorhynchs like *Cheliplana* (Karling, 1961; Schilke, 1970).

Hypotheses of hook movement and unanswered morphological and functional questions

Karling (1961) offered hypotheses of function based on morphological descriptions of various schizorhynchs. He described some functional details of the opening and closing mechanism in karkinorhynch proboscis as being puzzling. It is the goal of this study to clarify these details by describing the *Cheliplana* proboscis as a muscle articulation.

The mechanical description of tongue divarication or hook opening by Karling (1961) (Fig. 49) is applicable to most schizorhynchs. Because the one or more fibers of the trunk muscles that form the bulk of the tongues or hook supports are essentially constant in volume, contractions of their stacks of transverse myofibrils bundles result in a decrease in width and increase in length of these structures (Fig. 49C). Simultaneous contraction of the lateral abductor muscles are thought to divaricate the tongue tips or hooks as the tongue or hook moves forward. This mechanism is consistent with illustrations showing the bent hook supports of opened karkinorhynch proboscides (Karling, 1961; Beauchamp, 1961).

There are four potential mechanisms of hook closing in karkinorhynchs which take into account the lack of adductor (occlusor) muscles (Karling, 1961). First, the closing movement may be passive. The connective tissue of the nodus may be arranged to hold the hook supports in a closed position and thus closing may be the result of the elastic recoil of the connective tissue. Second, Karling (1961) suggested that in some karkinorhynchs, this passive elastic recoil is augmented by contraction of muscle fibers in the nodus. Third, the hooks of some karkinorhynchs may be actively adducted by muscle fibers at the base of the trunk muscles. Because the karkinorhynch proboscis may have evolved from longitudinally arranged fibers of a cup-shaped conorhynch (see above), the base of the trunk muscles in some species has muscle fibers of oblique or longitudinal orientation. Karling (1961) suggested that these muscle fibers might help adduct the hooks. Fourth, because the lateral portion of the flaired base of the hook extends further posteriorly than does the medial portion, the rotation of the hook to an opened position may force the transversely oriented myofibril bundles of the trunk muscles to curve around the posterolateral edge of the hook.

164

Thus, straightening of these trunk muscle fibers during contraction would tend to rotate the hooks back to a closed position.

I analyze the morphology of the *Cheliplana* proboscis in an attempt to answer the following questions. What soft tissue components adduct and abduct the hooks? How are compressional forces transmitted across the joint as the hooks manipulate prey items? How are the various muscles of the proboscis antagonized or supported? I place particular emphasis on the connective tissue elements, given their crucial role in other muscle articulations and in support and movement in general.

Materials and methods

Specimens of an unidentified species of *Cheliplana* were collected, partially prepared (see below) and supplied to me by M. Hooge (University of Maine). The specimens were extracted from samples of fine-grained subtidal sand using magnesium sulfate anesthetization (Sterrer, 1971) by M. Hooge on 1 February 2004 from San Felipe Bay (30° 54' 21.6" N, 114° 42' 35.5"W), San Felipe, Baja California, Mexico. Five specimens selected for histological study were relaxed in isotonic magnesium sulfate, fixed in warm Stefanini's fixative (Stefanini et al., 1967), washed in Millonig's phosphate buffer (Millonig, 1961), fixed in phosphate-buffered 1% (v/v) osmium tetroxide and dehydrated in acetone. Dehydration was accelerated with microwave radiation (Giberson & Demaree, 1995). Specimens in vials were placed on ice in a microwave oven with two water filled 300 ml beakers as water ballasts. The specimens were dehydrated by two 7 s irradiations at 650W separated by a 20 s interim. The specimens were then embedded in EMBed/Araldite epoxy resin (Mollenhauer, 1964) and shipped to me. I cut serial sections of 0.5 to 1.5 µm thickness using triangular Latta-Hartmann glass knives (Latta & Hartmann, 1950) outfitted with a sealed boat for collecting

epoxy sections on the surface of distilled water. The sections were stained with Toluidine blue/Basic fuchsin stain (1% Toluidine blue O (C.I. 52040) in 1% sodium borate and 0.1% Basic fuchsin (C.I. 42510); modified from Blaauw et al., 1987) to differentiate muscle and connective tissues. The sections were examined using brightfield and phase contrast microscopy.

M. Hooge prepared whole mounts of six worms to reveal musculature by staining F-actin with fluorescently labeled phalloidin (Alexa 488; Molecular probes, Eugene, OR; Hooge, 2001). The specimens were fixed for 1 h in 4% (w/v) formaldehyde, rinsed in PBS (phosphate-buffered saline), attached to a coverslip treated with poly-L-lysine, simultaneously permeabilized, and stained for 45 min with phalloidin-Alexa diluted in 0.2% (v/v) Triton X-100 in PBS, and mounted under a second coverslip with Fluoromount-G (Southern Biotechnology Associates, Inc.; Birmingham, AL). I visualized these specimens using laser scanning confocal and differential interference contrast microscopy. Since the specimens were pressed laterally between two coverslips (a squash preparation), the pharyngeal bulb was in an everted position with the dorsal and ventral hooks oriented in a plane parallel to the coverslips and perpendicular to the optical axis of the confocal microscope. Three-dimensional images of the pharyngeal bulb musculature were produced by stacking parasagittal images. Contours drawn from these three-dimensional images, along with measurements from the histological sections, were used to generate a three-dimensional reconstruction of the proboscidial bulb using 3D modeling software (Anim8or, http://www.anim8or.com).

Results

Below I present the results of my morphological analysis of the *Cheliplana* proboscis (Fig. 50). Where possible, I use the terminology of Karling (1961, 1989) or De Vocht and Schockaert (1999). The main components of the proboscis that I describe below are the dorsal and ventral hooks, the left and right lateral auxiliary apparati, the trunk muscles, the hook abductor muscles, the retractor muscle, the nodus connective tissue, and the previously undescribed medial longitudinal connective tissue fibers.

Hooks & lateral auxiliary apparati

The hooks of the undescribed species of *Cheliplana* are slender, hollow, and medially curving cones that are 17.5 to 20.0 μm in length and roughly circular in cross-section. The hooks possess a flaired posterior opening with thickened walls where they are attached to the anterior tips of the trunk muscles (Fig. 50A). At the level of the flaired base, the hook diameter is approximately 2.5μm. This diameter tapers to approximately 1.25μm at the midpoint of the shaft and continues to taper to an inward curving closed point. The curve in the shaft approximates a 90° bend in the mid-sagittal plane and thus the tip section is almost exactly perpendicular to the shaft base. The hooks lack medial processes.

The lateral auxiliary apparati (Fig. 48, 50, 52) are present on the left and right of the hook supports and are approximately 10μm long. The posterior end of each apparatus is located next to the nodus at the base of the hook supports.

Proboscidial musculature

<u>Trunk muscles</u>

The trunk muscles and the hook abductor muscles of the hook supports (Fig. 50, 51, 52) represent the intrinsic muscles of the proboscis. The trunk muscles form the medial half

Figure 50. The *Cheliplana* proboscis in lateral view. A. Laser scanning confocal microscopy image. This image is composed of a z-axis stack of optically sectioned images overlaid with a differential interference contrast image to visualize the hooks (the lateral auxiliary apparatus and the longitudinal medial connective tissue strands are not visible here, but their positions are noted. (Image daltonized for better contrast viewing with dichromatic colorblindness) B. The same lateral view of the three-dimensional computer model.

A

10.0 μm

Hook abductor muscles

Area of nodus

Area of lateral auxiliary apparatus

Hooks

Area of medial connective tissue

Trunk muscles

Proboscis retractor muscles

B

Hook abductor muscles

Nodus

Proboscis retractor muscles

Lateral auxiliary apparatus

Hooks

Medial Connective tissue

Trunk muscles

Figure 50

169
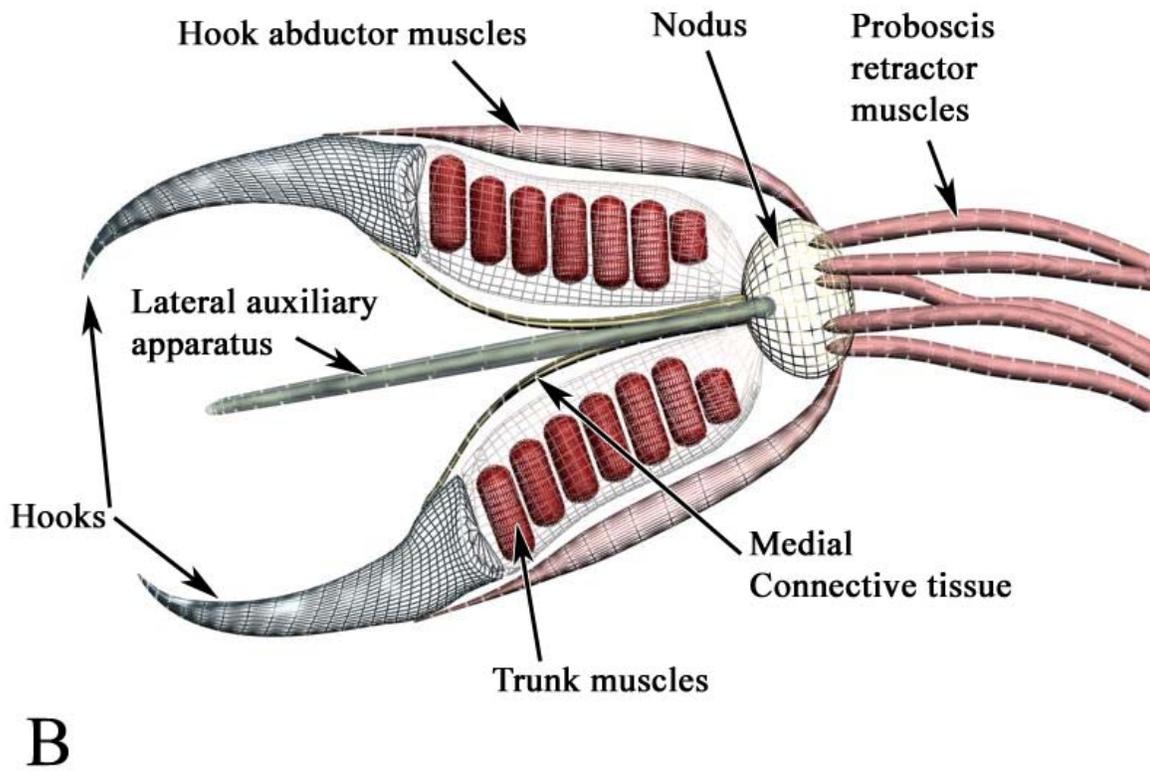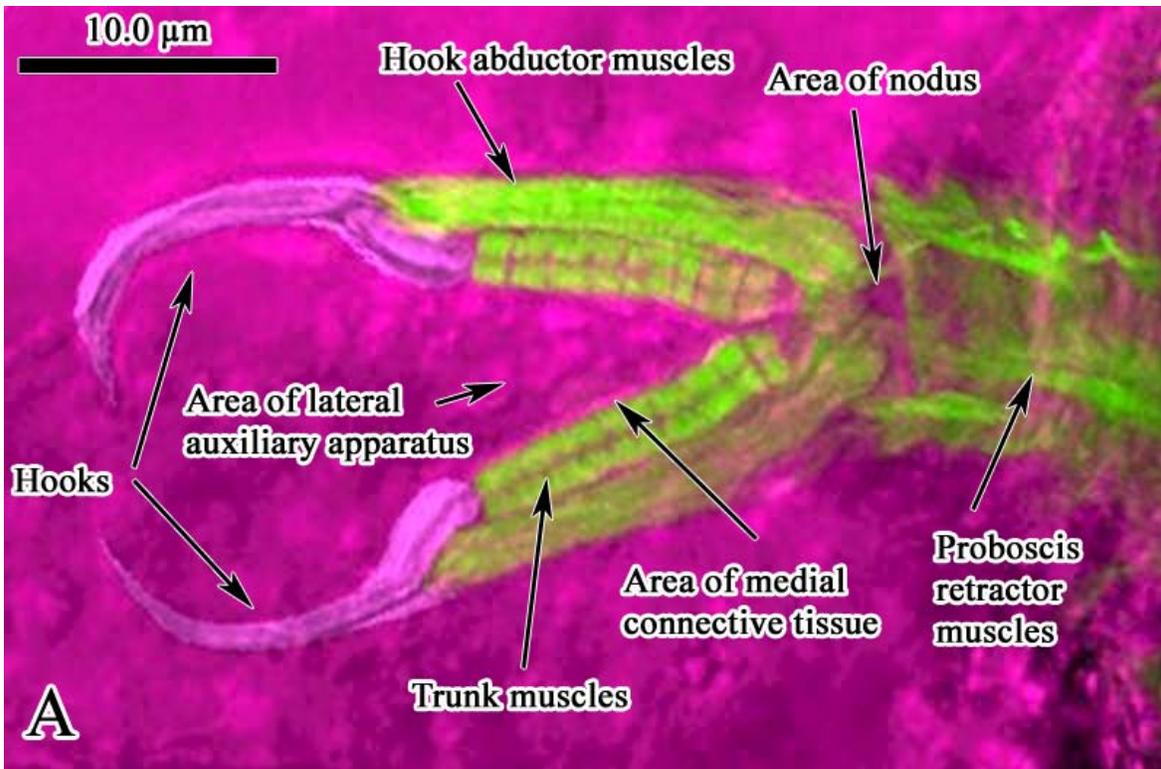
Figure 51. A laser scanning confocal microscopy image (A) of the *Cheliplana* proboscis musculature. As the fluorescent dye labels only the F-actin in the musculature, no other structures are seen. As illustrated in the labeled outline (B) below, the transverse alignment of the trunk muscle myofibril bundles, and the longitudinal orientation of the retractor and hook abductor muscles are clearly seen.
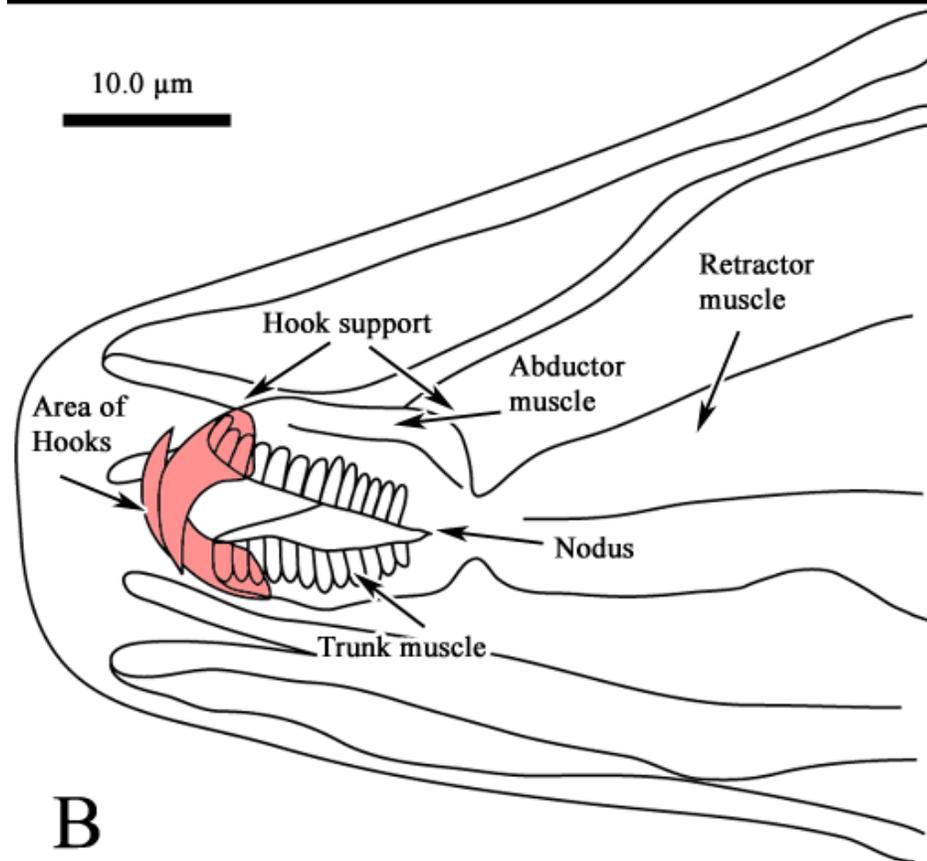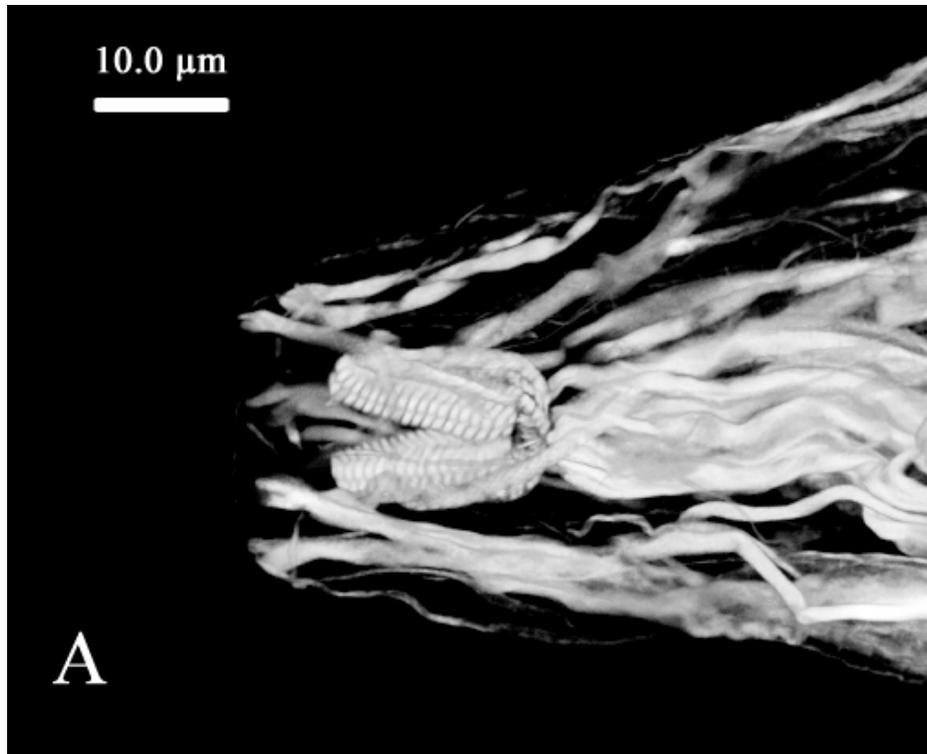
Figure 51
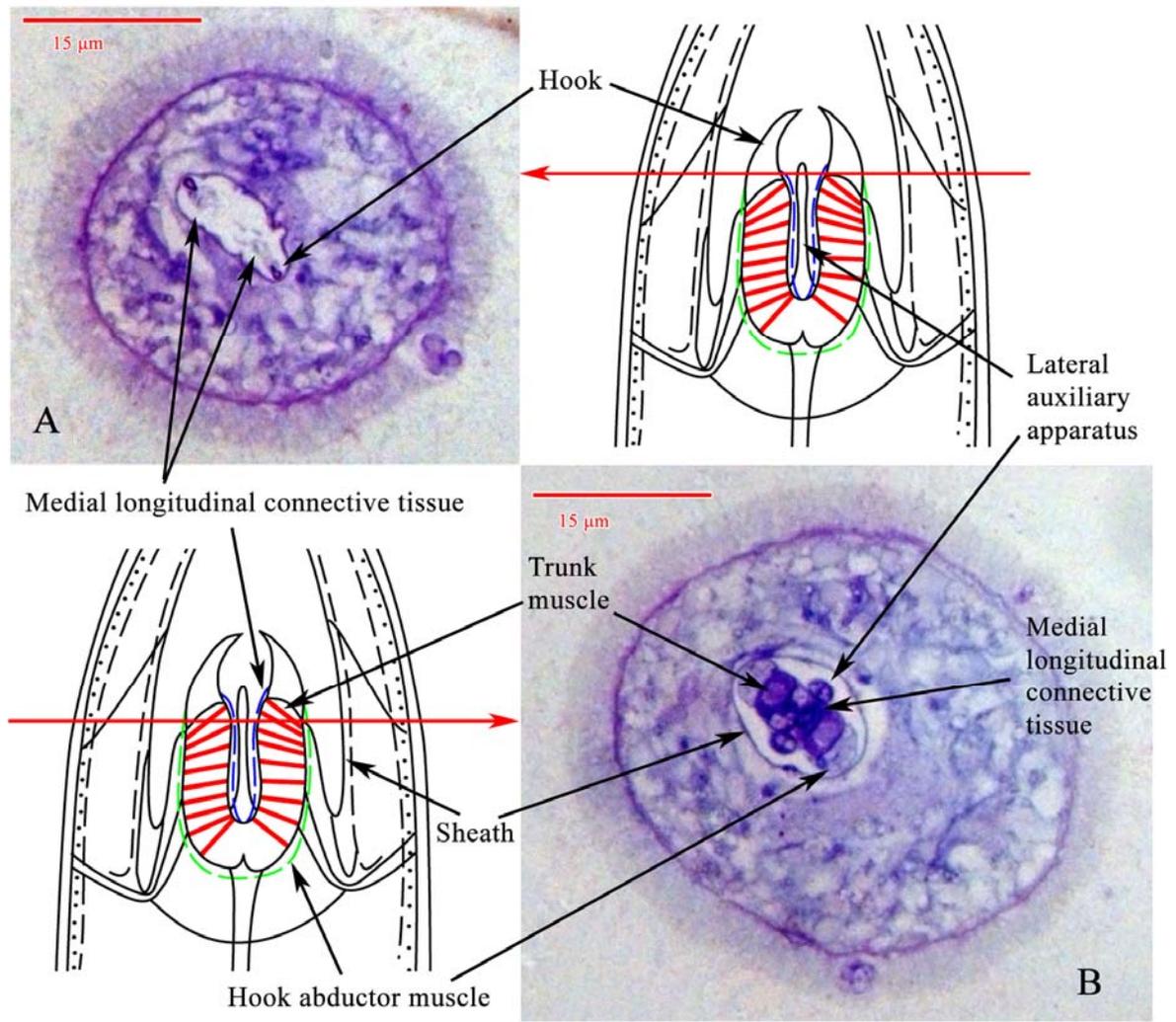
Figure 52. Transverse histological sections through the proboscis of *Cheliplana* at the levels indicated by the red horizontal arrows drawn on schematics reproduced from Fig. 49 E1. Section A is more anterior than section B. Note the medial longitudinal connective tissue strands of muscle along the inner surface of the hook shaft that may function in adduction (see text). (Brightfield microscopy of EMBed/Araldite epoxy resin section; Toluidine blue/Basic fuchsin stain)

of the dorsal and ventral hook supports. Each trunk muscle (Fig. 51) is formed of two stacks

of approximately 18 transverse strands. If these strands are synonymous with longitudinal

strands of the eukalyptorhynch conorhynch described by De Vocht (1991), they may

represent the actin myofilaments within bundles of myofibrils rather than individual cells.

When the hook supports are straight, the long axis of both stacks is roughly parallel to the

long axis of the proboscis. The stacks are formed by myofibril bundles layered one on top of

the other and their long axes are oriented in planes approximately perpendicular to the

longitudinal axis of the proboscis. They are not, however, parallel to each other or to the mid

sagittal plane (Fig. 51). They are instead obliquely arranged such that the lateral ends of the

myofibril bundles contact one another. There is an indentation at the midpoint of each bundle

of myofibrils that gives it a chevron-shaped appearance. Overall, the posterior end of the

trunk muscle is connected to the connective tissue nodus and the anterior end extends within

the flaired opening of the hooks.

Hook abductor muscles

The other intrinsic muscles of the proboscis are the hook abductors (Fig. 50, 51, 52).

These fibers have a longitudinal orientation when the hook supports are straight and extend

along the lateral edges of the dorsal and ventral trunk muscles. The hook abductor muscles

originate on the nodus lateral to the origin of the trunk muscles and insert on the external

posterolateral margin of the flaired hook base.

Retractor muscle

The retractor muscles are extrinsic to the proboscis and can be seen best in the three-

dimensional reconstructions generated by confocal microscopy (Fig. 51; also Fig. 50). These

medial fibers are oriented parallel to the long axis of the body and proboscis. The retractor

muscles insert on the connective tissue nodus that surrounds the nodal pore. The origin is well within the body and is thus obscured by the body wall musculature, but it is likely that they are anchored in the parenchyma of the body.

Connective tissue elements of the proboscis

<u>Nodus</u>

In confocal microscope images of fluorescently labeled musculature, the nodus appears as a small space (Fig. 50, 51) in the area where the trunk muscles, the hook abductor muscles, and the retractor muscles are connected at the base of the proboscis. In histological sections, this space is occupied with tissue with staining characteristics similar to collagen. The nodal pore appears as the space between the trunk and hood abductor muscles (Fig 49F, 50).

<u>Medial longitudinal connective tissue fibers</u>

The medial longitudinal connective tissue fibers (Fig. 52) have not been described previously and are dorsal and ventral connective tissue fibers that extend from an origin on the nodus to the posteromedial surfaces of the hook shafts. It is unclear whether these strands insert only at the above location or whether they are tightly bound along the length of the medial surface of the hook support as well as the hook shaft (they are represented in figure 53 as being only connected to the hook itself). In histological sections (Fig. 52), these connective tissue fibers show staining characteristics similar to collagen.

Discussion

The proboscis of *Cheliplana* likely functions as a muscle articulation. The musculature and connective tissue of the joint allows the proboscidial hooks to open and close with a wide range of motion that need not be dorsoventrally symmetrical (Karling,

1961; Beauchamp, 1961). Karling (1961) proposed a number of hypotheses of hook adduction and abduction based on a functional analysis of the morphology. I evaluate these hypotheses below, summarize the novel morphological details found in *Cheliplana*, and propose a hypothesis that may better describe the mechanism of the proboscis.

Opening

Karling (1961) and Schilke (1969) suggested that abductor muscles contract to rotate the hook tips open while the trunk muscles contract to provide skeletal support and resist the compressional forces exerted by the abductor muscles (Fig 49E). As the myofibril bundles of the trunk muscles in *Cheliplana* are transverse to the long axis of the hooks and hook supports, their orientation is appropriate to provide such skeletal support. Therefore my findings support those of Karling (1961) and Schilke (1969).

The trunk muscle will become wider during contraction of its transverse myofibril bundles. The overall effect of this contraction is an increase in the length of the trunk muscle and a decrease in its cross-sectional area. Thus, contraction of the trunk muscles may cause the hooks to be projected forward, away from the nodus. Co-contraction of the lateral abductor muscles, however, causes the extending trunk muscle to bend or bow laterally, resulting in the opening of the hooks.

Closing

Karling (1961) noted that in karkinorhynchs, like *Cheliplana*, the hook closing mechanism is uncertain because their proboscides lack adductor muscles. He proposed the following functional hypotheses of the closing mechanism.

The first hypothetical closing mechanism relies on the elasticity of the nodus to antagonize movements of the hook supports. This mechanism requires that the nodus

connective tissue fiber arrangement return the hook supports to a closed position after opening. In *Cheliplana*, no such arrangement was found. The nodus is a relatively small structure at the base of the hook supports to which the trunk muscles, the lateral abductor muscles, and the proboscis retractor muscles are all attached. Thus, the nodus may function primarily as an anchor point. Also, Karling (1961) noted asymmetrical movements of the hooks. Although asymmetrical closing could be caused by asymmetrical relaxation of the abductor muscles, if the nodus itself was primarily responsible for closing the hooks it may do so in a symmetrical manner because of its central location.

The second hypothesis suggests that transverse musculature below the nodus in some karkinorhynchs supplements the mechanism of the first hypothesis by providing additional closing force. I found no additional muscle fibers posterior to the node in *Cheliplana* (Fig 51). Furthermore, if these transverse muscle fibers were located posterior to the nodus, which may serve as a fulcrum, the posteriorly located transverse muscle fibers would open and not close the hooks.

The third mechanism, like the second, might not pertain to the specific morphology of *Cheliplana*. Some karkinorhynchs have a broad connection between the trunk muscles (Fig. 49D), perhaps reflecting their conorhynch ancestry. These broadly connected trunk muscles resemble a U-shape in which the myofibril bundles extend radially. Thus in the arms of the U-shape, the trunk muscle myofibril bundles are transversely oriented, while at the base of the U-shape, the myofibrils become progressively more longitudinal (as seen in Fig. 49 A2). Karling (1961) suggested that isolated activity of the myofibrils at the U-shape's base may extend the arms in a direction perpendicular to the axis of contraction (within the plane of the U-shape) and thus produce an opening motion. This hypothesis merits experimental tests,

176

perhaps microvideographical recordings. It is probably not, however, a mechanism used in *Cheliplana*. The myofibril bundles of the trunk muscles in *Cheliplana* are oriented parallel to one another in sequential transverse planes from the nodus to the hooks and there is only a very small connection between the trunk muscles at the nodus.

A fourth hypothesis can be derived based on Karling's (1961) illustration of movements in a karkinorhynch proboscis (Fig 49E). The anterior transverse myofibril bundles of the trunk muscles adjacent to the hooks are shown extending from the outer medial surface of the hook base to its outer lateral surface. Thus contraction of these myofibril bundles might rotate the hooks closed. This is unlikely in *Cheliplana*, because the transverse myofibril bundles lack analogous origin and insertion points. In fact, the relatively short transverse myofibril bundles of the trunk muscles that are visible within the hollow hooks may have internal, rather than external attachments to the hooks.

While the above hypotheses may explain hook closures in other schizorhynchs, they do not adequately describe the *Cheliplana* mechanism. Below, I describe a hypothesis that includes a previously undescribed component of the proboscis; the medial longitudinal connective tissue fibers.

Functional hypotheses of armed karkinorhynch proboscis movements

The major novel morphological finding of this study is the presence of the medial longitudinal connective tissue fibers of the dorsal and ventral hook carriers. These fibers exist in *Cheliplana*, and perhaps other karkinorhynchs, in the approximate location of the adductor muscles in the diascorhynch proboscis. They may function by resisting elongation of the trunk and thus antagonize the trunk muscles of the hook supports. A summary of their role is
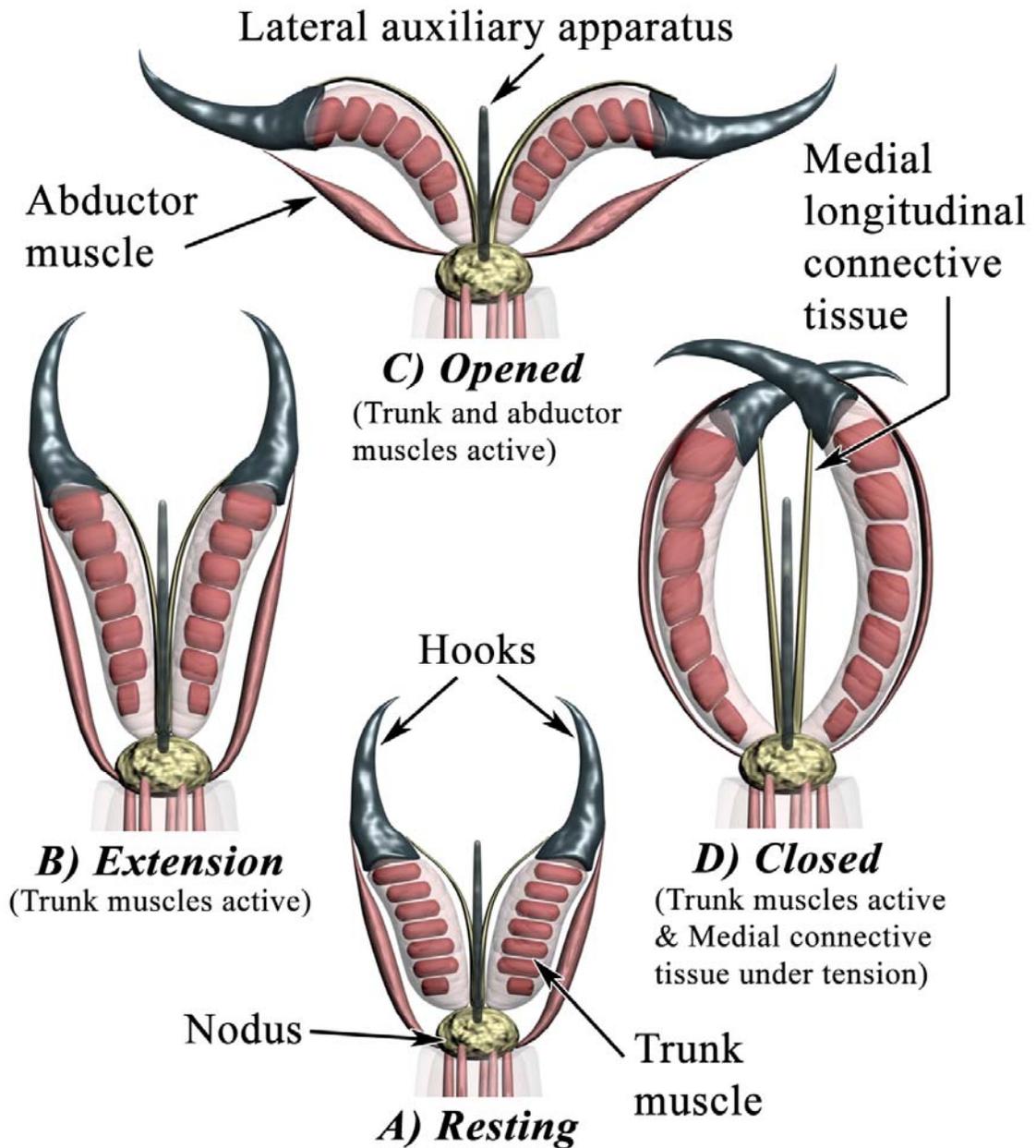
Figure 53. The proposed mechanism for the opening and closing of the *Cheliplana* proboscidial hooks. A) Resting phase; all muscles relaxed. B) Extension phase; trunk muscles activate and extend hooks. C) Opened phase; abductor muscles activate and bend the active trunk muscles. D) Closed phase; trunk muscles maximally contract and bend as they load medial longitudinal connective tissue strands in tension. The return to resting phase requires relaxation of the trunk muscles and contraction of the abductor muscles.

presented as a sequence of steps during which the hooks are rotated and translated during opening and closing movements (Fig. 53A-D).

Resting

The phase in which no muscles are active, and thus the proboscis is at rest is shown in Figure 53A. At rest, the aligned stack of transverse trunk muscle myofibril bundles may be straight. Preserved whole mounts of *Cheliplana* might give insight into hook form between this resting phase and the following extension phase. This is because during preservation, Karling (1961) noted that everted proboscides often perform a quick elastic grabbing movement that, in my specimens, may have resulted partially contracted but undivaricated hook supports. In the preparations I observed, the transverse myofibril bundles of the trunk muscles did not appear to be maximally contracted because the hook supports were generally straight even thought the lateral abductor muscles appeared taut.

Extension

Partial contraction of the hook support trunk muscles may result in protrusion of the hooks (Fig. 53B). Shortening of the transverse myofibril bundles of the trunk muscles decreases the cross-section of the trunk and thereby increases its length. As described by Karling (1961), the dorsoventral width of each hook support decreases as it lengthens.

Opening

Opening movements (Fig. 53C) result in the simultaneous lateral translation and rotation of the hooks such that the distance between them increases (the hooks divaricate) and the hook tips that are bent at almost 90° are brought nearly parallel to the proboscis longitudinal axis. This motion is often described as occurring in the mid-sagittal plane, but this may be an artifact of the whole mount squash preparation. Alternatively, the connective

179

tissue nodus might serve as an anchor to stabilize the hooks and hook supports during natural movements. Careful analysis of microscope video recordings of unrestrained specimens is needed.

The opening translation and rotation of the hooks may be accomplished by the co-activation of both the trunk and abductor muscles. During contraction, the trunk muscle may stiffen as it extends the hook forwards. The stiff trunk muscle may provide antagonistic support for the contraction of the abductor muscles. Because of their lateral locations in the hook support, contraction of abductor muscles may compress the lateral sides of the trunk muscles and thereby create a lateral bend (or bowing) in the hook supports (Fig. 53C). This lateral bowing of the hook supports might explain both the translation and rotation of the hooks.

Closing

Hook closure (Fig. 53D) may occur in two phases. The first is characterized by the partial contraction of the trunk muscles seen in the previous phases and the second requires maximal contraction of the trunk muscle placing the medial longitudinal connective tissue fibers in tension and thus actively adducting the hooks. In the first phase, closing the hooks requires relaxation of the abductor muscles while the trunk muscles continue contract. The rigidity of the trunk muscles may passively return the hook supports to the straight, extended position. In the second phase, further or maximal contraction of the trunk muscles result in the extension of the hook supports beyond the length to which the medial longitudinal connective tissue strands may extend. The connective tissue might limit further lengthening of the medial, but not the lateral sides of the hook supports, bending the supports towards the midline and closing the hooks.

<u>Retraction</u>

The retraction phase returns the hook supports from any other position back to the resting position. From either the closed or opened positions, relaxation of the trunk muscles causes the hook supports to straighten. Then, contractions of the abductor muscles return the hook supports to their shorter resting length.

Summary and future studies of the kalyptorhynch proboscis

It is probable that the proboscis of *Cheliplana* is a muscle articulation because its soft tissues are appropriately arranged to provide the functional requirements of this flexible joint type. First, the musculature may create force necessary for link movement; hook opening forces may be generated by the adductor and trunk muscles of the hook supports and closure may be the result of lengthening of the trunk muscles in an asymmetric manner imposed by the medial longitudinal connective tissue strands. Second, the soft tissue may form a compression bearing element. This element may be represented by the trunk muscles that stiffen during contraction. Compressive forces may be transmitted from one hook to the other through the stiffened trunk muscles connected at their bases by the nodus. The hook supports may be stiffest when the extension force of the trunk muscles, the tension in the medial longitudinal connective tissue strands, and the hook retraction forces generated by the abductor muscles are balanced. Third, arrangements of soft tissue (in this case both muscle and connective tissues) may provide antagonistic skeletal support. The medial longitudinal connective tissue strands, the hook abductor muscles and the trunk muscles provide mutual antagonistic support to open and close the hooks.

Whereas my morphological analysis of the *Cheliplana* proboscis reveals common muscle articulation functions, novel characteristics were also observed. The proboscis

181

mechanism does not make use of great numbers of complex muscle fiber orientations. Instead, two discrete and perpendicular muscles (the transverse myofibril bundles of the trunk and the longitudinal hook abductor muscles) and the tension-bearing medial longitudinal connective tissue fibers are connected by the nodus to form a muscular hydrostat capable of the functions of a muscle articulation joint. This construction illustrates that muscle articulations can be relatively simple mechanisms with few components. Additionally, the components that are used in tension may be formed of connective tissue rather than metabolically expensive muscle.

Better characterization of the karkinorhynch trunk muscles requires additional morphological investigations. What I have described as transverse bundles of myofibrils, based on De Vocht's (1991) description of conorhynch morphology, might also be muscle fibers or actin filaments functioning as cytoskeletal elements. Transmission electron microscopy of trunk muscle ultrathin sections and antibody labeling of myosin in the trunk might help distinguish between these possibilities.

As this study was limited to morphological descriptions only, I am planning future experimental studies of the kalyptorhynch proboscis to test the functional hypotheses presented above. Video recording of proboscidial hook movements during opening and closing behaviors will provide useful insights. Measurements of the bending angles and muscle length changes of the hook supports and of the displacements of the hook during abduction may be instructive in testing the functional roles of the muscular components of the proboscis. Additional possible experiments include using fluorescent calcium indicators to sense muscle contraction (e.g. Ito et al., 1988) while recording corresponding changes in microscopic tension during divarication of the hook supports (Anazawa et al., 1992). While

these further studies of microscopic structures might require specialized techniques, the transparency of these animals may aid *in vivo* investigations of muscle function.

Kalyptorhynchs may be a good model system to study the evolution of a muscle articulation. Karling (1961) noted that unarmed schizorhynch proboscides, from which armed karkinorhynch proboscides may have evolved, are used to wrap and adhere to prey items. Here contractions of transverse myofibril bundles of the trunk muscle fibers in the tongues are thought to produce the wrapping motion and it is possible that the curling motion is caused by a set of medial longitudinal connective tissue fibers. This would represent an opportunity to study the evolution of a muscle articulation because these tongues have no hooks that serve as the links required by muscle articulations. Furthermore, the proboscides of other schizorhynchs (i.e. the Diascorhynchidae) are well-developed with strong adductor and abductor muscles and jaws that are capable of interlocking biting motions. A comparative biomechanical analysis of unarmed schizorhynchs, armed karkinorhynchs and armed diascorhynchs may provide insight not only into the evolution of these animals, but into the evolution of an increasingly complex muscle articulation from a simple muscular hydrostat precursor. Finally, little is known about the control of proboscis behavior in schizorhynchs (or indeed in muscle articulations in general) and thus a comparative analysis may reveal changes in the requirements for control as the schizorhynch proboscis evolves.

Conclusions

Summary of general muscle articulation characteristics

Muscle articulations are flexible joints consisting of muscle and connective tissue between rigid links. These soft tissues are arranged to provide three critical functions that help define the flexible muscle articulation type joint.

First, the muscle and connective tissues of muscle articulations must form a compression-bearing element. This differentiates muscle articulations from other flexible joints, such as those between distal leg segments of some small insects (see Ch. 1). The simple insect joints are used primarily in tension because when loaded in compression, they buckle and cease to function. The joints between the valves of inarticulate brachiopods, the beaks of octopuses, the jaws of nereid polychaetes, and the hooks of kalyptorhynch flatworms do not buckle during the occlusion of their links because their soft tissues are arranged as compression-bearing elements and transmit reaction forces across the joint. In each of these structures, the soft tissues that form the compression-bearing element are arranged as muscular hydrostats.

Second, as the rigid links of muscle articulations do not make contact in the joint, they do not provide skeletal support for the contraction and lengthening of antagonistic muscles. The soft tissues themselves provide skeletal support by contracting to form stiffened supports against which muscles act and also to form pivots around which the links rotate.

Third, the muscle articulation itself generates the force to move the rigid links. Thus, muscle or, as seen in the kalyptorhynch proboscis, connective tissue fibers must be arranged antagonistically in order to adduct and abduct the links and return each other to resting length.

In the muscle articulations studied in this dissertation, a given orientation of soft tissue fibers typically has multiple functions. As an example, the transverse trunk muscle myofibril bundles in the karkinorhynch proboscis hook supports resist compression and also adduct the hooks.

Future muscle articulation studies

There are three general areas in which I am planning further biomechanical analyses that may improve theoretical understanding of muscle articulations: morphological analysis of additional examples (form), experimental tests of predicted function (function), and the investigation of neuromuscular control (control).

Form

Additional morphological analyses of undescribed muscle articulations will provide insight into the diversity of muscle articulation construction. The relatively few joints described in this dissertation show that muscle articulations encompass an impressive morphological diversity and that they are important for at least four unrelated and successful phyla of animals. Although their morphologies differ, they have convergently evolved the multiple soft tissue functions characteristic of a muscle articulation. I plan to study additional muscle articulations to provide additional insight into the theory of how muscle articulations work, how they have evolved, and to explore their importance within a wider group of organisms. Two additional possible examples include an arthropod and an onychophoran. Wood-boring beetle larvae show a great variation in mandibular morphology (Nieves-Aldrey et al., 2005), and in some groups, the mandibles are loosely connected and show a wide range of motions. The independently mobile jaws of *Peripatus* are embedded within the soft body (Manton & Harding, 1964) and might represent another muscle articulation.

Function

If experimental preparations can be successfully developed, I plan to further test the functional hypotheses resulting from the morphological descriptions to allow a more complete biomechanical description the *Nereis* pharynx, the *Cheliplana* proboscis, and future

potential muscle articulations. These functional studies might include the description of muscle activation sequences, the measurement of resultant movements (such as changes in muscle length and translations and rotations of links), and the characterization of the muscle and connective tissue mechanical properties.

The biomechanical analyses of muscle articulations may also become the basis for more ultimate questions; can the functional morphology of a muscle articulation be correlated with its use by an organism living in a particular ecological niche? Conversely, are there general biomechanical principles that explain why some groups of related organisms have evolved muscle articulations while others have not (e.g. armed karkinorhynch proboscides versus unarmed schizorhynch tongues)?

Finally, the three-dimensional reconstructions of these structures have helped to identify important mechanical characteristics (such as the proper spatial relations of structural components and actual location of rotational axes). In collaboration with engineers, I plan to develop and test physical models that may be useful in identifying conceptual errors and allow me to test the effects of changing dimensions (e.g. attachment points of muscle or connective tissue strands) or material properties of components (e.g. the elasticity of the links). Such model muscle articulations may additionally be practically useful if they inspire human-engineered robotic manipulators capable of complex and diverse movements.

Control

A major benefit of muscle articulations over many other types of joints is their ability to perform a variety of behaviors due to their remarkable range and diversity of motions. This benefit may come at the cost, however, of more complicated neuromuscular control. Although it is not a muscle articulation (the jaws bear a fibrous hinge), the pharyngeal

apparatus of the sea hare *Aplysia californica* supports a variety of functions (e.g., manipulating, swallowing, spitting, chewing etc.). While the control of these multiple functions comes from neural inputs, Ye et al (2006) and Novakovic et al. (2006) found that the relationship is bidirectional. Changes in the shape of one muscle alter the shapes of others around it, and these mechanical reconfigurations are affected by, but also have an effect on neural control. This is almost certainly the case in muscle articulations in which axes of rotation, planes of translations, and lengths of lever arms may be actively controlled. Thus, the analysis of muscle articulation neural input patterns, resulting in complex muscle activation patterns that allow multiple joint functions, is important not only for the understanding of how these joints function, but might help characterize the nature of the neuromuscular control and ultimately how complex behaviors are generated.

APPENDIX I: A device to monitor small movements in seawater

The recording of opening and closing movements in chapter three used a simple electronic circuit and miniature ball electrodes that were specifically designed for this purpose. This technique is described below as it was used in the experimental protocol of chapter three. A more generally applicable form of this technique has been published in Uyeno & Hsiao (2007).

The measurement of gape between the octopus beaks poses several technical challenges. First, the maximum distance change is relatively small (≤1cm) and must be accurately and precisely measured with a high special and temporal resolution and low noise. Second, the technique must be compatible with the high electrical conductivity of seawater. Third, the instrumentation attached to the beak must be designed to minimize the mechanical loading of the buccal mass joint in order to minimally alter its natural behavior. Fourth, the technique should output an analog electronic signal in order to be synchronized and recorded along with muscle activation data recorded as electromyographs. Fifth, as an electromyogram is being recorded concurrently, neither the signal generated by the electrical movement monitor nor its harmonics should be within the frequency range to produce artifacts in the electromyographical data. Sixth, the technique should employ a robust, stable, and cost effective construction design. Below is the description of the circuit, its construction, and issues of calibration and use.

Description of the circuit design

In reading the following set of circuit stage descriptions, please refer to the electronic circuit schematic shown in figure 54. The first stage of the circuit is an isolation transformer.
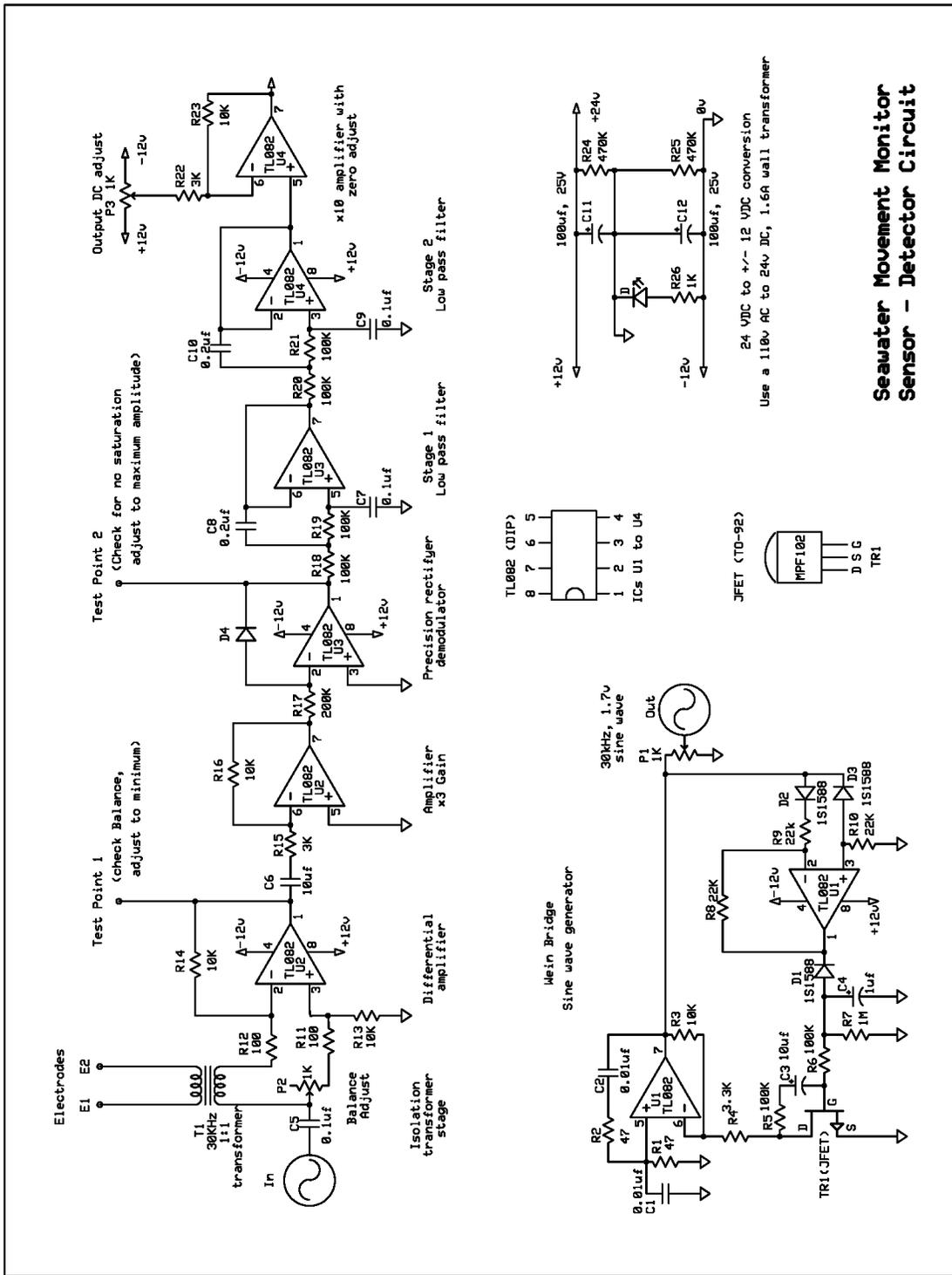
Figure 54. Movement monitor circuit schematic.

189

The electrodes are connected to the input of a high frequency response 1:1 transformer to help isolate circuit ground from the electrode reference ground. This transformer allows other voltage measurements, such as electromyography, to be made without artifacts and in isolation, because the electrical ground reference is independent. In this circuit, I use the low noise, high input impedance TL-082 general purpose operational amplifier as its maximal differential input voltages are ±15 v. Thus I modified a 24 volt AC power supply to provide ±12 volts (Fig. 54). This provided an adequate voltage range to ensure sufficient resolution.

The movement monitor circuit uses a front end 30 kHz sine wave generator with variable amplitude to generate the carrier frequency. This frequency was selected as it is well above the movement frequency, or even any known muscle activation frequencies. In this way the circuit does not add lower frequency noise. I chose a Wein bridge oscillator circuit was specifically selected because of its stability, exceptional low noise, and low distortion characteristics. In this bridge circuit the equivalent resistance of the electrodes is balanced using a potentiometer to nullify a reference voltage. Furthermore adjusting the reference voltage in this bridge circuit effectively nulls out baseline resistance and the desired motion signal can be highly amplified without increasing the artifacts due to the electrode properties.

Next, the signal is sent to a series of conditioning stages. First, the signal is amplified at high gain and demodulated. Demodulation is performed with a rectifier and two low pass filter stages (80 dB/decade). Finally, in the last stage, the extracted signal is amplified and baseline adjusted to zero for display and recording or digitizing.

The unique features of this circuit are the initial ground isolation in combination with a modified bridge circuit and carrier frequency generator. These combine to give a stable, low drift and low noise distance measurement.

Construction of the circuit board and considerations in electrode design

The device was originally designed and constructed using a prototyping circuit board; however a cleaner signal was obtained when the components were transferred to a printed circuit board. Both the schematic and the artwork used to create the printed circuit board were designed using ExpressPCB (Free CAD software found at http://www.expresspcb.com) This printed circuit board was made using an electronic trace template printed with etchant resistant ink, ferric chloride etchant and single sided copper clad circuit board. The printed circuit board artwork is reproduced in Figure 55.

The circuit uses a low current AC signal to avoid the polarization and plating of the sensor/detector electrodes. To limit lower frequency noise, these silver/silver chloride electrodes were made of the shortest possible lengths of 0.2 mm diameter wire insulated from the base to almost to the tip. The uninsulated tips were melted into matched 0.5 mm balls using a propane torch. The electrodes were then "chlorided" to stabilize the electrode potential (Geddes, 1972). This was accomplished by electrically connecting the electrodes and soaking the tips in chloriding solution (200 ml distilled H_2O, 100 g $FeCl_3$, 100 ml HCl) until a dull dark finish appeared on the exposed tips (about 10 min). After initial chloriding, I maintained the electrodes between experiments by immersing the tips in full strength commercial bleach (6% sodium hypochlorite by mass). I soldered the electrodes to copper leads to minimize the use of expensive silver wire. However, I found it important to insulate and not immerse this connection in water, as can generate current and artifactual noise.

System setup, calibration, and testing

The output signal of the circuit was recorded on a computer hard drive using an analog-to-digital converter card. The output was also monitored on an oscilloscope.
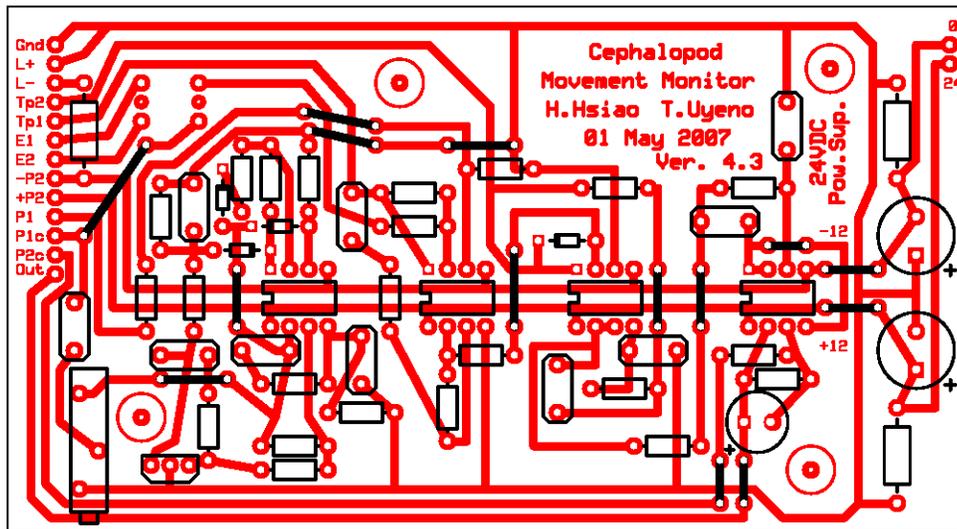
Figure 55. Movement monitor printed circuit board trace artwork. Note circuit is reproduced

here in actual 1:1 size for use in printed circuit board reproduction.

All the electrical systems associated with the buccal mass preparation were independently grounded so as not to introduce ground loop artifacts.

Accurate calibration allowed the measurement of actual gape distances. However, as changes in electrode tip shape and surface area as well as changes in the salinity of the water affect voltage output amplitudes, the circuit required calibration prior to each experiment. Using calipers attached to a micromanipulator, I measured the distance between the electrodes immersed in full-strength seawater (35 ppt) while recording the voltage output. The relationship between voltage and distance was described by computer fitting the appropriate function using the statistical software R (R Development Core Team, 2006). Because of the two-electrode design, this relationship cannot be entirely linear as field strength decreases and resistance increases with increases in distance. Figure 56 documents this effect using two electrodes with spherical tips of a diameter of 0.5 mm, immersed in seawater of 35 ppt and 21°C, and altering the distance between the tips from 0 mm to 10 mm. The relationship between voltage and distance can be described by a simple asymptotic function:

$$V = \frac{0.094D}{3.977 + D} \hspace{3cm} \text{Eq. 6}$$

where D is the distance (mm) and V is voltage (volts). Here it is important to either carefully adjust the DC offset (1K ohm potentiometer "P3" in Fig. 54) to zero, or standardize the voltage values after recording, such that both D and V are initially equal to zero.

I found that evaporation had to be controlled otherwise a significant amount of drift occurs. During a 10 h test to measure this effect, in which the salinity changed from 35ppt to 41 ppt, recordings from electrodes separated by 1 cm showed a drift of 9.1 mV/h. When the

193

test was performed again in a covered container the drift was negligible over the same period.

Finally, I found a warm-up period of approximately 4-8 minutes was necessary, as initial voltage output was low and rose to a stable reading prior to the end of that period.
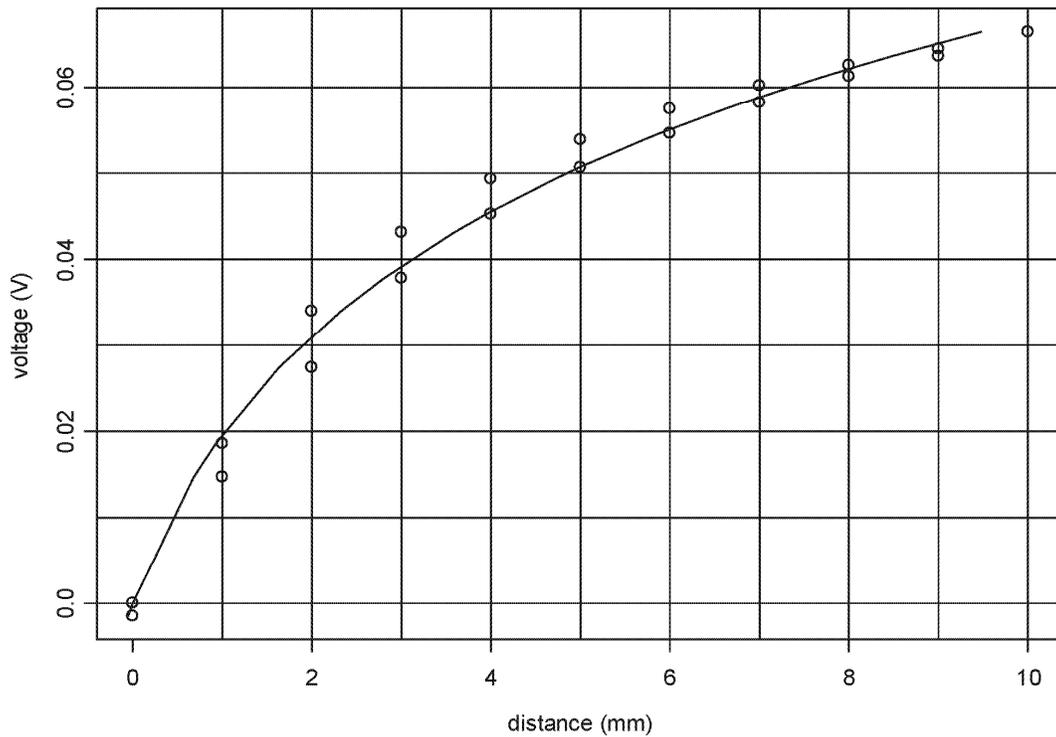
Figure 56. The movement monitor calibration correlating voltage output (volts) to distance (mm) between electrodes. Open circles represent voltage recordings at particular known inter-electrode distances and line of best fit is described by eq. 6.

APPENDIX II: Matlab code for EMG and movement monitor data analysis

The methods of chapter three included the use of fine wire electromyography (EMG) to record electrical signals that denote muscle activation patterns associated with beak openings and closings. As readily available analysis solutions were not available, I wrote the Matlab 7 (MathWorks, Natick, MA) computer language code below with the help of Dr. Randal Cole (Biomedical Engineering, UNC Chapel Hill, NC) and using helpful suggestions by Dr. Doug Altshuler (Biology, UC Riverside, CA).

The program analyzes raw EMG and movement monitor data recorded as an ASCII text file using the following methods: A spectral analysis of the raw data, using a fast fourier transform algorithm, is first performed to evaluate whether sampling rates were appropriate. Here, a 4 kHz sampling rate was shown to be adequate. The offset of the raw data was set to zero and the data was then rectified such that all points were positive. To create an envelope that described the rectified data, they were smoothed using a low pass, second order Butterworth filter with the time constant set to 79.5 ms. To correlate the filtered EMG data to events recorded by the movement monitor, I wrote a subroutine to identify muscle activity onset by defining these thresholds as activity above 2.5 standard deviations from the rectified EMG signal during a one second steady state period prior to a muscle activation.

Readout of the Matlab 7 code (File name: "octobeaks.m", ASCII text format):

```
% EMG/Movement Monitor Data Analysis Program (from text data file)
% written by R. Cole & T. Uyeno

% Variables
% A - the matrix
% A(:,1) - Channel 1 data
% A(:,2) - Channel 2 data
% A(:,3) - Channel 3 data
% timearr - the timeline
```

```matlab
% meancol1 - average value for channel 1 data
% meancol2 - average value for channel 2 data
% A1aver - channel 1 data rezeroed
% A2aver - channel 2 data rezeroed
% A1abs - rectified channel 1 data
% A2abs - rectified channel 2 data
% fftA1aver - frequency data for channel 1
% fftA2aver - frequency data for channel 2
% A1filt - Butterworth filtered channel 1 data
% A2filt - Butterworth filtered channel 2 data

clear all;
workdir = pwd;
[fname,pname] = uigetfile('*.txt','Select Excel File');
cd (num2str(pname));
A=load(fname);          %Reads the dat file and stores it in matrix A.
cd (num2str(workdir));

DisplayFileName = uicontrol('Style','text',...
      'Units','normalized',...
      'FontSize',12,...
      'Position',[.10 .96 .1 .03],...
    'String',fname);

[Rows,Columns]=size(A);

starttime=0;    % Arbitrary start time
endtime=(Rows-1)*0.00005;    % End time based on 20KHz sampling rate

timearr=[starttime:0.00005:endtime]; % Time array based on start end times

% Plotting the basic raw data
figure(1)
subplot(311)
plot(timearr,A(:,1));
subplot(312)
plot(timearr,A(:,2));
subplot(313)
plot(timearr,A(:,3));

% Calculating means and rezeroing data
    % Column 1
meancol1=mean(A(:,1));
if meancol1>0
    A1aver=A(:,1)-abs(meancol1);
else
    A1aver=abs(meancol1)+A(:,1);
end
    % Column 2
meancol2=mean(A(:,2));
if meancol2>0
    A2aver=A(:,2)-abs(meancol2);
else
    A2aver=abs(meancol2)+A(:,2);
end

% Rectifying data
```

196

```
A1abs=abs(A1aver);
A2abs=abs(A2aver);

% Filtering data (Dr. D. Altshuler's suggestion Butterworth filter)
[b,a] = butter(2, .0001); %.5 is 1/4 the cutoff frequency. Altshuler has
it between .01 and .001
A1filt = filtfilt(b,a,A1abs);
A2filt = filtfilt(b,a,A2abs);

% Analyzing filtered data (to make sure that the Butterworth filter is not
cutting off in range data)
meanA1=mean(A1filt);
A1filt=A1filt-mean(A1filt);
rr1=fft(A1filt,4096);
meanA2=mean(A2filt);
A2filt=A2filt-mean(A2filt);
rr2=fft(A2filt,4096);
figure(2)
subplot(211)
plot(fftshift(abs(rr1)))
subplot(212)
plot(fftshift(abs(rr2)))

% building frequency analysis diagram (using a fast fourier transform
using a frequency range of 4K)
fftA1aver=fft(A1aver,4096); % analyzing column 1
fftA2aver=fft(A2aver,4096); % analyzing column 2

% Plotting raw EMG data and frequency spectrum
figure(3)
subplot(221)
plot(timearr,A(:,1)) % plotting column 1 raw data
subplot(222)
plot(timearr,A(:,2)) % plotting column 2 raw data
subplot(223)
plot(fftshift(abs(fftA1aver))) % plotting column 1 frequency data
subplot(224)
plot(fftshift(abs(fftA2aver))) % plotting column 2 frequency data

% Plotting rezeroed, rectified, filtered EMG and movement data
figure(4)
subplot(421)
plot(timearr,A1aver) % plotting column 1 rezeroed data
subplot(422)
plot(timearr,A2aver) % plotting column 2 rezeroed data
subplot(423)
plot(timearr,A1abs) % plotting column 1 rectified data
subplot(424)
plot(timearr,A2abs) % plotting column 2 rectified data
subplot(425)
plot(timearr,A1filt) % plotting column 1 filtered data
subplot(426)
plot(timearr,A2filt) % plotting column 2 filtered data
subplot(427)
plot(timearr,A(:,3)) % plotting column 3 data
subplot(428)
plot(timearr,A(:,3)) % plotting column 3 data
```

```
% Plotting offset

n=1000;                                                     %n is
the number of points (or msec) for baseline reference
DURATION=1;
%DURATION is the time that onset has to stay above the threshold
FOLLOWTIME=1;
num_std=2.5;
%num_std is the number of standard deviation(std) for onset threshold

%A1abs is the EMG data vector for a given muscle
P1 = A1abs(1:n);
                    %P is the vector from the first n points of the emg1
vector
P2 = A2abs(1:n);

threshold1 = mean(P1) + std(P1)*num_std;
%threshold is the point beyond num_std deviations above the mean baseline
reference
threshold2 = mean(P2) + std(P2)*num_std;

figure (5)
subplot(211)
plot(timearr, A1abs, 'y'); hold on;
              %plot the entire vector in yellow first, then hold it
                                                            %Now,
plot the onset part over the orginal graph
for i = 1:length(A1abs)-FOLLOWTIME
    if abs(A1abs(i)) & abs(A1abs(i:i+FOLLOWTIME)) > threshold1
%DURATION is the time that data has to stay above threshold, 10msec for me
      plot(timearr(i:i+FOLLOWTIME),A1abs(i:i+FOLLOWTIME),'b');
%using a blue color
    end                                                     %if a
point in the data set is greater than the threshold and stays above the
threshold for 10 ms,
end                                                         %then
plot this point and the following 10 ms of data in a different color from
the original plot.

subplot(212)
plot(timearr, A2abs, 'y'); hold on;
for i = 1:length(A2abs)-FOLLOWTIME
    if abs(A2abs(i)) & abs(A2abs(i:i+FOLLOWTIME)) > threshold2
    plot(timearr(i:i+FOLLOWTIME),A2abs(i:i+FOLLOWTIME),'b');
    end
end
```

198

REFERENCES

Alexander RM. 1983. *Animal mechanics*. Blackwell Scientific Publication, Boston, MA. 301 pp.

Altman JS & Nixon M. 1970. Use of beaks and radula by *Octopus vulgaris* in feeding. *Journal of Zoology*. 161: 25-38.

Ambrose WG Jr. 1984a. Role of predatory infauna in structuring marine soft-bottom communities. *Marine Ecology – Progress Series*. 17: 109-115.

Ambrose WG Jr. 1984b. Influences of predatory polychaetes and epibenthic predators on the structure of a soft-bottom community in a Maine estuary. *Journal of Experimental Marine Biology and Ecology*. 81(2): 115-145.

Anazawa T, Yasuda K, & Ishiwata S. 1992. Spontaneous oscillation of tension and sarcomere length in skeletal myofibrils: Microscopic measurement and analysis. *Biophysical Journal*. 61: 1099-1108.

Arnold JM & Arnold KO. 1969. Some aspects of hole-boring predation by *Octopus vulgaris*. *American Zoologist*. 9(3): 991-996.

Bakken T & Wilson RS. 2005. Phylogeny of nereidids (Polychaeta, Nereididae) with paragnaths. *Zoologica Scripta*. 34(5): 507-547.

de Beauchamp P. 1927. Rhabdocoeles des sables à diatomées d'Arcachon I. Coup d'œil sur l'association Schizorhynchidae. *Bulletin de la Société Zoologique de France*. 52: 351-359.

de Beauchamp P. 1961. Classe des Turbellariés. In: *Traité de Zoologie: Anatomie, Systématique, Biologie* (Grassé P-P. ed.). Tome 4, Fascicule 1. Masson et Cie, Paris. p. 35-174.

Bennett HS, Wyrick AD, & Lee SW. 1976. Science and art in preparing tissues embedded in plastic for light microscopy, with special reference to a glycolmethacrylate, glass knives, and simple stains. *Stain Technology*. 51: 71-95.

Birkedal H, Broomell C, Khan RK, Slack N, Lichtenegger HC, Zok F, Stucky GD, & Waite JH. 2005. The jaws of *Nereis*: microstructure and mechanical properties. In: *Structure and Mechanical Behavior of Biological Materials* (Fratzl P, Landis WJ, Wang R, & Silver FH, Eds.) *Materials Research Society Symposium Proceedings*. Warrendale, PA. 874: L2.8-K2.8.

Blaauw EH, Jonkman MF, & Gerrits PO. 1987. A rapid connective tissue stain for glycol methacrylate embedded tissue. *Acta Morphologica Neerlando-Scandinavica*. 25: 167-172.

Boletzky Sv. 1999. Cephalopod development and evolution In: Advancing Research on Living and Fossil Cephalopods (Olóriz F& Rodríguez-Tovar FJ, Eds.) Kluwer Academic/Plenum Publishers, New York. p. 3-11.

Boletzky Sv. 2007. Origin of the lower jaw in cephalopods: a biting issue. *Paläontologische Zeitschrift*. In press.

Bonnaud L, Boucher-Rodoni R, & Monnerot M. 1997. Phylogeny of cephalopods inferred from mitochondrial DNA sequences. *Molecular Phylogenetics and Evolution*. 7(1): 44-54.

Boyle PR, Mangold K, & Froesch D. 1979a. The organization of beak movements in *Octopus*. *Malacologia*. 18: 423-430.

Boyle PR, Mangold K, & Froesch D. 1979b. The mandibular movements of *Octopus vulgaris*. *Journal of Zoology (London)*. 188: 53-67.

Brown B. 1993. Maine's baitworm fisheries: resources at risk? *American Zoologist*. 33: 568-577.

Brunet M. 1968. Turbellariés Karkinorhynchidae de la region de Marseille. Les genres *Cheliplana* et *Cheliplanella*. *Cahiers de Biologie Marine*. 9: 421-440.

Brusca RC & Brusca GJ. 2003. *Invertebrates*. Sinauer Associates, Inc. Sunderland, MA. 530 pp.

Bryan GW & Gibbs PE. 1979. Zinc – a major inorganic component of Nereid polychaete jaws. *Journal of the Marine Biological Association of the United Kingdom*. 59: 969-973.

Burns WA. 1978. Thick sections: technique and applications (Ch.4) In: *Diagnostic Electron Microscopy* (Trump BF & Jones RJ, Eds.) John Wiley & Sons, New York. Vol. 1. p. 141-166.

Cariello L & Zanetti L. 1977. α- and β-cephalotoxin: two paralyzing proteins from posterior salivary glands of *Octopus vulgaris*. *Comparative Biochemistry and Physiology*. 57(C): 169-173.

Clark RB. 1964. *Dynamics in metazoan evolution: the origin of the coelom and segments*. Clarendon Press, Oxford U.K. 313 pp.

Clarke MR. 1962. The identification of cephalopod "beaks" and the relationship between beak size and total body weight. *Bulletin of the British Museum (Natural History)* 8: 421–480.

Clarke MR. 1986. *A handbook for the identification of cephalopod beaks*. Clarendon Press, Oxford, U.K. 273 pp.

Clarke RB & Cowey JB. 1958. Factors controlling the change of shape of certain nemertean and turbellarian worms. *Journal of Experimental Biology*. 35(4): 731-748.

Commito JA & Shrader PB. 1985. Benthic community response to experimental additions of the polychaete *Nereis virens*. *Marine Biology*. 86(1): 101-107.

Commito JA. 1982. Importance of predation by infaunal polychaetes in controlling the structure of a soft-bottom community in Maine, USA. *Marine Biology*. 68(1):77-81.

Copeland M & Wieman HL. 1924. The chemical sense and feeding behavior of *Nereis virens*. Sars. *Biological Bulletin*. 47(4): 231-238.

Cortez T, Castro BG, & Guerra A. 1998. Drilling behaviour of *Octopus mimus* Gould. *Journal of Experimental Marine Biology and Ecology*. 224: 193-203.

Crompton AW. 1963. On the lower jaw of *Diarthrognathus* and the origin of the mammalian lower jaw. *Proceedings of the Zoological Society London* 140: 697-753.

Croneis C & Scott HW. 1933. Scolecodonts (abstract). *Geological Society of America Bulletin*. 44: 207.

Dales RP. 1962. The polychaete stomodaeum and the inter-relationships of the families of Polychaeta. *Proceedings of the Zoological Society of London*. 139: 389-428.

De Vocht AJ-P & Schockaert ER. 1999. The anatomy and ultrastructure of the proboscis in *Zonorhynchus*-species and implications for phylogenetic relationships within the Eukalyptorhynchia Meixner, 1928 (Platyhelminthes, Rhabdocoela). *Belgian Journal of Zoology*. 129(1): 219-234.

De Vocht AJ-P. 1989. Ultrastructure of the proboscis in Cystiplanidae (Platyhelminthes, Kalyptorhynchia). *Zoomorphology*. 109: 1-10.

De Vocht AJ-P. 1991. Anatomy and ultrastructure of the proboscis in *Mesorhynchus terminostylis* (Platyhelminthes, Rhabdocoela). *Hydrobiologia*. 227: 291-298.

Dilly PN & Nixon M. 1976. The cells that secrete the beaks in octopods and squids (Mollusca, Cephalopoda). *Cell and Tissue Research*. 167: 229-241.

Doe DA. 1976. The proboscis hooks in Karkinorhynchidae and Gnathorhynchidae (Turbellaria, Kalyptorhynchia) as basement membrane or intracellular specializations. *Zoologica Scripta*. 5: 105-115.

Dorgan KM, Jumars PA, Johnson B, Boudreau BP, & Landis E. 2005. Burrow extension by crack propagation. *Nature*. 433: 475.

Dorgan KM, Jumars PA, Johnson BD, & Boudreau BP. 2006. Macrofaunal burrowing: the medium is the message. *Oceanography and Marine Biology: An Annual Review*. 44: 85-121.

DuBrul EL. 1992. Origin and adaptation of the hominid jaw joint, Ch. 1 In: *The temporomandibular joint: a biological basis for clinical practice*. 4th Ed. (Sarnat BG & Laskin DM, Eds.) W.B. Saunders Company, Philadelphia, PA. 505 pp.

Ehlers E. 1864. *Die Borstenwürmer (Annelida Chaetopoda) nach systematischen und anatomischen Untersuchungen dargestellt*. Wilhelm Engelmann, Leipzig.

Ehlers U. 1986. Comments on a phylogenetic system of the Platyhelminthes. *Hydrobiologia*. 132: 1-12.

Eichwald, E. 1854. Die Grauwackenschichten von Liv-und Esthland. *Bulletin de la Société Imperiale des Naturalistes de Moscou*. 27: 111.

Elner RW & Campbell A. 1981. Force, function and mechanical advantage in the chelae of the American lobster *Homarus americanus* (Decapoda: Crustacea). *Journal of Zoology (London)*. 193: 269-86.

Evans SM. 1973. A study of fighting reactions in some Nereid polychaetes. *Animal Behaviour*. 21: 138-146.

Fauchald K & Jumars PA. 1979. The diet of worms: a study of polychaete feeding guilds. *Oceanography and Marine Biology. An Annual Review*. 17: 193-284.

Fauchald K & Rouse G. 1997. Polychaete systematics: past and present. *Zoologica Scripta*. 26(2): 71-138.

Fauchald K. 1977. *The polychaete worms; definitions and keys to the orders, families, and genera*. Natural History Museum of Los Angeles County. Los Angeles, CA. 188 pp.

Frye CJ & Feldmann RM. 1991. North American late Devonian cephalopod aptychi. *Kirtlandia*. 46: 49-71.

Gage PW, Moore JW, Westerfield M. 1976. An octopus toxin, maculotoxin, selectively blocks sodium current in squid axons. *Journal of Physiology*. 259: 427-443.

Ghiretti F. 1959. Cephalotoxin: the crab-paralysing agent of the posterior salivary glands of cephalopods. *Nature*. 183: 1192-1193.

Ghiretti F. 1960. Toxicity of octopus saliva against crustacea. *Annals of the New York Academy of Science*. 90: 726-741.

Giberson RT & Demaree RS Jr. 1995. Microwave fixation: understanding the variables to achieve rapid reproducible results. *Microscopy Research and Techniques*, 32: 246-254.

Giebel CG. 1849. Briefliche Mittheilungen an Herrn Beyrich. *Zeitschrift der Deutschen Geologischen Gesellschaft* 1(2): 99-100.

Giere O. 1993. *Meiobenthology: The microscopic fauna in aquatic sediments*. Springer-Verlag, Berlin. 328 pp.

Goerke H. 1971. Die Ernährungsweise der Nereis-Arten (Polychaeta, Nereidae) der deutschen Küsten. *Veröffentlichungen des Instituts für Meeresforschung in Bremerhaven*. 13: 1-50.

Gosline JM & Shadwick RE. 1983a. The role of elastic energy storage mechanisms in swimming: an analysis of mantle elasticity in escape jetting in the squid, *Loligo opalescens*. *Canadian Journal of Zoology*. 61: 1421-1431.

Gosline JM & Shadwick RE. 1983b. Molluscan collagen and its mechanical organization in squid mantle. In *The Mollusca, Metabolic Biochemistry and Molecular Biomechanics*. (Hochachka PW, Ed.) Academic Press, NY. Vol 1. p. 371-398.

Gosliner TM. 1994. Gastropoda: Opisthobranchia. In: *Microscopic Anatomy of Invertebrates* (Harrison FW, Ed.), Vol. 5: Mollusca I, Ch. 5. Wiley-Liss, New York. p. 253-355.

Gould SJ & Lewontin RC. 1979. The Spandrels of San Marco and the panglossian paradigm: A critique of the adaptationist programme. *Proceedings of the Royal Society of London, Series B.* 205(1161): 581-598.

von Graff L. 1882. *Monographie der Turbellarien. I Rhabdocoelida*. Verlag Wilhelm Engelmann, Leipzig. 442 pp.

von Graff L. 1905. Turbellaria I. Acoela. In: *Das Tierreich* (Schulze FE, Ed.). Königl. Preuss. Akademie der Wissenschaften zu Berlin. 23(23): 34-42.

von Graff L. 1913. Turbellaria. II. Rhabdocoelida. In: *Das Tierreich*. R. Friedländer und Sohn, Berlin. 35: 484 pp.

Gross AO. 1921. The feeding habits and chemical sense of *Nereis virens* Sars. *Journal of Experimental Zoology*. 32(3): 427-442.

Guerra A, Nixon M, & Castro BG. 1988. Initial stages of food ingestion by *Sepia officinalis* (Mollusca, Cephalopoda). *Journal of Zoology*. 214(2): 189-197.

Hanlon RT & Messenger JB. 1996. *Cephalopod behaviour*. Cambridge University Press. Cambridge, UK. 232 pp.

Haszprunar G & Schaefer K. 1997. Monoplacophora. In: *Microscopic Anatomy of Invertebrates* (Harrison FW, Ed.), Vol. 6B: Mollusca II Ch. 4. Wiley-Liss, New York. p. 415-457.

Hildebrand M. 1995. *Analysis of vertebrate structure*. 4th Ed. John Wiley & Sons, Inc., New York, NY. 657 pp.

Hofmann KD & Schiedges I. 1984. Brain hormone levels and feed-back regulation during gametogenesis, metamorpholsis and regeneration in *Platynereis dumerilii* – an experimental approach. *Fortschreitte der Zoologie*. 29: 73-79.

Holland BS, Stridsberg S, & Bergström J. 1978. Confirmation of the reconstruction of *Aptychopsis*. *Lethaia*. 11: 144.

Hooge MD. 2001. Evolution of body-wall musculature in the Platyhelminthes (Acoela, Catenulida, Rhabditophora). *Journal of Morphology*. 249: 171-194.

Hunt S & Nixon M. 1981. A comparative study of protein composition in the chitin-protein complexes of the beak, pen, sucker disc, radula and oesophageal cuticle of cephalopods. *Comparative Biochemistry and Physiology*. 68B: 535-46.

Hwang DF, Arakawa O, Saito T, Noguchi T, Simidu U, Tsukamoto K, Shida Y, & Hashimoto K. 1989. Tetrodotoxin-producing bacteria from the blue-ringed octopus *Octopus maculosus*. *Marine Biology*. 100(3): 327-332.

Hyman LH. 1959. Smaller coelomate groups, Ch. 21 In: *The invertebrates* Vol. 11. (Hyman LH, Ed.) McGraw-Hill Book Company, Inc., New York, NY. 783 pp.

ITIS. 2007. Retrieved [14 January 2007], from the Integrated Taxonomic Information System on-line database, http://www.itis.gov.)

Ito Y, Kuriyama H, & Parker I. 1988. Calcium transients evoked by electrical stimulation of smooth muscle from Guinea-pig ileum recorded by the use of Fura-2. *Journal of Physiology*. 407: 117-134.

Jansonius J & Craig JH. 1971. Scolecodonts: I. Descriptive terminology and revision of systematic nomenclature; II. Lectotypes, new names for homonyms, index of species. *Bulletin of Canadian Petroleum Geology*. 19(1): 251-302.

Johnsen S & Kier WM. 1993. Intramuscular crossed connective tissue fibers: skeletal support in the lateral fins of squid and cuttlefish (Mollusca: Cephalopoda). *Journal of Zoology (London)*. 231: 311-338.

von Karling TG. 1947. Studien über Kalyptorhynchien (Turbellaria). I. Die Familien Placorhynchidae und Gnathorhynchidae. *Acta Zoologica Fennica*. 50: 1-64.

von Karling TG. 1949. Studien über Kalyptorhynchien (Turbellaria). II. Die Familien Karkinorhynchidae und Diascorhynchidae. *Acta Zoologica Fennica*. 58: 1-42.

von Karling TG. 1950. Studien über Kalyptorhynchien (Turbellaria). III. Die Familie Schizorhynchidae. *Acta Zoologica Fennica*. 59: 1-33.

von Karling TG. 1961. Zur Morphologie, Entstehungsweise und Funktion des Spaltrüssels der Turbellaria Schizorhynchia. *Arkiv För Zoologi*. 13(11): 253-286.

von Karling TG. 1983. Structural and systematic studies on Turbellaria Schizorhynchia (Platyhelminthes). *Zoologica Scripta*. 12(2): 77-89.

von Karling TG. 1987. New taxa of Kalyptorhynchia (Platyhelminthes) from the N. American Pacific coast. *Zoologica Scripta*. 18(1): 19-32.

Kear AJ. 1994. Morphology and function of the mandibular muscles in some coleoid cephalopods. *Journal of the Marine Biological Association U.K*. 74: 801-22.

Kier WM & Smith AM. 1990. The morphology and mechanics of octopus suckers. *Biological Bulletin*. 178: 126-136.

Kier WM & Smith AM. 2002. The structure and adhesive mechanism of octopus suckers. *Integrative and Comparative Biology*. 42: 1146-1153.

Kier WM, Smith KK, Miyan JA. 1989. Electromyography of the fin musculature of the cuttlefish *Sepia officinalis*. *Journal of Experimental Biology*. 143: 17-31.

Kier WM, Smith KK. 1985. Tongues, tentacles and trunks: the biomechanics of movement in muscular-hydrostats. *Zoological Journal of the Linnean Soc*iety 83: 307-324.

Kier WM. 1982. The functional morphology of the musculature of squid (Loliginidae) arms and tentacles. *Journal of Morphology* 172: 179-192.

Kier WM. 1989. The fin musculature of cuttlefish and squid (Mollusca, Cephalopoda): Morphology and mechanics. *Journal of Zoology (London)*. 217: 23-38.

Kier WM. 1992. Hydrostatic skeletons and muscular hydrostats (Ch. 9) In: *Biomechanics (Structures and Systems): A Practical Approach* (Biewener AA, Ed.) IRL Press at Oxford University Press. New York. p. 205-231.

Kozloff EN. 1990. *Invertebrates*. Saunders College Publishing, New York, NY. 866 pp.

Latta H & Hartmann JF. 1950. Use of a glass edge in thin sectioning for electron microscopy. *Proceedings of the Society for Experimental Biology and Medicine*. 74: 436-439.

Lehmann U. 1970. Lias Anaptychen als Kieferelemente (Ammonoidea). *Paläontologische Zeitschrift*. 44: 25-31.

Lehmann U. 1971. New aspects in ammonite biology. *Proceedings of the North American Paleontological Convention* Field Museum of Natural History, Chicago IL. I: 1251-1269.

Lehmann U. 1972. Aptychen als Kieferelemente der Ammoniten. *Paläontologische Zeitschrift*. 49:34-48.

Lehmann U. 1981. *The Ammonites: their life and their world*. Cambridge University Press, New York, NY. 252 pp.

Levine HL. 1999. *Ancient invertebrates and their living relatives.* Prentice Hall, Upper Saddle River, NJ. 358 pp.

Lewis C, Olive PJW, & Bentley MG. 2003. Pre-emptive competition as a selective pressure for early repreoduction in the polychaete *Nereis virens*. *Marine Ecology Progress Series*. 254: 199-211.

Lewis DB & Whitney PJ. 1968. Cellulase in *Nereis virens*. *Nature (London)*. 220(5167): 603-604.

Lichtenegger HC, Schöber T, Ruokolainen JT, Cross JO, Heald SM, Birkedal H, Waite JH, & Stucky GD. 2003. Zinc and mechanical prowess in the jaws of *Nereis*, a marine worm. Proceedings of the National Academy of Science. 100(16): 9144-9149.

Littlewood DTJ, Rohde K, & Clough KA. 1999. The interrelationships of all major groups of Platyhelminthes: phylogenetic evidence from morphology and molecules. *Biological Journal of the Linnean Society*. 66: 75-114.

Lowenstam HA, Traub W, & Weiner S. 1984. Nautilus hard parts: A study of the mineral and organic constituents. *Paleobiology*. 10(2): 268-279.

Lu CC & Ickeringill R. 2002. Cephalopod beak identification and biomass estimation techniques: tools for dietary studies of southern Australian finfishes. *Museum Victoria Science Reports*. 6: 1-65.

Luchtel DL, Martin AW, Deyrup-Olsen I, & Boer HH. 1997. Gastropoda: Pulmonata. In: *Microscopic Anatomy of Invertebrates* (Harrison FW, Ed.), Vol. 6B: Mollusca II Ch. 5. Wiley-Liss, New York. p. 459-718.

Maly EJ, Schoenholtz S, & Arts MT. 1980. The influence of flatworm predation on zooplankton inhabiting small ponds. *Hydrobiologia*. 76: 233-240.

Manton SM & Harding JP. 1964. Mandibular mechanisms and the evolution of arthropods. *Philosophical Transactions of the Royal Society of London. Series B, Biological Sciences*. 247(737): 1-183.

Mare MF. 1942. A study of a marine benthic community with special reference to the micro-organisms. *Journal of the Marine Biological Association UK*. 25:517-554.

Markert S, Arndt C, Felbeck H, Becher D, Sievert SM, Hügler M, Albrecht D, Robidart J, Bench S, Feldman RA, Hecker M, & Schweder T. 2007. Physiological proteomics of the uncultured endosymbiont of *Riftia pachyptila*. *Science*. 315: 247-250.

Martens PM & Schockaert ER. 1986. The importance of turbellarians in the marine meiobenthos: a review. *Hydrobiologia*. 132(1): 295-303.

McCarthy JM & Joskowicz L. 2001. Kinematic synthesis Ch. 1. In: *Formal engineering design synthesis*. 1st Ed. (Antonsson EK & Cagan J, Eds.) Cambridge University

Press, Cambridge, U.K. 523 pp.

Meixner J. 1925. Beitrag zur Morphologie und zum System der Turbellaria-Rhabdocoela. I. Die Kalyptorhynchia. *Zeitschrift für Morphologie und Ökologie der Tiere*. 3: 255-343.

Meixner J. 1928. Aberrante Kalyptorhynchia aus dem Sande der Kieler Bucht. *Zoologischer Anzeiger*. 77: 229-253.

Meixner J. 1938. Turbellaria (Strudelwüermer). I. Allgemeines Teil. In: *Die Tierwelt der Nord- und Ostsee*, 33 (IVb) (Grimpe G, Wagler E, & Remane A; Eds.). Akademische Verlagsgesellschaft: Leipzig, Germany. 146 pp.

Messenger JB & Young JZ. 1999. The radular apparatus of cephalopods. *Philosophical Transactions of the Royal Society of London. Series B*. 354: 161-182.

Millonig G. 1961. Advantages of a phosphate buffer for OsO_4 solution in fixation. *Journal of Applied Physics*. 32: 1637.

Miron G, Desrosiers G, & Retière C 1992a. Organisation of fighting in the polychaete *Nereis virens* (Sars) and the effects of residency and orientation. *Behaviour*. 121:20-34.

Miron G, Desrosiers G, Retière C, & Masson S. 1992b. Variations in time budget of the polychaete *Nereis virens* as a function of density and acclimation after introduction to a new burrow. *Marine Biology*. 114(1): 41-48.

Mollenhauer HH. 1964. Plastic embedding mixtures for use in electron microscopy. *Stain Technology*. 39: 111-114.

Monks N & Palmer P. 2002. *Ammonites*. Smithsonian Institution Press, Washington DC. 176 pp.

Moore RC & Sylvester-Bradley PC. 1957. Taxonomy and nomenclature of aptychi. In: *Treatise on Invertebrate Paleontology* (Moore RC, Ed.), Vol. L: Mollusca 4, Cephalopoda, Ammonoidea. Geological Society of America and University of Kansas Press, Lawrence KA. p. L465-L471.

Mori J, Kubodera T, & Baba N. 2001. Squid in the diet of northern fur seals, *Callorhyinus ursinus*, caught in the western and central North Pacific Ocean. *Fisheries Research*. 52: 91-97.

Nesis KN. 1993. Cephalopods of seamounts and submarine ridges. In: *Recent advances in cephalopod fisheries biology* (Okutani T, O'Dor RK, Kubodera T. Eds.). Tokai University Press. Tokyo, Japan. p. 365-373.

Neustadter DM, Drushel RF, & Chiel HJ. 2002. Kinematics of the buccal mass during swallowing based on magnetic resonance imaging in intact, behaving *Aplysia californica*. *Journal of Experimental Biology*. 205: 939-958.

Nieves-Aldrey JL, Vardal H, & Ronquist F. 2005. Comparative morphology of terminal-instar larvae of Cynipoidea: phylogenetic implications. *Zoologica Scripta*. 34: 15-36.

Nigmatullin CM, Ostapenko AA. 1976. Feeding of *Octopus vulgaris* Lam. from the northwest African coast. *ICES CM 1976/K: Shellfish and Benthos Committee* 6: 1–15.

Nixon M & Boyle P. 1982. Hole-drilling in crustaceans by *Eledone cirrhosa*. *Journal of Zoology (London)*. 196: 439-444.

Nixon M & Budelmann BU. 1984. Scale-worms – occasional food of *Octopus*. *Journal of Molluscan Studies*. 50: 39-42.

Nixon M & Maconnachie E. 1988. Drilling by *Octopus vulgaris* (Mollusca, Cephalopoda) in the Mediterranean. *Journal of Zoology (London)*. 216: 687-716.

Nixon M & Mangold K. 1996. The early life of *Octopus vulgaris* (Cephalopoda: Octopodidae) in the plankton and at settlement: A change in lifestyle. *Journal of Zoology (London)*. 239(2): 301-327.

Nixon M, Maconnachie E, & Howell PGT. 1980. The effects on shells of drilling by *Octopus*. *Journal of Zoology (London)*. 191: 75-88.

Nixon M, Young JZ. 2003. *The brains and lives of cephalopods*. Oxford University Press. Oxford, UK. 392 pp.

Nixon M. 1969. Growth of the beak and radula of *Octopus vulgaris*. *Journal of Zoology (London)*. 159: 363-379.

Nixon M. 1979a. Has *Octopus vulgaris* a second radula? *Journal of Zoology (London)*. 187: 291-296.

Nixon M. 1979b. Hole-boring in shells by *Octopus vulgaris* Cuvier in the Mediterranean. *Malacologia*. 18: 431-443.

Nixon M. 1980. Salivary papilla of *Octopus* as an accessory radula for drilling shells. *Journal of Zoology (London)*. 190: 53-57.

Nixon M. 1984. Is there external digestion by *Octopus*? *Journal of Zoology (London)*. 202: 441-447.

Nixon M. 1987. Cephalopod diets. In: *Cephalopod life cycles* (Boyle PR, Ed.). Vol 2. Comparative Reviews. Academic Press. London, UK. p. 201-219.

Noble HW, Creanor SL. 1992. Comparative functional anatomy Ch. 2. In: *The temporomandibular joint: a biological basis for clinical practice*. 4th Ed. (Sarnat BG & Laskin DM, Eds.). W.B. Saunders Company, Philadelphia, PA. 505 pp.

Novakovic VA, Sutton GP, Neustadter DM, Beer RD, & Chiel HJ. 2006. Mechanical reconfiguration mediates swallowing and rejection in *Aplysia californica*. *Journal of Comparative Physiology A: Neuroethology, Sensory, Neural, and Behavioral Physiology*. 192: 857-870.

Nussbaum MC. 1985. *Aristotle's* De Motu Animalium. Princeton University Press, Princeton, NJ. 430 pp.

O'Dor RK, Pörtner HO, & Shadwick RE. 1990. Squid as elite athletes: locomotory, respiratory, and circulatory integration. In: *Squid as experimental animals* (Gilbert DL, Adelman WJ, & Arnold JM, Eds.). Plenum Press, New York. p. 481-503.

Olive PJW. 1993. Management of the exploitation of the lugworm *Arenicola marina* and the ragworm *Nereis virens* (Polychaeta) in conservation areas. *Aquatic Conservation*. 3: 1-24.

Paxton H. 1980. Jaw growth and replacement in Polychaeta. *Journal of Natural History* 14: 543-546.

Paxton H. 2004. Jaw growth and replacement in *Ophryotrocha labronica* (Polychaeta, Dorvilleidae). *Zoomorphology*. 123: 147-154.

Pechenik JA. 2004. *Biology of the Invertebrates* (5th ed.). McGraw-Hill, New York. 608 pp.

Pettibone MH. 1963. Marine polychaete worms of the New England region. I Aphroditidae through Trochochaetidae. *U.S. National Museum Bulletin*. 227(I): 1-356.

Pilato G. 1968a. La muscolatura dei Policheti. II. Muscolatura del bulbo faringeo di *Perinereis cultrifera* (Grube). *Archivio Zoologico Italiano*. 53: 169-187.

Pilato G. 1968b. La muscolatura dei Policheti. III Studio anatomico-funzionale della muscolatura della proboscide di *Perinereis cultrifera* (Grube). *Archivio Zoologico Italiano*. 53: 293-313.

Platt JR. 1964. Strong Inference. *Science*. 146(3642): 347-353.

Regnard E. 1913. Contribution a l'etude des *Nereis* de la région de Roscolf. *Memoires de la Société Zoologique de France*. 25: 72-111.

Reise K. 1981. High abundance of small zoobenthos around biogenic structures in tidal sediment of the Wadden Sea. *Helgoländer Meeresuntersuchungen*. 34: 413-425.

Remane A. 1933. Verteilung und organization der benthonischen microfauna der Kieler Bucht. *Wissenschaftliche Meeresuntersuchungen (Abt. Kiel)*. 21: 161-221.

Ricci C & Balsamo M. 2000. The biology and ecology of lotic rotifers and gastrotrichs. *Freshwater Biology*. 44: 15-28.

Rieger RM & Doe DA. 1975. The proboscis armature of Turbellaria-Kalyptorhynchia, a derivative of the basement lamina? *Zoologica Scripta*. 4: 25-32.

Rieger RM, Tyler S, Rieger GE, & Smith JPS. 1991. Turbellaria. In: *Microscopic Anatomy of Invertebrates*, Volume 3, Platyhelminthes and Nemertinea, (Harrison FW & Bogitsh BJ, Eds.), Wiley-Liss, New York. p. 7-140.

Robertson AL, Rundle SD, & Schmid-Araya JM. 2000. An introduction to a special issue on lotic meiofauna. *Freshwater Biology*. 44: 1-3.

Rouse GW & Fauchald K. 1997. Cladistics and polychaetes. *Zoologica Scripta*. 26: 139-204.

Rouse GW & Pleijel F. 2001. *Polychaetes*. Oxford University Press, Oxford, U.K. 354 pp.

Rudwick MJS. 1970. *Living and fossil brachiopods*. Hutchinson, London, U.K. 199 pp.

Santos MB, Clarke MR, & Pierce GJ. 2001. Assessing the importance of cephalopods in the diets of marine mammals and other top predators: problems and solutions. *Fisheries Research*. 52: 121-139.

Saulnier-Michel C. 1992. Polychaeta: digestive system, Ch. 2.3 In: *Microscopical anatomy of invertebrates: Annelida*, Vol 7. (Harrison FW & Gardiner SL, Eds.) Wiley-Liss, Inc., New York, NY. 418 pp.

Schilke K. 1969. Zwei neuartige Konstruktionstypen des Rüsselapparates der Kalyptorhynchia (Turbellaria). *Zeitschrift für Morphologie der Tiere*. 65: 287-314.

Schilke K. 1970. Zur morphologie und phylogenie der Schizorhynchia (Turbellaria Kalyptorhynchia). *Zeitschrift für Morphologie der Tiere*. 67: 118-171.

Schmidt-Nielsen K. 1998. *Animal physiology: adaptation and environment*. 5th Ed. Cambridge University Press, Cambridge, U.K. 612 pp.

Shimek RL & Steiner G. 1997. Scaphopoda. In: *Microscopic Anatomy of Invertebrates* (Harrison FW, Ed.), Vol. 6B: Mollusca II Ch. 6. Wiley-Liss, New York. pp. 719-781.

Smith JPS, Tyler S, & Rieger RM. 1986. Is the Turbellaria polyphyletic? *Hydrobiologia*. 132: 13-21.

Smith KK & Kier WM. 1989. Trunks, tongues, and tentacles: moving with skeletons of muscle. *American Scientist.* 77: 28-35.

Steer MA & Semmens JM. 2003. Pulling or drilling, does size or species matter? An experimental study of prey handling in *Octopus dierythraeus* (Norman, 1992). *Journal of Experimental Marine Biology and Ecology*. 290: 165-178.

Stefanini M, De Martino C, & Zamboni L. 1967. Fixation of ejaculated spermatozoa for electron microscopy, *Nature*, 216: 173-14.

Stephens GC. 1968. Dissolved organic matter as a potential source of nutrition for marine organisms. *American Zoologist*. 8: 95-106.

Sterrer W. 1971. Gnathostomulida: problems and procedures In: Proceedings of the First International Conference on Meiofauna. (Hulings NC, Ed.). *Smithsonian Contributions to Zoology,* Washington DC, Smithsonian Institution Press. 76: 9-15.

Szaniawski H. 1996. Scolecodonts, Ch. 12 In: *Palynology: principles and applications.* (Jansonius J & McGregor DC, Eds.) American Association of Stratigraphic Palynologists Foundation, p. 337-354.

Tanabe K & Fukuda Y. 1999. Morphology and function of cephalopod buccal mass, Ch. 19 In: *Functional morphology of the invertebrate skeleton.* (Savazzi E, Ed.) John Wiley & Sons, New York, NY, p. 245-262.

Tanabe K, Hirano H, & Kanie Y. 1980. The jaw apparatus of *Scalarites mihoensis*, a Late Cretaceous ammonite. *Professor Saburo Kanno Memorial Volume* p. 159-165.

Taylor GM, Palmer AR & Barton AC. 2000. Variation in safety factors of claws within and among six species of *Cancer* crabs (Decapoda: Brachyura). *Biological Journal of the Linnean Society*. 70: 37-62.

Taylor GM. 2000. Maximum force production: why are crabs so strong? *Proceedings of the Royal Society of London. B* 267: 1475-1480.

Thompson JT & Kier WM. 2001. Ontogenetic changes in fibrous connective tissue organization in the oval squid, *Sepioteuthis lessoniana*, Lesson, 1830. *Biological Bulletin*. 201: 136-153.

Toomey DF, Baesemann JF, & Lane HR. 1974. The biota of the Pennsylvanian (Virgilian) Leavenworth limestone, midcontinent region. Part 5: distribution of miscellaneous microfossils. *Journal of Paleontology* 48(6): 1156-1165.

Trueman ER & Wong TM. 1987. The role of the coelom as a hydrostatic skeleton in lingulid brachiopods. *Journal of Zoology (London)*. 213: 221-32.

Tunnicliffe V, McArthur AG, & McHugh D. 1998. A biogeographical perspective of the deep-sea hydrothermal vent fauna. *Advances in Marine Biology*. 34: 352-442.

Turek V. 1978. Biological and stratigraphical significance of the Silurian nautiloid *Aptychopsis*. *Lethaia.* 11: 127-138.

Turnbull FM. 1876. On the anatomy and habits of *Nereis virens. Transactions of the Connecticut Academy of Arts and Sciences*. 3(7): 265-280.

Uyeno TA & Hsiao HS. 2007. A novel device to monitor small changes in underwater distances. *Invertebrate Biology*. in press.

Uyeno TA & Kier WM. 2005. Functional morphology of the cephalopod buccal mass: A novel joint type. *Journal of Morphology*. 264: 211-222.

Uyeno TA & Kier WM. 2007. Electromyography of the buccal musculature of octopus (*Octopus bimaculoides*): a test of the function of the muscle articulation in support and movement. *Journal of Experimental Biology*. 210: 118-128.

Vogel S & Wainwright SA. 1969. *A functional bestiary, laboratory studies about living system.* Addison-Wesley, Reading MA. 106 pp.

Vogel S. 2003. *Comparative biomechanics: life's physical world*. Princeton University Press. Princeton NJ. 580 pp.

Voight JR. 2000. A deep-sea octopus (*Granelledone* cf. *boreopacifica*) as a shell-crushing hydrothermal vent predator. *Journal of Zoology (London)*. 252: 335-341.

Voltzow J. 1994. Gastropoda: Prosobranchia. In: *Microscopic Anatomy of Invertebrates* (Harrison FW, Ed.), Vol. 5: Mollusca I Ch. 4. Wiley-Liss, New York. p. 111-252.

Voss GL. 1977. Present status and new trends in cephalopod systematics. In: *The biology of cephalopods. Symposium of the Zoological Society of London* (Nixon M & Messenger JB, Eds.), Vol. 38 Academic Press, London, U.K. p. 49-60.

Wainwright SA, Biggs WD, Currey JD, & Gosline JM. 1982. *Mechanical design in organisms*. Princeton University Press, Princeton, NJ. 423 pp.

Wainwright SA. 1988. Form and function in organisms. *American Zoologist*. 28: 671-680.

Ward DV & Wainwright SA. 1972. Locomotory aspects of squid mantle structure. *Journal of Zoology (London).* 167: 437-449.

Wells MJ. 1978. *Octopus: physiology and behaviour of an advanced invertebrate*. Chapman and Hall, London, U.K. 417 pp.

Wilson RS. 2000. Family Nereididae. In: *Polychaetes and Allies: The Southern Synthesis* (Beesley PL, Ross GJB, & Glasby CJ. Eds.) CSIRO Publishing, Melbourne. p. 138-141.

Wilson WH Jr. & Ruff RE. 1988. Species profiles: life histories and environmental requirements of coastal fishes and invertebrates (North Atlantic) – sandworm and bloodworm. *U.S. Fisheries and Wildlife Service Biological Reports 82 (11.80). U.S. Army Corps of Engineers, TR EL-82-4.* 23 pp.

Ye H, Morton DW, & Chiel HJ. 2006. Neuromechanics of multifunctionality during rejection in *Aplysia californica. Journal of Neuroscience*. 26(42): 10743-10755.

Young JZ. 1965. The buccal nervous system of *Octopus. Philosophical Transactions of the Royal Society of London (B)* 249: 27–43.

Young JZ. 1971. *The anatomy of the nervous system of* Octopus vulgaris. Oxford, UK: Clarendon Press.

Young JZ. 1991. The muscular-hydrostatic radula supports of *Octopus*, *Loligo*, *Sepia* and *Nautilus*. *Journal of Cephalopod Biology*. 2: 65-93.

Zghal F & Amor ZB. 1986. Caractéristiques morphologiques du pharynx de *Nereis diversicolor* Müller, 1776 (Polychetes Nereidae). *Archives de l'Institute Pasteur de Tunis*. 63(2-3): 277-284.